Pathological modeling of tick-borne encephalitis virus infection and induced antiviral response in neurons and astrocytes using human neural progenitor-derived cells.

Mazigh Fares

agreenium
l'institut agronomique, vétérinaire & forestier de France

AgroParisTech

NNT° : 2018IAVF0025

THESE DE DOCTORAT

préparée à l'Institut des sciences et industries du vivant et de l'environnement (AgroParisTech)

pour obtenir le grade de

Docteur de l'Institut agronomique vétérinaire et forestier de France

Spécialité : Microbiologie

École doctorale n°581
Agriculture, alimentation, biologie, environnement et santé (ABIES)

par

Mazigh FARES

Pathological modeling of tick-borne encephalitis virus infection and induced antiviral response in neurons and astrocytes using human neural progenitor-derived cells.

Directrice de thèse : **Nadia HADDAD**
Co-directrice de thèse : **Muriel COULPIER**

Thèse présentée et soutenue à Maisons-Alfort, le jeudi 20 décembre 2018.

Composition du jury :

M. Hervé BOURHY, Directeur de recherche, Institut Pasteur Paris	Président
Mme Branka HORVAT, Directrice de recherche, INSERM	Rapporteure
M. Alain KOHL, Professeur, University of Glasgow	Rapporteur
Mme Thérèse COUDERC, Chargée de recherche, Institut Pasteur Paris	Examinatrice
Mme Sara SALINAS, Chargée de recherche, INSERM/Université de Montpellier	Examinatrice
Mme Nadia HADDAD, Professeure, École Nationale Vétérinaire d'Alfort	Directrice de thèse
Mme Muriel COULPIER, Chargée de recherche, Institut National de Recherche Agronomique	Co-directrice de thèse
M. Pierre-Emmanuel CECCALDI, Professeur, Institut Pasteur Paris – Université Paris-Diderot	Invité

UMR 1161 de Virologie (VIRO)

École Nationale Vétérinaire d'Alfort, 7 Avenue du Général de Gaulle, 94700, Maisons-Alfort, France

"Bernard of Chartres used to say that we are like dwarfs on the shoulders of giants, so that we can see more than they, and things at a greater distance, not by virtue of any sharpness on sight on our part, or any physical distinction, but because we are carried high and raised up by their giant size."

John of Salisbury, Metalogicon, 1159

Acknowledgements

Abstract

Title: Pathological modeling of tick-borne encephalitis virus infection and induced antiviral response in neurons and astrocytes using human neural progenitor-derived cells.

Keywords: Tick-borne encephalitis virus, Antiviral immunity, Human neural progenitor cells, Neurons, Astrocytes, Flavivirus

Tick-borne encephalitis virus (TBEV), a member of the *Flaviviridae* family, genus *Flavivirus*, is, from a medical point of view, the most important arbovirus in Europe and North-East Asia. It is responsible for febrile illness and, in some cases, for neurological manifestations ranging from mild meningitis to severe encephalomyelitis that can be fatal. Despite its medical importance, the neuropathogenesis induced by this zoonotic agent remains poorly understood. Here, we used human neural cells differentiated from fetal neural progenitor cells (hNPCs) to model the infection *in vitro* and to decipher the mechanisms by which the virus damages the human brain. Our results showed that neurons and glial cells, namely astrocytes and oligodendrocytes, were permissive to TBEV. Neurons were massively infected and subjected to a dramatic cytopathic effect (60% loss 7 days post-infection). Astrocytes were also infected, although at lower levels, and the infection had a moderate effect on their survival (30% loss 7 days post-infection), inducing a hypertrophied morphology characteristic of astrogliosis. Thus, two major cellular events described in TBEV-infected human brain (i.e. neuronal loss and astrogliosis) were reproduced in this *in vitro* cellular model, showing its relevance to study TBEV-induced neuropathogenesis. We therefore used it to tackle TBEV-induced antiviral response. Using PCR arrays, we first showed that TBEV induced a strong antiviral response characterized by the overexpression of viral sensors, cytokines and interferon-stimulated genes (ISGs). Then, setting up enriched cultures of human neurons and human astrocytes, we further showed that the two cellular types were participating in the global antiviral response. However, astrocytes developed a stronger antiviral response than neurons. These results, by demonstrating that human neurons and human astrocytes have unique antiviral potential, suggest that their particular susceptibility to TBEV infection is due to their different capacity to mount a protective antiviral response.

Résumé

Titre : Modélisation pathologique de l'infection par le virus de l'encéphalite à tiques et réponse antivirale induite dans les neurones et astrocytes dérivés de progéniteurs neuraux fœtaux humains

Mots-clés : Virus de l'encéphalite à tiques, Immunité antivirale, Cellules progénitrices neurales humaines, Neurones, Astrocytes, Flavivirus

Le virus de l'encéphalite à tiques (TBEV), membre de la famille des *Flaviviridae* et du genre *Flavivirus*, est d'un point de vue médical, l'arbovirus le plus important en Europe et en Asie du Nord-Est. Il est responsable de symptômes fébriles et de manifestations neurologiques allant de la méningite légère à l''encéphalomyélite sévère pouvant être fatale. En dépit de son importance médicale, la neuropathogenèse induite par cet agent zoonotique reste peu caractérisée. Ici, nous avons utilisé des cellules neurales humaines différenciées à partir de progéniteurs neuraux fœtaux pour modéliser l'infection *in vitro* et élucider les mécanismes par lesquels le virus endommage le cerveau humain. Nos résultats ont montré que les neurones et les cellules gliales (astrocytes et oligodendrocytes) étaient permissifs au TBEV. Les neurones étaient massivement infectés et la cible d'un effet cytopathique important (perte de 60 % des neurones 7 jours après l'infection). Les astrocytes étaient également infectés, bien qu'à des niveaux inférieurs, et l'infection avait un effet modéré sur leur survie (perte de 30 % des astrocytes 7 jours après l'infection), induisant une hypertrophie caractéristique d'une astrogliose. Ainsi, deux événements majeurs décrits dans les cerveaux de patients infectés par TBEV (perte neuronale et astrogliose) étaient reproduits dans ce modèle cellulaire *in vitro*, démontrant ainsi sa pertinence pour des études de neuropathogenèse. Nous l'avons donc utilisé pour étudier la réponse antivirale induite par TBEV. En utilisant des PCR arrays, nous avons d'abord montré que le virus induisait une forte réponse antivirale caractérisée par une surexpression de senseurs viraux, de cytokines et de gènes stimulés par l'interféron. Puis, en établissant des cultures enrichies en neurones humains et astrocytes humains, nous avons montré que ces deux types cellulaires participaient à la réponse antivirale globale. Cependant, les astrocytes élaboraient une réponse antivirale plus forte que les neurones. Ces résultats, en démontrant que les neurones humains et les astrocytes humains élaboraient chacun une réponse antivirale unique suite à l'infection, suggèrent que leur sensibilité particulière à TBEV serait due à leur capacité différente à établir une réponse antivirale protectrice.

Résumé substantiel

Le virus de l'encéphalite à tiques (TBEV) est un membre de la famille des *Flaviviridae* et du genre *Flavivirus*. D'un point de vue médical, il est l'arbovirus le plus important en Europe et en Asie du Nord-Est, avec en moyenne 8000 cas cliniques déclarés par an. L'infection par TBEV est souvent asymptomatique, mais les patients atteints peuvent développer un syndrome fébrile voire des manifestations neurologiques allant d'une méningite bénigne à une encéphalomyélite sévère pouvant être fatale. En dépit de son importance médicale, la neuropathogenèse induite par TBEV reste peu caractérisée. Ici, nous avons utilisé des cellules neurales humaines différenciées à partir de progéniteurs neuraux fœtaux (hNPCs) pour modéliser l'infection *in vitro* et élucider les mécanismes par lesquels le virus endommage le cerveau humain.

Afin de déterminer quel était le tropisme de TBEV dans les cellules neurales humaines dérivées de hNPCs, nous avons réalisé des immunomarquages avec des anticorps dirigés contre TBEV et contre des marqueurs spécifiques des neurones (HuC/HuD ou ßIII-Tubulin), des astrocytes (GFAP) ou des oligodendrocytes (Olig2), et nous les avons quantifiés en utilisant un imageur automatique (ArrayScan Cellomics Thermo Scientific). Nos résultats ont montré que les cellules neurales étaient permissives à TBEV. Les neurones étaient la cible principale du virus avec 55.2±3.8 % de neurones infectés. Les cellules gliales étaient également permissives au virus, avec 6.81±21.5 % d'oligodendrocytes infectés et 13.6±5.3 % d'astrocytes infectés. Ces résultats ont révélé un tropisme de TBEV pour les neurones et les oligodendrocytes et suggèrent une résistance des astrocytes à l'infection.

Nous avons ensuite évalué les dommages induits par TBEV dans les trois types de cellules. Nous avons réalisé des immunomarquages spécifiques de chacun des types cellulaires, comme précédemment. Nos résultats ont montré une perte importante et continue de neurones dès 72 heures post-infection (hpi). De manière inattendue, nous avons également observé une perte modérée d'astrocytes à un temps plus tardif (7 jours post-infection –jpi-), mais nous n'avons pas observé d'altération induite par TBEV dans la population d'oligodendrocytes. Cela suggère un impact diffèrent de TBEV sur les neurones et les cellules gliales humaines, confirmant que ces dernières seraient plus résistantes à la mort induite par TBEV.

Comme nous avons observé une diminution du nombre de neurones et d'astrocytes suggérant une mort cellulaire, nous avons cherché à déterminer par quelles voies la mort cellulaire était induite par TBEV dans les cultures. Pour cela, nous avons réalisé des PCR arrays nous permettant d'analyser l'expression de 84 gènes impliqués dans l'apoptose et de 84 gènes impliqués dans l'autophagie. Nos résultats ont mis en évidence une surexpression de plusieurs gènes impliqués dans l'apoptose, alors que peu de gènes impliqués dans l'autophagie étaient surexprimés. Nous avons confirmé la surexpression ou l'absence de surexpression de certains gènes (*TNFSF10*, *P53*, *BECN1* et *ATG3*) par qRT-PCR. De plus, un marquage TUNEL (Terminal deoxynucleotidyl transferase dUTP nick end labeling), spécifique des cassures double brin de l'ADN, avait monté une augmentation des figures d'apoptose dans les cultures neurales. De manière plus spécifique, nous avons observé, par immunomarquage, une induction du clivage de la Caspase 3 dans les neurones, suggérant une activation des voies de l'apoptose.

Par ailleurs, dans le but de déterminer si les cellules neurales dérivées de hNPCs développent une réponse antivirale contre TBEV, nous avons analysé par PCR array l'expression de 84 gènes impliqués dans la réponse antivirale humaine. Nos résultats ont montré que 23 gènes étaient surexprimés suite à l'infection par TBEV, parmi lesquels des récepteurs de reconnaissance de motifs moléculaires (PRR), des cytokines et des gènes stimulés par l'interféron (ISG). Nous avons confirmé la surexpression de 11 gènes par qRT-PCR, à savoir *DDX58* (RIG-I), *TLR3*, *IFIH1* (MDA5), *CXCL10*, *CCL5* (RANTES), *CXCL11*, *ISG15*, *OAS2*, *MX1*, *ISG56* et *IFI6*. Pour tous ces gènes, des cinétiques d'infection ont montré une surexpression dès 7 hpi, qui augmentait jusqu'à 14 jpi, sauf pour les cytokines dont l'expression diminuait à 14 jpi. Cela a montré une activation importante de la réponse antivirale dans les cultures.

Pour élucider si cette réponse antivirale était différente entre les neurones et les astrocytes, nous avons établi des cultures enrichies soit en neurones, soit en astrocytes, en utilisant la technologie MACS (Magnetic-Activated Cell Sorting), basée sur des billes magnétiques conjuguées à des anticorps anti-GLAST spécifiques des astrocytes. Nous avons respectivement enrichi la proportion de neurones, passant de 74.1±4.1 % dans les cultures non séparées à 94.1±0.4 % dans les cultures enrichies en neurones (En-Neurons), et la proportion d'astrocytes, passant de 20.8±4.9 % dans les cultures non séparées à 53.5±2.7 % dans les cultures enrichies en astrocytes

(En-Astrocytes). Nous avons ensuite analysé l'expression de gènes de la réponse antivirale dans les cultures En-Neurons, En-Astrocytes et non séparées. Nous avons montré une surexpression de gènes de la réponse antivirale à la fois dans les neurones et dans les astrocytes. En revanche, le niveau d'expression était plus important dans les astrocytes. Nous avons ensuite effectué des qRT-PCR pour confirmer cette surexpression à différents temps après l'infection. Nous avons confirmé que, dès 7hpi pour *IFIH1* (MDA5) et *OAS2*, et dès 24hpi pour *DDX58* (RIG I), *TLR3*, *MX1*, *CXCL10*, les gènes étaient surexprimés de manière plus importante dans les astrocytes que dans les neurones. *RSAD2* (viperin), un ISG décrit comme participant au contrôle de la réplication de TBEV dans les cellules neurales murines, suit le même profil d'expression. Globalement, nos résultats suggèrent que la sensibilité neuronale à TBEV pourrait être due à une réponse antivirale globale associée à l'absence de régulation de gènes clés de la réponse antivirale. A l'inverse, la résistance des astrocytes pourrait être due à une réponse antivirale plus forte et protectrice.

Les astrocytes humains induisaient donc une réponse antivirale protectrice, mais l'effet protecteur de cette réponse sur l'infection et la survie des neurones humains n'est pas caractérisé. Pour identifier un potentiel effet, nous avons infecté des cultures En-Neurons (contenant ≅95 % de neurones) et des cultures non séparées (contenant ≅75 % de neurones) avec TBEV et comparé leur taux d'infection. Dès 24 hpi, alors que TBEV infectait 66.5±3.8 % des neurones dans les cultures mixtes, le taux d'infection avait atteint 94±4.3 % des neurones dans les En-Neurons, suggérant fortement que la présence des astrocytes dans la culture diminuait l'infection des neurones. Cependant, la déplétion des astrocytes ne semblait pas impacter la survie des neurones dans les cultures infectées par TBEV à ce temps d'infection. Par ailleurs, l'impact de l'infection des neurones sur la survie des astrocytes n'est également pas connu. Pour identifier cet impact, nous avons infecté des cultures En-Astrocytes (contenant ≅35% de neurones) et des cultures non séparées (contenant ≅75% de neurones) avec TBEV et nous avons quantifié et comparé le nombre et l'infection des astrocytes dans les cultures. Nos résultats ont montré que la déplétion des neurones ne s'accompagnait pas d'une augmentation de l'infection des astrocytes. Cependant, la survie des astrocytes était restaurée dans les En-Astrocytes à 7jpi, en comparaison des cultures non séparées, suggérant que l'effet de TBEV sur

les astrocytes dans les cultures neurales dérivées de hNPCs serait médié par les neurones.

Ainsi, nos résultats montrent pour la première fois une étude comparative de l'impact de TBEV sur les neurones, astrocytes et oligodendrocytes humains. Nous avons mis en évidence une réponse antivirale induite par TBEV différente entre les neurones et les astrocytes humains, suggérant que même si les neurones sont des acteurs de l'immunité dans le CNS, la réponse antivirale qu'ils développent resterait plus faible que dans les astrocytes et nous émettons l'hypothèse que cette réponse conditionnerait la neuropathologie induite par TBEV. Par ailleurs, nous avons identifié des interactions entre les neurones humains et les astrocytes humains montrant que des cultures complexes sont nécessaires pour étudier la neuropathologie viroinduite.

Table of contents

List of abbreviations

2-5A	2'-5'-linked oligoadenylates
ACSA-1	Astrocyte cell surface antigen-1
AHFV	Alkhurma hemorrhagic fever virus
BBB	Blood-brain barrier
BDV	Borna disease virus
C	Capsid protein
CARD	Caspase activation and recruitment domains
CARDIF	CARD adapter inducing interferon beta
CCL	C-C motif chemokine ligand
CD	Cluster of differentiation
CHO	Chinese hamster ovary cells
CL	Containment level
CN	Cortical neurons
CNS	Central nervous system
CSF	Cerebrospinal fluid
d13	13 days of differentiation
DC	Dendritic cell
DENV	Dengue virus
DR	Death receptor
dsRNA	Double-stranded RNA
E	Envelop protein
ER	Endoplasmic reticulum
EU	European Union
GAG	Glycoaminoglycans
GAS	IFN-γ-activated sequence
GLAST	Glutamate aspartate transporter
GGYV	Gadgets Gully virus
GCN	Granule cell neurons
HG	Hazard group

gRNA	Genomic viral RNA
hNPC	Human neural progenitor cells
HS	Heparan sulfate
IFIT	Interferon induced protein with tetratricopeptide repeats 1
IFN	Interferon
IFNAR	Interferon alpha and beta receptor subunit
IFNGR	Interferon gamma receptor 1
IKKε	Inhibitor of nuclear factor kappa-B kinase subunit epsilon
IPS-1	Interferon beta promoter stimulator protein 1
iPSc	Induced pluripotent stem cells
IRF	Interferon regulatory factor
IRSE	IFN-stimulated response element
ISG	Interferon-stimulated gene
ISGF	Interferon-stimulated gene factor
JAK	Janus kinase
JEV	Japanese encephalitis virus
Kb	Kilobases
kDa	kilodalton
KFDC	Kyasanur forest disease virus
KSIV	Karshi virus
LACV	La Cross virus
LBP	Laminin binding protein
LGTV	Langat virus
LIV	Looping ill virus
LMS	Laminal membrane structures
M	Membrane protein
MAVS	Mitochondrial antiviral-signaling protein
MDA5	Melanoma differentiation-associated protein 5
MMP	Matrix metalloproteinase
Myd88	Myeloid differentiation primary response 88
NC	Nucleocapsid

NCR	Non-coding regions
NF-κB	Nuclear factor-kappa B
nm	Nanometer
NS	Non structural
OAS	oligoadenylate sythetase
OASL	5' oligoadenylate synthetase like
OHFV	Omsk hemorrhagic fever virus
ORF	Open reading frame
PAMP	Pathogen associated molecular patterns
PBMC	Peripheral blood mononuclear cell
pDC	Plasmacytoid dendritic cells
POWV	Powassan virus
prM	Membrane protein precursor
PKR	Protein kinase R
PRR	Pattern recognition receptors
PSA-NCAM	Polysialylated-neuronal cell adhesion molecule
RABV	Rabies virus
RANTES	Regulated on activation, normal T cell expressed and secreted
RER	Rough endoplasmic reticulum
RIG-I	Retinoic acid-inducible gene I
RFV	Royal Farm virus
RSAD2	Radical s-adenosyl methionine domain containing 2
sfRNA	Subgenomic *Flavivirus* RNA
SMS	Laminal membrane structures
siRNA	Small interfering RNA
ssRNA	Simple stranded RNA
STAT	Signal transducer and activator of transcription
TBE	Tick-borne encephalitis
TBEV	Tick-borne encephalitis virus
TBEV-Fe	Far Eastern tick-borne encephalitis virus
TBEV-Sib	Siberian tick-borne encephalitis virus

TBEV-Eu	European tick-borne encephalitis virus
TBFV	Tick-borne *Flavivirus*
TBK1	TANK binding kinase 1
THOV	Thogoto virus
TLR	Toll-like receptors
TMEV	Theiler's encephalomyelitis virus
TRAIL	TNF-related apoptosis inducing ligand
TRIF	TIR-domain-containing adapter-inducing interferon-ß
TRIM	Tripartite motif protein
TYK	Tyrosine kinase 2
UTR	Untranslated transcribed region
VISA	Virus-induced signaling adapter
VSV	Vesicular stomatitis virus
WNV	West Nile virus
XRN1	5′ 3′ exoribonuclease 1
YFV	Yellow fever virus
ZIKV	Zika virus

List of figures

List of tables

List of supplementary tables

Chapter I: Introduction

1.1. Tick-borne encephalitis virus

Tick-borne encephalitis virus (TBEV) is a member of the genus *Flavivirus* within the *Flaviviridae* family [1]. The genus *Flavivirus* comprises more than 53 known members, including Dengue viruses (DENV), yellow fever virus (YFV), Japanese encephalitis virus (JEV), West Nile virus (WNV), and Zika virus (ZIKV) that are serologically related and share common genome and structural organization [2,3]. About two thirds of flaviviruses are known to infect and to be transmitted to vertebrate species by arthropod vectors, and approximately 60% of them are able to induce encephalitis in the infected hosts [4].

The name '*flavivirus*' is derived from the Latin word *flavus* meaning yellow, signifying the jaundice caused by YFV [5]. In 2017, a proposal to change the family name from *Flaviviridae* to *Kitrinoviridae* was issued, *kitrino* meaning yellow in Greek, to avoid the ambiguity between the *Flavivirus* genus among the *Flaviviridae* family in the use of the words *Flavivirus* or flaviviral [6]. So far, the International Committee on Taxonomy of Viruses did not rule on the proposal.

TBEV is a member of the mammalian tick-borne flavivirus group (previously called TBEV serocomplex) (Figure 1). Along with other genetically and antigenically related viruses, this group includes Omsk hemorrhagic fever virus (OHFV), Langat virus (LGTV), Alkhurma hemorrhagic fever virus (AHFV), Kyasanur Forest disease virus (KFDV), Powassan virus (POWV), Royal Farm virus (RFV), Karshi virus (KSIV), Gadgets Gully virus (GGYV) and louping ill virus (LIV) [7,8]. Among those viruses, TBEV, LIV and POWV can cause encephalitis in humans [9].

The first description of a tick-borne encephalitis-like disease dates back to Scandinavian church records from the 18th century [10]. Descriptions of tick-borne encephalitis (TBE) can be found in several publications as early as the 19th century [11] but tick-borne encephalitis was first described as a clinical entity in 1931, in Austria [12]. TBEV, the causative agent of the disease, was isolated by Soviet scientists in the late 1930s, after several fatal encephalitis cases among the soldiers posted in the Taiga [11,13].

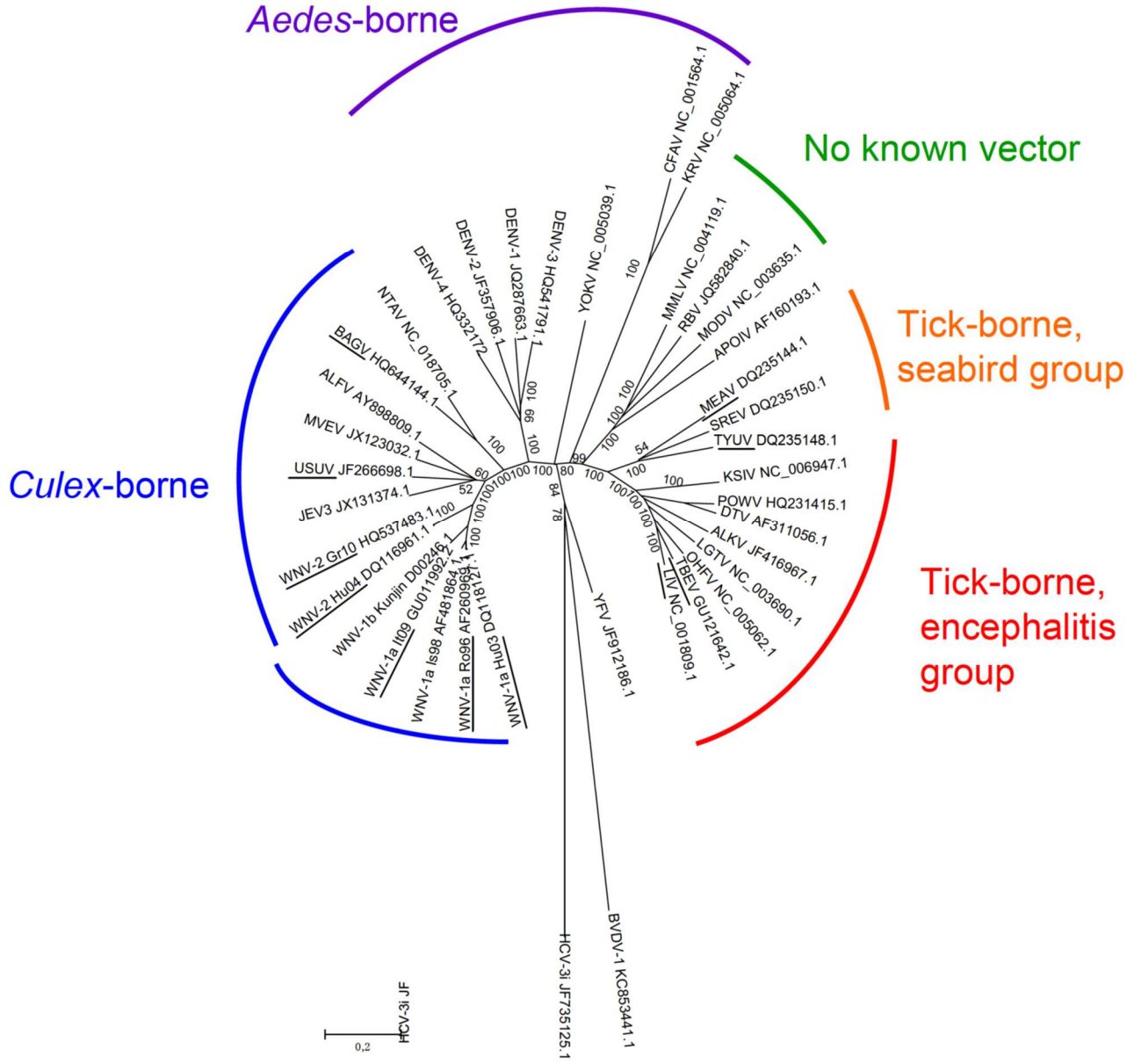

Figure 1 - Genetic relatedness of flaviviruses

The tree was build using genetic alignments of complete genomic sequences [14].

Three subtypes of TBEV are described [1]: [1/] the European subtype (TBEV-Eu) is prevalent in western, northern, central and eastern parts of Europe, [2/] the Far-Eastern subtype (TBEV-FE) is located mainly in eastern parts of the Russian Federation, in China and Japan, [3/] the Siberian subtype (TBEV-Sib) occurs in all parts of the Russian Federation, predominately in the Asian parts. All 3 subtypes co-circulate in the Baltics [15,16], the European part of the Russian Federation, and in Siberia [17]. All are pathogens of the risk group (RG) 3, and they have to be handled in a containment level (CL)-3 laboratory.

1.1.1 Genomic and structural organization

The genome of flaviviruses is a single positive stranded RNA of ≅10,8 kilobases (Kb) that serves three discrete roles within the life cycle, as [1/] the messenger RNA (mRNA) for translation of all viral proteins, [2/] a template during RNA replication, and [3/] genetic material packaged within new viral particles [18,19]. Furthermore, the genomic RNA is infectious by itself [20].

The genomic viral RNA (gRNA) is a single open reading frame (ORF) of ≅3,400 codons, flanked by a 5'- and a 3'-noncoding regions (NCR) of respectively ≅100 nucleotides and 350 to 750 nucleotides [21]. The ORF encodes a polyprotein that is processed by viral and host proteases into three structural and seven non-structural proteins (Figure 2). The 5'NCR carries two conserved stem-loop regions and a type I cap structure m7GpppAmpN2 [22–24]. The 3'NCR is made up of a stem-loop and two dumbbell sequences and, unlike cellular mRNAs, does not carry a poly-A tail [25]. However, for some variants and quasispecies of TBEV, an internal poly-A tract is included in the 3'-NCR variable region that enhances viral virulence [25–28]. Because they are located at the 5' and 3' ends of the flaviviral genome, the NCRs of flaviviruses play an important role in translation, RNA replication and packaging, as well as in immune modulation [29].

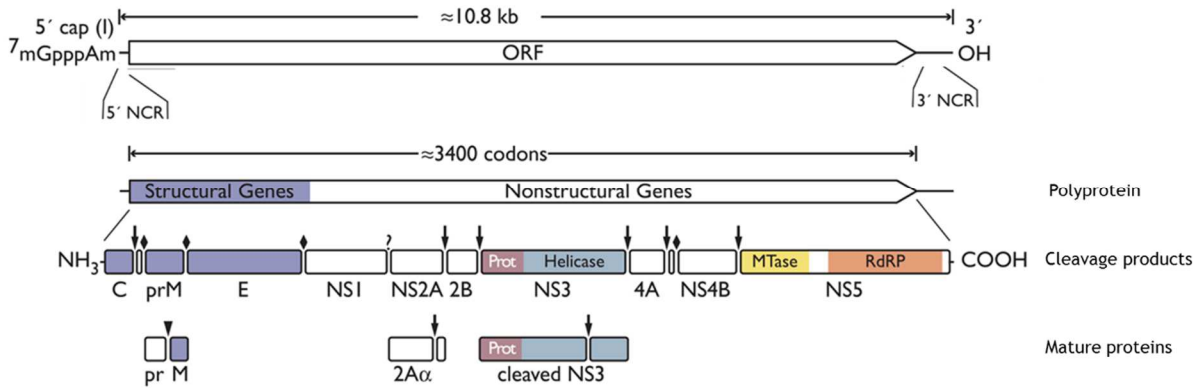

Figure 2 - *Flavivirus* genome and polyprotein structures.

A unique ORF is expressed and the produced polyprotein is processed by cleavage. The viral protein prM, NS2A and NS3 are then subject to maturation. Specific marks highlight cleavage sites for host signalase (♦), viral serine protease (🡻), furin or related protease (▼), and unknown proteases (?) [Adapted from 30].

The incomplete degradation of the gRNA by the host 5′-3′ exoribonuclease 1 (XRN1) produces long subgenomic flaviviral RNA (sfRNA) of 300 to 500 nucleotides, originating from the three dimensional structures of 3' NCR [31–33]. The produced sfRNAs interfere with RNAi complex mediators, inducing a decrease in siRNA response in tick cells [34] and/or in mammalian and mosquito cells [35,36]. Mosquito-borne flaviviruses sfRNAs also increase uncapped cellular mRNA stability by repressing XRN1 activity [37], interfere with type I interferon (IFN) signaling [38], and are essential for viral growth [39,40].

From a structural point of view, *Flavivirus* virions are small spherical particles of 35 nanometers (nm) to 55 nm, enclosing a 25 nm to 30 nm electron-dense core, that is presumed to contain one copy of the viral genome and hundreds of copies of Capsid (C) protein [41,42]. This nucleocapsid (NC) core is surrounded by a lipid envelope in which 180 copies of the Membrane (M, 8 kDa) and Envelope (E, 53 kDa) transmembrane proteins are anchored (Figure 3)[2,21,30,42]. The M protein produced during maturation of nascent virus particles within the secretory pathway is a small proteolytic fragment of the precursor prM protein [18]. The E glycoprotein, the major antigenic determinant on virus particles, is a class II viral fusion protein that forms an icosahedral network. It mediates binding and fusion during virus entry [43,44].

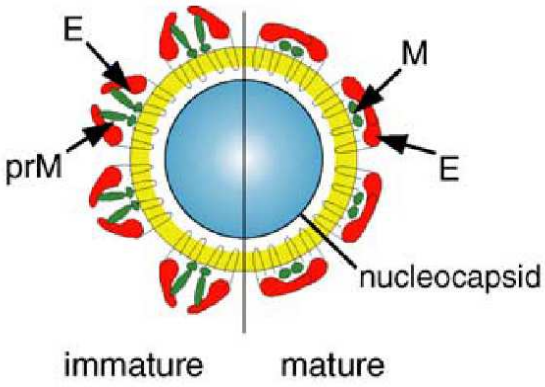

Figure 3 - Schematic diagram of the structural organization of TBEV particles.
The viral nucleocapsid (in blue), formed by the positive-stranded RNA genome and protein C, is surrounded by a lipid envelope (in yellow) in which prM/M (in green) and E (in red) proteins are carboxy-terminally anchored. prM and E form heterodimers in immature particles, whereas infectious, mature virus particles carry the small protein M and homodimers of protein E [9].

TBEV is very stable under natural conditions and the three subtypes are genetically and antigenically very similar. TBEV-Fe and TBEV-Sib are phylogenetically more closely related to each other than to TBEV–Eu, but the degree of variation in the amino acid level between strains within TBEV-Eu and TBEV-FE subtypes remains low [17,45]. The amino acid variability between the three subtypes is in the range of variation within flaviviruses (3±6% to 5±6%), while the nucleotide level variability is higher (1% to 16±9%). Sequences of the E protein differ by no more than 2±2%, suggesting a selection pressure favoring the conservation of the E protein [46]. As a result of this close antigenic relationship, there is a high degree of cross-protection between the subtype strains in mice [47,48]. Moreover, neutralizing antibodies against TBEV can also provide a protection against the infection by some other flaviviruses, such as Omsk Hemorrhagic Fever Virus (OHFV) [49].

1.1.2 Replication cycle

1.1.2.1. Binding and entry

The first step of *Flavivirus* entry involves the interaction of the E glycoprotein with cellular attachment factors that concentrate and recruit the virus, and primary receptors that bind the viral particles and induce endocytosis [50,51].

Negatively charged sulfated Glycoaminoglycans (GAG), which are abundantly expressed on numerous cell types, are utilized as attachment factors by several flaviviruses [52–56]. For TBEV, the GAG protein Heparan Sulfate (HS) mediates viral attachment but CHO epithelial cell lines lacking HS are still highly susceptible to TBEV, suggesting that other surface molecules, which might be laminin binding protein (LBP) [57] and human αVß3 integrin [58], are involved in viral attachment and entry [59,60].

After attachment, TBEV entry into the cell can occur through clathrin-mediated endocytosis [61] or through micropinocytosis, a clathrin-independent endocytosis [62]. This might be dependent on cell type and serotype [63]. So far, the entry receptors of TBEV are not deciphered. The virus utilizes either a ubiquitous receptor molecule or multiple receptors for cell entry, as TBEV infection has been observed in a variety of host cells and as it circulates in nature between arthropod vectors and their vertebrate hosts [59].

The internalized virus is then transported to the early/intermediate endosome that matures into a late endosome. The low pH in the endosome, at an optimum of pH=5.4±1, triggers conformational rearrangements of the class II fusion E protein [43,64], inducing the fusion of the viral particle with endosomal membrane and gRNA delivery into the cytoplasm (Figure 4) [65,66].

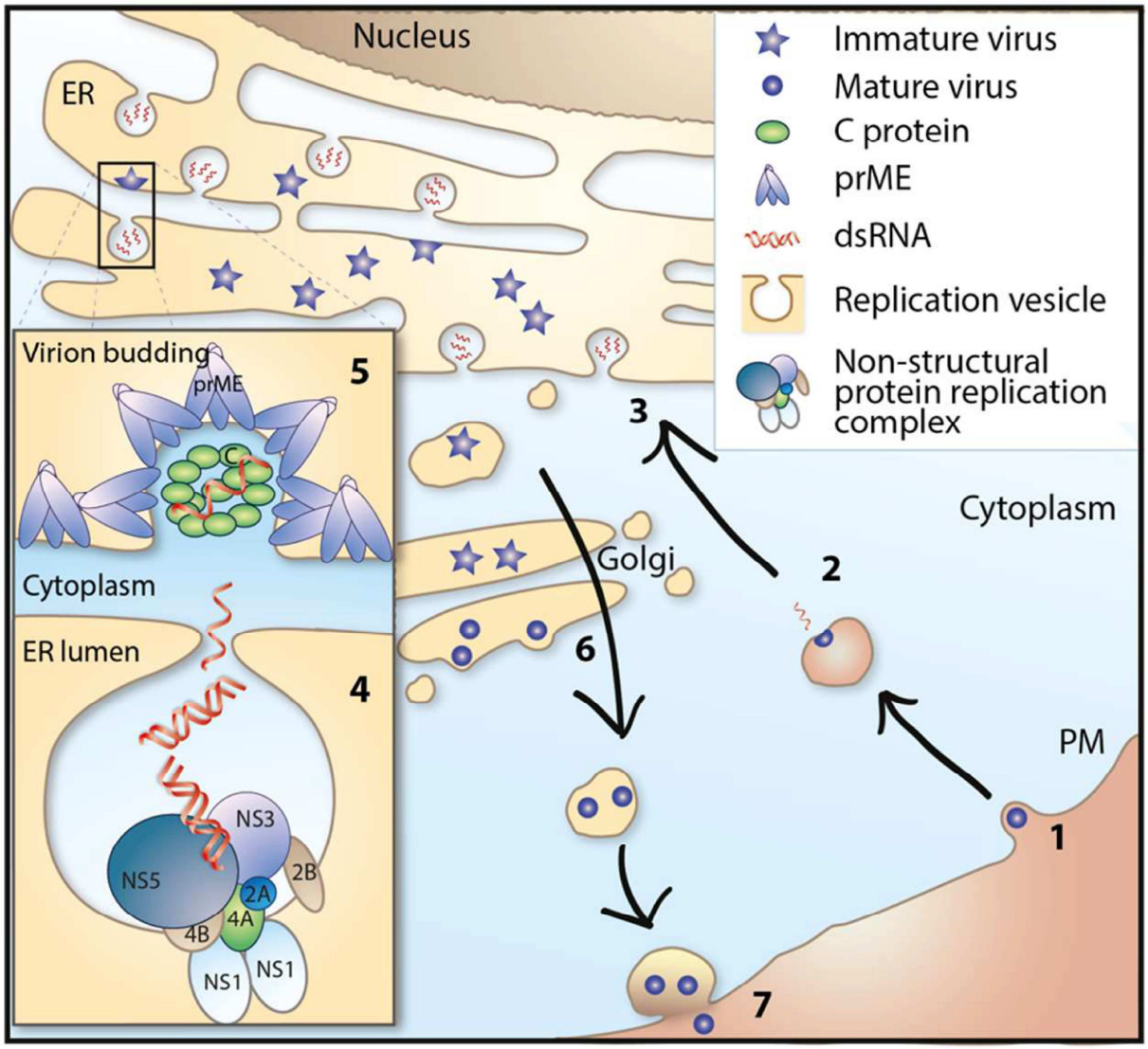

Figure 4 – Replication cycle of tick-borne encephalitis virus.

(1) Endocytosis. (2) Fusion with the membrane of the endosome and release of viral genome into the cytoplasm. (3) Translation of the polyprotein from viral genomic RNA and synthesis of negative strand RNA. (4) Genome replication in the ER. (5) Viral particle assembly and packaging of newly synthesized positive strands RNA. (6) Maturation of virions in the trans-Golgi Network and transport via the secretory pathway. (7) Release of mature virions from the cell. ER=endoplasmic reticulum. PM=plasma membrane [67]

1.1.2.2. Replication, assembly, maturation, and release.

Flaviviruses replicate in the cytoplasm of infected cells. The released gRNA acts as a template for mRNA synthesis [19]. The capped 5'-end of the viral genome, aided by 3'UTR elements, triggers the recruitment of eukaryotic initiation factors to form the ribosome complex [41]. The RNA is directly translated into a single polyprotein of 3411 amino acids and is then co- and post-translationally cleaved by NS2B/NS3 viral serine protease and host-encoded proteases such as signalase and furin [68,69]. The cleavage results into three structural proteins: C, prM, and E, and seven non-structural (NS) proteins: NS1 (glycoprotein), NS2A, NS2B (protease component), NS3 (protease, helicase and NTPase activity), NS4A, NS4B, NS5 (RNA-dependent polymerase) (Figure 2) [10,70,71].

The newly produced NS viral proteins remodel the rough endoplasmic reticulum (RER) membrane, forming membrane curvatures and invaginations where the replication complex forms, becoming viral replication hubs (Figure 4) [72–75]. NS3 and NS5 proteins will bind to the 5' cap structure of the gRNA and induce negative sense RNA synthesis that acts as a template for multiple rounds of capped positive-stranded viral RNA synthesis [41]. Intermediates of dsRNA are formed between positive and negative strands [76,77] and the replication occurs in a semi-conservative and asymmetric way, where positive-strands accumulate in a large excess over negative-strands [30,78]. The NS5 acts as a regulatory element of viral gRNA synthesis and replication (Reviewed by [79]) and TBEV NS5 mutant viral genome fails to replicate [80].

The assembly process is probably coupled with the replication and is initiated by association of C-dimers with newly synthesized viral gRNA, on the cytoplasmic side of the ER membrane, to form a nucleocapsid precursor [81]. The NC buds into the ER, thus acquiring an envelope. The assembly of NC and E-prM heterodimers forms immature non-infectious viral particles [71,82].

The immature viral particles accumulate in the ER lumen and are transported via the host secretory pathway to the Golgi. Maturation of TBEV occurs in the acidic environment of the late trans-Golgi network, when prM is cleaved by a cellular furin protease [69,83], associated with E protein conformational rearrangements [30,43]. The mature particles are released in the extracellular matrix by fusion of the transport vesicles with the plasma membrane (Figure 4) [9]. While flaviviral RNA

synthesis is detected after three to six hours of infection, the release of infectious viral particles begins after 12 hours [21].

1.2. Transmission and epidemiology of tick-borne encephalitis virus

As an arbovirus, TBEV is maintained in nature by hard ticks, which act as vectors of the virus [84,85]. In addition to tick bites, it can be transmitted to humans by consumption of unpasteurized dairy products from infected livestock [86]. Several confirmed or suspected cases of TBEV transmission by exposure to raw milk or dairy products were reported. While viremia in TBEV-infected livestock remains low [86-88], LGTV, a closely related virus, is stable for several days in milk at room temperature, and cheese making processes are likely to reduce viral loads [90], which suggests a similar stability for TBEV. Other transmission routes were also reported in rare or single occurrences, such as laboratory infection [91] and person-to-person transmission after an organ transplantation [92] or blood transfusion [93]. Transmission to infants through breastfeeding was suggested to be possible for several flaviviruses such as DENV [96], WNV [97], or YFV [98], but unlikely for ZIKV [94,95]. Even though reviews evoke this transmission route for TBEV [84,99], no evidence of TBEV presence in maternal milk or breastfeeding transmission was reported. Transmission through sexual intercourse was also reported for ZIKV and suggested for WNV and YFV, as they have been detected in semen [100], but there is no data supporting sexual transmission of TBEV in humans [101].

1.2.1. Risk areas and endemic zone

Tick-borne encephalitis Virus endemic zone spreads From Central, Northern and Eastern Europe to the Russian Far East, including Mongolia, northern China, and Japan (Figure 5) [84,102,103].

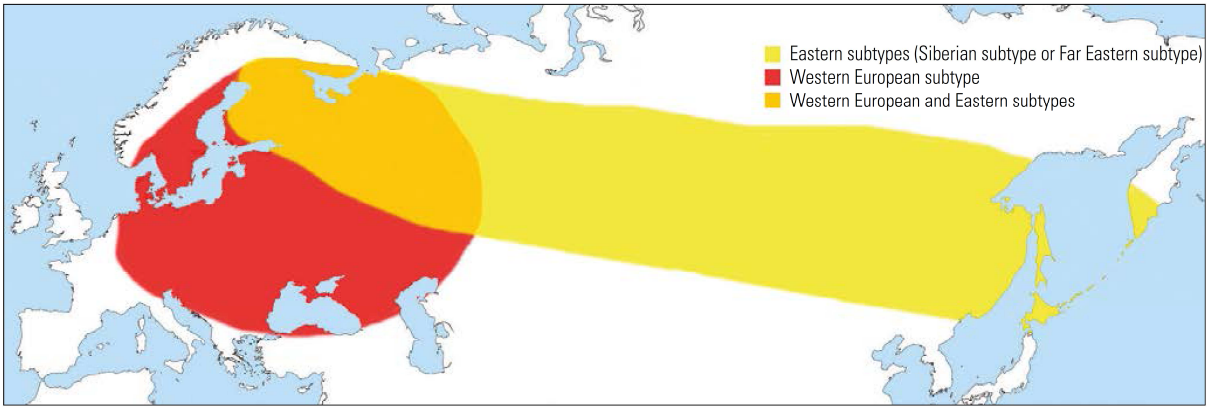

Figure 5 - Geographical distribution of Eastern and European subtypes of tick-borne encephalitis virus.
Endemic zone of TBEV-Eu (red), TBEV-FE (yellow) and overlapping areas (orange) are represented [104].

Since the 1990s, TBEV is expanding to previously unaffected areas such as Czech Republic, Germany, Norway, Slovenia, Sweden, Switzerland [105–107] and more recently, the Netherlands [108]. Endemic zones are also expanding in altitude, up to 1500 meters above sea level, as reported in Austria and Slovakia [109,110], However, it is possible that the attention drawn to the disease may have led to a higher number of registered cases [111]. A review from Charrel *et al*. [112] mapped at least 25 European and 7 Asian countries where TBEV is present. In France, fewer than 10 cases are reported yearly, mainly in the Alsace region, with a significant increase in 2016 [113]. As a consequence of the higher risk of TBE in Western Europe, it is listed as a disease under surveillance in the European Union (EU), and it joined the list of notifiable diseases in September 2012 [114–116]. Prior to the EU decision, the type of TBE cases routinely reported, the source and type of case-based data surveillance, the case definition, and the laboratory test used for diagnosis were country-dependent [107]. This might lead to a high number of underdiagnosed or unreported TBE cases, and in highly endemic countries, the number of reported cases does not adequately reflect the real risk of infection [111]. However, thanks to efficient vaccination campaigns, the disease incidence in some endemic countries, such as Austria, decreased importantly [117].

Between 1976 and 1989, TBEV was widely undiagnosed and fewer than 40,000 cases were reported in Europe, with an average of about 2,700 per year. TBEV reported incidence has increased since the 1990s, and between 1990 and 2007, nearly 160,000 TBE cases were documented worldwide, with an average of about

8,700 cases per year. This corresponds to an increase of TBE morbidity by more than 300% [111]. The most recent data about the morbidity worldwide [84] and in 20 EU member states [107] are from 2010. By crossing data from different reviews and databases [84,111,118–120], we were able to estimate the number of cases worldwide from 1985 to 2010 (Figure 6). Yearly, 10,000 to 12,000 clinical cases of TBE is often given as a reference, but although this estimate is above those recent data (about 6000 cases in 2010), this figure is believed to significantly underestimate the actual total, due to the high rate of asymptomatic cases [103].

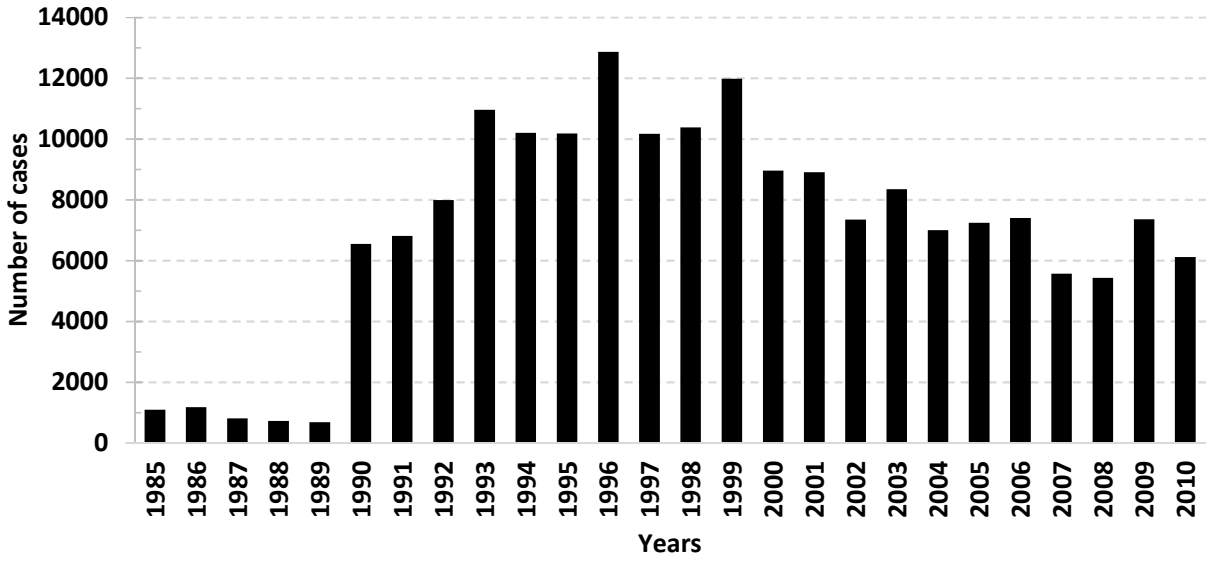

Figure 6 – Number of recorded TBEV human infections worldwide between 1985 and 2010.

Data gathered from [84,111,118–120]. Bulk data are in shown in Supplementary table 1.

Interestingly, the increase of the TBEV risk in Europe might be partly due to climate change, affecting vector biology, pathogen transmission [121] and density of hosts on which ticks feed [122]. Other factors might as well be involved, such as political or sociological changes and human behavior which influenced the tick bite exposure of humans and vaccination acceptance [121,123–127]. Those factors may have created favorable living conditions for ticks and thus led to a further spread of tick-borne diseases.

Symptomatic infection occurs in all age groups and genders but the case distribution may vary by region [103]. However, it is often more severe in adults and

elderly people and the seroconversion rate following vaccination decreases after the age of 50 [128,129].

1.2.2. Amplifying and spreading hosts

Ticks feed on a large span of hosts. In general, immature stages of ticks (larvae and nymphs) feed on small mammals and birds, while adults feed on large animals such as ungulates and livestock [130]. TBEV transmission to a vertebrate host occurs mainly after a tick bite, during a blood meal [131], and is indirectly facilitated by tick saliva through its contained analgesic, anti-inflammatory and anti-coagulant substances that allow the blood meal to be unnoticed [132].

Small rodents and insectivores, mainly yellow-necked field mice (*Apodemus flavicollis*) and bank voles (*Myodes glareolus*), act as a the main reservoir of TBEV, transmitting the virus to feeding ticks and amplifying tick populations [133,134]. In bank voles, TBEV RNA was found in the brain, where it can cause marginal clinical symptoms and mild meningoencephalitis [135,136]. Moreover, infected laboratory male mice can transmit TBEV to females through the sexual route, inducing increased embryonal mortality [137]. The virus is also transmitted vertically in *Myodes* red voles, through placenta to embryo [133]. This suggests a possible mechanism for tick-free long-term maintenance of TBEV in rodent hosts [138].

Birds can be infected by TBEV but they are more likely to play a role in dispersal of TBEV-infected ticks. TBEV was found in birds or bird-infesting ticks in the Baltic region of Russia [139], Siberia [140,141], Slovakia [142], Sweden [143], and Latvia [144]. Their role in virus circulation and dissemination is not clear and no outbreak was associated with this dispersal route but the involvement of birds in transport of TBEV-infected ticks from Russia to Japan was hypothesized [145].

In dogs, TBEV infection induces clinical signs similar to those observed in human cases, including fever, apathy and neurological signs such as paresis, seizures or hyperalgesia. The infection can be acute or chronic, and the outcome is often fatal [146]. The neuropathology of TBE in dogs was found consistent with observations in humans and laboratory mice [147]. Seropositive dogs were also found in Spain [148], a country that is not endemic for TBEV and where no human case was recorded [107], suggesting they can be sentinels for TBEV risk [149,150].

Ungulates can be infected by TBEV and clinical signs were sparsely reported in infected horses, including poor general condition, anorexia, ataxia, cramps, seizures, and paralyses [151,152]. Roe deer develop a short and low-grade viremia but are non-receptive hosts for TBEV [150]. TBEV-neutralizing antibodies and TBEV RNA were found in Dutch roe deer [153]. They can hence be used as sentinel [154]. It is unclear whether they contribute positively to TBEV dissemination and amplification, through co-feeding and transport of infected ticks [155], or negatively, by diverting questing ticks from hosts able to act as reservoir, such as rodents [122,156]. Furthermore, wild ungulates could also be infected, as TBEV-neutralizing antibodies were found in Flemish wild boars [157].

In sheep, goats, and cows, TBEV infection rarely causes clinical signs, and blood viremia is not detectable (or for very short time periods) [158,159]. Infectious virus is found in milk [86], and neutralizing antibodies are produced, suggesting that they can be used as sentinels in non-endemic or low prevalence areas [159,160].

Non-human primates are susceptible to infection and symptoms similar to those observed in mild humans cases as well as chronic infection were described [161,162]. The main reference for experimental infections on non-human primates was published in Russian in the 1980s [163–165]. However, there is no description of natural TBEV infection of non-human primates.

1.2.3. Biology of the vector

Ticks activity (including development, feeding, and movement) starts when the temperature is above 5°C and the humidity level is high (92% is optimal) [10]. The occurrence of these conditions is dependent on latitude and altitude, and is seen between spring and autumn in temperate climates [121]. New features in tick biology are observed, such as an increase in ticks activity [166], an acceleration in their life cycle [167,168] and a higher and northern distribution [124], increasing the risk of tick-bites for humans.

Ixodes ricinus (TBEV-Eu) and *Ixodes persulcatus* (TBEV-Sib and TBEV-FE) are the main vectors for TBEV. Their geographical distributions is represented in Figure 7, and partially overlaps with TBEV endemic zone. However, up to 18 species of ticks can be infected with TBEV [10,112]. Among those, *Boophilus microplus*, *Dermacentor reticulatus*, *D. silvarum*, *D. marginatus*, *Haemaphysalis concinna H. flava*, *H.*

longicornis or *Ixodes ovatus* have been found carrying TBEV or were associated with local outbreaks [84,169–173].

With respect to their role as vectors of TBEV, the critical ecological features of *I.ricinus* and *I.persulcatus* ticks that allow TBEV foci maintenance, and distinguish them from other sympatric (present in the same geographic areas) tick species are 1/ their long life cycle lasting two to six years [130,168], involving long survival of infected individuals 2/ the aggregated distribution of larvae and nymphs on hosts caused by the overlapping seasonal periods of feeding activity [174], and 3/ the range of small mammal species, such as birds and rodents, on which the immature stages feed and can get infected [85,175].

Figure 7 - Geographic distribution of TBEV-transmitting ticks

Ixodes ricinus and *Ixodes persulcatus* are present in the areas colored in red and yellow, respectively. Both species are present in the area colored in orange [Adapted from 176]

TBEV is maintained in tick population through three main ways [177] (Figure 8): transmission by feeding on an infected viremic animal [130,178]; transmission by co-feeding, meaning between ticks feeding in close proximity on the same host without systemic viremia [179–181]; or transstadial survival, through the life span of ticks [182,183]. Moreover, while they can carry TBEV throughout their life and through all stages, nymphs seem to be the most important stage for virus transmission [178].

Other transmission routes were also documented. Transovarial transmission to eggs occurs at a low ratio <1% [184] and sexual transmission from infected tick males

to females through saliva and/or seminal fluid was also evoked in reviews [84,135,185], but there is no data supporting this route.

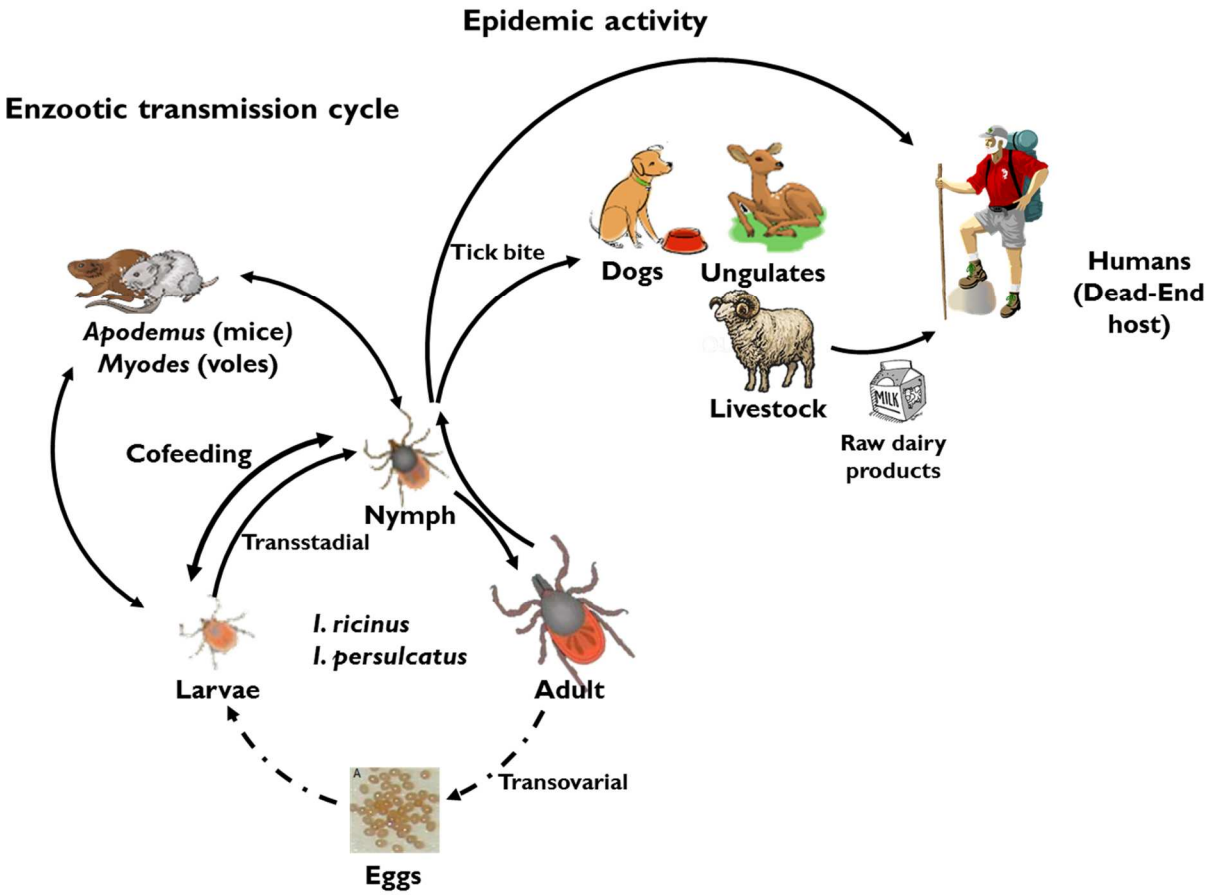

Figure 8 - Schematic transmission cycle of TBEV.

Tick larvaes, nymphs, and more rarely adults, feed on small rodents that represent the natural reservoir of TBEV. A mechanism known as cofeeding allows the transmission of the virus among the tick population, hence contributing to the maintenance of TBEV-infected ticks in the environment. The transmission to a various range of vertebrate hosts occurs by tick bites during a blood meal. Humans can be infected by TBEV after a bite of adult or nymph ticks, or by consumption of raw dairy products. Full arrows represent high rate transmission, dashed arrows represent low rate transmission. Adapted from [10,183,186,187]

1.3. Tick-borne encephalitis

1.3.1. Clinical presentation in humans

As with many arboviruses, the majority of TBEV infections are asymptomatic. Their proportion is difficult to establish because those with mild symptoms may be undiagnosed [188] but reviews suggest 70% to 95% of asymptomatic or sub-clinical cases [178,189]. The disease occurs in a biphasic course in about two thirds of neurologic cases [190]. The biphasic form is more often encountered with TBEV-Eu subtype infections (72-75%) [191,192] than with TBEV-Sib subtypes (21%) and TBEV-FE (3-8%) [193]. The monophasic form (one third of cases) is more severe and is more likely to involve central nervous system (CNS) alteration [191]. The incubation period after a tick bite varies from 2 to 28 days and usually lasts 7 to 14 days [102]. The following viremic phase lasts 2 to 8 days and is characterized by flu-like symptoms such as fever, headache, fatigue, nausea and aching back and limbs. Leukopenia and thrombocytopenia are common features, and abnormal liver functions are observed but rare [191,194,195]. In the biphasic course, those symptoms fade and patients experience a period without clinical signs assimilated to remission. The virus spreads eventually into the CNS and causes anorexia, fever, headache, vomiting, photophobia and possibly sensory changes, visual disturbance, paresis and paralysis. Those symptoms can culminate to coma and death quickly after manifestation of neurological symptoms [178]. The biphasic course of TBE is represented in Figure 9.

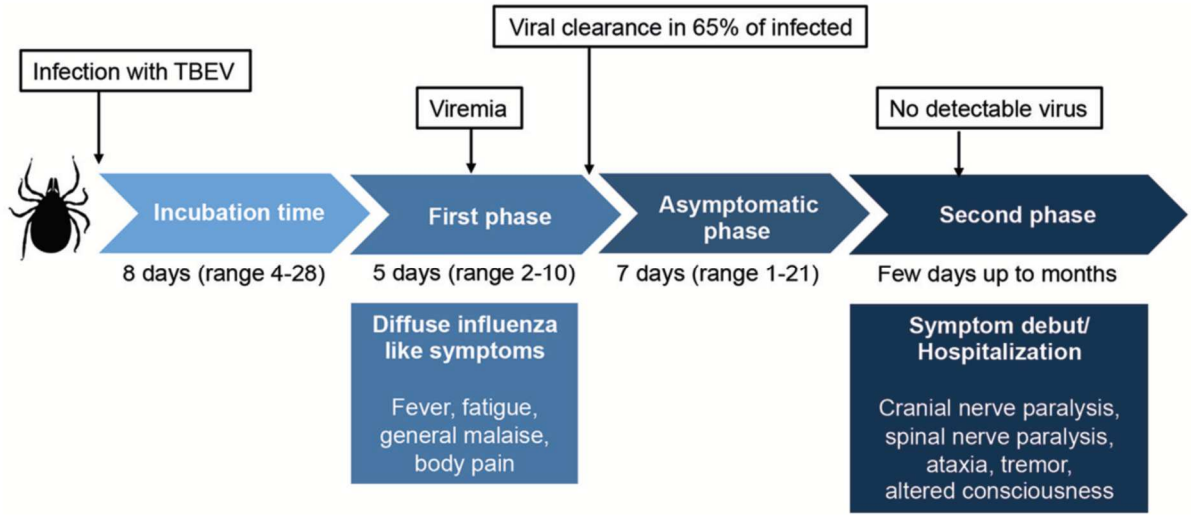

Figure 9 – Overview of the biphasic course of human TBEV infection.

Viral particles and nucleic acids are detected in the blood during the viremic phase that occurs usually one week after transmission. An asymptomatic period occurs in one third of the patients before experiencing the second phase of the disease. In this non-viremic phase, neurological symptoms, such as meningitis and encephalitis, occur. [196,197].

Meningitis is the most characteristic, clinical form of TBE, although not disease-specific, and is usually manifested by high hyperthermia, headache, nausea, vomiting, and vertigo. Encephalitis is mainly characterized by a disturbance of consciousness ranging from somnolence to stupor and, in rare cases, coma. Meningo-encephalomyelitis is the most severe form of the disease, characterized by flaccid paresis that usually develops during the febrile phase of the illness. Severe pain in the arms, back, and legs occasionally precedes the onset of paresis [189]. The severity of the disease varies depending on the subtype, TBEV-Sib and TBEV-FE inducing the most severe forms [198]. The outcome of the disease in humans (represented in Figure 10) is also influenced by factors such as the infecting dose, genetic susceptibility of the hosts, their immune status, and their age [84,199]. The fatality rate in adult patients is less than 2% for TBEV-Eu, 6-8% for the TBEV-Sib, and can reach 35% for TBEV-FE [102,198]. However, the high mortality figure observed with TBEV-FE subtype might be due to a lack of detection of mild cases, increasing the overall mortality rate [200]. A long-term morbidity is observed in 10 to 20% of the patients as a post-encephalitic TBE syndrome is defined, associated with temporary or permanent chronic neurological or neuropsychiatric symptoms, mainly cognitive and focal neurological signs, memory and concentration disturbance,

paresis, imbalance and headaches [201]. This chronic form is mainly induced by TBEV-Sib strains [193,202].

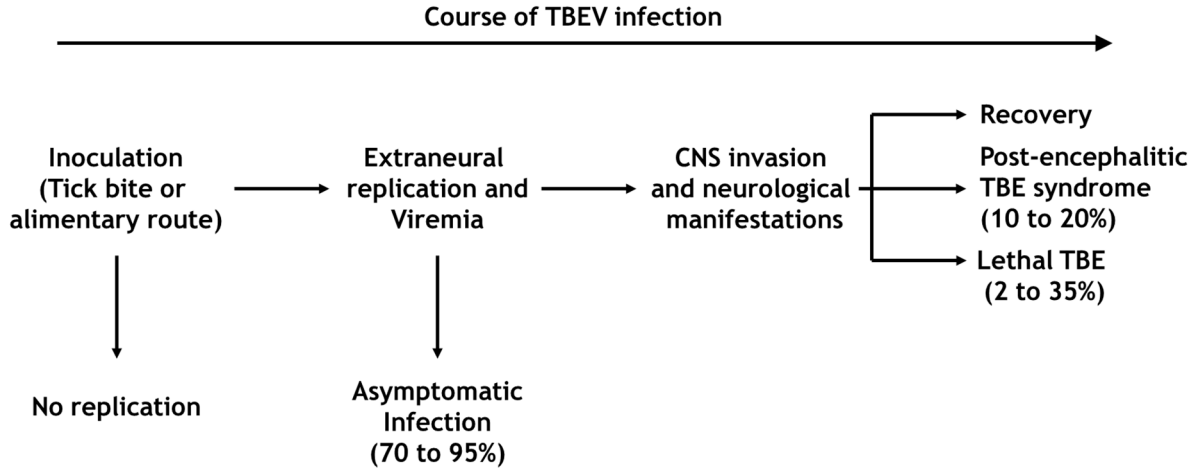

Figure 10 - Spectrum of possible outcomes of TBEV infection
[Adapted from 203]

1.3.2. Vaccination against TBEV in humans

Active immunization is the only option for prophylaxis against TBEV, as no antiviral treatment is presently available. Four widely used vaccines containing formalin or formaldehyde-inactivated TBEV derived from chicken embryonic fibroblast cells and using aluminum hydroxide as adjuvant are available, and they all require 3 doses for a complete course of immunization [204]. Two vaccines, based on the Neudoerfl and K23 European strains respectively, are currently in use in Western Europe: FSME-Immun® (Baxter, Austria) and Encepur® (Novartis Vaccines, Germany). Two other vaccines, based on the 205 or Sofjin Far-Eastern strains respectively, are in use in the Russian Federation: EnceVir® (Scientific Production Association Microgen, Russia) and TBE vaccine Moscow® (Federal State Entreprise of Chumakov Institute of Poliomyelitis and Viral Encephalitides, Russia Academy of Medical Sciences, Russia) [103,205]. A formalin-inactivated TBEV vaccine is also in use in China [206], but there is a lack of information about its composition, safety, efficacy and effectiveness [103]. The vaccines induce a protective response against the homologous subtypes, but they are also interchangeable and they are able to induce a cross-protective response against the other subtypes [47,48,204,207,208]. Clinical effectiveness of TBE vaccination in the field was demonstrated in Austria [209].

Langat virus (LGTV), a member of the mammalian tick-borne flavivirus group, is closely related to TBEV. It shares more than 80% amino acid identity with TBEV but is less virulent, and was previously used as a live-attenuated anti-TBEV vaccine. However, while LGTV-vaccination decreased the overall incidence, it resulted in meningoencephalitis in 1/10000 recipients, which led to its discontinuation [178]. It remains broadly used as an attenuated alternative for TBEV in research, as it is a HG-2 virus handled in a CL-2 laboratory.

1.3.3. Viral pathogenesis

Neurotropic viral infections initiate in the periphery (skin, mucosa, gut, or lung). Following TBEV inoculation by tick-bite, the first cells replicating the virus in the skin are probably epidermal dendritic cells (DCs), namely Langerhans cells [210]. They migrate to draining lymphatic nodes via the lymphatic system and the virus replicates in the lymphatic organs (spleen, liver and bone marrow), leading to dissemination in the periphery and viremia (Figure 11) [181,211]. When the infection occurs through the alimentary route, after consumption of raw milk or dairy products, the virus enters to the intestinal lumen and replicates in epithelial cells. It is then able to cross the intestinal epithelium by transcellular (through the cell) or paracellular (between cell junctions) routes, as shown *in vitro* on Caco-2 cell lines, and to join the blood circulation, leading to a systemic infection [62]. After hematogenic spread, the virus replicates in T- and B-cells, as well as in macrophages, and different organs are invaded, including sympathetic and parasympathetic ganglia, olfactory mucosa, and the brain parenchyma [193,201,212,213]. Viral neuropathogenicity involves three major properties: $^{1/}$ viremic capacity (capacity of the virus to highly replicate in peripheral tissues), $^{2/}$ neuroinvasiveness (capacity of the virus to cross the blood-brain barrier and enter the CNS), and $^{3/}$ neurovirulence (ability to replicate, spread, and cause neuropathology within the CNS) [9,203,214].

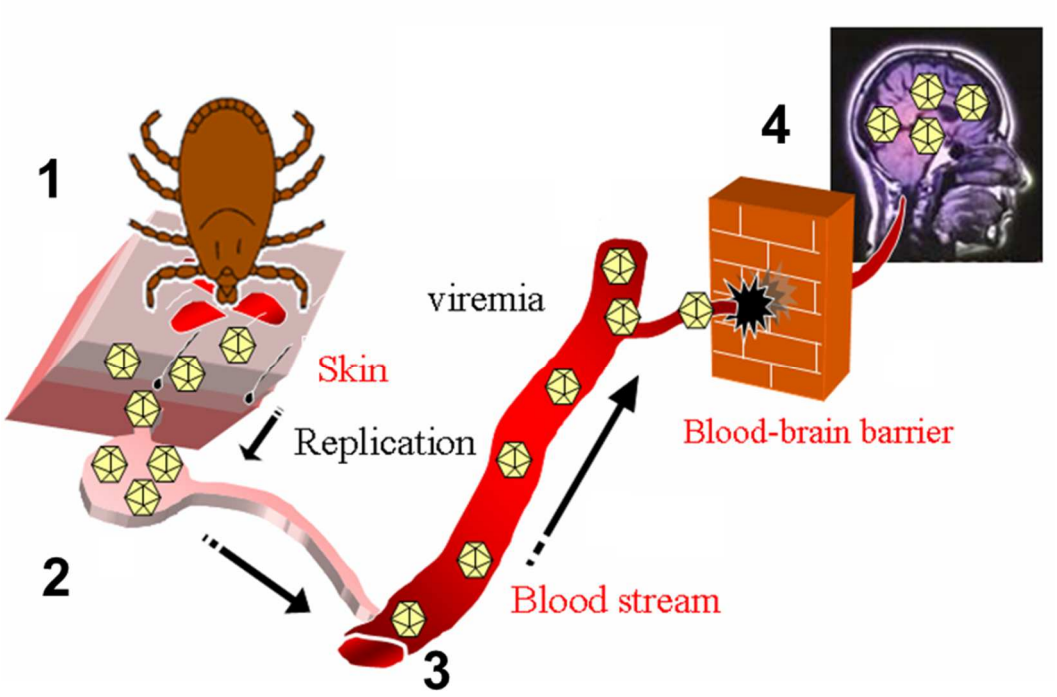

Figure 11 - TBEV invasion of the CNS following tick bite.

After a tick bite (1), TBEV replicates in epidermal dendritic cells that migrate to draining lymph nodes where it replicates massively (2), before reaching the circulatory system, leading to viremia (3). The virus could then cross the blood brain barrier (BBB) and enter the brain (4) (Adapted from [212]).

1.3.3.1. Models to study viral pathogenesis

- ***In vivo* animal models**

Animal models are an interesting approach to study neurotropic viral infections. They offer complexity, including developed brain structures and different immune entities, but they are unable to recapitulate the human brain physiology accurately [215,216]. They also have specific innate immune response features that differ from humans [217]. Moreover, it is difficult to study key cellular and molecular mechanisms underlying brain diseases pathology in whole-animal models [218].

The study of TBEV-induced neuropathology was mainly performed on laboratory mice. This is led by the availability of tools on mice, but also because they develop neurological signs similar to those observed in humans, such as meningoencephalitis [193,199,219–221]. Other animal models were also used in the past, such as chick embryos, suckling white rats, Syrian golden hamsters, sheep and monkeys (Reviewed

by [193]). However, all those models remain phylogenetically far from humans and the obtained results are difficult to translate to human neuropathogenesis [193].

- **Two-dimensional cell cultures**

The dominant models for studying neuroviral infections are the two-dimensional (2D) cell cultures in monolayer structures. They rely on cell adherence to the flat surface of the culture dish. The 2D cultures allow a simplified approach to study the brain diseases, at low cost, and with high reproducibility due to equal access of cells to nutrients and growth factors, resulting in homogenous growth and proliferation [222].

Immortalized cell lines are an easy model to study brain infection with viruses such as TBEV [223] and HSV1 [224]. However, genetic and signaling abnormalities found in these cultures require validation on a more stable model [225]. The 2D cell culture models were further enhanced by using primary cells, that can easily be obtained from mice [226], but in humans, experiments on those cells are limited by the difficulties to access cell sources such as embryos and cadavers [227]. Other limitations of those human cells cultures include that they might fail to mimic the complexity of the human brain if the cellular composition of brain cells, such as neurons or different glial cells, is not well characterized [225,228,229]. Supporting the importance of complex cultures, neurons were shown to act differently when co-cultured with astrocytes in comparison to neuronal monocultures [230]. To address these issues, human neural cells can be derived from human embryos or human iPSC of healthy patients or with pathological manifestations [231], and multicellular differentiated complex brain cell cultures have been used, for instance the study of the physiopathology induced by La Cross virus (LACV) [225] or impairment of neurogenesis by Borna disease virus (BDV) [232,233].

- **Three-dimensional models**

While the 2D cultures are useful to study viral interactions with neural cells, they do not represent the 3D architecture and different regions of the brain. To overcome this issue, new culture systems that allow reconstruction of architectural and three-dimensional features of the human brain were developed. They aim to

mimic the human brain tissue in a reproducible manner and provide high-throughput studies for drug and neurotoxic components screening.

Brain organotypic slices

Brain organotypic slices create a platform that simulates the *in vivo* architecture of the brain in an *in vitro* environment. They can be obtained from murine neonates or adults [234], but when obtained from older animals, the slices are thin and fragile [218] hence not representing an easy model for studies on a fully developed brain. More importantly, they can also be obtained from adult human donors, which offers a relevant environment of live human CNS tissue [235,236].

They allow to study both the infection and dissemination of neurotropic viruses within the CNS, but also the evaluation of antiviral molecules [237,238]. Compared to animal models, they are easier to prepare and have a lower maintenance cost [218]. So far, most infectious studies carried on viruses such an HSV-1 and ZIKV used organotypic slices obtained from rodents at prenatal or early postnatal stages [237–241], which makes the data harder to extrapolate to the human adult brain.

Neurospheroids and cerebral organoids

In the last decade, systems using human pluripotent-stem cells-derived three-dimensional (3D) cultures that model organogenesis and form brain region-specific structures were developed. Those three-dimensional models are composed of proliferative progenitor neural cells that produce specific brain-like structural organization, mimicking brain physiology and allowing a relevant modeling of neurodevelopmental disorders [242]. Those 3D models comprise two types: neurospheroids and cerebral organoids.

Neurospheroids (or neurospheres) originate from single cell suspension of neural progenitor cells, and are less complex than organoids. They are mainly used to study the proliferation, self-renewal capacity, and multipotency of neural stem cells and progenitor cells during development [218]. They are good models for the developing forebrain and cerebellum, but they fail to develop into other regions such as ventral midbrain. Neurospheroids were highly useful to model ZIKV-infection of the prenatal brain. Garcez and colleagues [243,244] used human iPSC-derived neurospheroids that mimic a three-month old brain development, and infected them with ZIKV for

24 hours to study the mechanisms by which the virus causes microcephaly. They showed that ZIKV reduces the size of human neurospheroids, by altering translation, cell cycle, and neural differentiation.

On the other hand, cerebral organoids are able to recapitulate the three-dimensional architecture of the brain tissue in a higher resolution than neurospheroids [218]. They can differentiate, self-organize and form distinct multiple neural populations forming brain-like structures, which makes them an ideal model for development, disease pathogenesis, and drug screening studies [245]. They are formed by culturing floating cells in spinning bioreactors that favor human pluripotent stem cells to compartmentalize in different brain regions leading to a specific brain structure [242]. They can also be generated by fusion of neurospheroids resembling different regions of the human brain, allowing the formation of forebrain-like organoids [246].

Cerebral organoids were used to mimic ZIKV-induced brain malformations and explore the interferon response [247]. Furthermore, a ZIKV inhibitor, azithromycin, was shown to reduce ZIKV infection in glioma cells but not in organoids [238,248], which suggests a limited effect on the fetal brain and shows the relevance of three-dimensional models.

While it is clear that cerebral organoids represent the future of *in vitro* brain models, the technology still faces several limitations [218]. First, the cerebral organoids developed are mostly based on spontaneous cell self-aggregation (Figure **12**), which makes each organoid typical and does not allow reproducibility [249]. Second, the organoids require several months of culturing, frequent change of a large medium volume and specific spinning bioreactors, which increases the costs. Additionally, while three-dimensional structures are formed, brain organoids do not always recapitulate embryonic human cerebral cortex cell composition, such as the absence of outer radial glia cells, nor allow proper development of certain structures, such as the subventricular zone (SVZ). They also fail to recapitulate many late brain development events, such as myelination and gliagenesis [218].

However, recent developments have improved reproducibility and miniaturized the bioreactors, allowing cost-effective and reproductive study of brain development-impairing viruses, such as ZIKV that causes microcephalies [249]. Furthermore, those organoids can produce mature glutamatergic and GABAergic

neurons, which allows studying neurogenesis, but they fail to generate other cell types such as astrocytes and oligodendrocytes [242,249].

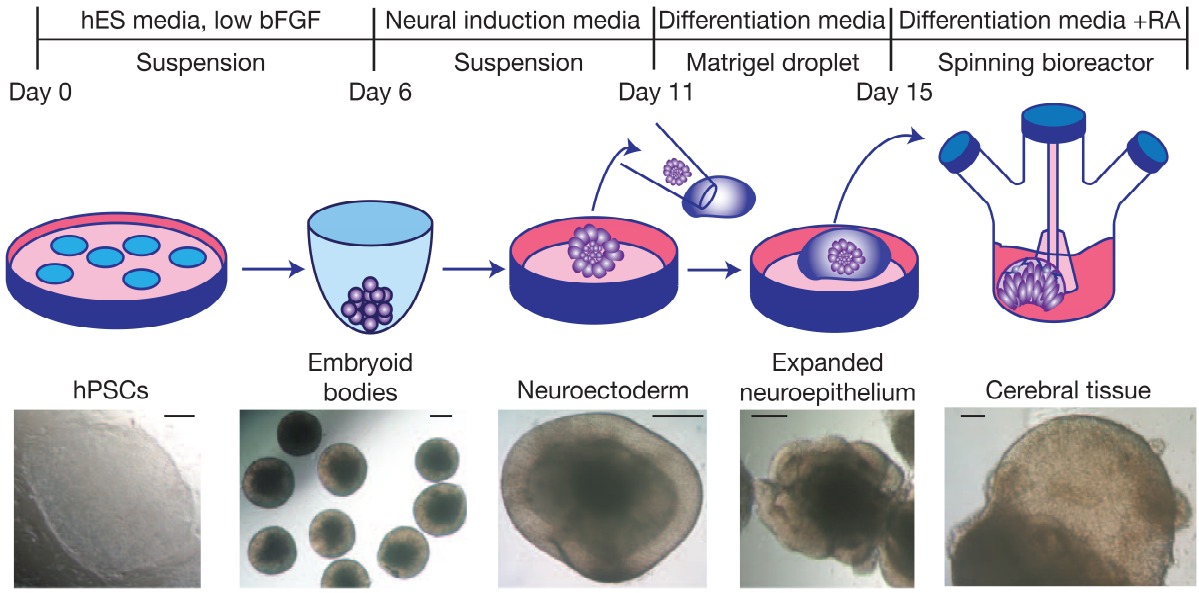

Figure 12 – Cerebral organoid cell culture system and representative images of each stage

bFGF, basic fibroblast growth factor; hES, human embryonic stem cell; hPSCs, human pluripotent stem cells; RA, retinoic acid [242].

1.3.3.2. TBEV in the brain

The CNS is separated from the blood circulation by a physical barrier called the blood-brain barrier (BBB). It represents a physical and metabolic barrier, aiming to selective transport and trafficking of molecules and cells from the blood circulation into the brain parenchyma [250]. It is composed of specialized endothelial cells that form tight cell-cell junctions, and interact with astrocytes and microglia to maintain its integrity [251]. While TBEV induces an increase in BBB permeability, its disruption is not a prerequisite to TBEV entry into the brain as it precedes CNS invasion [252], which was also observed with other flaviviruses such as JEV [253]. The mechanisms by which TBEV enters the CNS are not fully characterized, but they are likely to include:

1/ Direct infection of endothelial cells and transcellular migration by transcytosis through the endothelial cells layer without prior alteration of its integrity (Figure 13), as suggested in an *in vitro* model of the BBB [254],

2/ Transcellular or paracellular transport of infected peripheral blood mononuclear cells (PBMCs) by infiltration into the brain, via “Trojan horse” mechanism [255],

3/ Axonal transport of viral RNA in a retrograde way (towards the cell body) following a peripheral infection, shown in a rodent model *in vivo* [256] or in human neurons *in vitro* [221],

4/ High replication in the olfactory epithelium that might lead to CNS invasion through olfactory neurons [257], supported by accidental human laboratory infection with aerosols as a probable route of infection [91,258].

Paracellular entry of TBEV between endothelial cells of brain capillaries was also suggested [201], however, using an *in vitro* model of the BBB, Palus *et al.* [254] showed that the tight junctions of microvascular endothelial cells are not compromised, which does not argue in favor of this hypothesis.

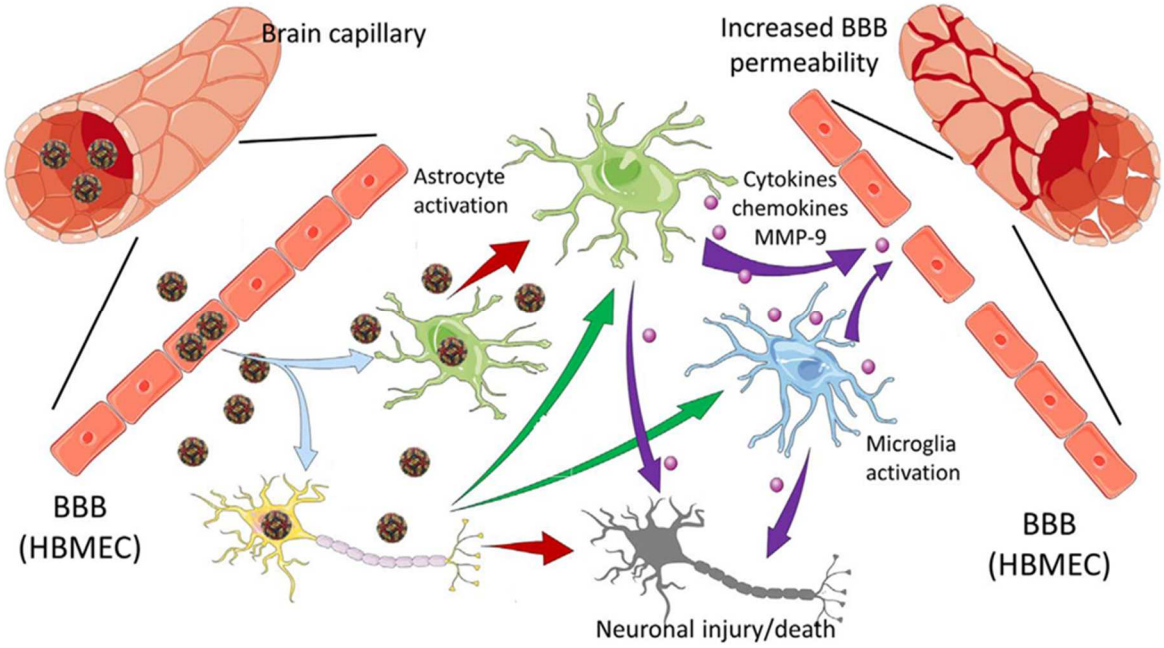

Figure 13 – TBEV entry to the brain and disruption of the BBB

TBEV enters the CNS, possibly by infection of HBMEC, and infects brain cells, such as neurons and astrocytes. Infected cells within the CNS induce a cytokine signaling, which will eventually lead to BBB breakdown and massive entry of the virus and immune cells. HBMEC= Human Brain Microvascular Endothelial cells [253].

Upon viral entry into the brain, TBEV induces non-specific pathological changes. Its antigens are detected in the pericaryon of large cerebellar neurons (Figure 14A).

Lesions, including inflammatory changes and neuronal damage (Figure 14b), are widespread in the spinal cord (anterior horns), the brainstem (medulla oblongata, pontine nuclei and tegmentum of pons), the cerebellum (dentate nucleus and Purkinje cells), and the striatum, while they were absent in meningeal structures, peripheral nerve and blood cells [259–262]. Microglial hypertrophy and astrogliosis were observed in human fatal cases of TBE (Figure 14C) [259].

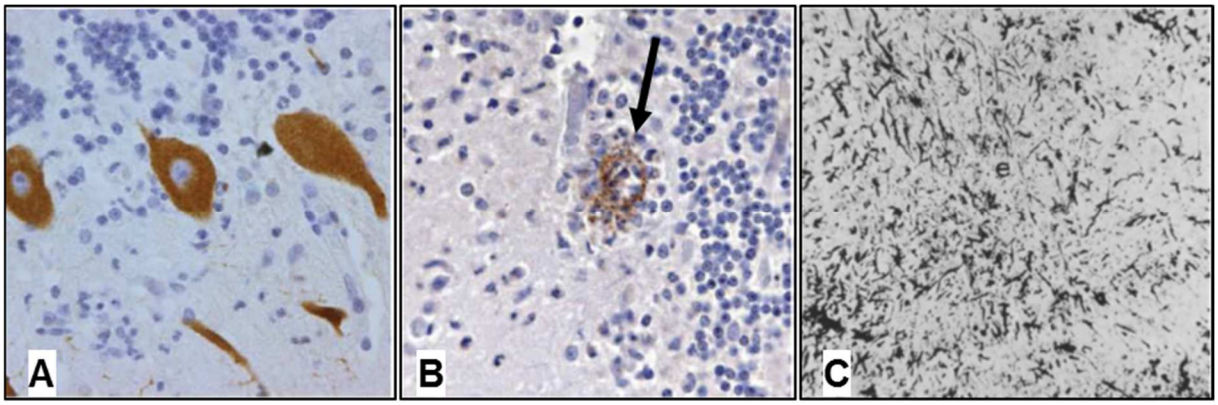

Figure 14 – Histology of human brains of fatal cases of TBE

(A) Immunolabeling of TBEV shows infection neurons (Purkinje cells in the cerebellum) and their processes (600x). (B) Immunolabeling of TBEV shows a disintegrating Purkinje cell associated with a mononuclear inflammatory cells (black arrow) (600x). (C) Proliferation and hypertrophy of microglia, stained with Gallyas' silver stain (figure adapted from [259] and [261]).

Neurons are the main target of TBEV [72,263]. TBEV antigens accumulate in the cell body, and spread to dendrites at later stages of infection (Figure 15A). The virus replicates in dendrites, causing a swelling, and induces a rough endoplasmic reticulum (RER) disorganization and degranulation, tubule-like structures, as well as the formation of specific laminal or smooth membrane structures (LMS or SMS) inside the cisternae of the RER, probably through budding from its membrane [72,223,264]. Those structures are probably intracellular membrane vesicles used by the virus to escape the immune system and delay IFN response signaling [265]. TBEV induces neuronal death but the underlying mechanisms are not fully understood. It might occur through direct and/or indirect effect, mediated by immune cells in the latter case. *In vivo* experiments showed that $CD8^{-/-}$ mice survive longer than immunocompetent mice following TBEV infection and cytotoxic CD8-positive T-cells

were observed in close contact with neurons in brains of fatal TBE cases *post mortem*, supporting a role for cell-mediated immunity in TBEV-induced neuropathogenesis [199,262]. However, so far, a direct effect remains considered as the major cause of TBEV-induced neuropathology [220]. Both apoptosis and necrosis may be involved, as the two processes have been described *in vivo*, in the brain of mice and monkeys [199,264,266,267] and *in vitro,* in human neuroblastoma cell cultures [223]. Caspase 3 was also observed in neurons of human fatal TBE cases analyzed *post mortem* (Figure 15B) [262]. In favor of an apoptotic death, E and NS3 proteins of LGTV have been shown to induce massive cell death in mouse neuroblastoma cell lines through caspase-3 or caspase 8 (for NS3 only) pathways [268,269]. However, this is not further supported by data obtained in primary cultures of murine neurons showing that apoptotic cells were rare [264]. In human cultures of neurons, no apoptotic figures were described either [72]. Furthermore, similar to other flaviviruses [270,271], TBEV induces autophagy in human neuronal cells, and this induction increases TBEV replication [72,223]. However, the mechanisms of TBEV-induced autophagy are not deciphered.

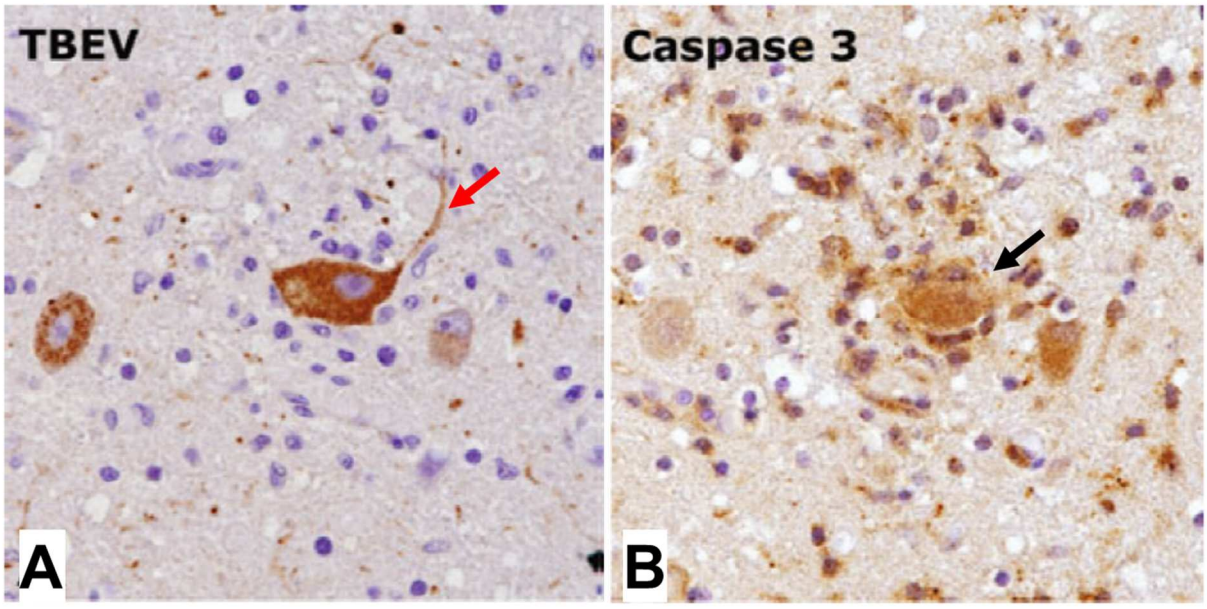

Figure 15 – Infection and induction of apoptosis in neurons of fatal human TBE cases

(A) Immunolabeling of TBEV in neuronal perikarya and processes (red arrow). (B) Immunolabeling of Caspase 3 in TBEV-expressing neurons (black arrow). Stainings in (A) and (B) were performed on consecutive tissue sections (Adapted from [261]).

In addition to neurons, the CNS encompasses glial cells, composed of microglia, astrocytes and oligodendrocytes. Microglia are macrophage-like resident cells [272,273]. They are involved in homeostatic functions such as clearance of necrotic and apoptotic cells and their debris [273]. Astrocytes are star-shaped cells that provide important structural, metabolic and trophic support to neurons [274] and are involved in the BBB formation and maintenance [275]. Following brain trauma or infection, both astrocytes and microglia undergo a process called astrogliosis and microgliosis, respectively, associated with reversible changes such as stimulus-dependent modification of gene expression, and thicker hypertrophic intermediate filaments, as well as long-lasting astrocytes scar formation that sequestrate the affected region of the CNS [276]. Oligodendrocytes are associated with neuronal axons through a myelin sheath and are involved in improving conduction of neuronal impulses. They produce soluble factors and maintain the ionic homeostasis of the brain, thus promoting neuronal survival [277–279]. TBEV infection of glial cells was first studied using immortalized cell lines. It was shown that TBEV replicates in cells of glial origin (glioblastoma cell lines), though in a lower extent than in cells of neural origin (neuroblastoma cell lines). Similar ultrastructural rearrangements and features of apoptosis were however observed in both cell types [223]. Further studies using primary cells from murine or human origins confirmed a low rate of infection of astrocytes (<20%) due to a fast IFN response, and showed ultrastructural modifications in the cytoskeleton, formation of tubule-like structures and limited necrotic figures [61,280]. While TBEV weakly altered astrocytes viability [263,280,281], it induced astrogliosis [259,280], as well as secretion of a large set of cytokines and matrix metalloproteinases (MMP), some of which, such as MMP-9, may play a role in the increase of BBB permeability [280]. As for oligodendrocytes, little is known in a TBEV-infectious context, but they are thought to be rarely infected [193]. However, microglial cells seem not to support TBEV replication [193], but the virus induces their activation [262,282], suggesting a cytokine response.

Furthermore, a cellular immune response is observed, and is represented by inflammatory infiltrates of CD3-, CD4-, and CD8-positive T cells and activated macrophages/microglia in parenchymal and perivascular compartments, and B cells mainly confined in the perivascular compartment (Figure 16) [261].

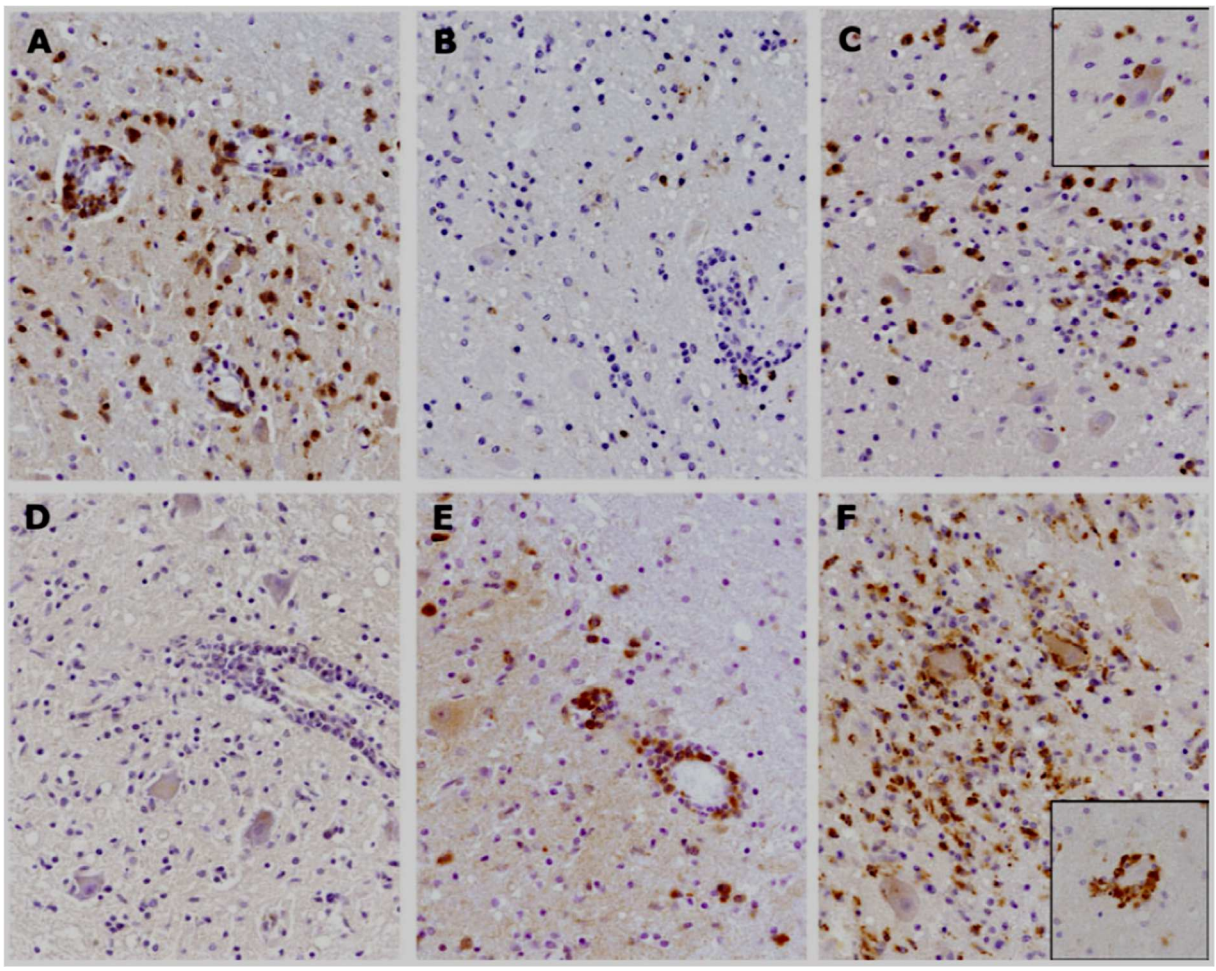

Figure 16 - Immunohistochemical characterization of inflammatory cell subsets and inflammation-assisted factors

T lymphocytes were detected in the parenchymal and perivascular compartment (A: anti-CD3, ×400; B: anti-CD4, ×400; C: anti-CD8, ×400). CD8-positive cytotoxic lymphocytes were predominant in the parenchyma (C), and were seen in contact to morphologically intact neurons (C, inset). B lymphocytes were mainly found in the perivascular compartment (D: anti-CD20, ×400; E: anti-CD79A, ×400). Numerous CD68-positive cells (F, ×400) were detected in both compartments, neuronophagias were observed (F, inset; ×600) [262].

While innate and adaptive immune cells infiltrates might play a role in TBEV-induced pathogenesis, experimental studies about TBEV-induced immunopathology and cellular immune response are limited [197].

During viral infection, innate immune cells, such as neutrophils, macrophages and natural killer (NK) cells provide a fast response aiming to control viral infection and replication. Neutrophils and macrophages are phagocytic cells that are recruited to the site of TBEV infection [181] and the macrophages present antigens to B- and T cells by increasing MHC expression [283]. They are susceptible to TBEV infection

and might participate in peripheral spread of the virus [181,284]. Mouse macrophages support TBEV replication [285], but whether it replicates in neutrophils is still unknown. NK cells represent innate lymphocytes that have the ability to respond against pathogens and kill virus-infected cells through the release of perforin and granzymes [286,287]. They also contribute to viral control of flaviviral infections [288,289] but little is known about their role in TBEV infection. Their cytotoxic responses involve induction of apoptosis by TRAIL and FAS-ligand in targeted cells [290,291]. They are detected in cerebrospinal fluid (CSF) of patients with TBE, indicating that they infiltrate through the BBB [292]. Furthermore, acute TBEV infection activates NK cells but impairs their functionality [293] and NK levels were transitorily stimulated in TBEV-infected mice [220,294].

In comparison, adaptive immunity cells, such as T and B cells, develop later after infection and provide a more specific response targeting viral antigens [295]. In mice, CD8-positive T cells are the main immune cells involved in TBEV-immunopathology [199] and they are strongly activated by TBEV infection [296]. However, breakdown of the BBB is not dependent on infiltration of CD8-positive T cells into the CNS after TBEV-infection [252]. In humans, they contribute to neuronal damage in TBEV-infected human brain, by releasing granzyme B, a serine protease inducing cell death by apoptosis and/or necrosis [261]. CD4-positive T cells have a protective role, confining TBEV spread [199], but they show only a low to moderate activation by TBEV infection [296].

1.4. Cell response to TBEV infection

The CNS is a sensitive organ where immune responses are highly regulated [297]. This regulation enhances protection of vital structures and non-renewable cells, such as neurons, from damage by inflammatory responses, and the CNS is considered as an immune regulated site [298,299].

In the homeostatic brain, the CNS parenchyma has poor lymphatic drainage [300] and is separated from the blood circulation by the BBB, protecting it from the entry of pathogens and circulating immune cells [301]. The meninges are accessible and patrolled by immune cells but the entry of monocytes, B and T cells is restrained. CNS cells express fas ligand (fasL) which induces death of fas-positive T cells that reach the CNS, independently from antigen recognition [302,303]. Furthermore, astrocytes and microglia inhibit T-cell proliferation and cytokine production, by inducing regulatory T cells [304]. Neurons also convert activated T cells to regulatory T cells [305]. Moreover, the low expression of major histocompatibility complex (MHC) class I and II prevents them from recognizing corresponding antigens [306].

Some pathogens, such as neurotropic viruses, are able to breach the physiological and immunological barriers and enter the CNS, either causing devastating inflammation or taking advantage of the immune environment of the CNS to persist as latent infections. Upon inflammation, immune reactions take place in the CNS due to immunostimulatory effects of locally produced cytokines, such as breakdown of the BBB, facilitation of antigen drainage to the periphery, DC appearance, and MHC upregulation [307]. Furthermore, all brain cells are able to mount an intrinsic antiviral response against pathogens.

1.4.1. Intrinsic immune response

1.4.1.1. Sensing of viral infection

Within the CNS, the innate immune response is the first line of defense against viral infections. It relies primarily on the recognition of pathogen associated molecular patterns (PAMPs) by cellular sensors known as pathogen recognition receptors (PRR), which induces antiviral response cascades and interferon (IFN) production. Different PRRs react with specific PAMPs, show distinct expression patterns, activate specific signaling pathways, and lead to distinct antiviral responses [308]. PRRs are either

localized at the cell or endosomal membranes, such as toll-like receptors (TLRs), or in the cytosol, such as RIG-I-like receptors (RLRs) [309].

- **RIG-I like receptors (RLR) pathway**

The three members of the RLR family are retinoic acid-inducible gene I (RIG-I), melanoma differentiation-associated 5 (MDA5) and laboratory of genetics and physiology 2 (LGP2). Those receptors have highly conserved structures. They carry two repeats of caspase activation and recruitment domain (CARD)-like region at the N-terminal end, which are important to downstream signaling through their interaction with other CARD-containing proteins. The middle portion contains the DExD/H helicase domain associated with an ATP-binding motif. The C-terminal region contains a repressor domain that inhibits downstream signaling [310].

Both RIG-I and MDA5 sense viral RNA with their helicase domain and induce downstream signaling through their card domain. LGP2 lacks the CARD homology and was thought to function as a negative regulator by interfering with viral RNA recognition by RIG-I and MDA5 [310]. It seems that it can on the contrary facilitate viral RNA recognition by other RLRs through its ATPase domain [311].

RLRs recognize double-stranded RNAs (dsRNAs) formed during flavivirus replication [312]. MDA5 recognizes long dsRNAs (>4kb), that can be generated as intermediates during viral infection and replication, while RIG-I can recognize short dsRNAs (≅300bp) and 5' di- and 5' tri-phosphorylated single stranded RNAs (ssRNAs) [313]. Because of this specific recognition of nucleic acids, RIG-I and MDA5 sense the replication of different viruses [314]. They can act in synergy, in a temporal manner, depending on PAMPs displayed along the infection [315].

Upon recognition of PAMPs, RLRs change their conformation and form oligomers through their CARD domains, which also interacts with the CARD domain in the N-terminal end of IPS-1 (also known as MAVS, VISA or CARDIF) that is localized at the external mitochondrial membrane [316]. IPS-1 recruits several proteins of the tumor necrosis factor (TNF) receptor-associated factor (TRAF) family [317]. TRAF proteins are E3-ubiquitine ligases that will recruit inhibitor of nuclear factor kappa-B kinase subunit gamma (IKK-γ) protein (also called NFκB essential modulator -NEMO-) that will activate the TBK1/IKKε and IKKα/IKKβ complexes. TRAF3 induces TBK1 and IKKε activation, that will form a complex with NEMO, NF-κB activating kinase associated

protein 1 (NAP-1), and similar to NAP-1 TBK1 adaptor (SINTBAD) proteins and induce IRF3 and IRF7 phosphorylation, conformational change, dimerization, and nuclear translocation of the dimers to induce type I IFN gene expression [318]. TRAF6 association with TAK1, TAB 1/2/3 and TANK proteins induces the formation of IKKα/IKKβ complex that induce nuclear translocation of NF-κB and proinflammatory cytokines production [319] (Figure 17).

TBEV infection induces the upregulation of both RIG-I and MDA5 in T98G neuroblastoma cell line, and both are involved in the enhanced activation of interferon regulatory factor 3 (IRF3) signaling and *RANTES* (CCL5) expression in human astrocytes [320,321]. However, IFN induction by the virus depends only on RIG-I, and not on MDA5, in human osteosarcoma cell lines U2OS [80]. The downstream adaptor of RLR signaling, IPS-1, is also important for restricting LGTV infection, as $IPS1^{-/-}$ mice show higher viral replication and increased mortality [282], supporting the involvement of RLRs in TBEV sensing.

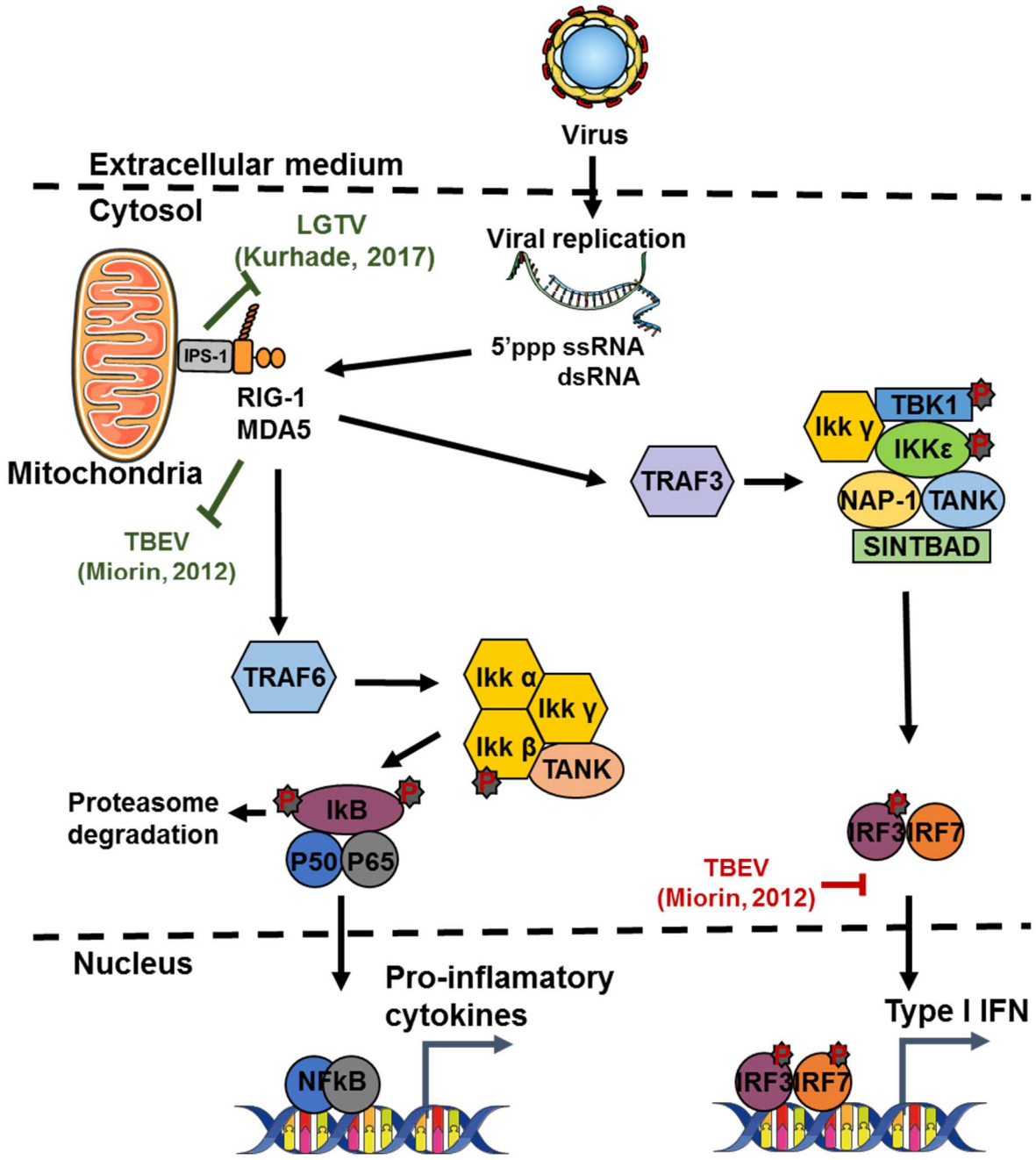

Figure 17 – RLR pathway and known TBEV interactions.

Known interactions inhibiting (green) or favoring (red) TBEV replication are represented.

- **Toll-Like Receptors pathway**

Double-stranded RNAs (dsRNAs) can also be recognized in the endosome by Toll-Like Receptor proteins (TLRs). TLRs are very conserved transmembrane proteins composed of an N-terminal ectodomain, involved in ligand recognition, a transmembrane domain, and a C-terminal cytosolic domain called tool interleukin-1 (TIR), that induce downstream signaling [322]. Among the 10 described TLRs in

mammals, TLR2 and TLR4 are involved in viral recognition at the cell membrane, while TLR3, TLR7, TLR8 and TLR9 are involved in viral sensing at membranes of endosomes [322]. The TLR pathway is represented in Figure 18.

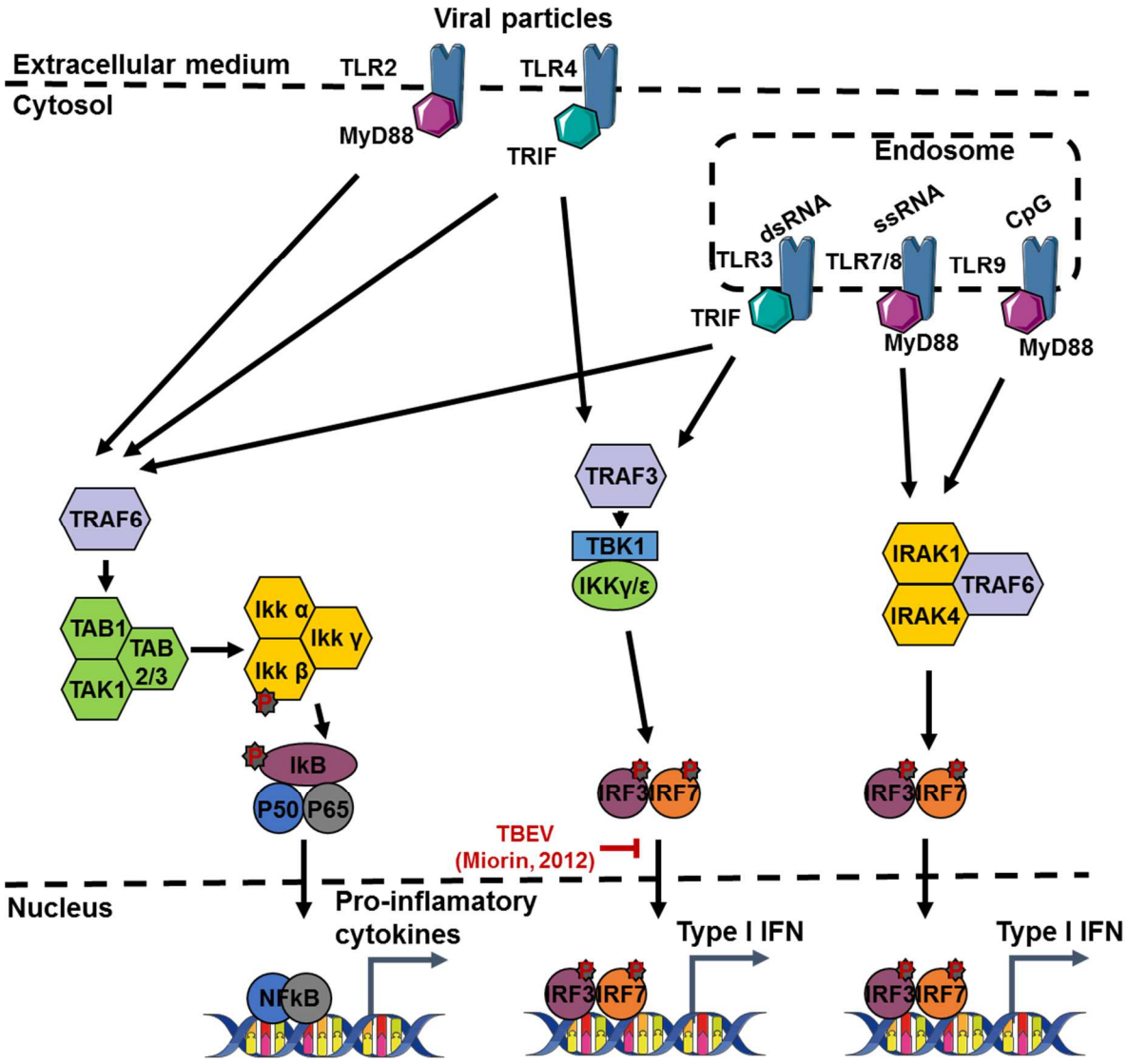

Figure 18 - TLR pathway and known TBEV interactions.

Known interactions inhibiting (green) or favoring (red) TBEV replication are represented.

TLR2 and TLR4, localized at the cell membrane, recognize viral glycoproteins, mainly localized at the surface of viral particles such as vesicular stomatitis virus (VSV) or Ebola viruses [323,324]. Their activation induces proinflammatory cytokine production but TLR2 and its internalization can also induce type I IFN by binding murine CMV [325].

Within the cell, viral nucleic acids are directed to the endosomal compartment through three main ways: 1/ degradation by cellular proteases of viral particles after entry by endocytosis, 2/ viral entry by membrane fusion, autophagy, and degradation of viral particles after viral entry and membrane fusion, and 3/ nucleic acid transfer to pDC through exosomes [326–328]. TLR3 recognizes dsRNAs that either form the viral genome or are replication intermediates [329]. TLR7 and TLR8 recognize ssRNA, and are involved in the sensing of ssRNA viral genomes. TLR7 induces type I IFN production while TLR8 induces mainly proinflammatory cytokines production through NF-κB activation [313,328]. TLR9 recognize non-methylated cytosine-guanosine motifs (CpG) that are present in the bacterial and viral DNA. They induce type I IFN production, but can also induce proinflammatory cytokines production through NF-κB activation [330].

TLRs binding to their ligand induces their dimerization and recruitment of TIR domain-containing adapters. There are four different adapters: myeloid differentiation primary response protein 88 (Myd88), TIR-associated protein/MyD88 adaptor like (TIRAP/MAL), TIR domain-containing adaptor protein inducing IFNβ/TIR-domain containing molecule 1 (TRIF/TICAM), and TRIF-related adaptor molecule (TRAM) [331].

TLR3 induces the activation of TRIF adapter, while TLR2, TLR4, TLR7, TLR8 and TLR9 activate both TRIF and MyD88 adapters. The C-terminal domain of TRIF binds TRAF 6 protein, while its N-terminal interacts with receptor interacting protein 1 (RIP1). The TRAF-RIP1 complex activates TAK1 kinase and NF-κB activation [332]. TRIF also interacts with TRAF3 to activate TBK1 and IKKε. The formed complex induces IRF3 and IRF7 phosphorylation and type I IFN production [333].

Myd88 is recruited to TLR receptors dimers through its TIR domain [334]. Its recruitment by TLR2 and TLR4 is facilitated by MyD88-adapter-like (MAL) protein [335]. Through its death domain (DD), Myd88 recruits kinase proteins of the IRAK family [336]. The formed complex dissociates from Myd88 and binds TRAF6. TRAF6 dimerization induces the formation of TAK1-TAB1/2/3 complex that autophosphorylates and phosphorylates the IKKα-IKKβ-IKKγ complex [337]. The phosphorylated IKK complex activates NF-κB, which translocate to the nucleus. Furthermore, TLR7, TLR8 and TLR9 can induce IRF3-IRF7 phosphorylation and translocation through the complexes Myd88/IRAK4/TRAF6 and TRAF6/IRAK1/IKKα [338]

TLRs involvement in TBEV sensing is not clear, as few laboratory experiments have investigated the importance of TLR3-TRIF pathway in tick-borne *Flaviviruses* (TBFV) [67]. TLR3 expression was not induced by TBEV in T98G neuroblastoma cell lines [320]. In TBE patients, TLR3 expression is associated with either a protective [339] or a more severe outcome/risk factor [340–342]. This led to the suggestion that TLR3 might support TBEV penetration through BBB and facilitate the onset of neurologic symptoms, but that within the CNS, its expression would be protective [339]. Indeed, TLR7 might act in a related way in LGTV infection, as it restricts viral replication and spread in the CNS in an IFN-independent manner, by activation of the inflammatory response, which might facilitate BBB disruption [343].

1.4.1.2. Interferon signaling

The activation of the PRR cascades results in the phosphorylation, oligomerization and then nuclear translocation of the transcription factors IRF3, IRF7 and/or NFκB [308,344,345]. Translocation of IRF3 and IRF7 induces the expression of specific cytokines called interferon (IFN). Three types of IFNs are produced by cells: type I IFN, type II IFN, and type III IFN (Figure 19).

- **Type I Interferon**

Type I IFNs are key innate immune regulators for viral infections within the CNS. They enclose 5 different classes: IFN-α (comprising 12 subtypes), IFN-ß, IFN-ω, IFN-ε, and IFN-κ that form a large family of cytokines that control early spread of viral infection. Most cells produce IFN-ß, whereas hematopoietic cells such as plasmacytoid dendritic cells (pDC) are specialized in IFN-α production [346]. IFN-ε and IFN-κ are not induced by PRRs activation, but are constitutively expressed. IFN-ε is expressed by epithelial cells of the female genital tract and protects against sexually transmitted infections such as HSV-2 and *Chlamydia muridarum* [347]. IFN-κ is produced by keratinocytes, and does not have a known subsequent antiviral activity [348]. IFN-ω is mainly produced by leucocytes and stimulate NK cells MHC class I expression [349].

Type I IFNs bind to a receptor composed of two major subunits, IFNAR 1 and IFNAR 2, constitutively associated with JAK1 and TYK2 kinases [350]. Binding of type I

IFN to its specific receptor, in a paracrine or autocrine manner, induces the trans-phosphorylation of the JAK tyrosine kinases, which phosphorylate tyrosine residues within the intracellular subunit of IFN receptors. These residues recruit STAT proteins that are then phosphorylated by the JAKs, allowing the formation of STAT1-STAT2 heterodimers associated with IRF9, known as ISGF3 transcription factor. These complexes translocate to the nucleus and bind the ISRE promoter, which induces the expression of hundreds of interferon stimulated genes (ISGs) [351,352].

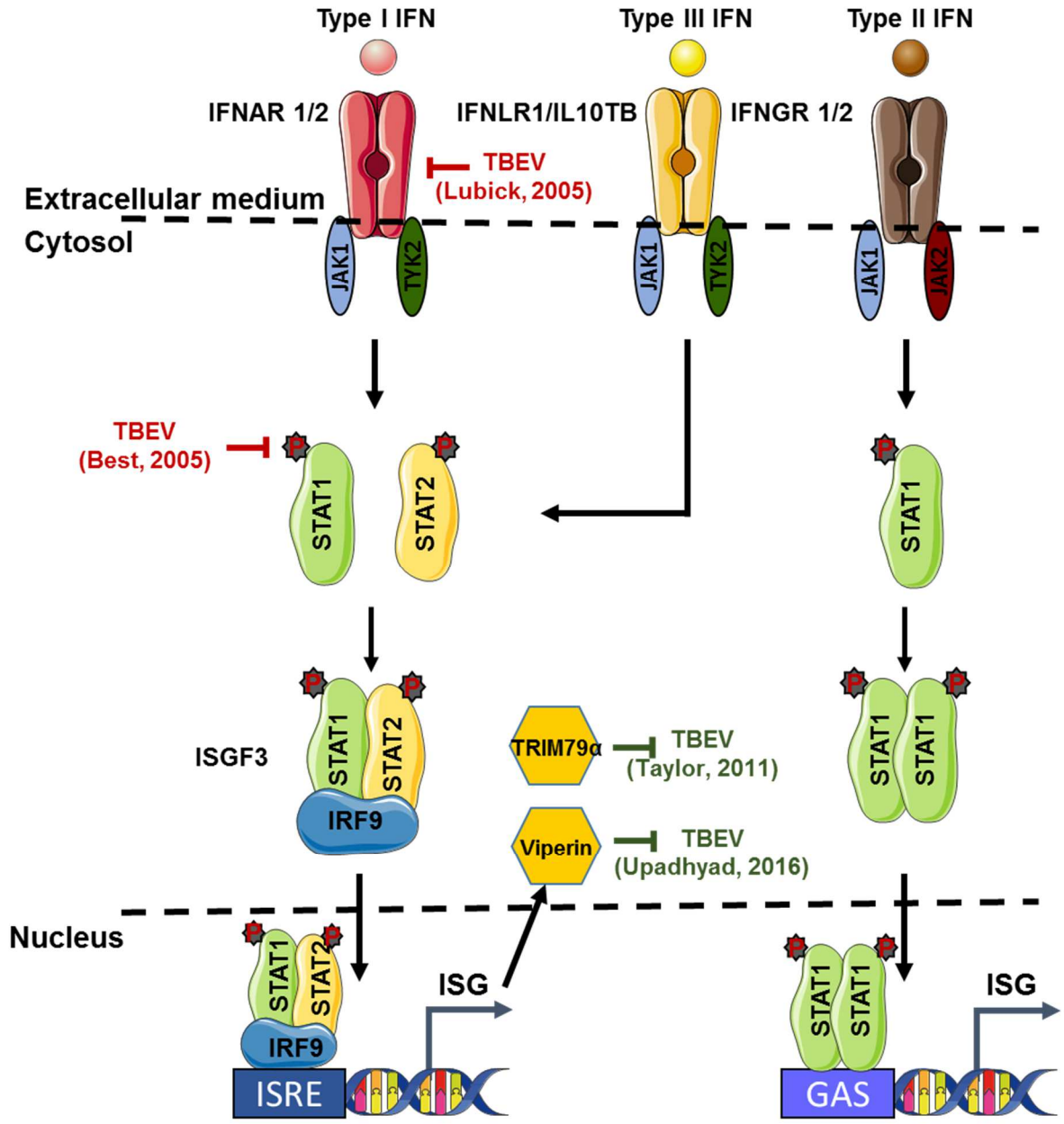

Figure 19 – Type I, type II, and type III interferon.

Known interactions inhibiting (green) or favoring (red) TBEV replication are represented.

- **Type II Interferon**

Type II IFN, represented by IFN-γ, binds to a receptor composed of the two subunits IFNGR1 and IFNGR2 [353]. Binding of IFN-γ to its receptor induces the activation of JAK1 and JAK2 proteins that are associated with the intracellular ends of its subunits. This leads to the phosphorylation and dimerization of STAT1 which will translocate to the nucleus and activate the IFN-γ-activated site (GAS) and the expression of genes such as ISGs [351,352]. IFN-γ is an important immune modulator. It is mainly produced by immune cells and stimulates macrophages differentiation, induces neutrophils activation, increases NK cells cytotoxicity and stimulates MHC class I and II expression [354].

- **Type III Interferon**

Type III IFNs, represented by IFN-λ1 (IL-29), IFN-λ2 (IL-28A), and IFN-λ3 (IL-28B), signal through a heterodimeric receptor complex including IFNLR1 and IL10TB subunits [355]. While IL-10TB subunit is widely distributed across cell types, IFNLR1 is restricted to epithelial cells and, as a consequence, many other cell types respond poorly to type III IFNs [356]. Although binding a different receptor, type III IFN induces a similar pathway than type I IFNs, through the JAK/STAT signaling [357]. It has an antiviral activity and is able to control rotavirus infection in the gut [358] and influenza infection in the respiratory tract [359]

- **Interferon and TBEV infection**

IFN response through IFNAR is important for control of TBEV, as its replication and infection are increased in $IFNAR^{-/-}$ murine astrocytes [281]. Type I IFN induction in TBEV-infected cells is protective [80,282,360] and they can inhibit LGTV replication in pretreated cell cultures [361,362]. Type III IFN slightly restricts LGTV replication in murine neuroblastoma cells [361] but unlike type I IFN, it does not mediate antiviral protection when used to pretreat human medulloblastoma cells derived from cerebellar neurons (DAOY) [362]. In DAOY cells, TBEV infection activates type III IFN, but not type I or type II IFN cascades [362]. Moreover, TBEV-NS5 induces the activation of IRF3 through IKKε and TBK1, resulting in the expression of

RANTES, while IRF7 and IKKε/NF-κB roles do not seem essential for TBEV-induced RANTES production [320,321].

TBEV evolved to escape IFN response, by sequestrating its gRNA and replication intermediate dsRNA in intracellular vesicles located in the ER membranes, delaying type I IFN production by hiding from PRR recognition factors and abrogating IRF-3 translocation to the nucleus [80,265]. Viral proteins of flaviviruses are known to antagonize type I IFN, particularly NS5 [Reviewed by 363] but also TBEV-NS1, as its overexpression *in vitro*, but not during viral replication, abrogates the IFN-ß signaling [80]. TBEV-NS5 protein inhibits IFNAR1 expression by binding to prolidase (Peptidase D or PEPD) involved in the IFN receptor maturation and cell surface expression [364]. LGTV- and TBEV-NS5 also interfere with JAK-STAT signaling pathway induced by type I (IFN-α) and II (IFN-γ) interferons. LGTV-NS5 binds to IFNAR and IFNGR receptors, blocking the phosphorylation of JAK1, TYK2, STAT1 and STAT2 (Figure 19) [361], while TBEV-NS5 abolishes STAT1 phosphorylation through its interaction with the PDZ protein Scribble [365]. The overall data suggest that the inhibition of neuronal outgrowths (neurites) by TBEV-NS5 interaction with Scribble, competing with Rac1 [366], is a side effect of IFN signaling inhibition.

1.4.1.3. Interferon-stimulated genes response

The JAK-STAT transduction pathway induces the expression of hundreds of interferon stimulated genes (ISGs) that can directly act on restraining the viral replication [367]. Some ISGs are directly involved in IFN signaling, such as RIG-I, MDA5 or STAT1. Others regulate this signaling, such as ISG15, or have intrinsic antiviral activities by modulating nucleic acid integrity (OAS/RNAse L, ADAR1, and APOBEC family members), viral entry (IFITM3), or protein translation (PKR, IFIT family members) [368].

A wide panel of ISGs are upregulated following TBEV infection, with amongst them IFIT1, IFIT2, RSAD2 (viperin), OASL, IFIT3, OAS2, ISG15 and ISG20 [362]. Here, I develop the functions and mechanisms of four ISGs that have been well characterized and are relevant in flavivirus-induced interferon response.

- **Mx proteins family**

Mx (Myxovirus resistance) proteins family encloses two members: MxA (or Mx1) and MxB (or Mx2). They inhibit several viruses by targeting viral nucleocapsids, resulting in viral inhibition prior to viral replication (Figure 20) [369,370]. MxA contains GTP binding domains in the N-terminal end and a specific effector domain for GTP hydrolysis in the C-terminal end [371], but the functions of the two domains are not essential for its activity and depend on the targeted virus [372,373].

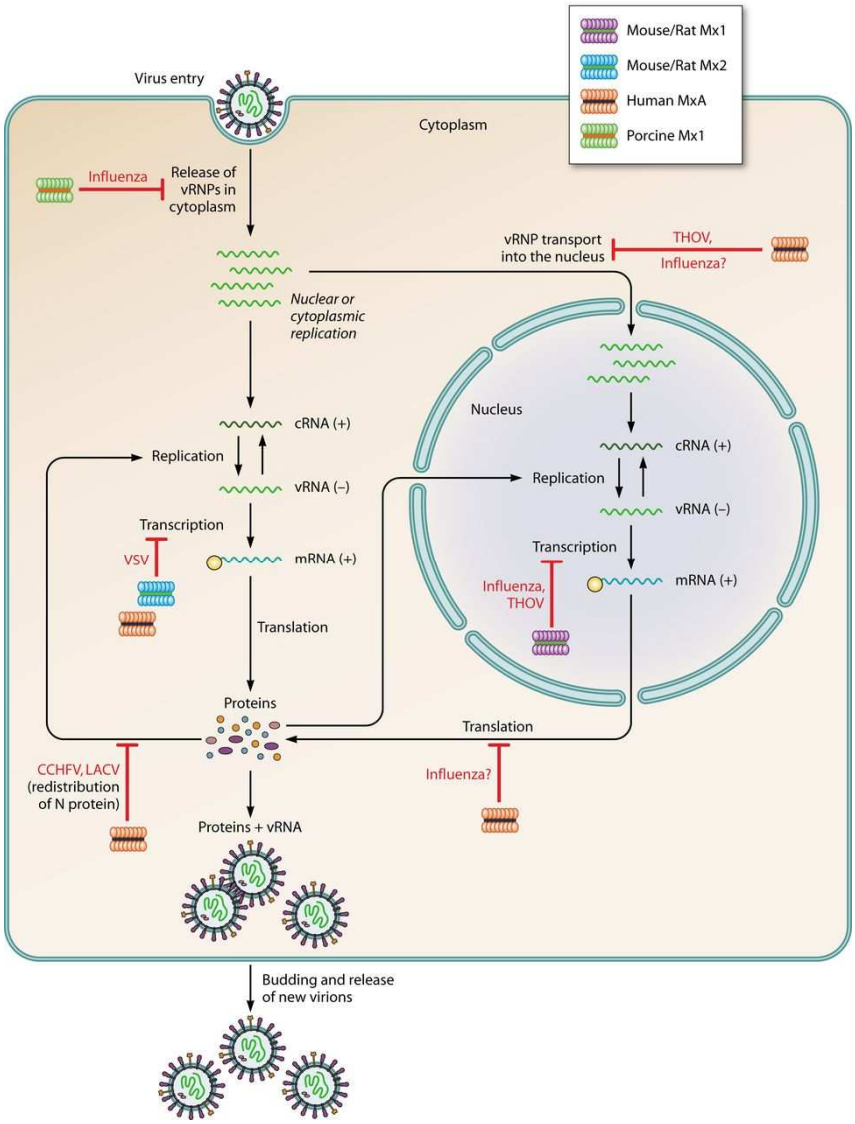

Figure 20 – Antiviral mechanisms of Mx proteins

Mx proteins family inhibit several steps in the life cycle of viruses. They block nuclear translocation of nucleocapsids of Influenza A virus and Thogoto virus (THOV) (1), and inhibits the secondary transcription and replication of their viral genome in the nucleus (2) or of vesicular stomatitis virus (VSV) in the cytoplasm (3). MxA also sequesters N protein of La Crosse virus (LACV) (4), thereby blocking genome replication. Furthermore, MxB inhibits uncoating, nuclear uptake and/or stability of HIV-1, preventing chromosomal integration [370]. N, nucleocapsid protein. Adapted from [374].

- **OAS/RNaseL proteins**

OAS genes are upregulated by IFN signaling and encode 2'-5' oligoadenylate synthetase (OAS) proteins. Double stranded-RNAs, originating from replicative intermediates ssRNAs, stem structures of ssRNAs, or viral dsRNA genomes activate OAS proteins inducing the polymerization of adenosine 5'-triphosphate (ATP) into 2'-5'-linked oligoadenylates (2-5A). These 2-5A oligomers bind to and activate latent RNase L that degrades single stranded RNA from cellular or viral origins [375] (Figure **21**). *OAS1b*, a murine gene also called *Flv* or *falvivirus resistance gene*, is known to induce a cell resistance to flaviviruses by an unknown mechanism independently of RNase L [376]. Furthermore, RNase L is also involved in control of flavivirus replication, such as WNV [377].

OAS1b is involved in the reduction of TBEV replication in transgenic mice [378]. In humans, polymorphism in *OAS2* and *OAS3* but not *OAS1* genes are associated with an increased susceptibility to TBEV-induced disease [379] and *2'-5'-oligoadenylate synthetase like* (*OASL*) and *OAS2* genes were overexpressed in TBEV-infected DAOY human neuroblastoma cell lines [362].

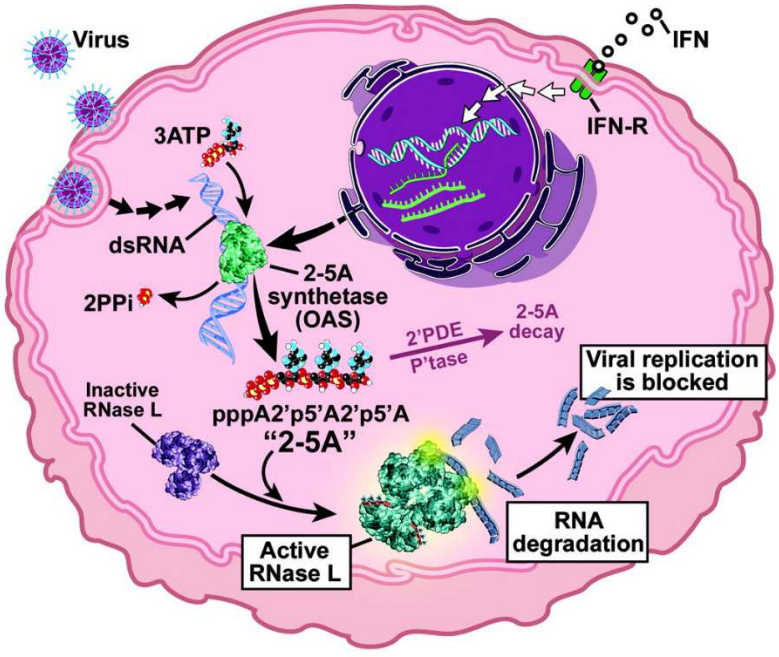

Figure 21 – OAS2/RNase L system.

IFN signaling induces transcription of *OAS* gene through ISRE promoter. They bind dsRNA and activate RNase L through 2-5A production, mainly (2′-5′)p3A3 and (2′-5′)p3A4, leading to ssRNA cleavage. PPi, pyrophosphate; 2′PDE, 2′-phosphodiesterase; P'tase, phosphatase; IFN-R, IFN receptor. Reproduced from [380].

- **TRIM proteins family**

The tripartite motif (TRIM) protein family comprises 66 members. They are E3 ligase proteins that contain an RBCC domain formed by a really interesting new gene (RING) domain, one or two B-boxes domains and a coiled-coil domain [381]. Their functions are highly dependent on the capacity of the C-terminal domain to recruit specific partners. The physiological role of several TRIMs is poorly understood but it is established that it can act in the cytoplasm or the nucleus, at multiple stages of the viral life cycles, and can target various viral [382]. They are mainly known to affect retroviral replication.

TRIMs regulate PRRs function and downstream signaling. For instance, TRIM4 and TRIM25 facilitate RIG-I oligomerization and stabilization by catalyzing the synthesis of unanchored K63-linked poly-Ub chains, which promotes the interaction of its CARD domains with IPS-1 [383,384]. TRIM65 also activates MDA5 by ubiquitination of its RNA helicase domain [385], but TRIM13 and TRIM59 act as inhibitors of MDA-5 induced cascades, inhibiting transcription of IRF3 and NF-κB genes [386,387]. Furthermore, TRIM56 interacts with TRIF and promotes TLR3 activation [388].

TRIMs are also able to restrict replication of several viruses. TRIM5α blocks the replication of human immunodeficiency virus-1 (HIV-1) and murine leukemia virus (MLV), at a stage following reverse transcription but before integration of viral DNA into the host chromosome [389,390]. TRIM52 interacts with NS2A protein of JEV and directs it to proteasome mediated degradation [391] and TRIM56 may restrict YFV and DENV with an unknown mechanism [388]. Taylor *et al.* [392] showed that TRIM79α, also known as TRIM30-3 or TRIM30D is upregulated in LGTV-infected mice. It binds TBEV-NS5 and mediates its proteasome independent lysosome-mediated degradation, inhibiting viral replication. However, the NS5 protein of WNV, a mosquito-borne flavivirus, was not recognized, showing a specific mode of action [392]. TRIM79α expression is also highly upregulated in TBEV-infected murine astrocytes [281]. However, as TRIM79α is specific for mice, other TRIM proteins might have a similar anti-TBEV role in humans.

- **Viperin**

Viperin, coded by the *RSAD2* gene, is an ISG with broad-spectrum antiviral activity induced both in an IFN-dependent manner and IFN-independent manner [393,394]. Viperin is a radical S-adenosylmethionine (SAM) domain-containing molecule, which uses a [4Fe-4S] cluster to cleave SAM. It targets different steps of the replication cycle of viruses, including CMV, influenza A virus, Sindbis virus, WNV and DENV.

Viperin interferes at several levels of TBEV replication cycle: selective blocking of genomic RNA synthesis [395], proper viral particle assembly [396], and induction of proteasome-dependent degradation of NS3 and NS3-interacting viral proteins [397]. Viperin also restricts LGTV replication in the brain in a region-specific manner. Its expression is higher in astrocytes than in cortical neurons (CN) and it restricts viral replication in both cell types, while viral replication in granule cell neurons (GCN) mediate a viperin-independent antiviral response [263].

1.4.1.4. Cytokines and chemokines

During viral infections, in addition to IFN production through IRF3-IRF7 nuclear translocation, PRRs-induced signaling activates downstream cascades that induce NF-κB nuclear translocation, leading to activation of pro-inflammatory cytokines.

Neurons, astrocytes, microglia and oligodendrocytes can produce inflammatory mediators, and cytokine receptors are expressed constitutively throughout the CNS. In pathophysiological conditions, microglia and macrophages are rapidly recruited to the site of insult, and produce cytokines and trophic factors that can either damage or protect neighboring cells [398].

- **Interleukins**

Up to date, more than 40 interleukins (IL) have been identified. During immune response, they have a role in activation, proliferation and of leucocytes [399]. Interleukin signaling is cell-type dependent and mainly regulated by JAK/STAT pathway [400,401]. The can have a pro-inflammatory role, such as IL-1, IL-6, IL-12, and IL-17, inducing leucocytes differentiation, activation, and proliferation. They

can also have an anti-inflammatory role, such as IL-4, IL-10, IL-13, and IL-22, which are secreted at later stages of inflammation

- **TNF**

Tumor necrosis factor-α (TNFα) is a central mediator of inflammation and is involved in the pathogenesis of several viral infections. TNF signaling is mediated by two receptors, p55 and p75, that are involved in either protective or deleterious effect on neurons. The downstream signaling activates NF-κB, induces neuronal apoptosis, and can disrupt the BBB [402,403]. It also modulates the inflammatory response, and regulate pro-inflammatory cytokines during JEV infection [404]. In the brain, astrocytes and microglia are able to synthesize TNF*a* [403].

TNF-related apoptosis-inducing ligand (TRAIL) is a member of the TNF family that promotes apoptosis in a wide variety of transformed and cancerous cells, by binding to and activating the death receptors DR4 and DR5 [405]. It can also mediate antiviral functions in an apoptosis-independent manner [406,407]. Furthermore, its expression can be induced by viruses such as measles virus [408] and DENV [406].

- **Chemokines**

Cytokines involved in immune cells migration are called chemokines. They are produced by a large number of cells and form gradients that attract leucocytes to the highest concentration.

There are two types of chemokines: homeostatic chemokines, which are constitutively produced in certain organs, and inflammatory chemokines, which are induced in response to immune response insults [409,410]. Depending on the position of cysteine residues at their N-ter end, they are subdivided into CCL, CSCL, CX3CL and XCL. Chemokines receptors are divided depending on the chemokine that they bind: CCR, CXCR, CX3CR and XCR. The chemokine-receptor are not exclusive, as different chemokines can bind to different receptors [409].

Among pro-inflammatory chemokines, C-X-C motif chemokine ligand (CXCL) 10 acts primarily on neutrophils as chemoattractant and activators [398]. It can also

mediate apoptosis in neurons [411], and viral infections induce its expression by astrocytes [412].

- **Cytokine response to TBEV-infection**

TBEV/LGTV infection induces an elevated production of several cytokines and chemokines, such as CCL3 (MIP1α), CCL4 (MIP1ß), CCL5 (RANTES), CXCL10 (IP-10), IL-6, TNFα as well as IL-1α/ß, IL-6, IL-8 IFN-α and IFN-γ [252,280,362], produced at least partly by glial cells (Zhang et al. 2016; Zheng et al. 2018). This production of cytokines is associated with an acute infection in HEK 293T cell lines, as cells infected in a persistent manner with LGTV did not upregulate cytokine-expressing genes [413]. The activation of the inflammatory response is important for the control of infection, as deletion in the *CCR5* gene, coding for the receptor of CCL5 (RANTES) is associated with severe tick-borne encephalitis syndromes [414].

1.4.2. Cell death

Cell death is an essential biological process for physiological growth and development. The classical forms of cell death include apoptosis, necrosis and autophagy [415]. They activate specific signaling pathways and display distinct morphological features. Cell death is a common outcome of virus infection. It can either slow down viral replication or enhance virus dissemination. Following viral infection, cell death can occur through one or several pathways.

1.1.2.1 Apoptosis

Apoptosis can be triggered by extrinsic signals, such as cytokines, or by intrinsic signals. Both rely on cysteine aspartyl proteases (caspase) signaling. Caspases are inactive zymogens that can be autoactivated (caspase 8, 9 and 10), or activated by a proteolytic cascade (caspase 3, 6 and 7) [416]. Both intrinsic and extrinsic pathways induce cell shrinkage, nuclear and chromatin condensation, DNA fragmentation, membrane blebbing and breakdown into apoptotic bodies.

The extrinsic pathway is stimulated by ligands of the TNF family, such as TNF, Fas ligand (FasL) and TRAIL. In the absence of TNFα, its receptor TNFR1 is associated

with NFR-associated death domain (TRADD), receptor interacting protein kinase (RIP1), cellular inhibitor of apoptosis 1 (cIAP1), cIAP2, TNFR-associated factor 2 (TRAF2) and TRAF5. This induces the formation of a complex at the plasma membrane termed complex I which activates cell survival through NF-κB signaling [417]. Binding of TNFα to its receptor TNFR1 leads to its internalization and the formation of a new complex including RIP1, RIP3, TRADD, FAS-associated protein with a death domain (FADD) and caspase-8. This complex is called cytosolic death-inducing signaling complex (DISC) or complex II. RIP1 and RIP3 are then cleaved by caspase 8, which induces the death signal by direct cleavage of caspases 3, 6 and 7, or by cleavage of Bid, a pro-apoptotic member of Bcl-2 family that will trigger Bax and Bak to initiate intrinsic apoptotic pathway [418].

On the other hand, the intrinsic pathway can be induced by a variety of intracellular stimuli that promote mitochondrial outer membrane permeabilization (MOMP) and the release of pro-apoptotic mitochondrial proteins. Among them, cytochrome c promotes the formation of a complex comprising Apaf-1 and caspase 9. This complex (called apoptosome) stimulates the autoactivation of caspase 9, which cleaves downstream effector caspases, such as caspase 3 [419]. The protein p53 (or TP53) is another inducer of intrinsic apoptotic pathway. Upon stress, p53 translocates to the mitochondria and interacts with Bcl-2 family members, leading to MOMP and apoptosis (Figure 22) [420].

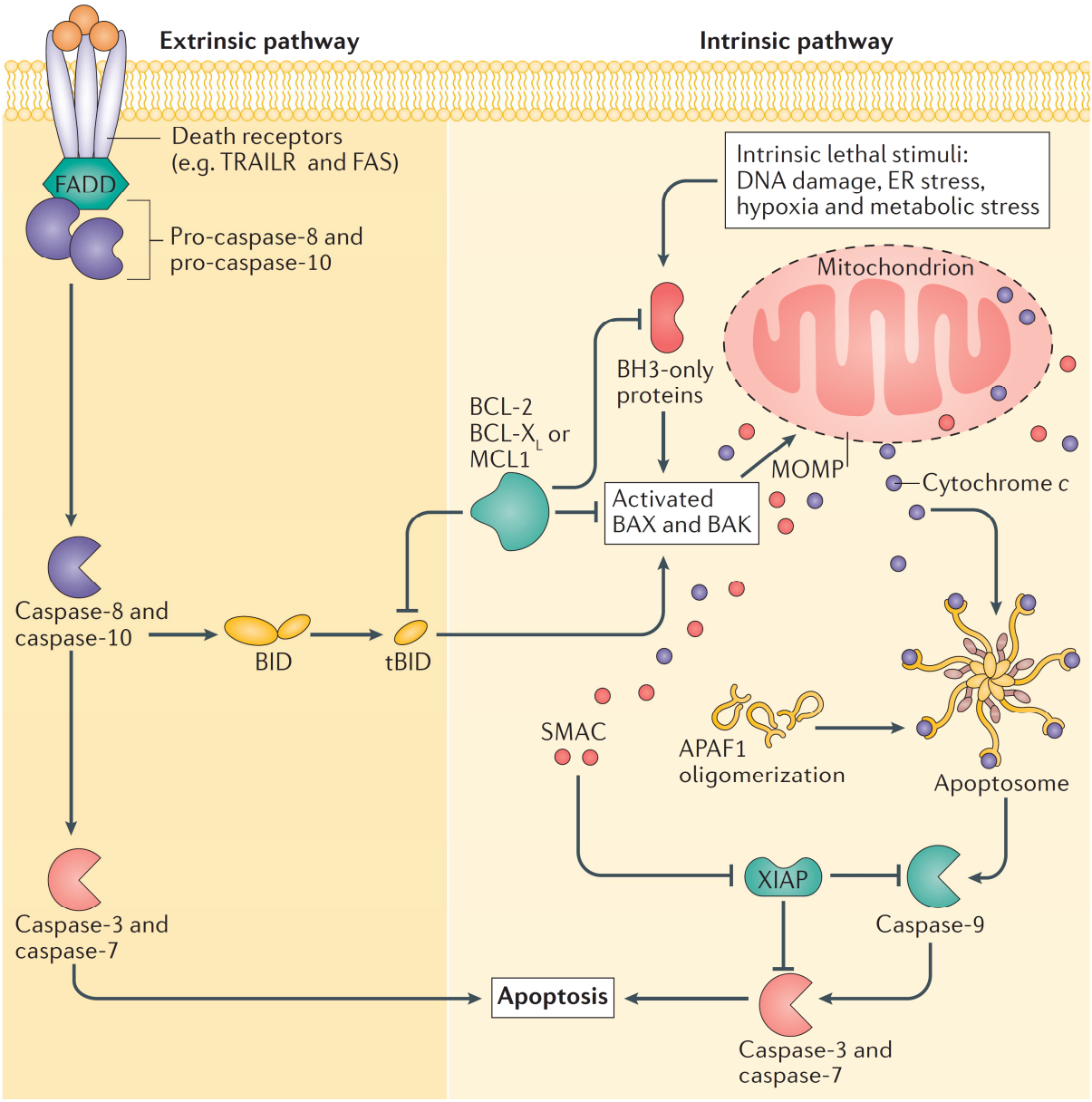

Figure 22 - Extrinsic and intrinsic apoptotic signaling pathways

See text for details. ER=endoplasmic reticulum, MCL1=myeloid cell leukaemia 1, tBID=truncated BID. [421].

1.1.2.2 Necroptosis

Necrosis has historically been considered an accidental form of death. However, evidence demonstrates that necrosis can be tightly regulated, involving specific ligands and genes. The terms programmed necrosis, necroptosis, or regulated necrosis are used to distinguish the programmed necrosis from the accidental necrosis [419]. Diverse signals, such as DNA damage, ATP depletion, or excessive

production of reactive oxygen species (ROS) can induce organelle distention and disruption, cell swelling, and the release of cytoplasmic content [422].

The most characterized pathway is through the signaling pathway of TNFα. It can also be induced by PRRs, but the mechanisms of this signaling are not known. TNFα induces the intrinsic pathway of apoptosis through activation of caspase 8. When caspase 8 is deleted or inhibited, apoptosis cannot be initiated, which results in necroptosis [423].

1.1.2.3 Autophagy

Autophagy pathways are divided into three classes: microautophagy (engulfment of the cytoplasm at the lysosomal membrane, mainly characterized in yeasts), chaperon-mediated autophagy (directs unfolded proteins towards the lysosome for degradation), and macroautophagy, by which cells undergo partial autodigestion to provide nutrients that are necessary to maintain cell viability [424,425]. Macroautophagy is the most well characterized of the three types and is highly conserved [426]. Here, the focus is made on macroautophagy, hereafter referred to as autophagy, because of its involvement in antiviral response and cell death.

Autophagy is mainly activated by stimuli such as starvation, deficiency of nutrients, hypoxic conditions, ER stress, and high temperatures [427]. It plays a role in physiological processes including immunity, survival, development and homeostasis [428]. While it is established that autophagy represents a cytoprotective process, it was suggested that it can also have pro-death functions [427,428]. However, the autophagic death is still in debate, and there is conflicting literature about whether autophagy is simply associated with other types of cell death or if it is a distinct cell death process [429].

Upon autophagy induction, cytoplasmic material is engulfed by double membranes, starting from the formation of a cup-shaped structure called the phagophore to the sequestration into double membrane vesicles, called autophagosomes. Autophagosomes eventually fuse with acidic lysosomes and form autolysosomes, where cargo is degraded [430].

The autophagic processes involve key factors among which several autophagy-related (Atg) proteins (Figure 23).

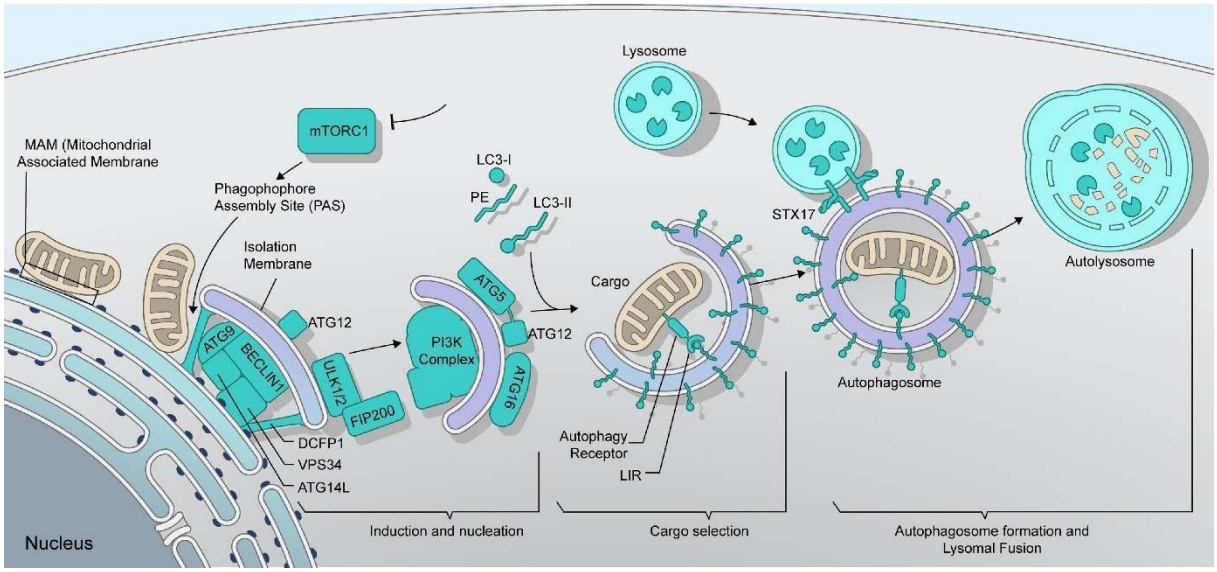

Figure 23- Regulatory processes of autophagy

Autophagy is initiated through inhibition of mTORC1. This results in the recruitment of coordinated induction of nucleation factors that assemble the mitochondrial associated membrane (MAM). The nucleation is followed by conjugation of phosphatidylethanolamine (PE) onto LC3-I, which activates its binding onto the autophagosome membrane by LC3-II. Cargo selection and closure of the autophagosomal membrane allows mature autophagosome formation, which fuses with lysosomes, forming autolysosome, in which cargo is degraded [426,430].

In normal conditions, mammalian target of rapamycin complex 1(mTORC1) strictly inhibits induction of autophagy by imposing an inhibitory phosphorylation on Unc-51-like kinase (ULK1). Under stress conditions, several factors remove this inhibition, such as PTEN, AMPK, and TSC2 [431]. The formation of ULK1 initiation complex, by activation of ULK1 and its association with Atg13/FIP200/Atg101, allows the isolation membrane to expand and leads to the formation of a pre-autophagosomal structure (PAS). This involves the phosphatidylinositol-3-kinase class III (PI3K III) complex that includes Vps34, Beclin 1 (Atg6), and Atg14 [432].

During autophagosome formation, two ubiquitin-like systems, the Atg12 and the Atg8 conjugation systems, are involved to achieve a proper elongation of the phospholipidic isolation membrane (Figure 23). The Atg12 conjugation is initiated by a cascade of ubiquitination involving E1-like Atg7 and E2-like Atg10/Atg5. Atg5 forms then a multimeric complex with Atg12 and Atg16 [433]. Rather than conjugating to another protein, Atg8 conjugation system involves the attachment of ubiquitin-like (Ubl) Atg8/LC3 to phosphatidylethanolamine (PE). Atg8/LC3 is processed by Atg4 and

binds Atg7, which is also involved in the Atg12-Atg5 conjugation. Activated Atg8/LC3 is then transferred to the E2-like enzyme Atg3 and conjugated to PE, forming a tightly membrane-associated form of Atg8/LC3-PE complex [425]. Moreover, Atg12–Atg5 conjugate has an E3-like activity for Atg8/LC3 lipidation [434], and Atg12–Atg5-Atg16 is also required for the correct localization of Atg8/LC3 [435].

For its last steps, autophagy involves the docking of completed autophagosomes with lysosomes. This process involves lysosomal protein LAMP-2 and GTP-binding protein Rab7. Autophagosome fusion with lysosome creates a structure called autolysosome. Within this structure, lysosomal enzymes (mainly cathepsins B, D and L) degrade the constituents of the inner autophagosomal membrane [436,437]

Autophagy is activated upon infection by several viruses, including flaviviruses such as DENV [438,439], WNV [440], ZIKV [426], and TBEV [72]. It can either serve pro- or antiviral functions during viral infections. For instance, ZIKV inhibits Akt-mTOR signaling to induce autophagy and increase virus replication [271]. Moreover, TLRs activation, such as TLR3, TLR4, and TLR7, are able to induce autophagy in macrophages [441,442]

Supporting antiviral function, autophagy induction reduced Sindbis virus replication and induced neuronal apoptosis by interaction of Beclin with the anti-apoptotic protein Bcl-2 [443]. In contrast, studies have shown that autophagy processes can negatively regulate antiviral response to VSV. Indeed, Atg5-Atg12 conjugate binds to RIG-I, impairing its function and abolishing IFN production [444], and autophagy defective cells enhance RLR signaling and resistance to VSV [445]. To counteract this antiviral effect, viruses have evolved to avoid autophagic processes. HSV-1 inhibits autophagy by targeting Beclin 1, and the abolition of this inhibition reduced viral neurovirulence [446,447]. Furthermore, TBEV hides from PRRS in intracellular vesicles that are thought to be induced by autophagy [265]. Several viruses also evolved to use autophagy processes to the benefit of their own replication. Indeed, autophagy can be hijacked and enhance the replication of several viruses, including ZIKV [271], DENV [438], HCV [448], and TBEV [72]

Objectives

TBEV infects the human brain and induces a wide range of neurological disruptions that are likely to be due to neuronal impairment. Several studies, performed on rodent *in vivo* and *in vitro* or on transformed/immortalized human brain cell lines, showed that TBEV infects neurons and astrocytes and impairs cells homeostasis. *Post mortem* analyses of brains from fatal TBE patients provided more knowledge on infected cells in humans and the inflammatory response and infiltrates. Furthermore, primary or iPSC-induced neurons and astrocytes allowed the analysis of human neural cells, and underlined structural changes induced by TBEV.

However, studies using human cells only focused on a specific cell type, neurons or astrocytes, which is not representative of cellular interactions within the CNS. Taking this into account, the **first objective** of my thesis was to develop a model of TBEV infection using a well characterized human differentiated neurons, astrocytes, and oligodendrocytes cultures derived from human neural progenitor cells (hNPCs). This type of multicellular cultures was used by our team and others for studying viruses such as BDV and LACV, highlighting differential impacts on the cell types or a high production of cytokines which can be important for signaling to neighboring cells.

While co-cultures provide a more complex environment than monocultures to study brain cells interactions, it is mandatory to unravel the specific responses of each cell type. For instance, astrocytes and neurons are producers of interferon and respond to its signaling, but in our knowledge, no comparative analysis of the induced antiviral response were performed. The **second objective** of my thesis was then to set up a method for separation of differentiated neurons and astrocytes. To achieve a satisfactory level of enrichment and viability of each cell type, we used magnetic cell sorting, which allows a fast, cost effective and adaptable sorting of cells based on membrane markers.

The enriched populations of neurons and astrocytes, associated with hNPC-differentiated co-cultures of the two cell types, represent original tools to decipher neurotropic viral infections of brain cells and the interactions between the

cell types. Using these newly established cultures, my **third objective** was to use the enriched neurons and astrocytes to decipher the mechanisms of antiviral response in both cell types. We formulated the hypothesis that the physiopathology of TBEV infection and the differential impact observed on neurons and astrocytes is associated to different levels and kinetics of antiviral response that controls viral replication. Exploring this hypothesis will help understand neuronal susceptibility and vulnerability to TBEV-infection.

Overall, this project represents a proof of concept that hNPCs-derived neural cells in co-cultures are adaptable to study the interactions between neurotropic viruses and neurons, astrocytes, and oligodendrocytes, and more interestingly, the interactions between neurons and astrocytes in an infectious environment.

Chapter II: Results

2.1. TBEV infects human brain cells differentiated from fetal neural progenitors

Cultures of human neural progenitor cells (hNPCs) and hNPCs-derived neural cells were previously developed in the laboratory and were used to study the mechanisms by which Borna Disease Virus impairs neuronal differentiation [232,233]. Here, we used hNPCs-derived neural cells to study TBEV-induced neuropathogenesis (experimental design shown in Figure 24). To avoid variability in the differentiation outcome, we exclusively used hNPCs from passage 13 to 15.

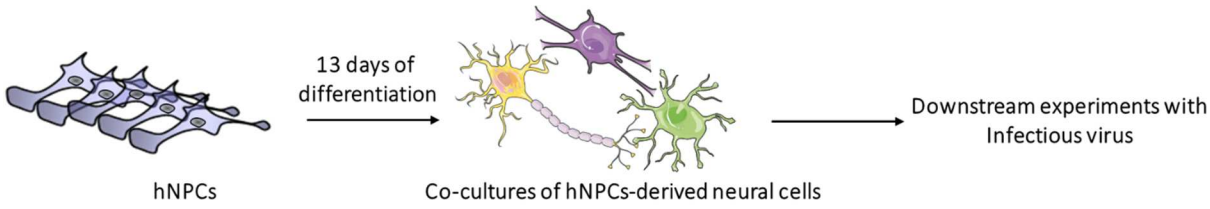

Figure 24 – Experimental design for hNPC-derived neural cells applications.
hNPCs are differentiated into neurons (yellow), astrocytes (green) and oligodendrocytes (magenta). Infections and downstream experiments involving infectious virus are performed at d13 of differentiation. The figure was created using Servier Medical Art (smart.servier.com), licensed under a CC BY 3.0 attribution.

Upon withdrawal of growth factors, hNPCs generate three cell types: neurons, astrocytes and oligodendrocytes. It was previously shown that neurons and astrocytes are the most numerous cells present in the co-cultures [232,233]. However, no enumeration was performed for oligodendrocytes. To precise the relative percentage of each cell population, we first reexamined the cell type composition of hNPCs-derived neural cultures. We differentiated hNPCs for 13 (d13) to 21 days (d21) and performed fluorescent immunostaining using antibodies against HuC/HuD or βIII-Tubulin to mark neurons, GFAP to mark astrocytes and Olig2 to mark oligodendrocytes (Figure 25a). Those markers are widely used for neural cells stainings and are localized either in the nucleus (HuC/HuD and Olig2) or in the cytoskeleton (βIII-Tubulin and GFAP). We automatically quantified neurons and oligodendrocytes using an automated microscope (ArrayScan Cellomics, Thermo Scientific). Due to technical reasons, it was not possible to enumerate GFAP-positive cells using the ArrayScan. Astrocytes were hence considered the remaining

population, and we further confirmed astrocytes enumeration by manual quantification of GFAP-immunostained cells. Our results using automated quantification showed that neural co-cultures contained 77.1±3.2% of neurons, 21.5±4.1% of astrocytes, and 1.4±1.0% of oligodendrocytes at d13 (Figure 25b), confirming previous results in the laboratory. Manual quantification of astrocytes by enumeration of GFAP-positive cells showed a proportion of 22.8±5.6 of astrocytes at d13, which is similar to enumeration of astrocytes using the ArrayScan (Figure 25c). Cell type composition was stable between d13 and d21, confirming that all hNPCs had exited the cell cycle and had entered neuronal or glial pathways by d13.

In all the following experiments, we used 13 day old differentiated hNPCs and performed TBEV infections (Hypr strain) at MOI 10^{-2}. We examined the capacity of the virus to infect, replicate and disseminate into the culture by immunofluorescence at 14 hours post-infection (hpi) as well as days 1, 2, 3, 4, and 7 post-infection (dpi), using an antibody specific to the domain 3 of TBEV envelop (TBEV-E3) (Figure 26a). Observation and enumeration of immunostained cells revealed that while 7.3±0.7% of cells were infected at 14hpi, their number increased to reach 45±4% at 72hpi, the peak of infection (Figure 26b). We constantly observed a decrease in the number of infected cells at 7dpi. This demonstrated that the virus infects and disseminates efficiently in hNPCs-derived brain cells. We further confirmed this by quantification of the viral genome either in the supernatant or intracellularly by RT-qPCR (Figure 26c) and by quantification of infectious particles in the supernatant by TCID50 assays (Figure 26d), from 14hpi to 7dpi. We observed similar profiles, showing an increase in viral genome and particles up to 48-72h followed by a decrease from 96h to 7 days.

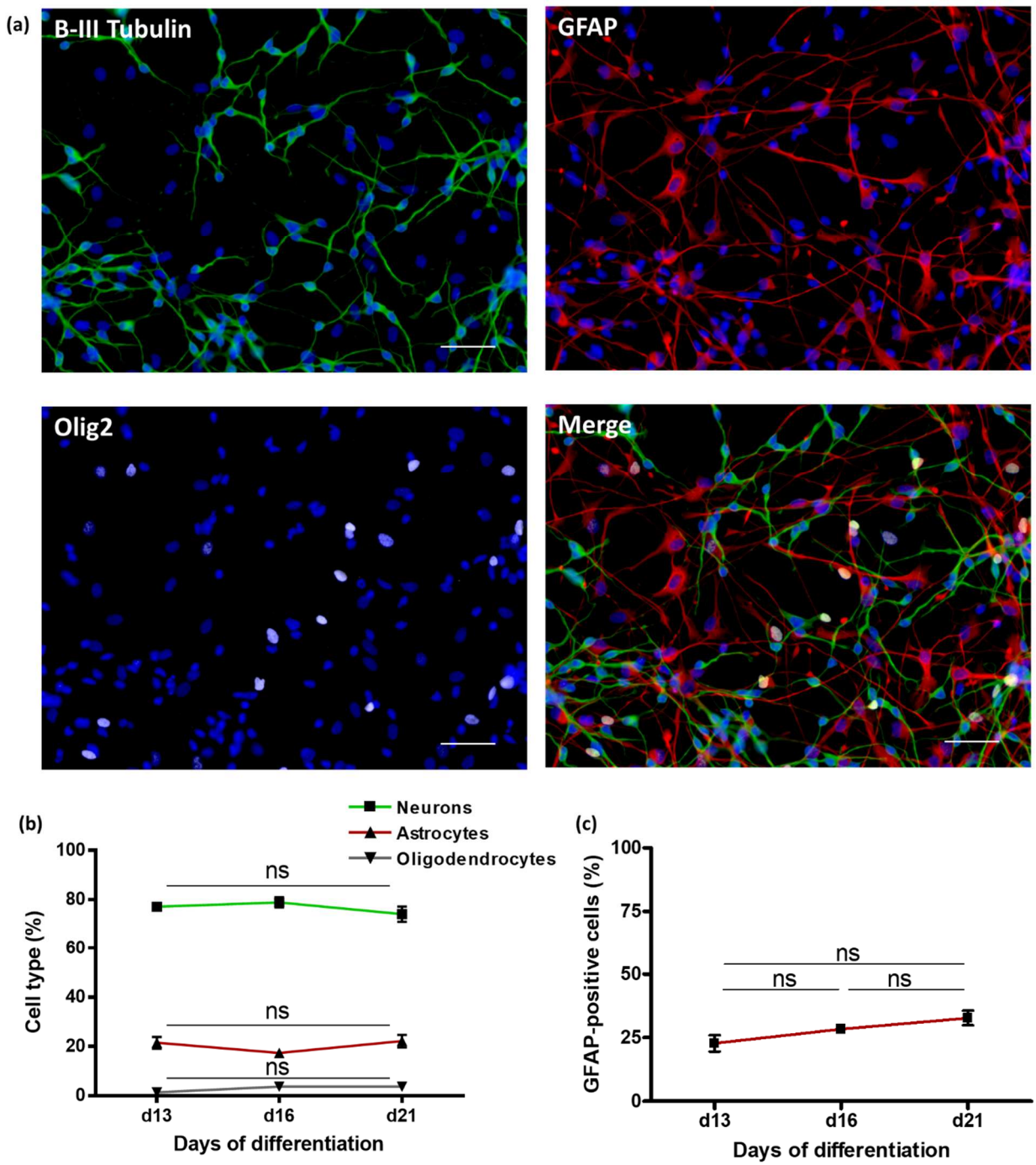

Figure 25 – Cellular composition of hNPCs-derived co-cultures.

(a) Immunostaining of neurons (βIII-Tubulin), astrocytes (GFAP), and oligodendrocytes (Olig2). Scale bar=50µm. (b) Quantification of neurons (HuC/HuD positive cells), astrocytes (HuC/HuD-negative and Olig2-negative cells) and oligodendrocytes (Olig2-positive cells) using the ArrayScan Cellomics. (c) Quantification of astrocytes by manual quantification of GFAP-positive cells using imageJ software. Data in (b) and (c) are expressed as mean±SD. Statistical analyses were performed using one-way ANOVA analysis (Bonferroni's Multiple Comparison Test) on Graphpad Prism V4.0.3, ns=non-significant ($p>0.05$).

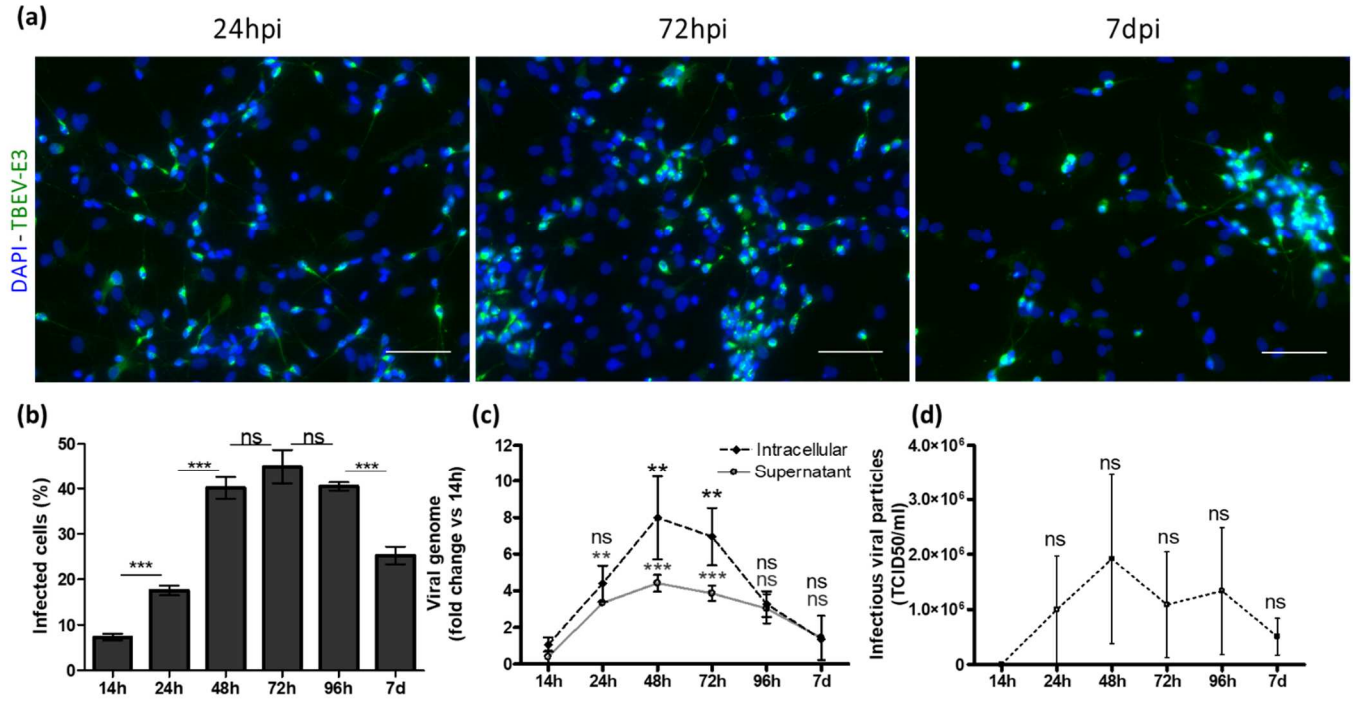

Figure 26 – TBEV infection and replication of hNPCs-derived neural cells.
(a) Immunostaining of TBEV-E3 protein (green) in infected cells at 24hpi, 72hpi, and 7dpi using an anti-TBEV-E3 polyclonal antibody. Nuclei were counterstained with (4',6-diamidino-2-phenylindole) (DAPI, Blue). Scale bar=100µm. (b) Number of infected cells during the course of infection. TBEV-E3 immunostaining was quantified with an ArrayScan Cellomics. (c) Viral genome was quantified by RT-qPCR. d) Infectious particles in the supernatant were quantified by TCID50 plaque assays on Vero cells. Results in (b), (c) and (d) are representative of at least 2 independent experiments performed in triplicate. Data are expressed as mean±SD. Statistical analyses were performed using one-way ANOVA analysis (Bonferroni's Multiple Comparison Test) on Graphpad Prism V4.0.3, ns=non-significant ($p>0.05$); ***=$p<0.001$.

2.2. TBEV infects human neurons, astrocytes, and oligodendrocytes

Human neurons have been shown to be widely infected by TBEV *in vitro* and *in vivo*, but human astrocytes and endothelial cells are also susceptible to the virus infection *in vitro* [72,254,261,280], while oligodendrocytes susceptibility to TBEV is not characterized. To identify TBEV tropism in our cultures, we infected human neural cells and performed immunostainings at different time points (14hpi to 7dpi), using anti-TBEV-E3 antibody and antibodies specific for brain cell markers, as described above. Microscopy analyses showed that, as early as 14hpi, TBEV infected human neurons, astrocytes and oligodendrocytes. Viral antigens were distributed in the cytoplasm, but accumulation of envelop protein was also observed in neurites

and astrocytes outgrowth (Figure 27a). Enumeration of cells from 14hpi to 7dpi revealed that the most important population among infected cells was neurons (81.4±3.5% to 92.2±1.1%) followed by astrocytes (6.2±1.4% to 11.7±5.2%) and oligodendrocytes (1.6±0.3% to 12.1±1.7%) (Figure 27b). We further determined the percentage of infected neurons, astrocytes and oligodendrocytes among their respective subpopulations over time (Figure 15c). Similar profiles were observed between neurons and astrocytes. Infection increased up to 48-72hpi and then decrease by 7dpi. Oligodendrocytes had a similar profile in the beginning of infection but there was no decrease at 7dpi. Importantly, whereas 55.2±3.8% of neurons and 68±21.5% of oligodendrocytes were infected at the peak of infection (72hpi), there was no more than 13.6±5.3% of infected astrocytes. This revealed a similar tropism of TBEV for both neurons and oligodendrocytes and strongly suggested a particular resistance of astrocytes to TBEV infection.

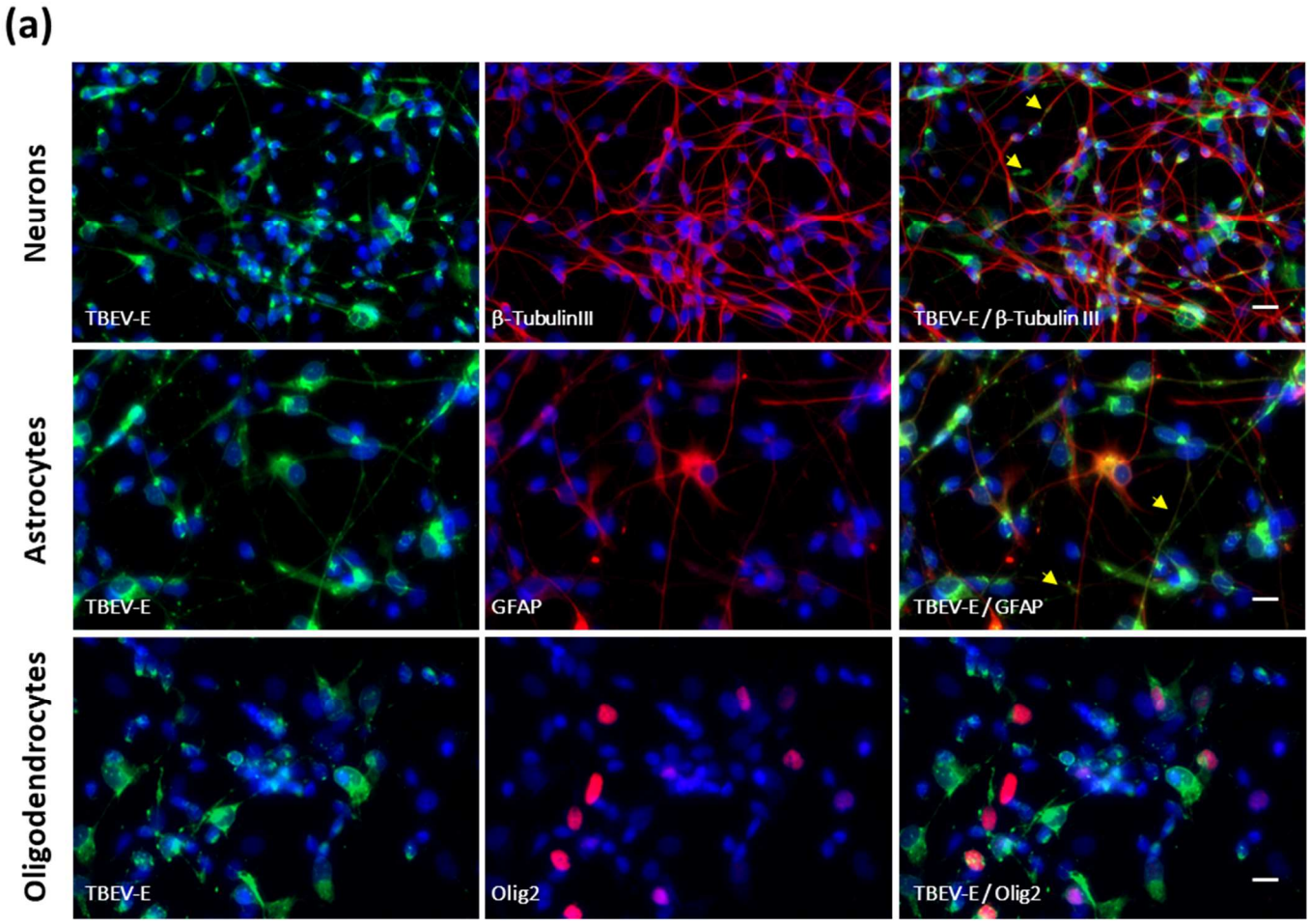

See Figure 27 caption on next page

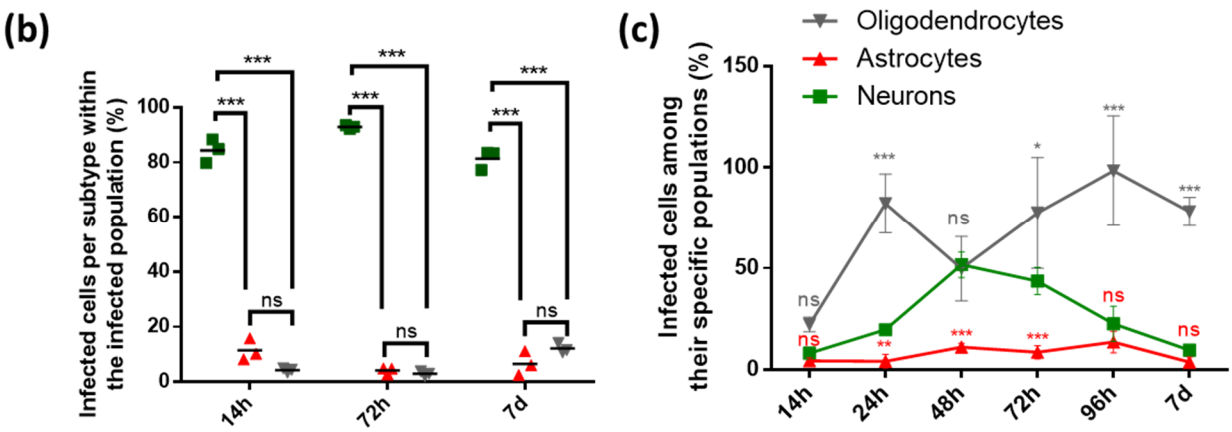

Figure 27 – TBEV infects human neurons, astrocytes, and oligodendrocytes.
TBEV-infected hNPCs-derived neural cells were immunostained with antibodies against βIII-Tubulin (neurons), GFAP (astrocytes), Olig2 (oligodendrocytes), and TBEV-E3 (TBEV) from 14hpi to 7dpi. (a) Photomicrographs showing immunostained cells at 14hpi. Arrowheads show accumulation of viral envelop in neurons and astrocytes outgrowths. Nuclei were counterstained with DAPI. Scale bar=20µm. (b) quantification of TBEV-infected cells per subtype. (c) percentage of infected cells within neuronal (green), astroglial (red) and oligodendroglial (grey)populations, respectively. Cells in (b) and (c) were enumerated using an ArrayScan Cellomics. Astrocytes were estimated as HuC/HuD-negative and Olig2-negative cells. Results are representative of at least 2 independent experiments performed in triplicate. Data in (b) and (c) are expressed as mean±SD. Statistical analyses were performed (vs neurons) using one-way ANOVA analysis (Bonferroni's Multiple Comparison Test) on Graphpad Prism V6.0.1, ns=non-significant ($p>0.05$), *=$p<0.05$, ***=$p<0.001$.

2.3. TBEV induces massive neuronal loss whereas it moderately affects glial cells viability

We showed that TBEV infected neurons, astrocytes, and oligodendrocytes, and that it efficiently replicates in hNPCs-derived neural cultures. We then sought to evaluate TBEV-induced damage on the different cell types, by enumerating their number. As all cells are post-mitotic and quiescent in our cultures, a decrease in their number would indicate a decrease in their viability. We immunostained non-infected (NI) and TBEV-infected neural cells with an antibody directed against βIII-Tubulin or HuC/HuD. Microscopic analysis showed a strong alteration in neurite network at 14dpi (Figure 28a) and an alteration in the number of neurons (Figure **28**b), suggesting that TBEV damages the neurons. Quantification of neurite length using HCS Studio Cell Analysis software V6.6.0 (Thermo Scientific) confirmed neurites alteration as a ≅50% decrease in length was observed as early as 72hpi in TBEV-infected cells compared to their matched NI controls (Figure 28c). Further

analyses of ßIII-Tubulin expression by qRT-PCR showed a decrease in *ßIII-Tubulin* mRNAs as early as 72hpi (Figure 28d). Next, we quantified the number of neurons from 14hpi to 14dpi. We observed that the neuronal population decreased significantly from 72hpi continuously up to 14dpi (Figure 28e), which shows that TBEV alters neuronal viability.

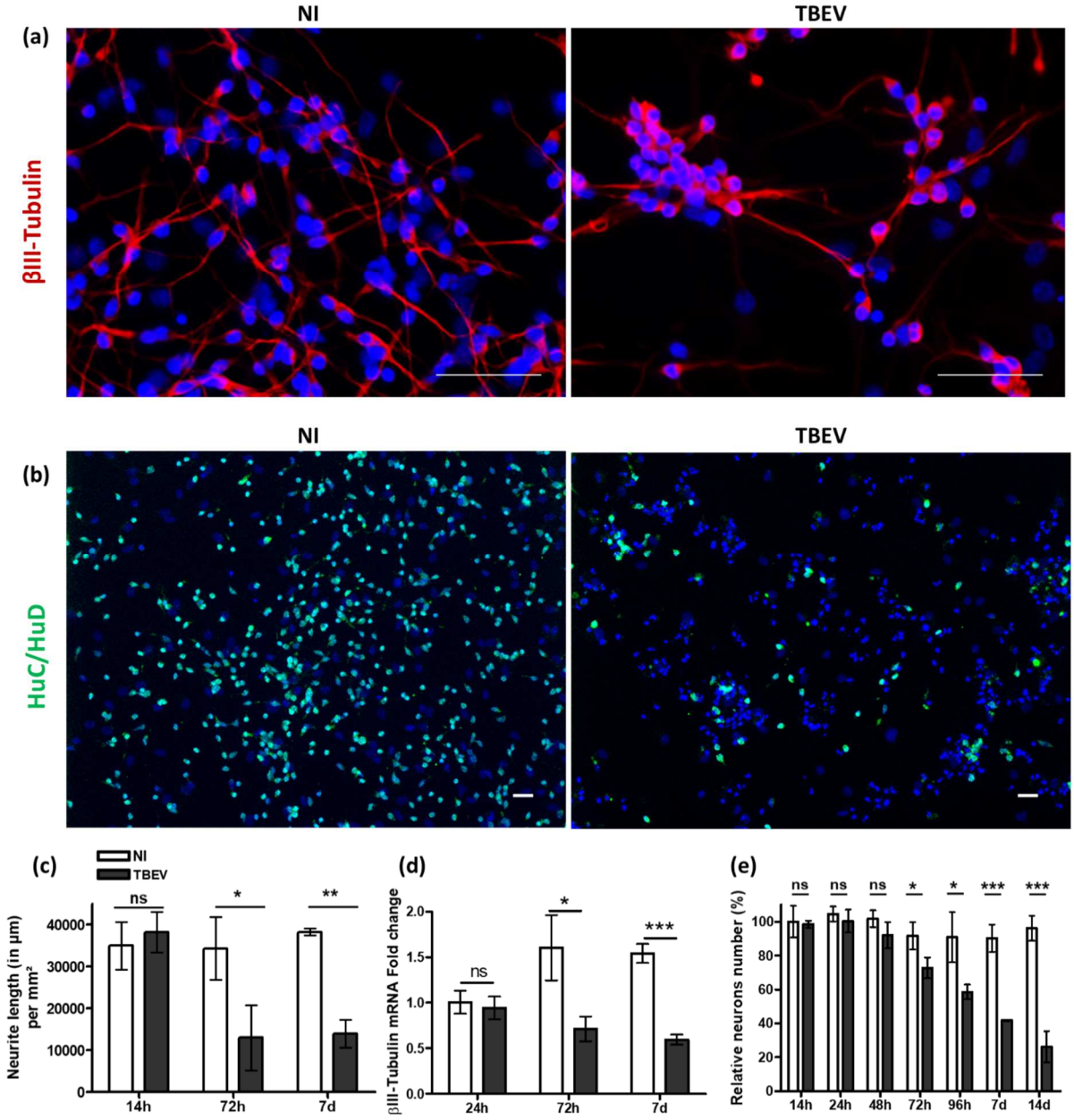

Figure 28 – Impact of TBEV on human neurons.

Immunostaining of (a) ßIII-Tubulin (red) and (b) HuC/HuD (green) in TBEV-infected cells at 14dpi and their matched NI controls. Nuclei were counterstained with DAPI. Scale bars=100µm. (c) evaluation of neurite network density (Neurite length per mm²) using an ArrayScan Cellomics. (d) quantification of *ßIII-Tubulin* mRNAs by qRT-PCR. (e) enumeration of HuC/HuD-positive neurons, using an ArrayScan Cellomics. The number of HuC/HuD-positive cells was normalized to HuC/HuD count in non-infected d13-differentiated cells. X-axis in (c), (d) and (e) represent times post-infection. Results are expressed as mean±SD and

are representative of at least two independent experiments performed in triplicates. Statistical analyses were performed using a two-tailed unpaired t test on Graphpad Prism V4.0.3, ns=non-significant ($p>0.05$); *=$p<0.05$; **=$p<0.01$; ***=$p<0.001$

We have shown that astrocytes are permissive to TBEV although they are infected at lower rates than neurons and oligodendrocytes (Figure 27c). To address the impact of TBEV infection on astrocytes population, we infected hNPCs-derived co-cultures and performed immunostainings of GFAP. Fluorescent imaging showed a difference in astrocytes morphology upon TBEV infection reminiscent of astrogliosis, although not in a systematic way (Figure 29a). qRT-PCR analyses showed variable levels of *GFAP* mRNA between experiments and did not reveal any significant tendency (Figure 29b). We further analyzed the number of astrocytes from 24hpi to 7dpi by manual enumeration of GFAP-positive cells. At 72hpi, a time point at which neuronal loss had already occurred, there was no significant alteration in astrocytes number. However, at 7dpi, we observed a significant decrease of ±30% in their number in TBEV-infected cultures compared to their matched NI controls (Figure **29**c). These data showed that astrocytes, although affected in their number at later stage of TBEV infection, were more resistant than neurons.

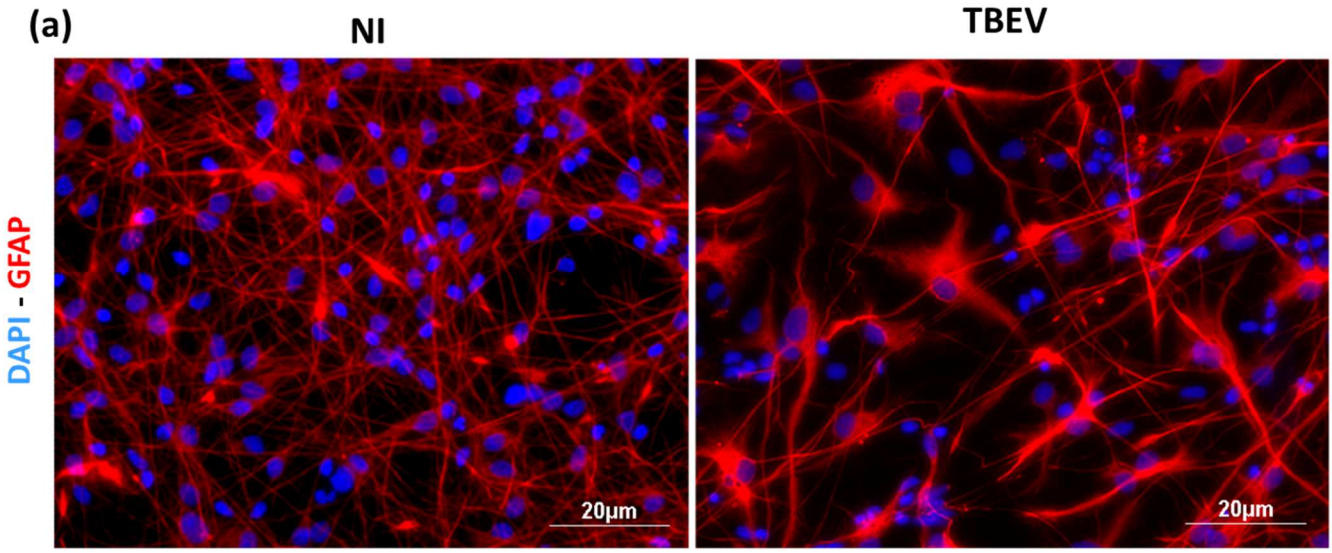

See Figure 29 caption on next page

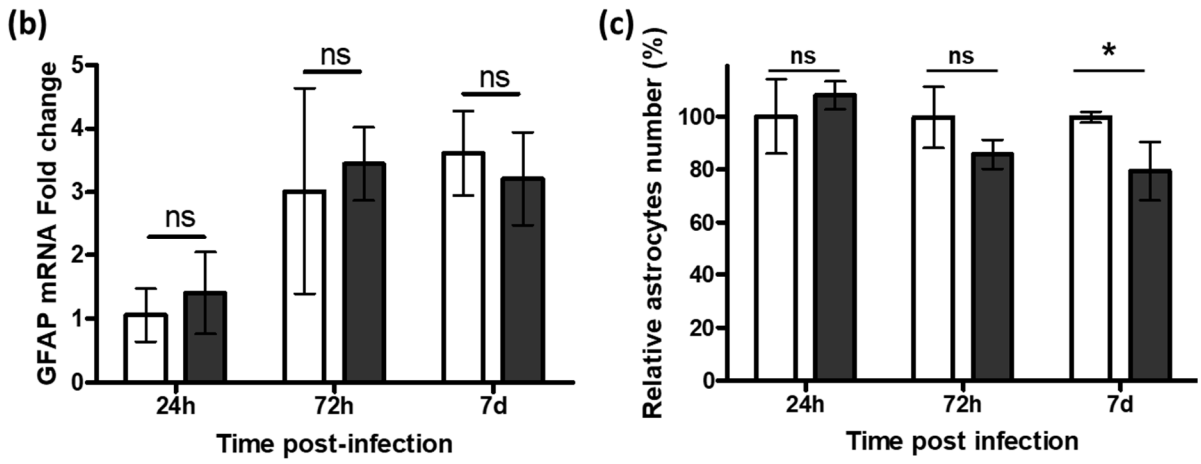

Figure 29 - Impact of TBEV on human astrocytes.
(a) Immunostaining of GFAP in non-infected (NI) and TBEV infected hNPCs-derived neural cells at 7dpi. Scale bar=20µm. (b) quantification of GFAP mRNAs by qRT-PCR. (c) Manual quantification of GFAP-positive cells using ImageJ software. The number of GFAP-positive cells was normalized to NI cells at d13. The results are expressed as mean±SD and are representative of three independent experiments performed in triplicates. Statistical analyses were performed using a two-tailed unpaired t test on Graphpad Prism V4.0.3, ns=non-significant ($p>0.05$); *=$p<0.05$.

Our data also showed that oligodendrocytes, like neurons, were strongly infected by TBEV (Figure 27c). We thus questioned whether TBEV affects their viability. Automated enumeration of Olig2-positive cells did not reveal any significant difference in their number when TBEV-infected cultures were compared to their matched NI cultures (Figure 30), thus showing that despite direct TBEV infection, oligodendrocytes were not affected in their viability.

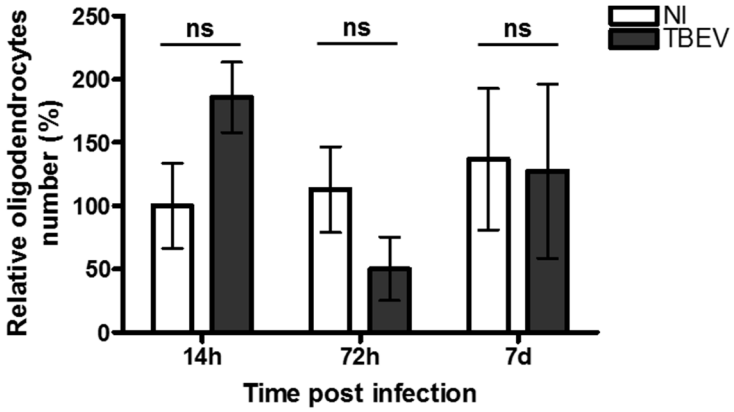

Figure 30 - Impact of TBEV on human oligodendrocytes.
Immunostained cells with Olig2 were quantified using an ArrayScan Cellomics. The number of Olig2 was normalized to NI cells at d13. Results are representative of two independent experiments performed in triplicates. Data are represented as mean±SEM. Statistical analyses were performed using a two-tailed unpaired t test on Graphpad Prism V4.0.3, ns=non-significant ($p>0.05$).

Thereby, our results showed that TBEV infection differently affected three human cellular subpopulations of the CNS, namely neurons, astrocytes and oligodendrocytes. Whereas neurons massively died, astrocytes were moderately affected and oligodendrocytes were not impaired in their survival. This further showed that glial cells were less susceptible to TBEV infection and less affected by TBEV-induced death than neuronal cells.

2.4. TBEV-induced cell death: apoptosis or autophagy?

As the survival of TBEV-infected neurons and astrocytes was reduced as compared to their uninfected counterparts, we sought to determine the molecular mechanisms that could underlie cell death. Apoptosis and autophagy are two pathways by which TBEV alters the cells [72,223]. In order to determine if these two pathways could be involved in TBEV-induced neural cell death, we used human PCR arrays (SABiosciences) to analyze the expression of 84 apoptosis-related genes and 84 autophagy-related genes. Transcripts from hNPCs derived neural cells infected with TBEV for 72 hours were pooled from biological triplicates and compared to their matched NI controls. Studied genes are shown in Table 1 and Table 2. After application of an arbitrary cut off (fold regulation of 3), according to the manufacturer's instructions, our preliminary data showed the upregulation of 15 genes in the apoptosis pathway (*TNFSF10*, *CASP1*, *BIRC3*, *BCL2A1*, *TNFRSF9*, *CASP4*, *TNF*, *CD40*, *HRK*, *CASP8*, *TNFRSF1B*, *CASP5*, *CD70*, *BCL2L10*, and *CASP14*) and 9 upregulated genes in autophagy pathway (*TNFSF10*, *CTSS*, *TNF*, *IGF1*, *TGM2*, *CASP8*, *NFKB1*, *TMEM74*, *DRAM1*, and *EIF2AK3*) (Figure 31a, Supplementary table 2 and Supplementary table 3). *TNFSF10*, coding for TNF-related apoptosis inducing ligand (TRAIL) protein that is involved in the induction of apoptosis, was the most expressed gene in both PCR arrays. In order to validate the PCR array, we addressed the expression of *TNFSF10* (a gene that was found upregulated by TBEV) and *TP53* (*p53*), *Atg3* and *BECN1* (three genes that were not regulated) by RT-qPCR at different time points after infection (Figure 31b). *TNFSF10* up-regulation was confirmed and we further showed that it took place as early as 7hpi and continuously increased up to 14dpi. In contrast, kinetic analyses by qRT-PCR revealed a slight increase in *TP53* and *Atg3* from 48hpi that was not previously shown by PCR array. Finally, the absence

of regulation of *Beclin1*, a major gene of autophagy, was also confirmed at all time points studied.

Table 1 - Apoptosis pathways and genes listed by RT^2 Profiler PCR array Human Apoptosis

Upregulated genes are underlined and presented in bold

Induction of Apoptosis	
Death Domain Receptors	CRADD, FADD, **TNF**, TNFRSF10B (DR5).
DNA Damage & Repair	ABL1, CIDEA, CIDEB, TP53 (p53), TP73.
Extracellular Apoptotic Signals	CFLAR (Casper), DAPK1, TNFRSF25 (DR3).
Other Pro-Apoptotic Genes	BAD, BAK1, BAX, BCL10, BCL2L11, BID, BIK, BNIP3, BNIP3L, **CASP1** (ICE), CASP10 (MCH4), **CASP14**, CASP2, CASP3, **CASP4**, CASP6, CASP8 (FLICE), CD27 (TNFRSF7), **CD70** (TNFSF7), CYCS, DFFA, DIABLO (SMAC), FAS (TNFRSF6), FASLG (TNFSF6), GADD45A, HRK, LTA (TNFB), NOD1 (CARD4), PYCARD (TMS1, ASC), TNFRSF10A (TRAIL-R), TNFRSF9, **TNFSF10** (TRAIL), TNFSF8, TP53BP2, TRADD, TRAF3.
Anti-Apoptotic	
AKT1, BAG1, BAG3, BAX, BCL2, BCL2A1 (BFL1), BCL2L1 (BCLXL), BCL2L10, BCL2L2, BFAR, **BIRC3** (c-IAP2), BIRC5, BIRC6, BNIP2, BNIP3, BNIP3L, BRAF, CD27 (TNFRSF7), CD40LG (TNFSF5), CFLAR (Casper), DAPK1, FAS (TNFRSF6), **HRK**, IGF1R, IL10, MCL1, NAIP (BIRC1), NFKB1, NOL3, RIPK2, TNF, XIAP (BIRC4).	
Regulation of Apoptosis	
Negative Regulation of Apoptosis	BAG1, BAG3, BCL10, BCL2, **BCL2A1** (BFL1), BCL2L1 (BCLXL), **BCL2L10**, BCL2L2, BFAR, BIRC2 (c-IAP1), **BIRC3** (c-IAP2), BIRC6, BNIP2, BNIP3, BNIP3L, BRAF, CASP3, CD27 (TNFRSF7), CD40LG (TNFSF5), CFLAR (Casper), CIDEA, DAPK1, DFFA, FAS (TNFRSF6), IGF1R, MCL1, NAIP (BIRC1), NOL3, TP53 (p53), TP73, XIAP (BIRC4).
Positive Regulation of Apoptosis	ABL1, AKT1, BAD, BAK1, BAX, BCL2L11, BID, BIK, BNIP3, BNIP3L, **CASP1** (ICE), CASP10 (MCH4), CASP14, CASP2, CASP4, CASP6, **CASP8** (FLICE), CD40 (TNFRSF5), **CD70** (TNFSF7), CIDEB, CRADD, FADD, FASLG (TNFSF6), **HRK**, LTA (TNFB), LTBR, NOD1 (CARD4), PYCARD (TMS1, ASC), RIPK2, **TNF**, TNFRSF10A (TRAIL-R), TNFRSF10B (DR5), TNFRSF25 (DR3), **TNFRSF9**, **TNFSF10** (TRAIL), TNFSF8, TP53 (p53), TP53BP2, TRADD, TRAF2, TRAF3.
Death Domain Receptors	
CRADD, DAPK1, FADD, TNFRSF10A (TRAIL-R), TNFRSF10B (DR5), TNFRSF11B (OPG), TNFRSF1A (TNFR1), **TNFRSF1B**, TNFRSF21, TNFRSF25 (DR3), TRADD.	
Caspases & Regulators	
Caspases	**CASP1** (ICE), CASP10 (MCH4), CASP14, CASP2, CASP3, **CASP4**, **CASP5**, CASP6, CASP7, CASP8 (FLICE), CASP9, CFLAR (Casper), CRADD, PYCARD (TMS1, ASC).
Caspase Activation	AIFM1 (PDCD8), APAF1, BAX, **BCL2L10**, **CASP1** (ICE), CASP9, NOD1 (CARD4), PYCARD (TMS1, ASC), TNFRSF10A (TRAIL-R), TNFRSF10B (DR5), TP53 (p53).
Caspase Inhibition	CD27 (TNFRSF7), XIAP (BIRC4).

Table 2 - Autophagy pathways and genes listed by RT^2 Profiler PCR array Human Autophagy

Upregulated genes are underlined and presented in bold

Autophagy Machinery Components	
Autophagic Vacuole Formation	AMBRA1 (NYW1), Atg12, Atg16L1, Atg4A, Atg4B, Atg4C, Atg4D, Atg5, Atg9A, Atg9B, BECN1, GABARAP, GABARAPL1, GABARAPL2, IRGM, MAP1LC3A, MAP1LC3B, RGS19, ULK1, WIPI1.
Vacuole Targeting	Atg4A, Atg4B, Atg4C, Atg4D, GABARAP.
Protein Transport	Atg10, Atg16L1, Atg16L2, Atg3, Atg4A, Atg4B, Atg4C, Atg4D, Atg7, Atg9A, GABARAP, GABARAPL2, RAB24.
Autophagosome-Lysosome Linkage	DRAM1, GABARAP, LAMP1, NPC1.
Ubiquitination	Atg3, Atg7, HDAC6.
Proteases	Atg4A, Atg4B, Atg4C, Atg4D.
Regulation of Autophagy	
Co-Regulators of Autophagy & Apoptosis	AKT1, APP, Atg12, Atg5, BAD, BAK1, BAX, BCL2, BCL2L1 (BCLXL), BECN1, BID, BNIP3, CASP3, **CASP8** (FLICE), CDKN1B (P27KIP1), CDKN2A (p16INK4a), CLN3, CTSB, CXCR4, DAPK1, **DRAM1**, **EIF2AK3**, FADD, FAS (TNFRSF6), HDAC1, HTT, IFNG, **IGF1**, INS, MAPK8 (JNK1), MTOR, **NFKB1**, PIK3CG, PRKAA1 (AMPK), PTEN, SNCA, SQSTM1, TGFB1, **TGM2**, **TNF**, **TNFSF10** (TRAIL), TP53 (p53).
Co-Regulators of Autophagy & the Cell Cycle	BAX, CDKN1B (P27KIP1), CDKN2A (p16INK4a), IFNG, PTEN, RB1, TGFB1, TP53 (p53).
Autophagy Induction by Intracellular Pathogens	**EIF2AK3**, IFNG, LAMP1.
Autophagy in Response to Other Intracellular Signals	CTSD, **CTSS**, DRAM2 (TMEM77), EIF4G1, ESR1 (ERα), GAA, HGS, MAPK14 (p38ALPHA), PIK3C3 (Vps34), PIK3R4, RPS6KB1, **TMEM74**, ULK2, UVRAG.
Chaperone-Mediated Autophagy	HSP90AA1, HSPA8.

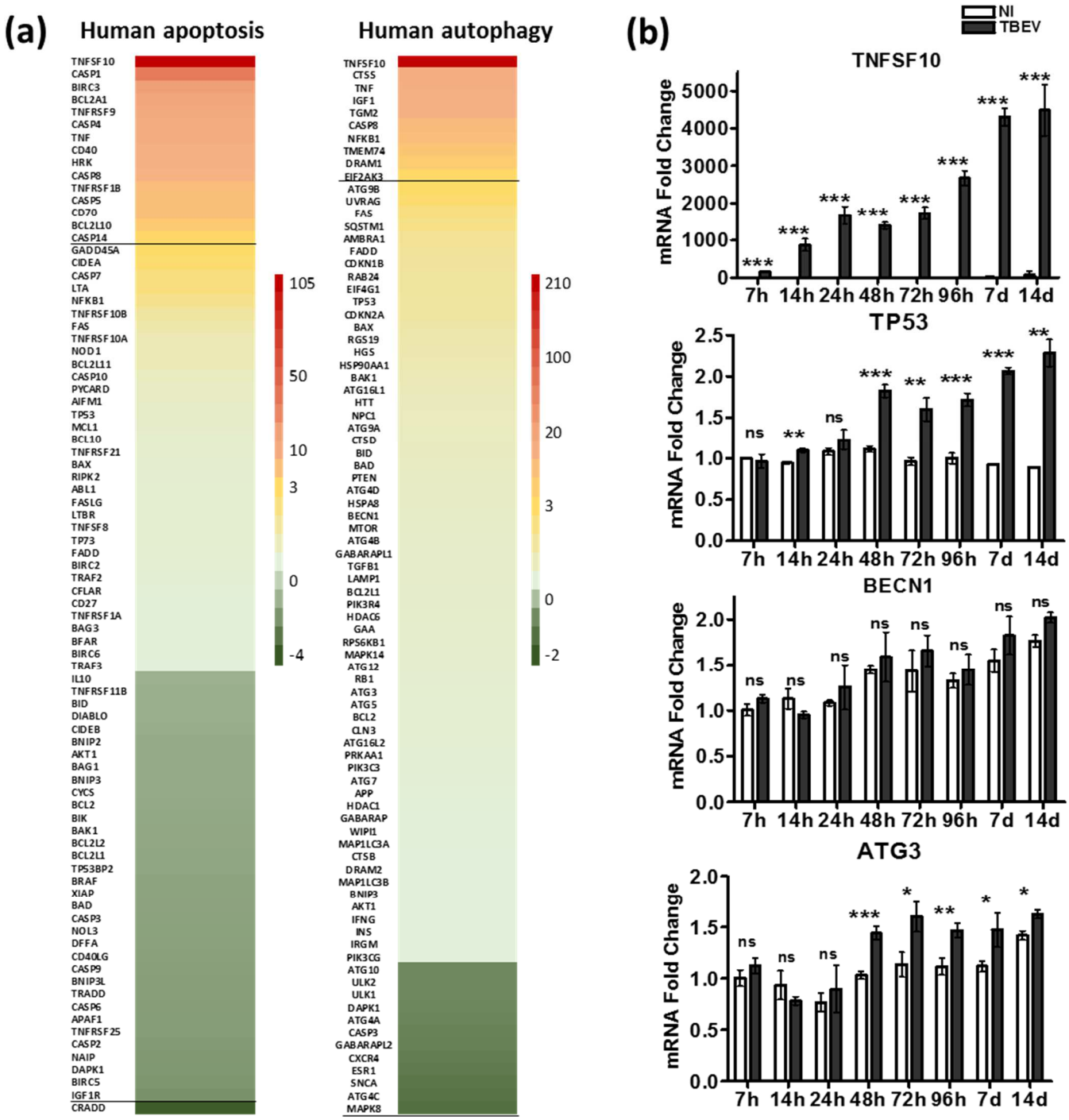

Figure 31 – TBEV-regulation of genes involved in apoptosis and autophagy pathways in hNPCs-derived neural cells.

(a) Fold regulation of 84 human apoptosis genes and 84 human autophagy genes at 72hpi. The heat map shows their differential expression. The most upregulated genes are colored in red and the most downregulated genes are colored in green, according to the color code. The black lines indicate the arbitrary cutoff of three. Genes between the two lines are considered non-regulated. (b) qPCR analysis of apoptosis and autophagy response genes. Data are expressed as mean±SD. Statistical analyses were performed using a two-tailed unpaired t test on Graphpad Prism V4.0.3, ns=non-significant ($p>0.05$); *=$p<0.05$; **=$p<0.01$; ***=$p<0.001$.

Thus, although we observed an up-regulation of co-regulators of apoptosis and autophagy (*TNFSF10*, *TNF*, *CASP8*, *NFKB1*, *IGF1*, *TGM2*), there was little to no modulation of key genes involved in autophagy, such as Atg3 and BECN1. On the contrary, there was a marked induction of apoptotic pathways, suggesting that apoptosis could have driven TBEV-induced neural cell death. We therefore performed DAPI staining on hNPCs-derived neural cells and analyzed nuclei morphology. We observed pyknosis (nuclear shrinkage) and formation of apoptotic bodies in several cells (Figure 32a). To confirm the occurrence of apoptotic events, we also performed a TUNEL assay. Quantification of TUNEL staining revealed an increase in TBEV-infected cultures from 72hpi to 14dpi compared to their matched NI controls (Figure 32b). To address activation of apoptosis pathways in the specific neuronal population, we quantified cleaved caspase 3 immunostaining in neurons (HuC/HuD- and cleaved caspase 3 positive cells). Caspase 3 cleavage in neurons was higher in TBEV-infected cultures at 72hpi and 7dpi (Figure 32c). Thus, our results confirmed that apoptosis was involved in TBEV-induced cell loss, in particular in neurons.

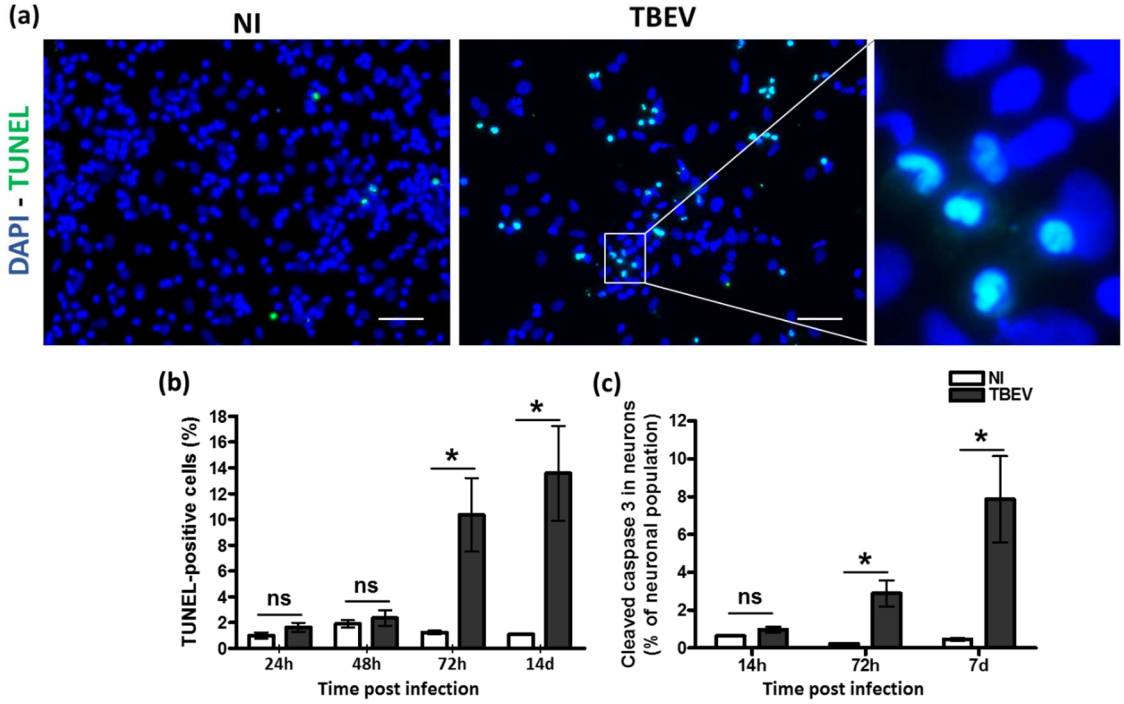

Figure 32 – Apoptosis in TBEV-infected neural cells.
(a) TBEV-infected cells at 7dpi and their matching NI controls were stained using TdT-mediated dUTP Nick-End Labeling (TUNEL) assays. Note the TUNEL staining (in green) and pyknotic cells on the magnification image of TBEV-infected cells. (b) Quantification of TUNEL-positive cells using an ArrayScan Cellomics. (c) Quantification of cleaved caspase 3 and HuC/HuD immune-positive cells, normalized to the neuronal population at each time point. Data in b) and c) are expressed as mean±SD, and are representative of one experiment performed in triplicate. Statistical analyses were performed using a two-tailed unpaired t test on Graphpad Prism V4.0.3, ns=non-significant ($p>0.05$); *=$p<0.05$.

2.5. Human neural cells develop a strong antiviral response to TBEV infection

When infected with a virus, cells are capable of defending themselves by expressing factors that will tend to control viral replication. In order to determine whether TBEV infected human neural cells are able to develop such an antiviral response, we analyzed the expression of 84 genes involved in human antiviral response by using a specific PCR array (SABiosciences). Transcripts from hNPCs-derived neural cells infected with TBEV for 24h were pooled from biological triplicates and compared with their matched NI-controls. All genes studied are shown in Table 3.

Table 3 - Antiviral response pathways and genes listed by RT2 Profiler PCR array Human Antiviral response

Upregulated genes are underlined and presented in bold

Toll-Like Receptor (TLR) Signaling	
Toll-Like Receptors & Chaperones	CTSB, CTSL, **CTSS**, **TLR3**, TLR7, TLR8, TLR9.
Signaling Downstream of Toll-Like Receptors	CHUK (IKKα), FOS, IKBKB (IKKβ), IRAK1, IRF3, IRF5, **IRF7**, JUN, MAP2K1 (MEK1), MAP2K3 (MEK3), MAP3K7 (TAK1), MAPK1 (ERK2), MAPK14 (p38ALPHA), MAPK3 (ERK1), MAPK8 (JNK1), **MYD88**, NFKB1, **NFKBIA** (IκBα, MAD3), RELA, RIPK1, SPP1, TBK1, TICAM1 (TRIF), TNF, TRAF3, TRAF6.
Toll-Like Receptor Signaling Responsive Genes	CCL3 (MIP-1A), **CCL5** (RANTES), CD40 (TNFRSF5), CD80, CD86, **CXCL10** (INP10), **CXCL11** (I-TAC, IP-9), **CXCL9** (MIG), IFNA1, IFNA2, **IFNB1**, IL12A, IL12B, **IL15**, IL1B, IL6.
NOD-Like Receptor (NLR) Signaling	
Receptors & Signaling Molecules	AIM2.
NOD-Like Receptors & Signaling Molecules	CARD9, **CASP1** (ICE), HSP90AA1, **MEFV**, NLRP3, NOD2, **OAS2**, PSTPIP1, PYCARD (TMS1, ASC), PYDC1 (POP1), SUGT1.
NOD-Like Receptor Signaling Responsive Genes	IL1B, IL18.
RIG-I-Like Receptor Signaling	
Receptors & Chaperones	CYLD.
RIG-I-Like Receptors & Chaperones	DAK, **DDX58** (RIG-I), **DHX58** (LGP2), **IFIH1** (MDA5), **ISG15** (G1P2), **TRIM25**.
Signaling Downstream of RIG-I-Like Receptors	Atg5, AZI2, CASP10 (MCH4), CASP8 (FLICE), CHUK (IKKα), DDX3X, FADD, IKBKB (IKKβ), IRF3, IRF7, MAP3K1 (MEKK1), MAP3K7 (TAK1), MAPK14 (p38ALPHA), MAPK8 (JNK1), MAVS, NFKB1, **NFKBIA** (IκBα, MAD3), PIN1, RELA, RIPK1, TBK1, TNF, TRADD, TRAF3, TRAF6.
RIG-I-Like Receptor Signaling Responsive Genes	**CXCL10** (INP10), IFNA1, IFNA2, **IFNB1**, IL12A, IL12B, **CXCL8**.
Type I Interferon Signaling & Response	
Type I Interferon Signaling	IFNA1, IFNA2, IFNAR1, **IFNB1**, **STAT1**.
Interferon Responsive Genes	**APOBEC3G**, **IL15**, **ISG15** (G1P2), **MX1**, **TLR3**.

After applying an arbitrary cut-off (fold regulation >3), 23 genes were shown to be upregulated in TBEV-infected cells among which were PRRs, cytokines including IFNβ, and ISGs (Figure 33a, Supplementary table 4). The overexpression of nine of

those genes was confirmed using qRT-PCR, namely *DDX58* (RIG-I), *TLR3*, and *IFIH1* (MDA5) as PRRs, *CXCL10*, *CCL5* (RANTES), and *CXCL11* as proinflammatory cytokines, and *ISG15*, *OAS2*, and *MX1* as ISGs. For these nine genes as well as two additional ISGs, *ISG56* and *IFI6*, kinetic analysis revealed that the antiviral response was initiated as early as 7hpi and maintained up to 14dpi, with the exception of proinflammatory cytokines whose expression decreased at 14dpi (Figure 33b). Thus, TBEV-infected hNPCs-derived neural cells developed a strong antiviral response in order to control TBEV replication.

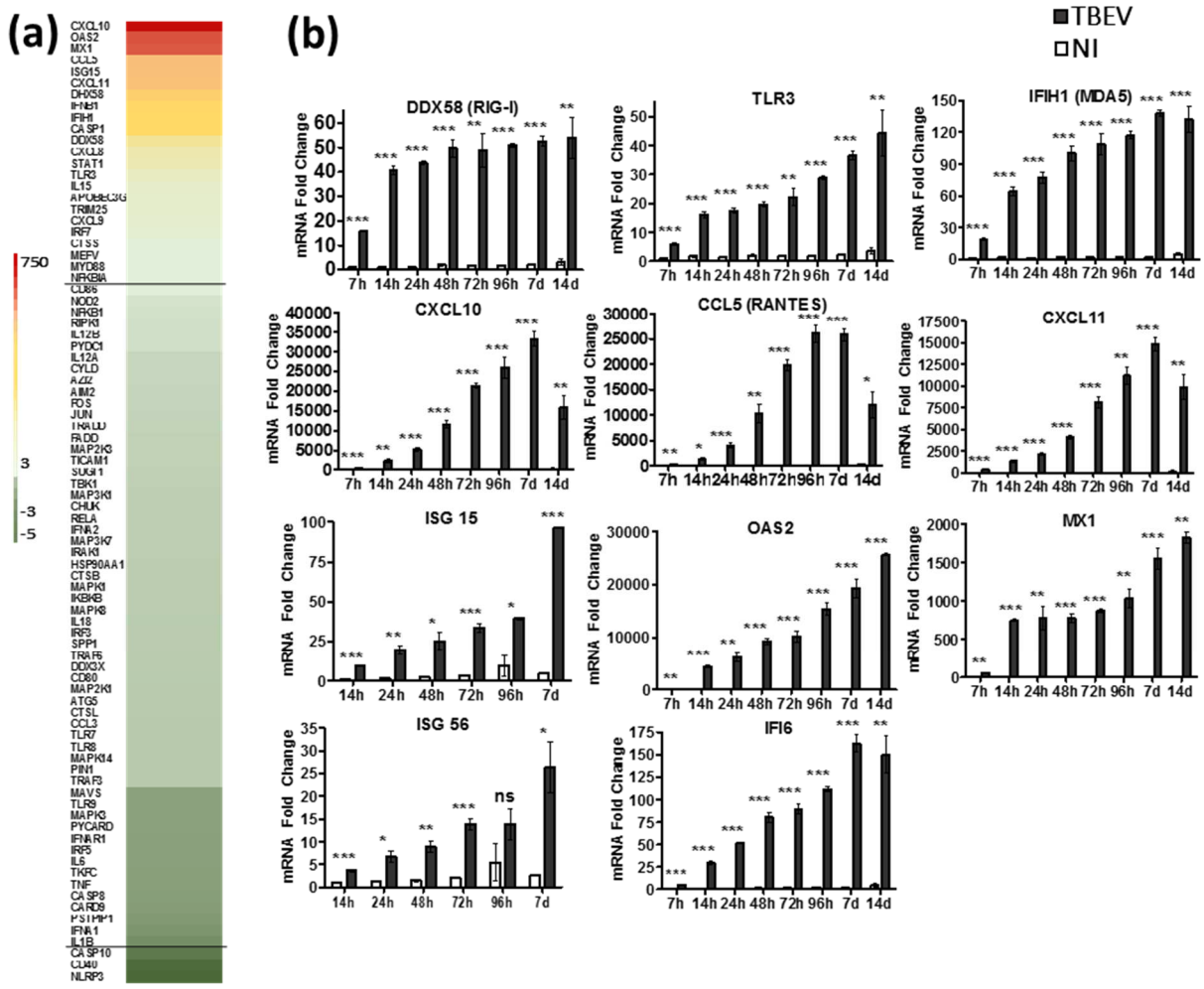

Figure 33 - TBEV-induced antiviral response in hNPCs-derived neural cells.
(a) TBEV-infected neural cells and their matched NI controls were analyzed 24hpi using an RT^2 Profiler PCR array specific to human antiviral response. The heat map shows the differential expression of 84 human genes. The most upregulated genes are colored in red and the most downregulated genes are colored in green, according to the color code. The black lines indicate the arbitrary cutoff of 3. Genes between the two lines are considered non-regulated. Results are representative of one experiment performed on pooled triplicates. (b) qPCR analysis of key antiviral response genes expression. Data were normalized using ΔΔCt. They are expressed as mean±SD. Results are representative of two experiments performed in triplicate. Statistical

analyses were performed using a two-tailed unpaired t test on Graphpad Prism V4.0.3, ns=non-significant ($p>0.05$); *=$p<0.05$; **=$p<0.01$; ***=$p<0.001$

2.6. TBEV induces an antiviral response in human neurons and human astrocytes

Our results showed a strong antiviral response in TBEV-infected hNPCs-derived neural cells and a difference in susceptibility and vulnerability of human neurons, astrocytes and oligodendrocytes. Thus, we hypothesized that intrinsic capacities to antiviral defense, specific to each cellular type, may underlie these differences. In order to test this hypothesis, we developed a protocol to obtain enriched cultures either in neurons (further called En-Neurons) or in astrocytes (further called En-Astrocytes).

2.6.1. Experimental design for enrichment of neurons and astrocytes

To obtain enriched cultures of neurons and astrocytes, we used Magnetic-Activated Cell Sorting (MACS) technology (Miltenyi Biotec). This method is based on antibody-conjugated magnetic beads passed through a magnet-associated column. While fast ready-to-use kits are commercialized for the isolation of murine neurons and astrocytes, there is no equivalent for human neural cells. We thus developed a two-step binding protocol based on biotinylated-cell specific antibodies and anti-biotin conjugated microbeads. Two cell specific antibodies were available for human neural cell sorting. They were directed against either Polysialylated Neuronal Cell Adhesion Molecule (PSA-NCAM) to bind neurons, or Glutamate Aspartate Transporter (GLAST or ACSA-1) to bind astrocytes. We evaluated the expression of PSA-NCAM and GLAST in hNPCs-derived neural cells using fluorescent antibodies and qRT-PCRs. Although PSA-NCAM mRNA was detected (Figure 34a), we did not observe any immuno-positive staining using a specific antibody (Figure 34b). Accordingly, cell-sorting experiments using PSA-NCAM-associated magnetic beads did not result in binding neuronal cells nor in sorting the cells into two distinct populations. Using LD columns that are designed for positive selection (binding the population of interest and stringent depletion of unbound cells), we quickly observed a clogging of the column that did not allow the pursuit

of the sorting. Hence, it was not possible to perform a positive selection of neurons using anti-PSA-NCAM specific antibodies. We thus sought to perform the cell sorting by negative selection of neurons using an anti-GLAST antibody. We first verified that GLAST mRNAs were detectable by qRT-PCR (Figure 34c) and that GLAST antibodies allowed the recognition of astrocytes in the hNPCs-derived neural cells (Figure 34d). MS columns optimized for negative selection (depleting strongly magnetically labeled cells) were used. The MS columns showed a slight clogging, and were suitable for the pursuit of cell sorting protocol.

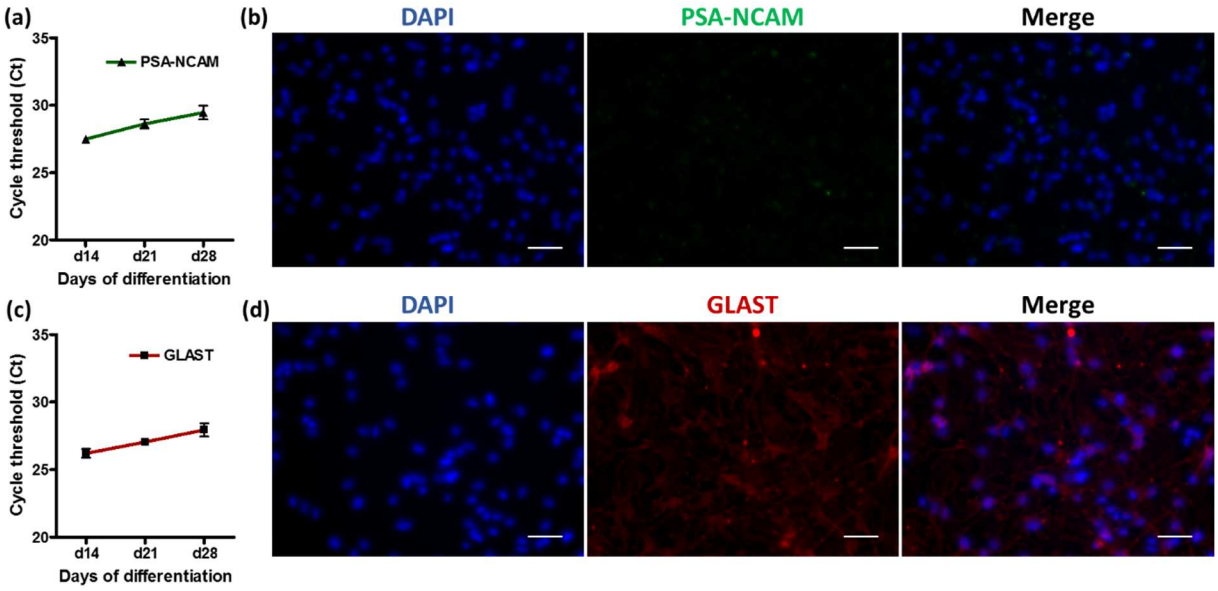

Figure 34 - Expression of GLAST and PSA-NCAM in hNPCs-derived neural cells.
hNPCs were differentiated for 14 to 28 days and PSA-NCAM or GLAST were detected by qRT-PCR (a,c) or by immunostaining (b,d) at d14. Non-normalized cycle threshold (Ct) are shown in (a) and (c). Note the absence of PSA-NCAM immunostaining (panel b), and presence of GLAST immunostaining (red, panel d). Cells were counterstained with DAPI. Scale bar = 50µm.

Combining anti-GLAST antibodies and MS columns, we used the experimental setting as shown in Figure 35a (fully described in material and method section). Thirteen day-old differentiated neural cells were sub-cultured and either directly plated as previously described (unsorted cells) or loaded on MS columns after incubation with an anti-GLAST antibody and anti-biotin microbeads. Enriched neurons were recovered from the flow through whereas enriched astrocytes were obtained after elution of the bound population. We faced two challenges: [1/] meet the right conditions for neurons survival after sorting and [2/] perform an efficient

antibody based cell sorting. We worked on optimizing the medium composition to enhance neuronal survival. We observed that supernatant of co-cultures (containing ≅30% astrocytes) used as conditioned medium is favorable for neuronal survival without further addition of growth or neurotropic factors. We further confirmed that unsorted cells were comparable to non-subcultured neural cells. There was indeed no obvious difference in cell morphology, as observed by phase contrast imaging. Short neuronal outgrowths were visible as early as 24h after sorting and a normal network of neurites had grown after 3 to 4 days, showing that neurons were not affected by the sorting protocol (Figure 35b). Next, to assess the enrichment of each subpopulation in enriched fractions, we performed fluorescent immunostainings using antibodies directed against specific cell markers: HuC/HuD for neurons, GFAP for astrocytes and Olig2 for oligodendrocytes (Figure 35c). Immunofluorescence imaging analysis showed viable cells in each fraction. Astrocytes had a normal morphology immediately after adhesion. Oligodendrocytes were observed both in the En-Neurons and En-Astrocytes cultures. We then enumerated the three cell types in each culture. In unsorted cells, the culture was similar to the non-subcultured one (74.1±4.1% neurons and 20.8±4.9% astrocytes). In En-Neurons, neuronal population increased to 94.1±0.4 of neurons, and in En-Astrocytes, astrocytes population increased to 53.5±2.7% of astrocytes. The oligodendrocytes represented 10.8±0.5% of En-Astrocytes cultures and 2.8±0.2% of En-Neurons cultures (Figure 35d). Thus, we developed a method to obtain cultures enriched in either neurons or astrocytes that is suitable to address neural cells response to viral infections.

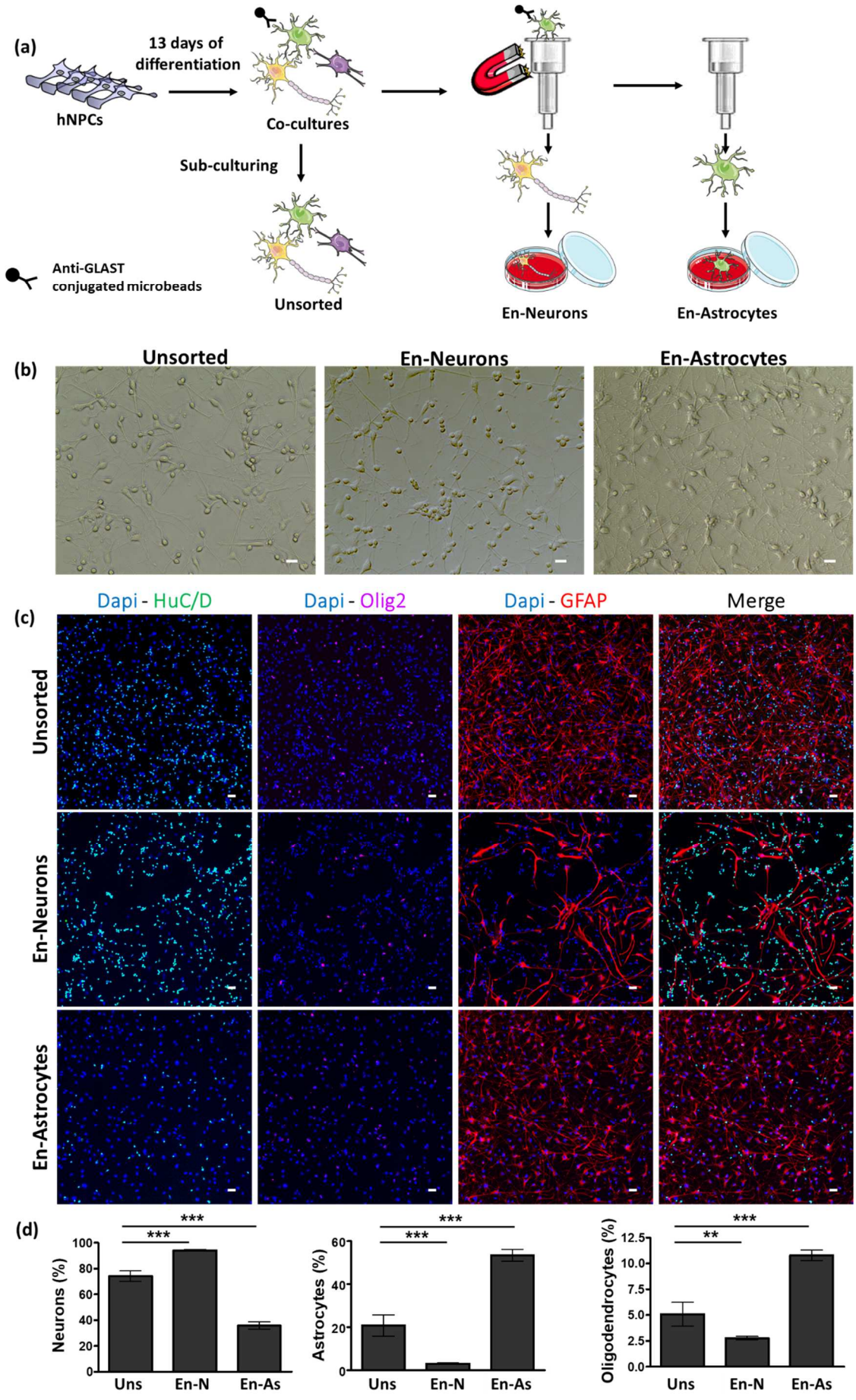

See Figure 35 caption on next page

Figure 35 – Enrichment of human neurons and human astrocytes by Magnetic-Activated Cell sorting.

(a) Experimental setting for magnetic sorting of neurons and astrocytes using MACS. The figure was created using Servier Medical Art (smart.servier.com), licensed under a CC BY 3.0 attribution. (b) hNPCs-derived neural cells at d13 of differentiation were sorted using the developed MACS protocol. Phase-contrast micrographs of cells were acquired 24h after sorting. Scale bars=20µm. (c) Unsorted cultures (Uns), enriched neurons (En-N) and enriched astrocytes (En-As) were immunostained with anti-HuC/HuD (neurons, green), anti-GFAP (astrocytes, red), and Anti-Olig2 (oligodendrocytes, magenta) antibodies. Scale bars=100µm. (d) sorted and unsorted hNPCs-derived neural cells were immunostained with specific antibodies and enumerated with an ArrayScan Cellomics 4 days after sorting. Data are representative of 4 experiments performed in triplicate. Statistical analyses were performed using a two-tailed unpaired t test on Graphpad Prism V4.0.3, ns=non-significant ($p>0.05$); **=$p<0.01$; ***=$p<0.001$.

2.6.2. Antiviral response to TBEV infection is weaker in human neurons than in human astrocytes

As a difference in neurons and astrocytes susceptibility and vulnerability to TBEV infection may be explained by a different basal level expression of antiviral response genes, we first used the previously described PCR array to compare the level of expression of 84 human antiviral response genes in NI En-Neurons and NI En-Astrocytes. In both cultures, the basal level of expression was low. Most of the genes were indeed weakly expressed, as shown by Ct values >30 (50 genes in astrocytes and 42 genes in neurons) (Supplementary table 5). Importantly, for most studied genes, there was no major difference in their level of expression in En-neurons and En-astrocytes (Figure 36a). Seventeen genes were differentially expressed in our experimental setting (fold >3), with either a higher expression in astrocytes (*CASP1*, *CTSL*, *FOS*, *IFIH1* –MDA5-, *IL12A*, *IRF3*, *ISG15*, *MAP2K3*, *STAT1*, *TICAM1*, *TLR3*, *TRADD*, *TRAF3*, and *TRIM25*) or in neurons (*CARD9*, *IFN6,* and *TLR9*). However, all genes were distributed along the black line on the scatter plot (Figure 36a) indicating that while their expression might be slightly different, it tends to be globally comparable in neurons and astrocytes. Using RT-qPCR analyses, we further analyzed *OAS2* and *IFNa* expression and showed no difference in En-Neurons and En-Astrocytes, therefore validating the PCR array results (Figure 36b). The expression of RSAD2 (viperin) was also compared, and again, no difference was observed (figure 13b). Thus, our results suggested that the overall basal expression levels of antiviral response genes are comparable between En-Neurons and En-Astrocytes.

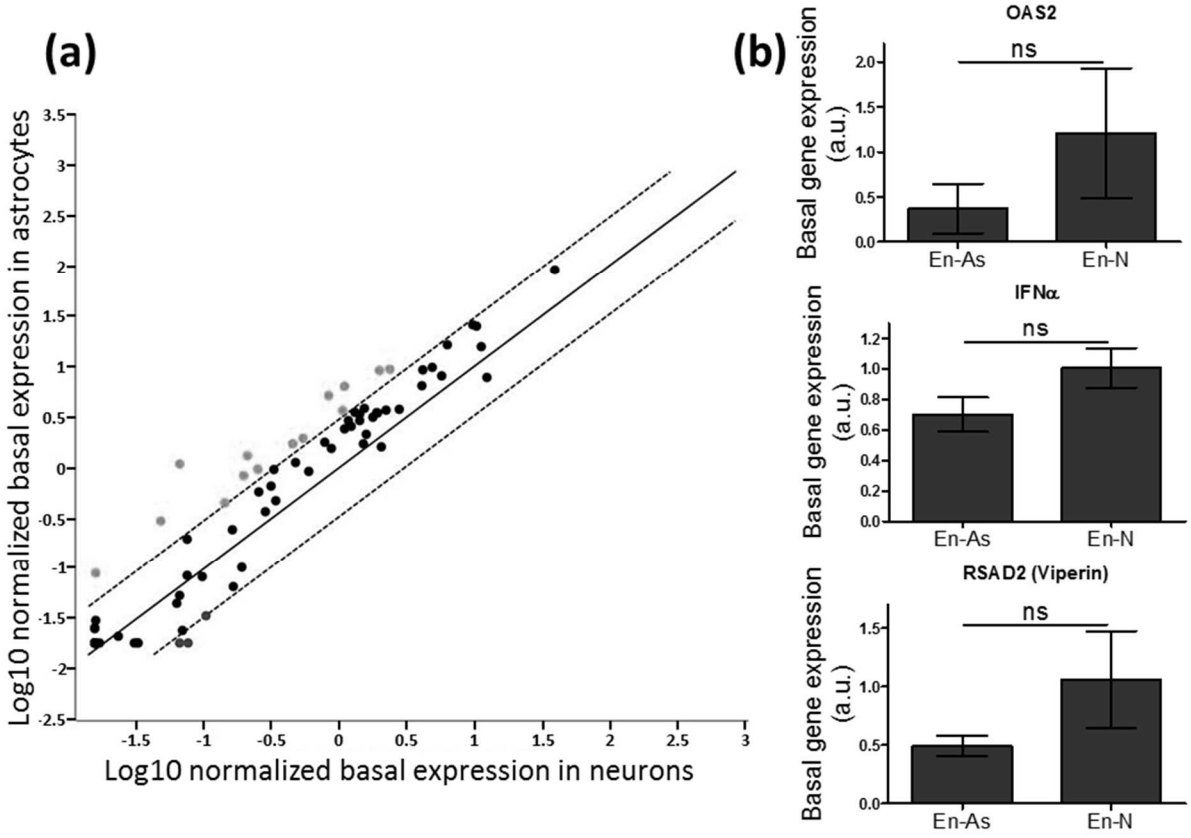

Figure 36 – Basal level of antiviral response genes in En-Neurons and En-Astrocytes.

(a) Scatterplot of basal levels of antiviral response genes analyzed using an Antiviral Response PCR array. Genes along the black line have similar expression levels between neurons and astrocytes. Dotted lines represent the arbitrary cut off (fold expression=3). Each grey dot represents a gene with a fold expression >3 and each black dot represents a gene with a fold expression <3. Data are representative of one experiment performed with material from pooled triplicates. (b) qPCR analysis of antiviral response genes in TBEV-infected En-Astrocytes (En-As) and En-Neurons (En-N). Fold expression normalized to *HPRT1* using ΔΔCt is shown in arbitrary units (a.u.). The results are expressed as mean±SD. Data are representative of two independent experiments performed in triplicate. Statistical analyses were performed using a two-tailed unpaired t test on Graphpad Prism V4.0.3, ns=non-significant ($p>0.05$); *=$p<0.05$; **=$p<0.01$; ***=$p<0.001$.

The difference in susceptibility and vulnerability might also be explained by differential levels of antiviral response gene expression. We then sought to determine whether neurons and astrocytes were capable of producing a different antiviral response upon TBEV infection, qualitatively and/or quantitatively. We first verified that unsorted cells had the same antiviral response as non-subcultured neural cells. This was indeed the case, as shown in Supplementary table 4 and Supplementary table 5. Thus, the

sub-culturing of cells did not activate any antiviral program. Using the PCR array, we then compared the expression of antiviral response genes in En-Neurons, En-Astrocytes and unsorted cultures infected with TBEV for 24 hours (Figure 37a). Most genes that were up-regulated in En-Neurons were also up-regulated in En-Astrocytes, except for two of them, coding for the cytokines IL15 and IL12B. This suggested the activation by TBEV of a similar antiviral program in both human neurons and human astrocytes. However, genes up-regulation was stronger in En-Astrocytes than in En-Neurons, showing that, while similar genes were overexpressed in the two cellular types, they were not induced with the same intensity. This revealed that although using a similar program, astrocytes were capable of developing a stronger antiviral response than neurons upon TBEV infection. To validate the PCR array results and to get further insight into the kinetics of expression of these genes, we performed a qRT-PCR analysis at 7hpi, 24hpi, and 72hpi for *DDX58* (RIG-I), *IFIH1* (MDA5), *TLR3*, *OAS2*, *MX1*, and *CXCL10* genes (Figure 37b). Analysis of *RSAD2* (viperin) was added, as it is known to be an important player in TBEV antiviral response [396,397]. All genes were significantly more overexpressed in En-Astrocytes than in En-Neurons at 24hpi, including *RSAD2*, which confirmed the PCR array data. Interestingly, five of those genes (*DDX58*, *IFIH1*, *TLR3*, *OAS2*, and *RSAD2*) were significantly more up-regulated in En-Astrocytes as early as 7hpi and four of them (*IFIH1*, *TLR3*, *OAS2*, and *RSAD2*) were not up-regulated at all at this time point in En-Neurons. Furthermore, in En-Neurons, *RSAD2* was not upregulated at any time point considered. This showed that, in addition to a weaker antiviral response in En-Neurons compared to En-Astrocytes, the antiviral response was delayed and one gene, *RSAD2*, coding for viperin, was not upregulated. Thus, TBEV activated a globally similar antiviral program in both neurons and astrocytes, but with a different intensity and kinetics, which could conduct to a reduced efficiency in neurons. However, part of the activated program was different, as at least one gene, *RSAD2*, was upregulated in astrocytes but not in neurons.

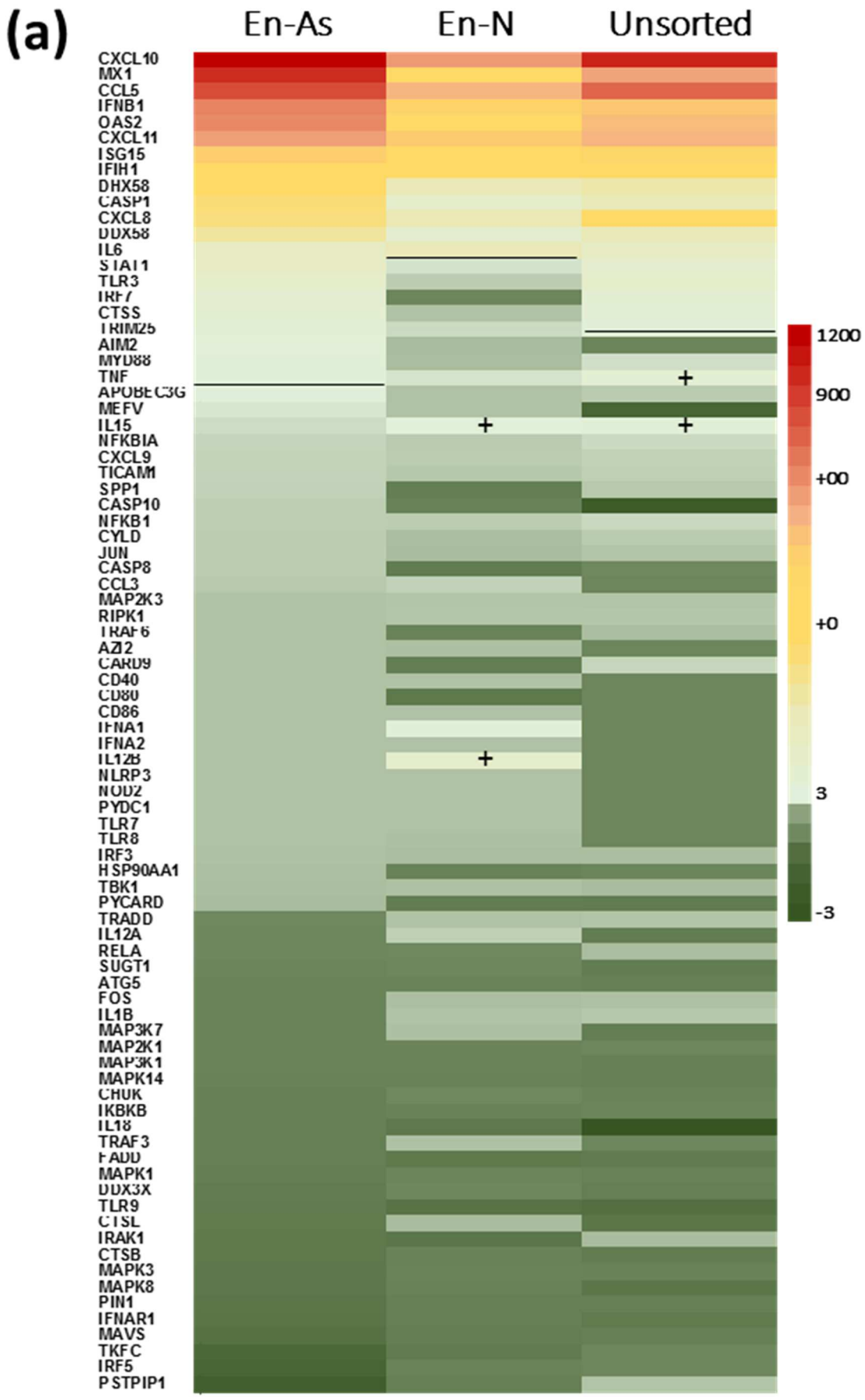

See Figure 37 caption on next page

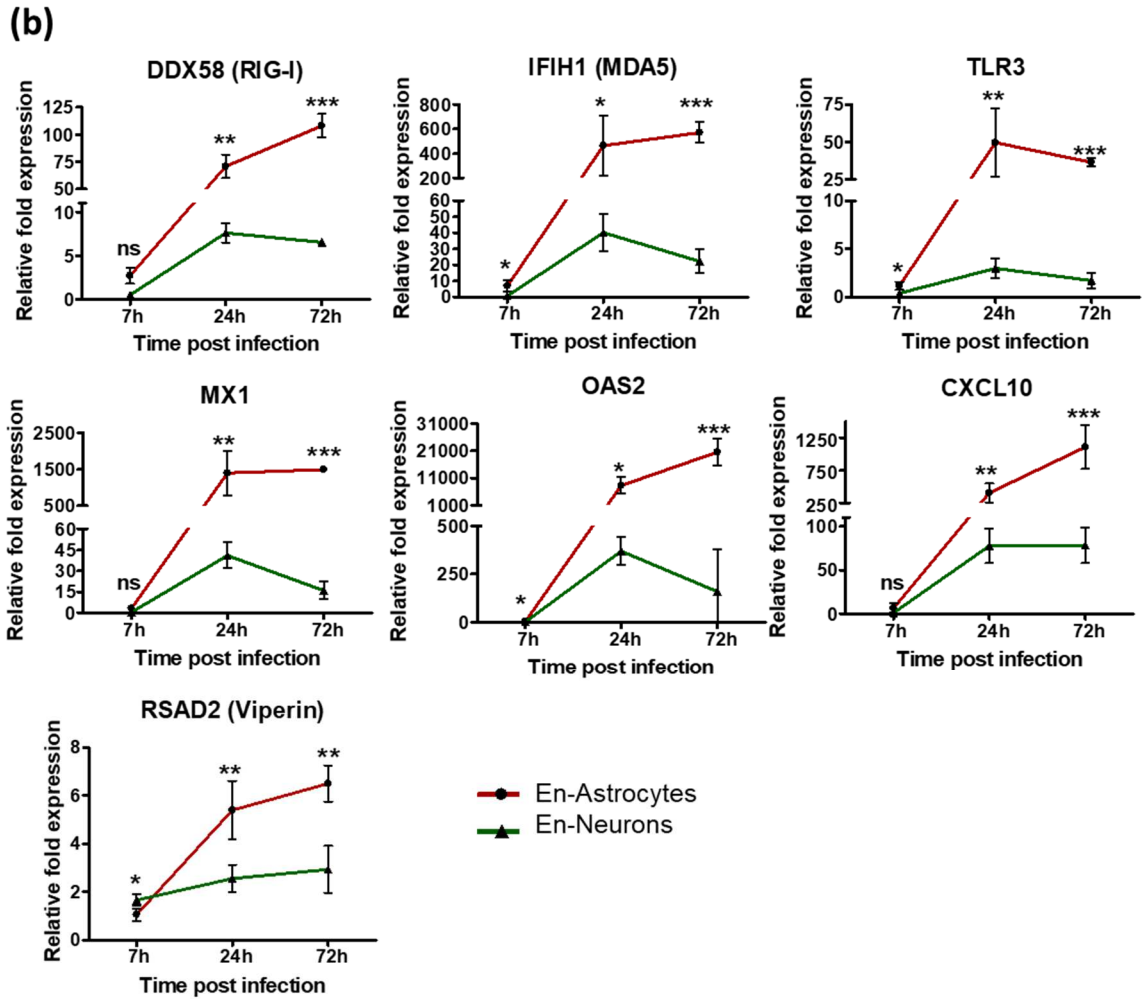

Figure 37 - Antiviral response in En-Neurons and En-Astrocytes, and unsorted cells.

(a) TBEV-infected En-Neurons, En-Astrocytes, and unsorted cultures were analyzed 24hpi using an RT² Profiler PCR array specific for human antiviral response. The heat map shows the differential expression of the 84 human genes, related to their matched NI controls, in each culture. The most upregulated genes are colored in red and the most downregulated genes are colored in green, according to the color code. The black lines indicate the arbitrary cutoff of three. Genes between the two lines are considered non-regulated, except for the genes noted (+). (b) qPCRs analyses of antiviral response genes expression in En-Neurons (red) and En-Astrocytes (green). The results are expressed as mean±SD. They are representative of 2 independent experiments performed in triplicate. Statistical analyses were performed using two-tailed unpaired t test on Graphpad Prism V4.0.3, ns=non-significant ($p>0.05$); *=$p<0.05$; **=$p<0.01$; ***=$p<0.001$.

2.7. Complex interplay between neurons and astrocytes modulates TBEV infection in each cell type

2.7.1. Astrocytes modulate TBEV infection in neurons

Our data suggested that human astrocytes strongly defend themselves against TBEV infection, limiting viral replication by mounting a strong antiviral response. However, whether they can participate in the defense of human neurons was not clear. To tackle this question, we infected unsorted cultures (containing ≅75% of neurons and 20% of astrocytes) and En-Neurons cultures (containing ≅95% of neurons and less than 5% of astrocytes) with TBEV at MOI 10^{-2} for 24 hours and compared the percentage of infected neurons. At 24hpi, whereas 66.5±3.8% of neurons were infected in unsorted cultures (shown as 100%), TBEV infected 94.4±4.3% of neurons in En-Neurons cultures (increase of ≈40%), showing that the presence of astrocytes in the culture was associated with a lower TBEV infection in neurons (Figure 38a). In an attempt to determine whether this increase in neurons infection was associated with an increase in neuronal loss, we performed a HuC/HuD immunostaining and enumerated neurons in both cultures at 24hpi (Figure 38b). As expected, there was no significant difference in unsorted cells. We made a similar observation in En-Neurons, showing that a higher number of infected neurons was not correlated to an increase in neuronal death at this time point. We sought to enumerate neurons at 72hpi, a later time point; however, neurons had formed clusters in En-Neurons cultures, which did not allow their enumeration. Thus, our results strongly suggested that human astrocytes modulated TBEV-infection of human neurons whereas it remains unclear whether this has an impact on neuronal death.

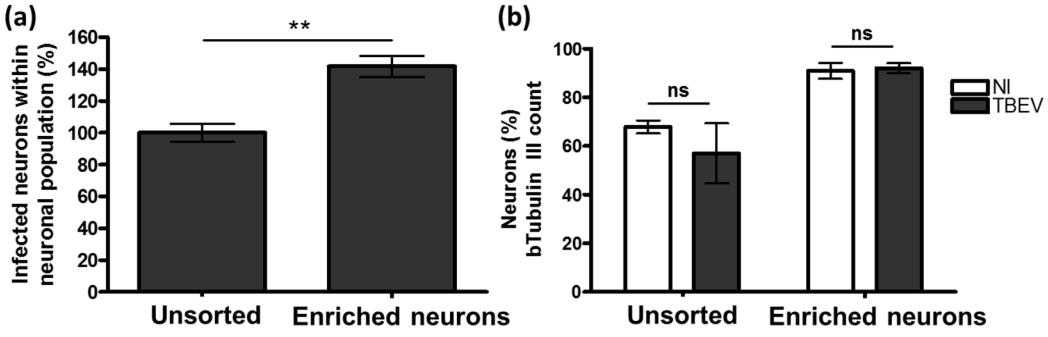

Figure 38 – TBEV infection and impact on neurons in En-Neurons.
Co-immunostaining was performed on En-Neurons and matching unsorted cultures 24hpi. B-III Tubulin and TBEV-E3 (a) and ß-III Tubulin (b) were manually enumerated using ImageJ

software. Results are representative of two experiments performed in triplicate. Data are expressed as mean±SEM. Statistical analyses were performed using a two-tailed unpaired t test on Graphpad Prism V4.0.3, ns=non-significant ($p>0.05$); **=$p<0.01$.

2.7.2. Neurons modulate astrocytes fate in TBEV-infected cells

We further questioned whether human neurons are also capable of modulating TBEV infection and fate of human astrocytes. After immunostaining with GFAP and TBEV antibodies, we manually enumerated and compared the percentage of infected astrocytes in both unsorted cultures (containing ≅75% of neurons) and En-Astrocytes cultures (containing ≅35% of neurons). We did not observe any significant difference at any time point studied (Figure 39a). However, whereas enumeration of total astrocytes did not show any difference at 24hpi, it revealed a difference later on, at 7dpi (Figure 39b). As previously shown, the number of astrocytes had decreased in unsorted cells at this time point. On the contrary, we did not observe a decrease in their number in En-Astrocytes, showing that protection of astrocytes was correlated to a lower level of neurons in the culture. This was also correlated to a lower level of TBEV gRNA, as shown in Figure 39c. Thus, our results, by showing that a higher number of neurons correlated with a higher level of TBEV replication and to a decrease in the number of astrocytes number strongly suggested that the presence of neurons modulates astrocytes fate.

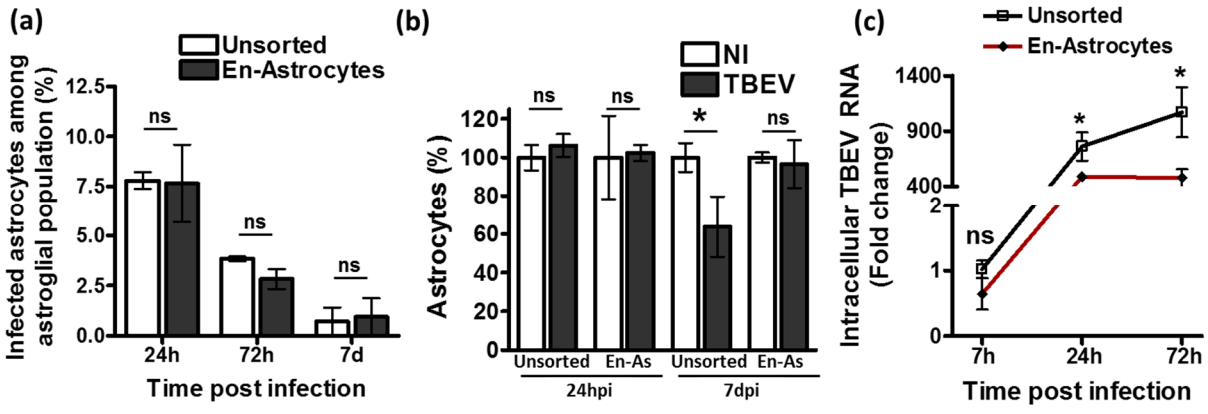

Figure 39 - TBEV impact on astrocytes in En-Astrocytes.
Unsorted cultures and En-Astrocytes were infected with TBEV and immunostained with GFAP and TBEV-E3 antibodies at different time points after infection (a) or with GFAP antibodies 24hpi or 7dpi along with their matched NI controls (b). Staining in (a) and (b) was manually enumerated using ImageJ software. (c) Unsorted cultures and En-Astrocytes were infected with TBEV and the intracellular viral load was analyzed by RT-qPCR at 7hpi, 24hpi and 72hpi.

Results in (a), (b), and (c) are representative of two independent experiments. Data are expressed as mean±SD. Statistical analyses were performed using a two-tailed unpaired t test on Graphpad Prism V4.0.3, ns=non-significant ($p>0.05$); *=$p<0.05$.

2.8. Preliminary data: siRNA transfections to downregulate PRRs

We previously showed, by PCR array and qPCRs, a strong up-regulation of the genes encoding the PRRs RIG-I (*DDX58*), TLR3 and MDA5 (*IFIH1*) in TBEV-infected hNPCs-derived neural cells (Figure 33). To determine which PRRs are involved in TBEV recognition in human neural cells, we sought to down-regulate the expression of these three genes by siRNAs transfection. We first worked on optimizing the conditions of transfection by adjusting: 1/ siRNA concentration vs transfectant volume ratio and 2/ siRNA pretreatment time before infection. We showed that *ApoE* expression was not influenced by TBEV infection (Figure 40). Hence, we used *siApoE*, which targets the gene coding for ApoE, a factor involved in the lipid metabolism, as a transfection control. Once the optimal conditions set up (see details in the methods section), we observed a down-regulation of more than one log of *ApoE* mRNA expression upon siRNA transfection (Figure 40).

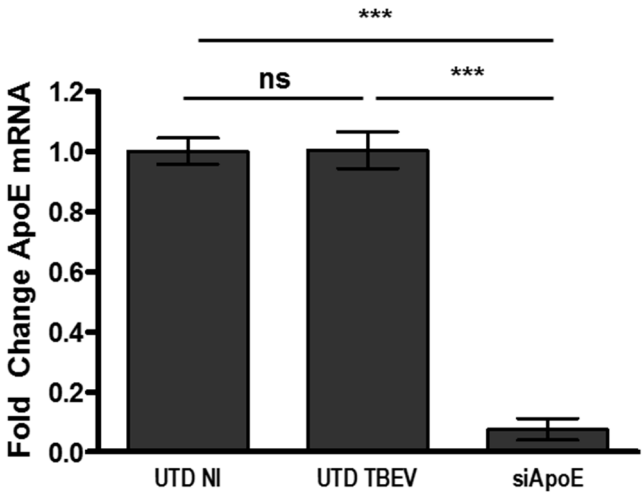

Figure 40 – Down-regulation of *ApoE* mRNA expression.
hNPCs-derived neural cells at d13 of differentiation were transfected with 25nM siApoE and infected after 48h with TBEV. Analysis was performed 24hpi. Data are expressed as mean±SD. Statistical analyses were performed using a two-tailed unpaired t test on Graphpad Prism V4.0.3, ns=non-significant ($p>0.05$); ***=$p<0.001$. UTD=untransfected, NI= non-infected

Using those conditions, we transfected hNPCs-derived cells with siRNAs targeting the genes encoding *ApoE*, RIG-I (*DDX58*), TLR3 and MDA5 (*IFIH1*), and we infected the cells 48 hours after transfection. We analyzed the expression of targeted genes by qPCRs at early time points, at 7hpi and 14hpi. The down-regulation

of ApoE expression was confirmed (>90% downregulation of *ApoE* mRNA at 7hpi and 14hpi). We also observed a down-regulation in *DDX58* mRNA expression of ≅60% at both 7hpi and 14hpi. The expression of *IFIH1* and *TLR3* mRNA was also decreased but only at 14hpi (Figure 41).

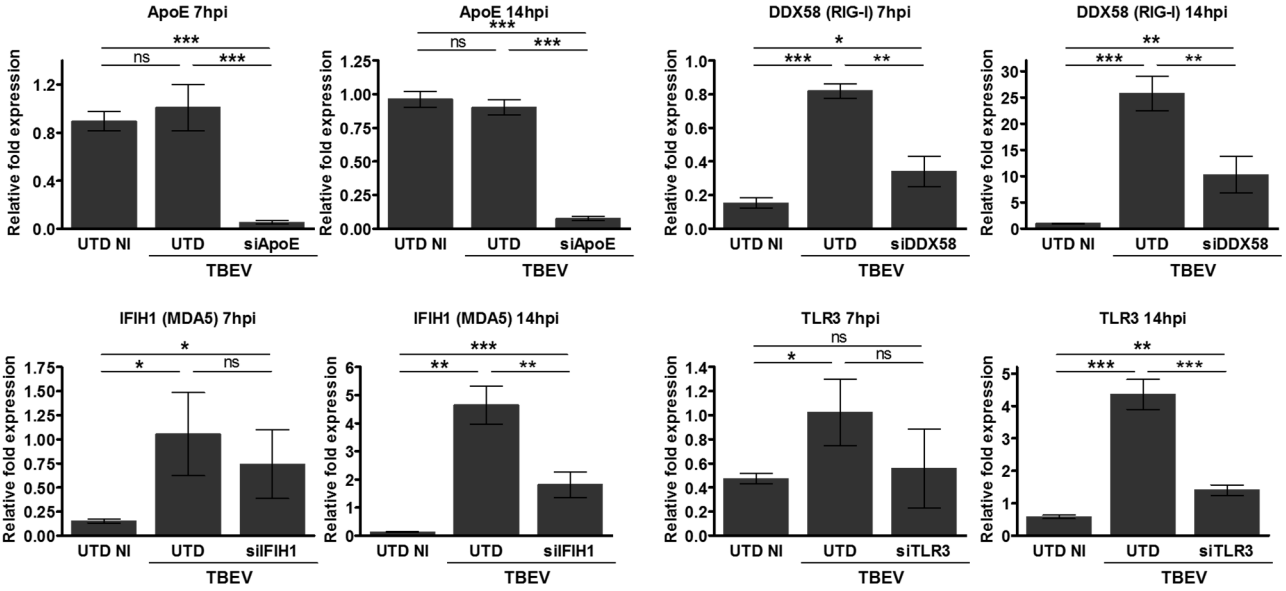

Figure 41 – siRNA-gene down-regulation in hNPCs-derived neural cells.
hNPC-derived neural cells were pretreated with siRNAs for 48h and infected with TBEV. Analysis was performed by qPCR 7hpi and 14hpi. UTD=untransfected, NI= non-infected. Data are expressed as mean±SD. Statistical analyses were performed using a two-tailed unpaired t test on Graphpad Prism V4.0.3, ns=non-significant ($p>0.05$); *=$p<0.05$.

To address whether the down-regulation of PRRs affected viral replication and induction of antiviral response genes, we performed qPCR analysis of intracellular viral gRNA and of two ISGs (*OAS2* and *IFI6*). While we did not observe a significant change of TBEV replication at 7hpi, transfection with si*TLR3* increased TBEV genome loads at 14hpi (Figure 42). Furthermore, in TBEV-infected cells, *siTLR3* and *siIFIH1* transfection induced an increase in ISGs expression when compared to non-treated controls. Interestingly, downregulation of *DDX58* led to a decrease in *OAS2* expression at 4hpi, but *IFI6* expression remained unaffected. These preliminary results, showing a down-regulation of *OAS2* gene expression in *siDDX58*-treated cells and an increase of both ISGs in *siTLR3*-treated cells, suggested a possible involvement of RIG-I and TLR3 in TBEV-induced antiviral response. These observations need to be confirmed by further experiments.

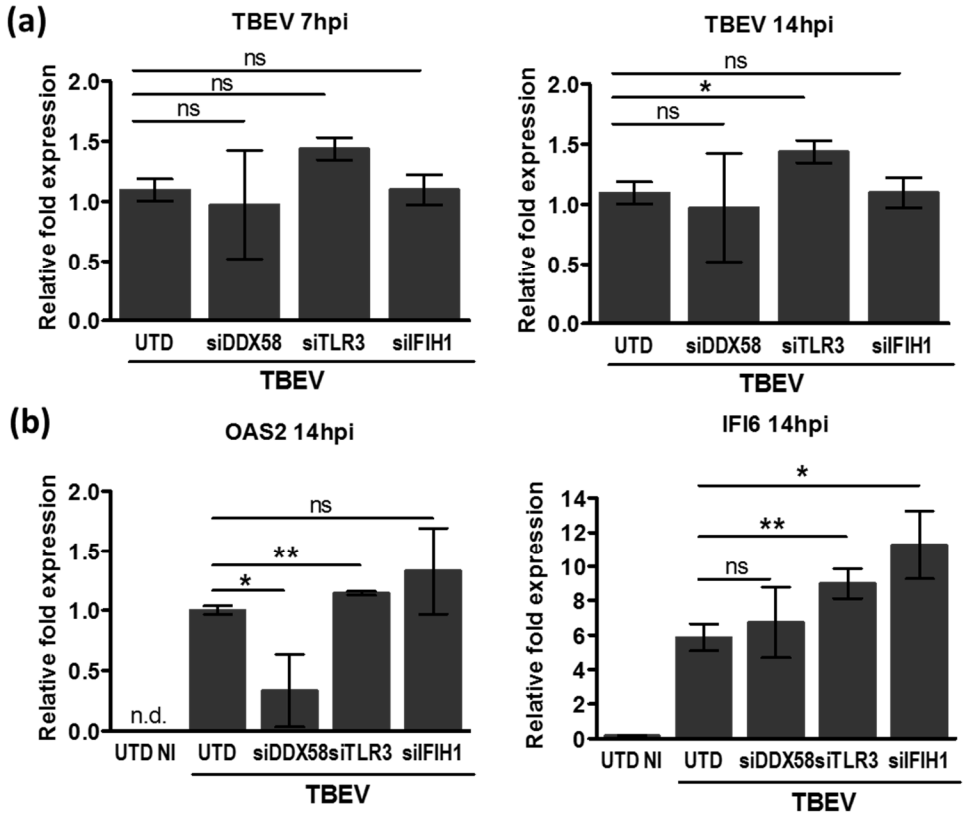

Figure 42 – Involvement of PRRs in viral sensing and ISGs induction.
hNPC-derived neural cells were pretreated with siRNAs for 48h and infected with TBEV. Analysis of TBEV intracellular genome (a) and of the ISGs *OAS2* and *IFI6* (b) was performed by qPCR 7hpi and 14hpi. UTD=untransfected, NI= non-infected. Data are expressed as mean±SD. Statistical analyses were performed using a two-tailed unpaired t test on Graphpad Prism V4.0.3, ns=non-significant ($p>0.05$); *=$p<0.05$; **=$p<0.01$.

Chapter III: Discussion

Despite its importance in human health, TBEV-induced neuropathogenesis is poorly understood. For a long time, human and mice neural cell lines *in vitro* and rodents *in vivo* were the only available models for the study of anti-TBEV immunity and TBEV-induced neuropathology [61,199,264,281,282,362]. Pathogenicity of TBEV in mice was shown to correlate with severity of infection in humans [449]. However, data obtained with cell lines could be biased, as it occurs that the identity of immortalized cell lines is often mistaken [450] and, more importantly, they differ in their signaling from the primary cells or *in vivo* situation [451,452]. Moreover, studies have highlighted species differences. More specifically, it has been shown that each mammalian specie possess a specific IFN response and a unique repertoire of ISGs [217], which limits extrapolation of knowledge on viral infections and antiviral response from mice to humans. In the last years, relevant contributions using iPSc-induced or primary human neurons and astrocytes were made [72,280], but the studies focused mainly on structural changes and inflammatory response. Here, we developed and characterized a new human physiological model to understand the antiviral response developed during TBEV infection and in particular the specificities of 2 main cell types within the CNS, neurons and astrocytes. We further explored the association between antiviral response and neuropathogenesis. Using hNPCs that differentiate into specialized brain cells and generate cultures containing neurons, astrocytes and oligodendrocytes [232,233], we showed that TBEV preferentially infects and damages human neurons. We further highlighted that TBEV induced an antiviral immune response in human neural cells. This antiviral response was however more strongly induced in astrocytes compared to neurons which led us to suggest that the particular neuronal susceptibility and vulnerability to TBEV infection is due, at least partly, to their inability to develop a protective antiviral response.

- **Human Neural Stem cells as a source of neural cultures**

The characterization of cell type composition of *in vitro* models is critical, as the CNS encloses regions with variable cellular compositions, and it is likely that the susceptibility of each cell type as well as their interactions shape the

susceptibility of specific regions to specific viruses. Despite that, studies using primary or iPSc-induced human or murine neurons or astrocytes disclose scarce data about the cellular heterogeneity of the cultures, and their cellular purity was poorly characterized. In this study, we have used a well-characterized hNPCs-derived neural cells culture that contains approximately 75% of neurons, 20% of astrocytes and less than 5% of oligodendrocytes. An important limitation of this model is that it is still far from representing the human brain, as the ratios of these cell types are not representative of the overall brain cellular composition [453], yet they might represent specific regions where the ratio of neurons to astrocytes is favorable to the former cell type. Moreover, as hNPCs are prepared from fetal brain tissue [232], the derived neural cultures lack microglia, an important player in CNS that derive from primitive myeloid precursors [454].

There is no evidence that microglia cells are permissive to TBEV. However, microglial cells respond to the brain infection by inducing their proliferation and activation, as shown in postmortem human brain tissues [261]. This activation is likely to be involved in neuronal damage and brain tissue destruction. It seems plausible that microglial cells are activated following a direct infection by TBEV, as they can be also be infected by other flaviviruses. ZIKV infects microglia and leads to their activation and the induction of an inflammatory response [455]. Microglia are also susceptible to JEV with no apparent cytopathogenic effect, but the virus can be transmitted to neighboring cells in a cell-dependent manner [456].

Further work assessing microglial susceptibility to TBEV, and its implication in the pathogenesis of the adult human brain is needed. Organotypic brain slices collected from human donors could provide a complementary view to our study by investigating TBEV infection of microglia in a multicellular environment. Microglia with a functional immune response can be developed in iPSC-derived human cerebral organoids, and be associated with neurons and other glial cells [457], which might allow the study of broader cellular interactions in a three dimensional environment.

- **A differential susceptibility of human neural cells to TBEV**

TBEV infects and replicates mainly in neurons, as shown in human and mouse neurons [72,264]. Glial cells are also susceptible to TBEV infection, as *in vitro* cultures showed ≅20% of infection in primary human and in primary rat astrocytes [61,280], but TBEV infection in oligodendrocytes had not been reported so far.

Here, we showed that primary human neurons and astrocytes are permissive to TBEV infection. This is the first direct comparison between the two cell types using co-culture of human neural cells, showing that susceptibility to TBEV infection is higher in neurons compared to astrocytes (more than 3 folds in the specific populations), and confirming that neurons are the main target of TBEV. Moreover, we revealed for the first time that human oligodendrocytes are highly permissive to TBEV infection, but we did not observe any evidence damage induced by the infection.

Other neurotropic viruses have been reported to infect and replicate in various cells of the brain. Both neurons and astrocytes are susceptible to LACV [225]. JEV can infect immature neurons [458,459] and astrocytes [460] [459,460] while ZIKV infects mainly neural stem cells, but also astrocytes [228,461]. Immature neurons are susceptible to ZIKV infection, but mature differentiated neurons are more resistant to the virus [462].

Oligodendrocytes infection by viruses is not well known. ZIKV was shown to infect oligodendrocytes within murine myelinating cultures, and to cause neuronal demyelination [463]. Theiler's murine encephalomyelitis virus (TMEV), murine leukemia viruses (MLV), and spongiogenic murine retroviruses also infect murine oligodendrocytes or oligodendrocytes progenitors, which also leads to neuronal demyelination, or to the impairment the differentiation of oligodendrocytes progenitors [464–466]. Oligodendrocytes are also injured during HIV-1 neurotropic infection [467].

Whether TBEV induces an alteration of the myelin sheath similarly to other viruses that infect oligodendrocytes has not been investigated. This could represent a mechanism of indirect neuronal alteration that does not involve cell death.

- **A differential impact of TBEV on human neural cells**

TBEV induces ultrastructural changes in infected neurons and astrocytes [61,72,264,280], it is however unclear whether it induces cell death exclusively by apoptosis, or if other cell death mechanisms, involving necrosis or autophagy, are involved. Apoptotic figures were observed in human neuroblastoma [223], but only limited apoptotic cells were observed in primary human neurons [72]. Our data showed that TBEV induces neuronal death by apoptosis and a massive neuronal loss. Bílý *et al*. [72] have also observed a maintenance of viral titers in neuronal cultures up to 13dpi and suggested a persistent infection. The kinetic studies we performed on hNPC-derived co-cultures showed a decrease of TBEV titers at later time points and do not favor the hypothesis of TBEV persistence in the brain. Because neurons survive hardly for a long time in cultures depleted of astrocytes, we were not able to perform longer time point analyses of viral replication in enriched-neuronal cultures. Furthermore, we observed an impairment of neurites network at 72hpi, which was stable up to 7dpi.The kinetics of this neurites loss, showing the same network density at 72hpi and 7dpi while neuronal count decreases suggests a retrograde neuronal degeneration. This mechanism of neuronal damage is well described in Rabies virus (RABV) infections [468].

Apoptotic figures were also observed in glioblastoma [223] but only marginal necrotic cells were present in human [280] and rat [61] astrocytes. Unexpectedly, our data showed a decrease in astrocytes number at later time points (7dpi) but we did not observe pyknosis or any other cell death figures in astrocytes. As rat primary astrocytes viability was not impaired, Potokar et al. [61] previously suggested they might act as a reservoir for TBEV during chronic infections of rodents. However, our data have shown that human astrocytes are also impaired in their survival, and are not likely to act as a source of TBEV within the CNS. Moreover, an increase in GFAP production was previously observed in human astrocytes [280], as well as structural changes of the cytoskeleton [61]. We observed an astroglial hypertrophy, suggesting astrogliosis but we did not observe an increase in GFAP transcripts. Furthermore, the hypertrophy was not accompanied by astrocytes proliferation, another figure of astrogliosis, which questions its occurrence.

Our results did not reveal a significant impairment of oligodendrocytes viability, however, we relied on Olig2 nuclear protein to mark cells from the oligodendroglial lineage, which allowed us to perform automated olig2-positive cells enumeration using an Arrayscan Cellomics. However, Olig2 is mainly expressed in oligodendrocytes progenitor cells, and directed them to an oligodendroglial fate [469]. Furthermore, while we did not observe Olig2 co-localization with neuronal or astroglial markers, Olig2 can be expressed in subpopulations of neurons [470] and astrocytes [471]. The use of mature oligodendrocytes markers such as O4 and MBP [472] will provide a complementary picture of the impact of TBEV infection on mature oligodendrocytes.

Hence, here, we confirm, using neurons and glial cells differentiated from the same culture, that astrocytes are more resistant to TBEV-infection than neurons. While the infection is lower and the replication is weaker, their viability is impaired during long-term infection.

- **The antiviral response in neurons and astrocytes: a link to pathogenesis?**

Two possible reasons could explain the difference in TBEV impact on neurons and astrocytes.

TBEV entry might be mediated by a specific receptor in neurons. For instance, AXL, the entry receptor of ZIKV, is known to be strongly expressed in astrocytes, but weakly in neurons [473], which is consistent with the virus tropism. Our results showed a higher infection in neurons (8.0±0.8%) than in astrocytes (4.3±1.5%) early after infection (14hpi), which suggests that viral entry is facilitated in neurons in comparison to astrocytes. However, while heparin sulfates are involved in TBEV attachment, the specific receptors mediating viral entry are not known, which does not allow us to address this possibility as a differential mechanism between neurons and astrocytes.

The different impact of TBEV infection on neurons and astrocytes might also be due either to a high basal level of antiviral response genes expression in astrocytes or to a difference in intrinsic capacity of neurons and astrocytes to develop a protective antiviral response upon TBEV infection. We observed a high difference in TBEV infection at 72hpi between neurons and astrocytes (Infection

of 43.6±6.7% of neuron and 8.5±3.3% of astrocytes). This suggests that astrocytes limit strongly viral replication compared to neurons. Our data did not show a significant difference in basal levels of antiviral response genes in neurons and astrocytes. However, while we showed the induction of the same antiviral program in both En-Neurons and En-Astrocytes, we observed a higher global expression in astrocytes compared to neurons. Previous work performed on mice revealed that IFN is essential for viral control and protection of the CNS [360] and that the cell-type- and region-specific IFN activation is protective and determines tropism of TBEV [263,282]. Astrocytes are the main IFN-producing cells in response to several neurotropic viruses (LACV, VSV, TMEV, and RABV [474,475]), and they mount a fast type I IFN response following TBEV infection [281]. Other flaviviruses, such as WNV, infect astrocytes in a similar manner, replicating slowly and inducing a strong IFN I response as well [476,477]. For a long time, neurons were considered immunologically quiescent cells, but it is now well established that they are able to produce IFN and mount an IFN response by expressing ISGs, hence participating to the antiviral response [478]. This response is specific to neuronal subtypes, and neurons from different regions of the brain have a different antiviral response and susceptibility to flaviviruses such as WNV and TBEV [263,479]. Our results demonstrate for the first time that TBEV induces a global antiviral response in human neurons that is weaker than the induced antiviral response in human astrocytes.

As neurons from different regions have specific antiviral responses, neuronal susceptibility might also be due to the lack of expression of one or few factor that restrict TBEV replication. Our data showed a higher expression of PRRS, ISGs, and proinflammatory cytokines in astrocytes compared to neurons. Among these genes, the expression of *RSAD2*, coding for the ISG viperin, was significantly upregulated in astrocytes but not in neurons. Viperin was shown to inhibit the replication of several viruses in mice, including TBEV and WNV [395,396]. Its expression is not necessary to control TBEV replication in granule cell neurons (GCN) of the cerebellum, but it is essential for a protective IFN-response in astrocytes and in cortical neurons (CN) of the cerebral cortex [263], showing a cell type specific mode of action. Whether the antiviral response in hNPCs-derived neurons lacks specific factors that are expressed in other neural types is unknown. Using iPSc to generating hNPCs that differentiate in different types of neurons

might help to tackle this question. Furthermore, our results raise the question of the involvement of viperin in TBEV control in human neural cells, but whether its ectopic expression can enhance the control of TBEV replication in neurons is unclear.

- **Interplays between neurons and astrocytes, a love and hate relationship**

Cellular environment is critical for viral clearance within the CNS. Control of the replication of an avirulent strain of WNV in astrocytes was hypothesized to be associated with milder neuropathology [477], suggesting that antiviral response in astrocytes may protect neurons. Furthermore, combined IFN responses of neurons and astrocytes together, but not separately induced a protective response in the murine olfactory bulb, through activation of macroglia [480]. Moreover, IFN response in astrocytes was shown to be crucial for protection of neighboring cells by suppressing TBEV-replication in the CNS [281]. However, astrocytes can also be deleterious to neurons, and microglia can induce this neurotoxic state [481].

Using enriched cultures of neurons, we showed that depletion of astrocytes strongly increased infection in neurons, suggesting that astrocytes not only control TBEV replication, but that they also limit neurons infection possibly through inducing a specific antiviral response. On the contrary, little is known about how neurons affect astrocytes infection and injury. We showed that decrease in neurons number led to a restoration in astrocytes viability at 7dpi. Thus, our results suggest that neurons have a harmful impact on astrocytes. This could be due to a higher replication of TBEV in neurons, which would lead to an increase in astrocytes infection and injury. However, analysis of astrocytes infection in En-Astrocytes cultures did not show an increase in their infection, which does not favor this possibility. Another explanation could be the release of proapoptotic factors by neurons in the extracellular medium. We observed an increase of *TNFSF10* transcripts, coding for TRAIL, following TBEV infection. TRAIL is a proapoptotic factor that that can be produced by neurons or astrocytes, and both cells are sensitive to its signaling, although TRAIL receptors, DR4 and DR5, are weakly expressed in astrocytes [482]. It can also be induced by IFN signaling

in humans, but only weakly in mice [217]. Further work is necessary to investigate TRAIL producing cells and its involvement in both neuronal and astroglial impairment.

Based on our results and data from the literature, we propose a model for TBEV interactions with human neural cells represented in Figure 43.

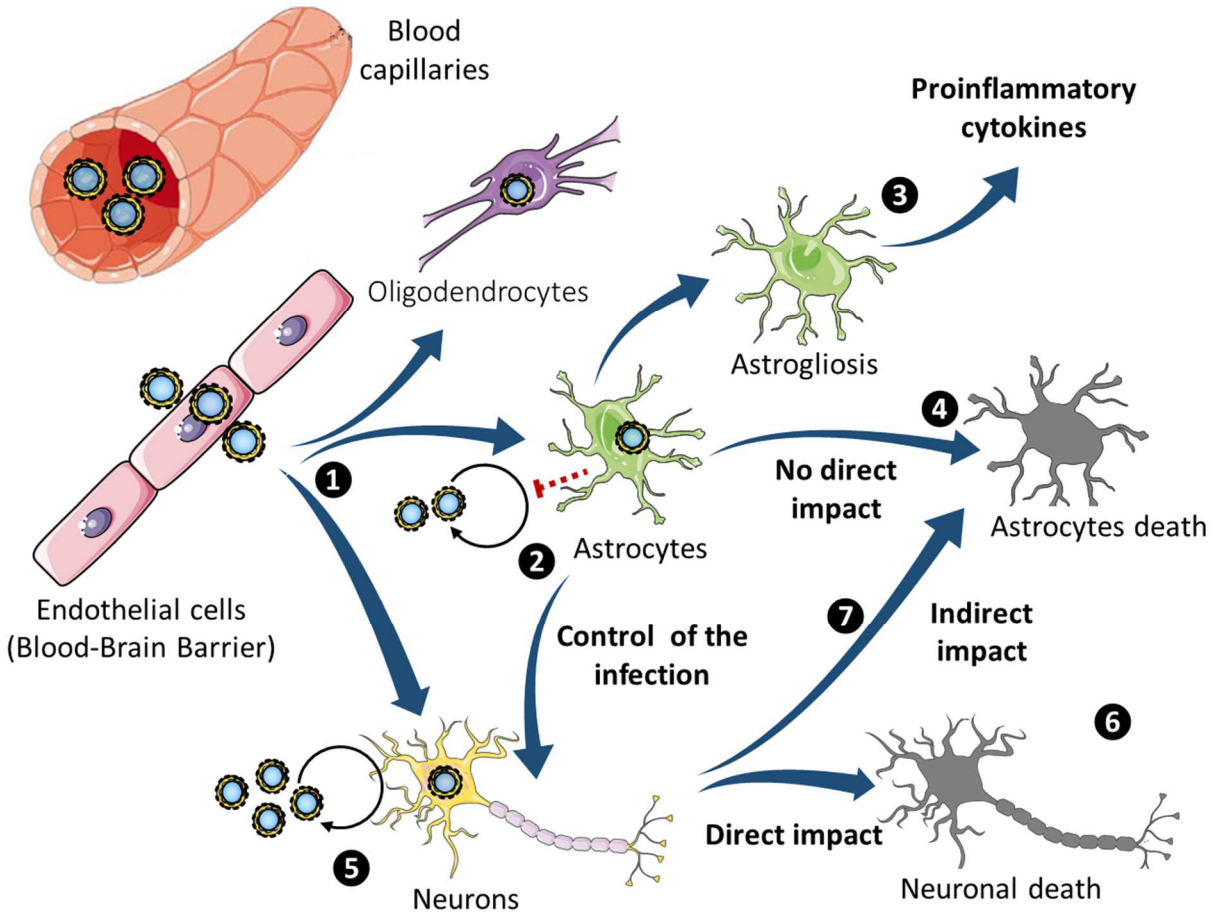

Figure 43 – Physiopathogenic model for TBEV induced pathogenesis in the human brain
After crossing the BBB, TBEV infects neurons, astrocytes and oligodendrocytes (1). Astrocytes control the infection by developing a strong antiviral response that is also beneficial for neurons (2). They also enter a reactive stage and express strongly pro-inflammatory cytokines (3), but are not damaged by the infection (4). Neurons, on the other hand, are highly susceptible to TBEV (5), which induce their alteration, probably by direct mechanisms (6), but also astroglial damage by an indirect mechanism (7). Figure adapted from [254] and created using Servier Medical Art (smart.servier.com), licensed under a CC BY 3.0 attribution.

Overall, our study, using human brain cells derived from fetal neural progenitors, led to the development of a new and highly relevant model that mimics major events of TBEV infection in the human brain. This allowed us to compare, for the first time, the impact of TBEV on human neurons, astrocytes and oligodendrocytes. We highlighted that TBEV infection induces a different antiviral response in human neurons and human astrocytes, which supports the concept that although neurons have an active immune role in the CNS, their intrinsic antiviral response is weaker than astrocytes response, and we hypothesized that this response conditions the neuropathology induced by the virus. We further identified a complex interplay between neurons and astrocytes showing the usefulness of complex cultures for the study of virus-induced neuropathogenesis.

Material and methods

Human neural progenitor cells culture

Human neural progenitor Cells (hNPCs) were prepared from the CNS of one first-trimester human embryo as described in [232]. Human embryos were obtained after legal abortion with written informed consent of the patient and procedures for the procurement and use of this human fetal CNS tissue were approved and monitored by the *Comité Consultatif de Protection des Personnes dans la Recherche Biomedicale* of Henri Mondor Hospital, France. Briefly, the cortex was dissected and cut into 1mm^3 tissue pieces. After mechanical dissociation, single-cell suspensions were cultured in Dulbecco's modified Eagle medium-F12 (DMEM-F12; 1/1; Invitrogen Life Technologies) supplemented with B27 (Invitrogen Life Technologies) and containing epidermal growth factor (EGF) and basic fibroblast growth factor (bFGF) at 20ng/ml (R&D Systems), heparin (5µg/ml, Sigma), 100U penicillin, and 1,000U streptomycin (Invitrogen Life Technologies). This cell suspension generated proliferating clones containing human Neural Progenitor Cells (hNPCs) in floating spheres (neurospheres). Cells were further expanded and maintained in suspension as neurospheres in uncoated tissue culture dishes in advanced Dulbecco's modified Eagle medium-F12 (DMEM-F12 Adv.; Invitrogen Life Technologies) supplemented with L-glutamine (2mM; Gibco), apotransferrin (0.1mg/ml; Sigma), insulin (25µg/ml; Sigma), and progesterone (6.3 ng/ml; Sigma). Medium, referred to as N2A medium, was changed twice a week, and the growth factors EGF and bFGF (both at 20 ng/ml; Abcys, Eurobio) were added three times a week to maintain undifferentiated cells. For infection, cells were cultured as monolayers by seeding them in matrigel-coated dishes (1/1,000; BD Biosciences) in N2A medium. They were subcultured using TrypLE (Invitrogen Life Technologies) when 80% confluence was reached. Cells were maintained at 37°C in a humidified atmosphere containing 5% CO2.

Neural stem cells differentiation

Undifferentiated proliferative hNPCs were subcultured using TrypLE and replated on a matrigel-coated dish at an average density of 30,000 cells/cm^2. Differentiation was induced as described in [232]. Briefly, one day after plating, N2A medium was replaced with 1:1 N2A and Neurobasal supplemented with L-glutamine and B27

without vitamin A (Invitrogen Life Technologies) (referred to as NBC) with withdrawal of EGF and bFGF. Differentiation conditions were maintained for 13 days before infection with medium replacement twice a week. 24-well plates (IBIDI) were used for fluorescent immunostainings and 6-well plates (Falcon) were used to prepare lysates for RNA and protein analysis.

Virus and infection

Hypr strain (provided by Dr S.Lecollinet, ANSES, France) is a well-characterized representative of European subtype TBE virus. Its complete sequence was described previously in [483] (GenBank accession number U39292). Hypr strain was first isolated in 1953 from the blood of a 10-year-old child with TBE in Czechoslovakia, and propagated through numerous suckling mouse brain passages [483]. Viral amplification was performed by successive passages on confluent Vero cells cultured in MEM medium (ThermoFisher) supplemented with 2% Fetal Bovine Serum (FBS). The supernatant was cleared by centrifugation (10000rpm, 10minutes) and aliquots were frozen prior to infection. Virus titers were estimated by plaque assays on Vero cells covered with a sterile v/v solution of PBS-Carboxymethyl cellulose (CMC) 3,2% and MEM 2X. Cells were colored with violet crystal for lysis quantification.

Cell transfection

Neural differentiation was induced as described above. hNPCs differentiated for 13 days were exposed to transfection complexes for 48 h prior to TBEV infection. HiPerfect transfection reagent (Qiagen) and siRNAs (25nM to 200nM) directed against *IFIH1*, *DDX58*, *TLR3*, *ApoE* or a non-targeting siRNAs (ON-TARGETplus siRNAs, Dharmacon) were used.

Intracellular RNA extraction

Cells were lysed using the *Lysis buffer MR1* of *NucleoMag® 96 RNA* kit (Macherey Nagel). RNAs and protein were extracted as two separate fractions using this same kit associated with a *King Fisher Duo* automate (Fisher Scientific) following provided instructions. RNAs were eluted in water.

Viral RNA extraction

Infected cells supernatants were first centrifuged at 4,000rpm to eliminate all cellular fragments before freezing. Extraction was performed using *QIAamp Viral RNA Mini Kit* (Qiagen) following manufacturer's spin protocol instructions.

PCR array analysis

Intracellular RNAs were extracted as described previously and RNAs of biological triplicates were pooled for each condition. Retrotranscription of the RNAs pool (250 to 500 ng) was performed using the *RT² First Strand Kit* (SA Biosciences, Qiagen). Obtained cDNAs were processed on *RT² Profiler PCR array* arrays (Human antiviral response PAHS—122Z, human apoptosis PAHS—012Z and human autophagy PAHS-084Z), following strictly manufacturer's instructions. Data were normalized for *HPRT1* gene expression and analyzed using the 2ΔΔCt (Livak & Schmittgen, 2001) for relative quantification on Qiagen Data analysis center (http://www.qiagen.com/fr/shop/genes-and-pathways/data-analysis-center-overview-page/).

Reverse transcription and quantitative polymerase chain reaction analysis

Total RNA concentration in the samples was quantified on a Nanodrop (Fisher Scientific). Reverse transcription of 160 to 250ng of RNA was performed using *SuperScript™ II Reverse Transcriptase* kit (ThermoFisher Scientific) following the manufacturer's instructions.

Real-time PCR was performed using 2µl of cDNA and *QuantiTect SYBR green PCR master* (Qiagen) with a LightCycler 96 (Roche Applied Science) on a 20µl reaction mixture. Gene expression was normalized with the ΔΔCt method (Livak & Schmittgen, 2001), with *GAPDH* or *HPRT1* as a housekeeping gene. The primer pairs used for gene expression analysis are show in Table 4. The amplification protocol used on the LightCycler96 is represented in Table 5.

Table 4 - Primer pairs used for qRT-PCR analyses.

Gene name	3' primer	5' primer
GAPDH	CACCATCTTCCAGGAGCGAG	GAGAtgAtgACCCTTTTGGC
HPRT1	GGACTAATTAtgGACAGGACTG	GCTCTTCAGTCTGATAAAATCTAC
TBEV	GGGCGGTTCTTGTTCTCC	ACACATCACCTCCTTGTCAGACT
GFAP	AGGTCCAtgTGGAGCTTGAC	GCCATTGCCTCATACTGCGT
ßIII-tubulin	CAACAGCACGGCCATCCAGG	CTTGGGGCCCTGGGCCTCCGA
TLR3	GCTGCAGTCAGCAACTTCAT	AGGAAAGGCTAGCAGTCATCC
DDX58 (RIG-I)	GAGAAAAAGTGTGGCAGCCT	ATATCCGGAAGACCCTGGAC
IFIH1 (MDA5)	TGCCCAtgTTGCTGTTAtgT	GTCTGGGGCAtgGAGAATAA
Caspase 1	TTTCCGCAAGGTTCGATTTTCA	GGCATCTGCGCTCTACCATC
TNFSF10	AGCAAtgCCACTTTTGGAGT	TTCACAGTGCTCCTGCAGTC
PSA-NCAM	AGTCCAAGGGGAACCCAGT	TAGTGTCTGAtgGGGGAGCC
GLAST	ACAtgAAGGAACAGGGGCAG	CACGGGGGCATACCACATTA
CXCL10	GCAGGTACAGCGTACGGTTC	CAGCAGAGGAACCTCCAGTC
CXCL11	AtgCAAAGACAGCGTCCTCT	CAAACAtgAGTGTGAAGGGC
CCL5 (RANTES)	TGTACTCCCGAACCCATTTC	TACACCAGTGGCAAGTGCTC
RSAD2 (viperin)	GTCCCTGGCATACAGAGACTG	GCTCAGAGGTTGCCTGAACA
IFI6	TCGCTGAtgAGCTGGTCTGC	ATTACCTAtgACGACGCTGC
OAS2	TGTTTTCCGTCCATAGGAGC	CTGATCGACGAGAtgGTGAA
MX1	CTACACACCGTGACGGATAtg	CGAGCTGGATTGGAAAGCCC
Beclin 1	ACCTCAGCCGAAGACTGAAG	AACAGCGTTTGTAGTTCTGACA
Atg3	ACAtgGCAAtgGGCTACAGG	CTGTTTGCACCGCTTATAGCA
P53	GAGGTTGGCTCTGACTGTACC	TCCGTCCCAGTAGATTACCAC
IFNα (1 and 13)	GACTCCATCTTGGCTGTGA	TGATTTCTGCTCTGACAACCT
IFNβ	CAACTTGCTTGGATTCCTACAAAG	TATTCAAGCCTCCCATTCAATTG
ISG15	CACCGTGTTCAtgAATCTGC	CTTTATTTCCGGCCCTTGAT
ISG56	GGACAGGAAGCTGAAGGA	AGTGGGTGTTTCCTGCAA
Trim5α	TGCCTCTGACACTGACTAAGAAGAtg	GGGCTAAGGACTCATTCATTGG

Table 5 - Amplification program on LightCycler96 (Roche).

Program	Cycles	Duration	T°	Acquisition	Ramp
Preincubation	1 cycle	900 s	95°c	-	4,4 °C/s
Three step amplification	40 cycles	30 s	95°c	-	4,4 °C/s
		30 s	60°c	-	2,2 °C/s
		30 s	72°c	-	4,4 °C/s
Melting	1 cycle	10 s	95°c	-	4,4 °C/s
		60 s	58°c	-	2,2 °C/s
	Continuous	1s	95°c	5 acq/°C	0,2 °C/s
Cooling	1 cycle	30s	40°c	-	2,2 °C/s

Immunofluorescence and TUNEL analyses

Cells were fixed for 20 minutes in PBS-PFA 4% (Electron Microscopy Sciences) and immunofluorescent stainings were performed for HuC/HuD (Thermofisher, A-21271), βIII-Tubulin (Sigma, #T8660), GFAP (Dako, #M076101-2 or #Z033429-2), Olig2 (R&D Systems #AF2418), TBEV-E3 (Kind gift of Dr S.Lecollinet, ANSES, France), cleaved caspase 3 (Cell Signaling Technology, #9662), GLAST (Miltenyi Biotec #130-095-814) or PSA-NCAM (Miltenyi Biotec #130-093-273). For all antibodies, cells were blocked 1h in a solution of PBS supplemented with 3% BSA 0.3% (Sigma) and Triton X-100 (VWR) solution and primary antibodies were incubated overnight in a solution of PBS supplemented with 1% BSA 0.1% Triton X-100 overnight at +4°C. Secondary immunostaining was performed with anti-IgG antibodies coupled with Alexa Fluor (Molecular Probes, Invitrogen, France). For the assessment of cell death, terminal deoxynucleotidyltransferase-mediated dUTP-biotin nick end labeling (TUNEL) staining was performed using DeadEnd™ Fluorometric TUNEL System (Promega, #G3250) according to the manufacturer's instructions. For all immunostainings, nuclei were stained with 4',6-diamidino-2-phenylindole (DAPI) (Life Technologies) at 0,1 ng/ml. Images of cells Immunostained with βIII-Tubulin, GFAP, βIII-Tubulin-GFAP and GFAP-TBEV were acquired with an *AxioObserver Z1* (Zeiss) inverted microscope using ZEN software (Zeiss). In every experiment, three wells per condition were analyzed and an average of 1,200 cells were manually enumerated using ImageJ 1.49m software. Images of cells TUNEL-stained or immunostained with HuC/HuD, TBEV and Olig2 antibodies were acquired using the Cellomics ArrayScan automated microscope (Thermofisher Scientific). Cell enumeration and neurite length measurement was automatically performed using Colocalization or Neuronal profiling bio applications on HCS Studio Cell Analysis Software V6.6.0 (Thermofisher Scientific). In every experiment, three wells per condition were analyzed and an average of 5,000 cells per well were enumerated.

Magnetic-activated cell sorting

Co-cultures of neural cells differentiated for 13 days (60 million cells) were detached using Gibco™ TrypLE™ Select Enzyme (1X) (Fisherscientific, #12563011) and collected in N2A-NBC medium. A fraction was collected to be centrifuged, resuspended in fresh N2A-NBC medium and subcultured as unsorted cultures. The remaining cells were

centrifuged at 80g speed for 10 minutes and resuspensded in 80µl sorting buffer per 10^7 cells. Sorting buffer is a solution of PBS supplemented with 0.5% BSA and 10% Kynurenic acid solution 10x. Kynurenic acid solution 10x is a solution of H2O supplemented with Kynurenic acid (1,89mg/ml), MgCl2 0,1M, NaOH 9mM, Hepes 5mM and 0.25‰ Phenol Red. Details of the preparation procedure is disclosed by Welsh *et al.*, [485]. Cell sorting was performed by positive selection of astrocytes using Anti-GLAST (ACSA-1) MicroBead Kit (Miltenyi Biotec #130-095-826). In brief, resuspended cells were incubated 10 minutes at 4°C with 20µl anti-GLAST (ACSA-1) Biotin conjugated antibodies per 10^7 cells. After washing, centrifugation and resuspension in sorting buffer as before, cells were incubated with AntiBiotin MicroBeads for 15 minutes at 4°C. The labelled cells were washed in excess using sorting buffer, centrifugated and resuspended in 500µl N2A-NBC. The magnetic sorting of the cells was performed using an MS columns (Miltenyi Biotec, #130-042-201) that was placed in a MiniMACS™ separator (Miltenyi Biotec #130-090-312). The sorted and unsorted cells were seeded at density of 100,000 cells per cm^2 in a v/v mix of fresh N2A-NBC medium and N2A-NBC conditioned medium (supernatant of 13d old co-cultures conditioned for 48 hours) on 24-wells µ-Plates (Ibidi, #82406). The negative selected cells were considered enriched neurons (En-Neurons) and the positive selected cells were considered enriched astrocytes (En-Astrocytes). Half the medium was changed every two days and replaced with fresh N2A-NBC.

Statistical analyses

Data are represented as mean±SD. Statistical analysis were performed on GraphPad Prism V4.03 or V6.0.1 using an unpaired Student's t test or a one-way ANOVA analysis (Bonferroni's Multiple Comparison Test), as described in the figures legend.*=($p<0,05$), **=($p<0,01$), ***=($p<0,001$), non-significant (ns)= ($p>0,05$).

References

1. Fauquet C, International Committee on Taxonomy of Viruses. Virus taxonomy¤: classification and nomenclature of viruses¤; 8th report of the International Committee on Taxonomy of Viruses. Elsevier/Academic Press; 2005.
2. Westaway EG, Brinton MA, Gaidamovich SYa, Horzinek MC, Igarashi A, Kääriäinen L, Lvov DK, Porterfield JS, Russell PK, Trent DW. Flaviviridae. Intervirology. 1985;24: 183–192. Available: http://www.ncbi.nlm.nih.gov/pubmed/3000978
3. Simmonds P, Becher P, Bukh J, Gould EA, Meyers G, Monath T, Muerhoff S, Pletnev A, Rico-Hesse R, Smith DB, Stapleton JT, Ictv Report Consortium IR. ICTV Virus Taxonomy Profile: Flaviviridae. J Gen Virol. Microbiology Society; 2017;98: 2–3. doi:10.1099/jgv.0.000672
4. Gould EA, Moss SR, Turner SL. Evolution and dispersal of encephalitic flaviviruses. Emergence and Control of Zoonotic Viral Encephalitides. Vienna: Springer Vienna; 2004. pp. 65–84. doi:10.1007/978-3-7091-0572-6_6
5. Mukhopadhyay S, Kuhn RJ, Rossmann MG. A structural perspective of the flavivirus life cycle. Nat Rev Microbiol. 2005;3: 13–22. doi:10.1038/nrmicro1067
6. Kuhn JH, Integrated N, Detrick F, View N, View GV, Kuhn JH. Rename genus Flavivirus (Revised submission). 2017;
7. Calisher CH. Antigenic classification and taxonomy of flaviviruses (family Flaviviridae) emphasizing a universal system for the taxonomy of viruses causing tick-borne encephalitis. Acta Virol. 1988;32: 469–78. Available: http://www.ncbi.nlm.nih.gov/pubmed/2904743
8. Porterfield JS. The basis of arbovirus classification. Med Biol. 1975;53: 400–5. Available: http://www.ncbi.nlm.nih.gov/pubmed/1207193
9. Mandl CW. Steps of the tick-borne encephalitis virus replication cycle that affect neuropathogenesis. Virus Res. 2005;111: 161–174. doi:10.1016/j.virusres.2005.04.007
10. Lindquist L, Vapalahti O. Tick-borne encephalitis. Lancet (London, England). 2008;371: 1861–71. doi:10.1016/S0140-6736(08)60800-4
11. Graščenkov NI. Tick-Borne Encephalitis in the USSR. Bull World Health Organ. 1964;30: 187–196.
12. Schneider H. Über epidemische akute 'Meningitis serosa.' Klin Wochenschr. 1931;44:350452.
13. Zlobin VI, Pogodina V V., Kahl O. A brief history of the discovery of tick-borne encephalitis virus in the late 1930s (based on reminiscences of members of the expeditions, their colleagues, and relatives). Ticks Tick Borne Dis. Elsevier; 2017;8: 813–820. doi:10.1016/j.ttbdis.2017.05.001
14. Beck C, Jimenez-Clavero M, Leblond A, Durand B, Nowotny N, Leparc-Goffart I, Zientara S, Jourdain E, Lecollinet S. Flaviviruses in Europe: Complex Circulation Patterns and Their Consequences for the Diagnosis and Control of West Nile Disease. Int J Environ Res Public Health. 2013;10: 6049–6083. doi:10.3390/ijerph10116049
15. Golovljova I, Vene S, Sjölander KB, Vasilenko V, Plyusnin A, Lundkvist Å¤. Characterization of tick-borne encephalitis virus from Estonia. J Med Virol. Wiley Subscription Services, Inc., A Wiley Company; 2004;74: 580–588. doi:10.1002/jmv.20224
16. Lundkvist A, Vene S, Golovljova I, Mavtchoutko V, Forsgren M, Kalnina V, Plyusnin A. Characterization of tick-borne encephalitis virus from latvia: Evidence for co-circulation of three distinct subtypes. J Med Virol. John Wiley & Sons, Inc.; 2001;65: 730–735. doi:10.1002/jmv.2097
17. Kollaritsch H, et al. Background Document on Vaccines and Vaccination against Tick-borne Encephalitis (TBE). World Heal Organ. 2011; 1–70. Available: http://www.who.int/immunization/sage/6_TBE_backgr_18_Mar_net_apr_2011.pdf

18. Lindenbach BD, Rice CM. Molecular biology of flaviviruses. Adv Virus Res. 2003;59: 23–61. doi:10.1016/S0065-3527(03)59002-9
19. Mandl CW, Heinz FX, Stöckl E, Kunz C. Genome sequence of tick-borne encephalitis virus (Western subtype) and comparative analysis of nonstructural proteins with other flaviviruses. Virology. 1989;173: 291–301. doi:10.1016/0042-6822(89)90246-8
20. Mandl CW, Ecker M, Holzmann H, Kunz C, Heinz FX. Infectious cDNA clones of tick-borne encephalitis virus European subtype prototypic strain Neudoerfl and high virulence strain Hypr. J Gen Virol. 1997;78: 1049–1057. doi:10.1099/0022-1317-78-5-1049
21. Chambers TJ, Hahn CS, Galler R, Rice CM. Flavivirus genome organization, expression, and replication. Annu Rev Microbiol. 1990;44: 649–688. doi:10.1146/annurev.mi.44.100190.003245
22. Furuichi Y, Shatkin AJ. Viral and cellular mRNA capping: past and prospects. Adv Virus Res. 2000;55: 135–184. doi:10.1016/S0065-3527(00)55003-9
23. Cleaves GR, Dubin DT. Methylation status of intracellular dengue type 2 40 S RNA. Virology. 1979;96: 159–165. doi:10.1016/0042-6822(79)90181-8
24. Cahour A, Pletnev A, Vazeille-Falcoz M, Rosen L, Lai C-J. Growth-Restricted Dengue Virus Mutants Containing Deletions in the 5′ Noncoding Region of the RNA Genome. Virology. Academic Press; 1995;207: 68–76. doi:10.1006/VIRO.1995.1052
25. Wallner G, Mandl CW, Kunz C, Heinz FX. The flavivirus 3'-noncoding region: extensive size heterogeneity independent of evolutionary relationships among strains of tick-borne encephalitis virus. Virology. 1995. pp. 169–178. doi:10.1006/viro.1995.1557
26. Asghar N, Lindblom P, Melik W, Lindqvist R, Haglund M, Forsberg P, Verby AK, Shild Andreassen Å, Lindgren -Eric, Johansson M, Ahmed N. Tick-Borne Encephalitis Virus Sequenced Directly from Questing and Blood-Feeding Ticks Reveals Quasispecies Variance. PLoS One. 2014;9. doi:10.1371/journal.pone.0103264
27. Asghar N, Lee Y-P, Nilsson E, Lindqvist R, Melik W, Kröger A, Överby AK, Johansson M. The role of the poly(A) tract in the replication and virulence of tick-borne encephalitis virus. Sci Rep. Nature Publishing Group; 2016;6: 39265. doi:10.1038/srep39265
28. Hoenninger VM, Rouha H, Orlinger KK, Miorin L, Marcello A, Kofler RM, Mandl CW. Analysis of the effects of alterations in the tick-borne encephalitis virus 3′-noncoding region on translation and RNA replication using reporter replicons. 2008; doi:10.1016/j.virol.2008.04.035
29. Ng WC, Soto-Acosta R, Bradrick SS, Garcia-Blanco MA, Ooi EE. The 5′ and 3′ untranslated regions of the flaviviral genome. Viruses. 2017;9: 1–14. doi:10.3390/v9060137
30. Lindenbach BD, Murray CL, Thiel H-J, Rice CM. Flaviviridae. In: Knipe DM, Howley PM, editors. Fields Virology. 6th ed. Philadelphia: Lippincott Williams & Wilkins, a Wolters Kluwer business; 2013. pp. 712–746. doi:10.1016/0038-092X(88)90131-4
31. Chapman EG, Costantino DA, Rabe JL, Moon SL, Wilusz J, Nix JC, Kieft JS. The structural basis of pathogenic subgenomic flavivirus RNA (sfRNA) production. Science (80-). 2014;344: 307–310. doi:10.1126/science.1250897
32. Clarke BD, Roby JA, Slonchak A, Khromykh AA. Functional non-coding RNAs derived from the flavivirus 3′ untranslated region. Virus Res. Elsevier; 2015;206: 53–61. doi:10.1016/J.VIRUSRES.2015.01.026
33. MacFadden A, Òdonoghue Z, Silva PAGC, Chapman EG, Olsthoorn RC, Sterken MG, Pijlman GP, Bredenbeek PJ, Kieft JS. Mechanism and structural diversity of exoribonuclease-resistant RNA structures in flaviviral RNAs. Nat Commun. 2018;9: 119. doi:10.1038/s41467-017-02604-y
34. Schnettler E, Tykalová H, Watson M, Sharma M, Sterken MG, Obbard DJ, Lewis SH, McFarlane M, Bell-Sakyi L, Barry G, Weisheit S, Best SM, Kuhn RJ, Pijlman GP, Chase-Topping ME, Gould EA, Grubhoffer L,

Fazakerley JK, Kohl A. Induction and suppression of tick cell antiviral RNAi responses by tick-borne flaviviruses. Nucleic Acids Res. Oxford University Press; 2014;42: 9436–46. doi:10.1093/nar/gku657

35. Schnettler E, Sterken MG, Leung JY, Metz SW, Geertsema C, Goldbach RW, Vlak JM, Kohl A, Khromykh AA, Pijlman GP. Noncoding flavivirus RNA displays RNA interference suppressor activity in insect and Mammalian cells. J Virol. 2012;86: 13486–500. doi:10.1128/JVI.01104-12
36. Moon SL, Dodd BJT, Brackney DE, Wilusz CJ, Ebel GD, Wilusz J. Flavivirus sfRNA suppresses antiviral RNA interference in cultured cells and mosquitoes and directly interacts with the RNAi machinery. Virology. 2015;485: 322–329. doi:10.1016/J.VIROL.2015.08.009
37. Moon SL, Anderson JR, Kumagai Y, Wilusz CJ, Akira S, Khromykh AA, Wilusz J. A noncoding RNA produced by arthropod-borne flaviviruses inhibits the cellular exoribonuclease XRN1 and alters host mRNA stability. Rna. 2012;18: 2029–2040. doi:10.1261/rna.034330.112
38. Schuessler A, Funk A, Lazear HM, Cooper DA, Torres S, Daffis S, Jha BK, Kumagai Y, Takeuchi O, Hertzog P, Silverman R, Akira S, Barton DJ, Diamond MS, Khromykh AA. West Nile Virus Noncoding Subgenomic RNA Contributes to Viral Evasion of the Type I Interferon-Mediated Antiviral Response. J Virol. 2012;86: 5708–5718. doi:10.1128/JVI.00207-12
39. Pijlman GP, Funk A, Kondratieva N, Leung J, Torres S, van der Aa L, Liu WJ, Palmenberg AC, Shi P-Y, Hall RA, Khromykh AA. A Highly Structured, Nuclease-Resistant, Noncoding RNA Produced by Flaviviruses Is Required for Pathogenicity. Cell Host Microbe. 2008;4: 579–591. doi:10.1016/j.chom.2008.10.007
40. Roby JA, Pijlman GP, Wilusz J, Khromykh AA. Noncoding subgenomic flavivirus RNA: Multiple functions in west Nile virus pathogenesis and modulation of host responses. Viruses. Multidisciplinary Digital Publishing Institute (MDPI); 2014;6: 404–427. doi:10.3390/v6020404
41. Garcia-Blanco MA, Vasudevan SG, Bradrick SS, Nicchitta C. Flavivirus RNA transactions from viral entry to genome replication. Antiviral Res. Elsevier; 2016;134: 244–249. doi:10.1016/J.ANTIVIRAL.2016.09.010
42. Murphy FA. 8 – Togavirus Morphology and Morphogenesis. The Togaviruses. 1980. pp. 241–316. doi:10.1016/B978-0-12-625380-1.50013-8
43. Rey F a, Heinz FX, Mandl C, Kunz C, Harrison SC. The envelope glycoprotein from tick-borne encephalitis virus at 2 A resolution. Nature. 1995. pp. 291–298. doi:10.1038/375291a0
44. Ferlenghi I, Clarke M, Ruttan T, Allison SL, Schalich J, Heinz FX, Harrison SC, Rey FA, Fuller SD. Molecular Organization of a Recombinant Subviral Particle from Tick-Borne Encephalitis Virus. Mol Cell. Cell Press; 2001;7: 593–602. doi:10.1016/S1097-2765(01)00206-4
45. Grard G, Moureau G, Charrel RN, Lemasson JJ, Gonzalez JP, Gallian P, Gritsun TS, Holmes EC, Gould EA, de Lamballerie X. Genetic characterization of tick-borne flaviviruses: New insights into evolution, pathogenetic determinants and taxonomy. Virology. 2007;361: 80–92. doi:10.1016/j.virol.2006.09.015
46. Ecker M, Allison SL, Meixner T, Heinz FX. Sequence analysis and genetic classification of tick-borne encephalitis viruses from Europe and Asia. J Gen Virol. 1999;80: 179–185.
47. Holzmann H, Vorobyova MS, Ladyzhenskaya IP, Ferenczi E, Kundi M, Kunz C, Heinz FX. Molecular epidemiology of tick-borne encephalitis virus: cross-protection between European and Far Eastern subtypes. Vaccine. Elsevier; 1992;10: 345–349. doi:10.1016/0264-410X(92)90376-U
48. Fritz R, Orlinger KK, Hofmeister Y, Janecki K, Traweger A, Perez-Burgos L, Barrett PN, Kreil TR. Quantitative comparison of the cross-protection induced by tick-borne encephalitis virus vaccines based on European and Far Eastern virus subtypes. Vaccine. Elsevier; 2012;30: 1165–1169. doi:10.1016/J.VACCINE.2011.12.013
49. Chidumayo NN, Yoshii K, Kariwa H. Evaluation of the European tick-borne encephalitis vaccine against Omsk hemorrhagic fever virus. Microbiol Immunol. 2014;58: 112–118. doi:10.1111/1348-0421.12122
50. Smit JM, Moesker B, Rodenhuis-Zybert I, Wilschut J. Flavivirus Cell Entry and Membrane Fusion. Viruses.

2011;3: 160–171. doi:10.3390/v3020160

51. Perera-Lecoin M, Meertens L, Carnec X, Amara A. Flavivirus Entry Receptors: An Update. Viruses. 2014;6: 69–88. doi:10.3390/v6010069
52. Chen Y, Maguire T, Hileman RE, Fromm JR, Esko JD, Linhardt RJ, Marks RM. Dengue virus infectivity depends on evelope protein binding to target cell heparan sulfate. Nat Med. 1997;3: 866–871. doi:10.1038/nm0897-866
53. Hilgard P. Heparan Sulfate Proteoglycans Initiate Dengue Virus Infection of Hepatocytes. Hepatology. 2000;32: 1069–1077. doi:10.1053/jhep.2000.18713
54. Germi R, Crance J-M, Garin D, Guimet J, Lortat-Jacob H, Ruigrok RWH, Zarski J-P, Drouet E. Heparan Sulfate-Mediated Binding of Infectious Dengue Virus Type 2 and Yellow Fever Virus. Virology. 2002;292: 162–168. doi:10.1006/viro.2001.1232
55. Lee E, Lobigs M. E protein domain III determinants of yellow fever virus 17D vaccine strain enhance binding to glycosaminoglycans, impede virus spread, and attenuate virulence. J Virol. 2008;82: 6024–33. doi:10.1128/JVI.02509-07
56. Kozlovskaya LI, Osolodkin DI, Shevtsova AS, Romanova LI, Rogova Y V., Dzhivanian TI, Lyapustin VN, Pivanova GP, Gmyl AP, Palyulin VA, Karganova GG. GAG-binding variants of tick-borne encephalitis virus. Virology. Elsevier Inc.; 2010;398: 262–272. doi:10.1016/j.virol.2009.12.012
57. Zaitsev BN, Benedetti F, Mikhaylov AG, Korneev D V., Sekatskii SK, Karakouz T, Belavin PA, Netesova NA, Protopopova E V., Konovalova SN, Dietler G, Loktev VB. Force-induced globule-coil transition in laminin binding protein and its role for viral-cell membrane fusion. J Mol Recognit. Wiley-Blackwell; 2014;27: 727–738. doi:10.1002/jmr.2399
58. Malygin AA, Bondarenko EI, Ivanisenko VA, Protopopova E V., Karpova GG, Loktev VB. C-terminal fragment of human laminin-binding protein contains a receptor domain for venezuelan equine encephalitis and tick-borne encephalitis viruses. Biochem. SP MAIK Nauka/Interperiodica; 2009;74: 1328–36. doi:10.1134/S0006297909120050
59. Kroschewski H, Allison SL, Heinz FX, Mandl CW. Role of heparan sulfate for attachment and entry of tick-borne encephalitis virus. Virology. 2003;308: 92–100. doi:10.1016/S0042-6822(02)00097-1
60. Mandl CW, Kroschewski H, Allison SL, Kofler R, Holzmann H, Meixner T, Heinz FX. Adaptation of Tick-Borne Encephalitis Virus to BHK-21 Cells Results in the Formation of Multiple Heparan Sulfate Binding Sites in the Envelope Protein and Attenuation In Vivo. J Virol. 2001;75: 5627–5637. doi:10.1128/JVI.75.12.5627
61. Potokar M, Korva MMMMM, Jorgačevski J, Avšič-Županc T, Zorec R, Jorgacevski J, Avsic-Zupanc T, Zorec R, Jorgačevski J, Avšič-Županc T, Zorec R, Jorgacevski J, Avsic-Zupanc T, Zorec R, Jorgačevski J, Avšič-Županc T, Zorec R. Tick-borne encephalitis virus infects rat astrocytes but does not affect their viability. PLoS One. 2014;9: e86219. doi:10.1371/journal.pone.0086219
62. Yu C, Achazi K, Möller L, Schulzke JD, Niedrig M, Bücker R. Tick-borne encephalitis virus replication, intracellular trafficking, and pathogenicity in human intestinal Caco-2 cell monolayers. PLoS One. 2014;9: 1–10. doi:10.1371/journal.pone.0096957
63. Acosta EG, Castilla V, Damonte EB. Alternative infectious entry pathways for dengue virus serotypes into mammalian cells. Cell Microbiol. 2009;11: 1533–1549. doi:10.1111/j.1462-5822.2009.01345.x
64. Corver J, Ortiz A, Allison SL, Schalich J, Heinz FX, Wilschut J. Membrane fusion activity of tick-borne encephalitis virus and recombinant subviral particles in a liposomal model system. Virology. Academic Press; 2000;269: 37–46. doi:10.1006/viro.1999.0172
65. Stiasny K, Allison SL, Schalich J, Heinz FX. Membrane interactions of the tick-borne encephalitis virus fusion protein E at low pH. J Virol. American Society for Microbiology Journals; 2002;76: 3784–90.

doi:10.1128/JVI.76.8.3784-3790.2002

66. Van Der Schaar HM, Rust MJ, Chen, Van Der Ende-Metselaar H, Wilschut J, Zhuang X, Smit JM. Dissecting the cell entry pathway of dengue virus by single-particle tracking in living cells. Farzan M, editor. PLoS Pathog. Public Library of Science; 2008;4: e1000244. doi:10.1371/journal.ppat.1000244
67. Lindqvist R, Upadhyay A, Överby A. Tick-Borne Flaviviruses and the Type I Interferon Response. Viruses. Multidisciplinary Digital Publishing Institute; 2018;10: 340. doi:10.3390/v10070340
68. Rice CM, Lenches EM, Eddy SR, Shin SJ, Sheets RL, Strauss JH. Nucleotide sequence of yellow fever virus: implications for flavivirus gene expression and evolution. Science. American Association for the Advancement of Science; 1985;229: 726–33. doi:10.1126/SCIENCE.4023707
69. Stadler K, Allison SL, Schalich J, Heinz FX. Proteolytic Activation of Tick-Borne Encephalitis Virus by Furin. J Virol. 1997;71: 8475–8481. doi:10.1128/jvi.00037-07
70. Heinz FX, Allison SL. Flavivirus Structure and Membrane Fusion. Adv Virus Res. 2003;59: 63–97. doi:10.1016/S0065-3527(03)59003-0
71. Apte-Sengupta S, Sirohi D, Kuhn RJ. Coupling of replication and assembly in flaviviruses. Curr Opin Virol. Elsevier; 2014;9: 134–142. doi:10.1016/j.coviro.2014.09.020
72. Bílý T, Palus M, Eyer L, Elsterová J, Vancová M, Růžek D. Electron Tomography Analysis of Tick-Borne Encephalitis Virus Infection in Human Neurons. Sci Rep. Nature Publishing Group; 2015;5: 10745. doi:10.1038/srep10745
73. Mackenzie JM, Khromykh AA, Westaway EG. Stable Expression of Noncytopathic Kunjin Replicons Simulates Both Ultrastructural and Biochemical Characteristics Observed during Replication of Kunjin Virus. Virology. Academic Press; 2001;279: 161–172. doi:10.1006/VIRO.2000.0691
74. Welsch S, Miller S, Romero-Brey I, Merz A, Bleck CKE, Walther P, Fuller SD, Antony C, Krijnse-Locker J, Bartenschlager R. Composition and Three-Dimensional Architecture of the Dengue Virus Replication and Assembly Sites. Cell Host Microbe. Cell Press; 2009;5: 365–375. doi:10.1016/j.chom.2009.03.007
75. Roosendaal J, Westaway EG, Khromykh A, Mackenzie JM. Regulated cleavages at the West Nile virus NS4A-2K-NS4B junctions play a major role in rearranging cytoplasmic membranes and Golgi trafficking of the NS4A protein. J Virol. American Society for Microbiology; 2006;80: 4623–32. doi:10.1128/JVI.80.9.4623-4632.2006
76. Överby AK, Weber F. Hiding from intracellular pattern recognition receptors, a passive strategy of flavivirus immune evasion. Virulence. 2011;2: 238–40. doi:10.4161/viru.2.3.16162
77. Miorin L, Romero-Brey I, Maiuri P, Hoppe S, Krijnse-Locker J, Bartenschlager R, Marcello A. Three-dimensional architecture of tick-borne encephalitis virus replication sites and trafficking of the replicated RNA. J Virol. 2013;87: 6469–81. doi:10.1128/JVI.03456-12
78. Chu PWG, Westaway EG. Replication strategy of Kunjin Virus: Evidence for recycling role of replicative form RNA as template in semiconservative and asymmetric replication. Virology. Academic Press; 1985;140: 68–79. doi:10.1016/0042-6822(85)90446-5
79. Selisko B, Wang C, Harris E, Canard B. Regulation of Flavivirus RNA synthesis and replication. Curr Opin Virol. NIH Public Access; 2014;9: 74–83. doi:10.1016/j.coviro.2014.09.011
80. Miorin L, Albornoz A, Baba MM, D'Agaro P, Marcello A. Formation of membrane-defined compartments by tick-borne encephalitis virus contributes to the early delay in interferon signaling. Virus Res. Elsevier B.V.; 2012;163: 660–666. doi:10.1016/j.virusres.2011.11.020
81. Dokland T, Walsh M, Mackenzie JM, Khromykh AA, Ee K-H, Wang S. West Nile Virus Core Protein: Tetramer Structure and Ribbon Formation. Structure. Cell Press; 2004;12: 1157–1163. doi:10.1016/J.STR.2004.04.024
82. Elshuber S, Allison SL, Heinz FX, Mandl CW. Cleavage of protein prM is necessary for infection of BHK-21

cells by tick-borne encephalitis virus. J Gen Virol. Microbiology Society; 2003;84: 183–191. doi:10.1099/vir.0.18723-0

83. Guirakhoo F, Heinz FX, Mandl CW, Holzmann H, Kunz C. Fusion activity of flaviviruses: Comparison of mature and immature (prM-containing) tick-borne encephalitis virions. J Gen Virol. 1991;72: 1323–1329. doi:10.1099/0022-1317-72-6-1323
84. Süss J. Tick-borne encephalitis 2010: Epidemiology, risk areas, and virus strains in Europe and Asia-An overview. Ticks Tick Borne Dis. 2011;2: 2–15. doi:10.1016/j.ttbdis.2010.10.007
85. Labuda M, Randolph SE. Survival strategy of tick-borne encephalitis virus: Cellular basis and environmental determinants. Zentralblatt für Bakteriol. 1999;289: 513–524. doi:10.1016/S0934-8840(99)80005-X
86. Cisak E, Wójcik-Fatla A, Zajac V, Sroka J, Buczek A, Dutkiewicz J. Prevalence of tick-borne encephalitis virus (TBEV) in samples of raw milk taken randomly from cows, goats and sheep in Eastern Poland. Ann Agric Environ Med. 2010;17: 283–286. doi:17283 [pii]
87. Caini S, Szomor K, Ferenczi E, Székelyné Gáspár A, Csohán A, Krisztalovics K, Molnár Z, Horváth JK. Tick-borne encephalitis transmitted by unpasteurised cow milk in Western Hungary, September to October 2011. Eurosurveillance. 2012;17: 13–17.
88. Hudopisk N, Korva M, Janet E, Simetinger M, Grgič-Vitek M, Gubenšek J, Natek V, Kraigher A, Strle F, Avšič-Županc T. Tick-borne encephalitis associated with consumption of raw goat milk, Slovenia, 2012. Emerg Infect Dis. 2013;19: 806–808. doi:10.3201/eid1905.121442
89. Van Tongeren HA. Encephalitis in Austria. IV. Excretion of virus by milk of the experimentally infected goat. 1955;
90. Offerdahl DK, Clancy NG, Bloom ME. Stability of a Tick-Borne Flavivirus in Milk. Front Bioeng Biotechnol. Frontiers Media SA; 2016;4: 40. doi:10.3389/fbioe.2016.00040
91. Avšič-Županc T, Poljak M, Matičič M, Radšel-Medvešček A, LeDuc JW, Stiasny K, Kunz C, Heinz FX. Laboratory acquired tick-borne meningoencephalitis: characterisation of virus strains. Clin Diagn Virol. 1995;4: 51–59. doi:10.1016/0928-0197(94)00062-Y
92. Lipowski D, Popiel M, Perlejewski K, Nakamura S, Bukowska-Ośko I, Rzadkiewicz E, Dzieciątkowski T, Milecka A, Wenski W, Ciszek M, Dębska-Ślizień A, Ignacak E, Cortes KC, Pawełczyk A, Horban A, Radkowski M, Laskus T. A Cluster of Fatal Tick-borne Encephalitis Virus Infection in Organ Transplant Setting. J Infect Dis ®. 2017;896: 896–901. doi:10.1093/infdis/jix040
93. Wahlberg P, Saikku P, Brummer-Korvenkontio M. Tick-borne viral encephalitis in Finland. The clinical features of Kumlinge disease during 1959–1987. J Intern Med. Wiley/Blackwell (10.1111); 1989;225: 173–177. doi:10.1111/j.1365-2796.1989.tb00059.x
94. Besnard M, Lastere S, Teissier A. Evidence of perinatal transmission of Zika virus, French Polynesia. Euro Surveill. 2014;19: 8–11.
95. Cavalcanti MG, Cabral-Castro MJ, Gonçalves JLS, Santana LS, Pimenta ES, Peralta JM. Zika virus shedding in human milk during lactation: an unlikely source of infection? Int J Infect Dis. International Society for Infectious Diseases; 2017;57: 70–72. doi:10.1016/j.ijid.2017.01.042
96. Barthel A, Gourinat A-C, Cazorla C, Joubert C, Dupont-Rouzeyrol M, Descloux E. Breast Milk as a Possible Route of Vertical Transmission of Dengue Virus? Clin Infect Dis. Oxford University Press; 2013;57: 415–417. doi:10.1093/cid/cit227
97. Centers for Disease Control and Prevention (CDC). Possible West Nile virus transmission to an infant through breast-feeding--Michigan, 2002. MMWR Morb Mortal Wkly Rep. 2002;51: 877–8. Available: http://www.ncbi.nlm.nih.gov/pubmed/12375687
98. Kuhn S, Twele-Montecinos L, MacDonald J, Webster P, Law B. Case report: probable transmission of

vaccine strain of yellow fever virus to an infant via breast milk. CMAJ. CMAJ; 2011;183: E243-5. doi:10.1503/cmaj.100619

99. Bogovic P. Tick-borne encephalitis: A review of epidemiology, clinical characteristics, and management. World J Clin Cases. 2015;3: 430. doi:10.12998/wjcc.v3.i5.430
100. Counotte MJ, Kim CR, Wang J, Bernstein K, Deal CD, Broutet NJN, Low N. Sexual transmission of Zika virus and other flaviviruses: A living systematic review. PLOS Med. Public Library of Science; 2018;15: e1002611. doi:10.1371/JOURNAL.PMED.1002611
101. Sexual transmission of ZIKV meeting of experts. Sexual transmission of Zika Virus: Current status, challenges and research priorities: Summary of discussions [Internet]. Geneva; 2017. Available: http://www.who.int/reproductivehealth/zika/sexual-transmission-experts-meeting/en/
102. Dumpis U, Crook D, Oksi J. Tick-borne encephalitis. Clin Infect Dis. 1999;28: 882–890. Available: http://cid.oxfordjournals.org/content/28/4/882.short
103. WHO. Vaccines against tick-borne encephalitis: WHO position paper. Wkly Epidemiol Rec. 2011;24: 241–256. doi:10.1371/jour
104. Valarcher JF, Hägglund S, Juremalm M, Blomqvist G, Renström L, Zohari S, Leijon M, Chirico J. Tick-borne encephalitis. Rev Sci Tech. 2015;34: 453–66. Available: http://www.ncbi.nlm.nih.gov/pubmed/26601448
105. Laursen K, Knudsen JD. Tick-borne Encephalitis: A Retrospective Study of Clinical Cases in Bornholm, Denmark. Scand J Infect Dis. 2003;35: 354–357. doi:10.1080/0036554021000027001
106. Skarpaas T, Ljøstad U, Sundøy A. First human cases of tickborne encephalitis, Norway. Emerg Infect Dis. 2004;10: 2241–2243. doi:10.3201/eid1012.040598
107. ECDC. Epidemiological situation of tick-borne encephalitis in the European Union and European Free Trade Association countries. ECDC Technical Report. Stockholm; 2012. doi:10.2900/62311
108. De Graaf JA, Reimerink JHJ, Voorn GP, De Vaate EALB, De Vries A, Rockx B, Schuitemaker A, Hira V. First human case of tick-borne encephalitis virus infection acquired in the Netherlands, July 2016. Eurosurveillance. 2016;21: 4–6. doi:10.2807/1560-7917.ES.2016.21.33.30318
109. Heinz FX, Stiasny K, Holzmann H, Kundi M, Sixl W, Wenk M, Kainz W, Essl A, Kunz C, Six W, Wenk M, Kainz W, Essl A, Kunz C. Emergence of tick-borne encephalitis in new endemic areas in Austria: 42 years of surveillance. Eurosurveillance. 2015;20: 16–19. doi:10.2807/1560-7917.ES2015.20.13.21077
110. Lukan M, Bullova E, Petko B. Climate warming and tick-borne encephalitis, Slovakia. Emerg Infect Dis. Centers for Disease Control and Prevention; 2010;16: 524–6. doi:10.3201/eid1603.081364
111. Süss J. Tick-borne encephalitis in Europe and beyond--the epidemiological situation as of 2007. Euro Surveill. 2008;13: 2–9.
112. Charrel RN, Attoui H, Butenko AM, Clegg JC, Deubel V, Frolova T V., Gould EA, Gritsun TS, Heinz FX, Labuda M, Lashkevich VA, Loktev V, Lundkvist A, Lvov D V., Mandl CW, Niedrig M, Papa A, Petrov VS, Plyusnin A, Randolph S, Süss J, Zlobin VI, de Lamballerie X. Tick-borne virus diseases of human interest in Europe. Clin Microbiol Infect. 2004;10: 1040–1055. doi:10.1111/j.1469-0691.2004.01022.x
113. Velay A, Solis M, Kack-Kack W, Gantner P, Maquart M, Martinot M, Augereau O, De Briel D, Kieffer P, Lohmann C, Poveda JD, Cart-Tanneur E, Argemi X, Leparc-Goffart I, de Martino S, Jaulhac B, Raguet S, Wendling MJ, Hansmann Y, Fafi-Kremer S. A new hot spot for tick-borne encephalitis (TBE): A marked increase of TBE cases in France in 2016. Ticks Tick Borne Dis. 2017; doi:10.1016/j.ttbdis.2017.09.015
114. Amato-Gauci AJ, Zeller H. Tick-borne encephalitis joins the diseases under surveillance in the European Union. Eurosurveillance. 2012;17: 1–2.
115. European Commission. Commission Implementing Decision of 8 August 2012 amending Decision 2002/253/EC laying down case definitions for reporting communicable diseases to the Community

network under Decision No 2119/98/EC of the European Parliament and of the Counci [Internet]. Official Journal of the European Union. 2012. Available: http://eur-lex.europa.eu/legal-content/EN/TXT/PDF/?uri=CELEX:32012D0506&qid=1428573336660&from=EN#page=32)

116. European Commission. Commission Implementing Decision (EU) 2018/945 of 22 June 2018 on the communicable diseases and related special health issues to be covered by epidemiological surveillance as well as relevant case definitions. Official Journal of the European Union. Brussels; 2018.
117. Heinz FX, Stiasny K, Holzmann H, Grgic-Vitek M, Kriz B, Essl A, Kundi M. Vaccination and tick-borne encephalitis, central Europe. Emerg Infect Dis. 2013;19: 69–76. doi:10.3201/eid1901.120458
118. Donoso Mantke O, Escadafal C, Niedrig M, Pfeffer M. Tick-borne encephalitis in Europe, 2007 to 2009. Eurosurveillance. 2011;16.
119. Poblete-Durán N, Prades-Pérez Y, Vera-Otarola J, Soto-Rifo R, Valiente-Echeverría F, Mccormick C. Who Regulates Whom? An Overview of RNA Granules and Viral Infections. Viruses. Multidisciplinary Digital Publishing Institute (MDPI); 2016;8. doi:10.3390/v8070180
120. WHO. Centralized information system for infectious diseases (CISID) [Internet]. WHO - Regional Office for Europe; 2018 [cited 9 Aug 2018]. Available: http://data.euro.who.int/cisid/
121. Kříž B, Beneš Č, Danielová V, Daniel M. Socio-economic conditions and other anthropogenic factors influencing tick-borne encephalitis incidence in the Czech Republic. Int J Med Microbiol Suppl. 2004;293: 63–68. doi:10.1016/S1433-1128(04)80010-X
122. Pugliese A, Rosà R. Effect of host populations on the intensity of ticks and the prevalence of tick-borne pathogens: How to interpret the results of deer exclosure experiments. Parasitology. Cambridge University Press; 2008. pp. 1531–1544. doi:10.1017/S003118200800036X
123. Randolph SE, Asokliene L, Avsic-Zupanc T, Bormane A, Burri C, Gern L, Golovljova I, Hubalek Z, Knap N, Kondrusik M, Kupca A, Pejcoch M, Vasilenko V, Zygutiene M. Variable spikes in tick-borne encephalitis incidence in 2006 independent of variable tick abundance but related to weather. Parasit Vectors. 2008;1: 44. doi:10.1186/1756-3305-1-44
124. Süss J, Klaus C, Gerstengarbe FW, Werner PC. What makes ticks tick? Climate change, ticks, and tick-borne diseases. J Travel Med. 2008;15: 39–45. doi:10.1111/j.1708-8305.2007.00176.x
125. Šumilo D, Asokliene L, Bormane A, Vasilenko V, Golovljova I, Randolph SE. Climate Change Cannot Explain the Upsurge of Tick-Borne Encephalitis in the Baltics. PLoS One. 2007;2. doi:10.1371/journal.pone.0000500
126. Šumilo D, Bormane A, Asokliene L, Vasilenko V, Golovljova I, Avsic-Zupanc T, Zdenek H, Randolph SE. Socio-economic factors in the differential upsurge of tick-borne encephalitis in Central and Eastern Europe. Rev Med Virol. 2008;18: 81–95. doi:10.1002/rmv
127. Šumilo D, Asokliene L, Avsic-Zupanc T, Bormane A, Vasilenko V, Lucenko I, Golovljova I, Randolph SE. Behavioural responses to perceived risk of tick-borne encephalitis: Vaccination and avoidance in the Baltics and Slovenia. Vaccine. 2008;26: 2580–2588. doi:10.1016/j.vaccine.2008.03.029
128. Weinberger B, Keller M, Fischer KH, Stiasny K, Neuner C, Heinz FX, Grubeck-Loebenstein B. Decreased antibody titers and booster responses in tick-borne encephalitis vaccinees aged 50-90 years. Vaccine. Elsevier Ltd; 2010;28: 3511–3515. doi:10.1016/j.vaccine.2010.03.024
129. Stiasny K, Aberle JH, Keller M, Grubeck-Loebenstein B, Heinz FX. Age affects quantity but not quality of antibody responses after vaccination with an inactivated flavivirus vaccine against tick-borne encephalitis. PLoS One. 2012;7: 1–7. doi:10.1371/journal.pone.0034145
130. Süss J. Epidemiology and ecology of TBE relevant to the production of effective vaccines. Vaccine. 2003;21: S19–S35. doi:10.1016/S0264-410X(02)00812-5
131. Nuttall PA, Labuda M. Tick–host interactions: saliva-activated transmission. Parasitology. 2004;129: S177–

S189. doi:10.1017/S0031182004005633

132. Sauer R, McSwain L, Bowman AS, Essenberg RC. Tick Salivary Gland Physiology. AIllIU Rev Entomol. 1995;40: 245–67. doi:10.1146/annurev.ento.40.1.245

133. Bakhvalova VN, Potapova OF, Panov V V, Morozova O V. Vertical transmission of tick-borne encephalitis virus between generations of adapted reservoir small rodents. Virus Res. Elsevier; 2009;140: 172–178. Available: https://www.sciencedirect.com/science/article/pii/S0168170208004103

134. Jaenson TGT, Hjertqvist M, Bergström T, Lundkvist \AAke, Lundkvist A. Why is tick-borne encephalitis increasing? A review of the key factors causing the increasing incidence of human TBE in Sweden. Parasit Vectors. 2012;5: 184. doi:10.1186/1756-3305-5-184

135. Tonteri E, Kipar A, Voutilainen L, Vene S, Vaheri A, Vapalahti O, Lundkvist ??ke. The three subtypes of tick-borne encephalitis virus induce encephalitis in a natural host, the bank vole (Myodes glareolus). PLoS One. 2013;8: 15–19. doi:10.1371/journal.pone.0081214

136. Knap N, Korva M, Dolinšek V, Sekirnik M, Trilar T, Avšič-Županc T. Patterns of Tick-Borne Encephalitis Virus Infection in Rodents in Slovenia. Vector-Borne Zoonotic Dis. Mary Ann Liebert, Inc. 140 Huguenot Street, 3rd Floor New Rochelle, NY 10801 USA ; 2012;12: 236–242. doi:10.1089/vbz.2011.0728

137. Gerlinskaya LA, Bakhvalova VN, Morozova O V., Tsekhanovskaya NA, Matveeva VA, Moshkin MP. Sexual transmission of tick-borne encephalitis virus in laboratory mice. Bull Exp Biol Med. Kluwer Academic Publishers-Plenum Publishers; 1997;123: 283–284. doi:10.1007/BF02445427

138. Estrada-Peña A, De La Fuente J. The ecology of ticks and epidemiology of tick-borne viral diseases. Antiviral Res. 2014;108: 104–128. doi:10.1016/j.antiviral.2014.05.016

139. Movila A, Alekseev AN, Dubinina H V., Toderas I. Detection of tick-borne pathogens in ticks from migratory birds in the Baltic region of Russia. Med Vet Entomol. 2013;27: 113–117. doi:10.1111/j.1365-2915.2012.01037.x

140. Moskvitina NS, Korobitsyn IG, Tyutenkov OY, Gashkov SI, Kononova Y V, Moskvitin SS, Romanenko VN, Mikryukova TP, Protopopova E V, Kartashov MY, Chausov E V, Konovalova SN, Tupota NL, Sementsova AO, Ternovoy VA, Loktev VB. The Potential Role of Migratory Birds in the Spread of Tick-borne Infections in Siberia and the Russian Far East. 2014; doi:10.1016/j.als.2015.01.005

141. Mikryukova TP, Moskvitina NS, Kononova Y V., Korobitsyn IG, Kartashov MY, Tyuten′kov OY, Protopopova E V., Romanenko VN, Chausov E V., Gashkov SI, Konovalova SN, Moskvitin SS, Tupota NL, Sementsova AO, Ternovoi VA, Loktev VB. Surveillance of tick-borne encephalitis virus in wild birds and ticks in Tomsk city and its suburbs (Western Siberia). Ticks Tick Borne Dis. Urban & Fischer; 2014;5: 145–151. doi:10.1016/J.TTBDIS.2013.10.004

142. Csank T, Bhide K, Bencúrová E, Dolinská S, Drzewnioková P, Major P, Korytár Ľ, Bocková E, Bhide M, Pistl J. Detection of West Nile virus and tick-borne encephalitis virus in birds in Slovakia, using a universal primer set. Arch Virol. 2016;04: 1–5. doi:10.1007/s00705-016-2828-5

143. Waldenström J, Lundkvist A, Falk KI, Garpmo U, Bergström S, Lindegren G, Sjöstedt A, Mejlon H, Fransson T, Haemig PD, Olsen B. Migrating birds and tickborne encephalitis virus. Emerg Infect Dis. Centers for Disease Control and Prevention; 2007;13: 1215–1218. doi:10.3201/eid1308.061416

144. Kazarina A, Japiņa K, Keišs O, Salmane I, Bandere D, Capligina V, Ranka R. Detection of tick-borne encephalitis virus in I. ricinus ticks collected from autumn migratory birds in Latvia. Ticks Tick Borne Dis. 2015;6: 178–180. doi:10.1016/j.ttbdis.2014.11.011

145. Suzuki Y. Multiple transmissions of tick-borne encephalitis virus between Japan and Russia. Genes Genet Syst. 2007;82: 187–195. doi:10.1266/ggs.82.187

146. Leschnik MW, Kirtz GC, Thalhammer JG. Tick-borne encephalitis (TBE) in dogs. Int J Med Microbiol. 2002;291: 66–69. doi:10.1016/S1438-4221(02)80014-5

147. Weissenbock H, Suchy A, Holzmann H, Weissenböck H, Suchy A, Holzmann H, Weissenbock H, Suchy A, Holzmann H. Tick-borne encephalitis in dogs: Neuropathological findings and distribution of antigen. Acta Neuropathol. Springer-Verlag; 1998;95: 361–366. doi:10.1007/s004010050811
148. García-Bocanegra I, Jurado-Tarifa E, Cano-Terriza D, Martínez R, Pérez-Marín JE, Lecollinet S. Exposure to West Nile virus and tick-borne encephalitis virus in dogs in Spain. Transbound Emerg Dis. 2018; 1–8. doi:10.1111/tbed.12801
149. Pfeffer M, Dobler G. Tick-borne encephalitis virus in dogs - is this an issue? Parasit Vectors. BioMed Central Ltd; 2011;4: 59. doi:10.1186/1756-3305-4-59
150. Imhoff M, Hagedorn P, Schulze Y, Hellenbrand W, Pfeffer M, Niedrig M. Review: Sentinels of tick-borne encephalitis risk. Ticks Tick Borne Dis. Elsevier GmbH.; 2015;6: 592–600. doi:10.1016/j.ttbdis.2015.05.001
151. Rushton JO, Lecollinet S, Hubálek Z, Svobodová P, Lussy H, Nowotny N. Tick-borne Encephalitis Virus in Horses, Austria, 2011. 2013;19: 2011–2013.
152. Klaus C, Hörügel U, Hoffmann B, Beer M. Tick-borne encephalitis virus (TBEV) infection in horses: Clinical and laboratory findings and epidemiological investigations. Vet Microbiol. 2013;163: 368–372. doi:10.1016/j.vetmic.2012.12.041
153. Jahfari S, de Vries A, Rijks JM, Van Gucht S, Vennema H, Sprong H, Rockx B. Tick-Borne Encephalitis Virus in Ticks and Roe Deer, the Netherlands. Emerg Infect Dis. 2017;23: 4–6. doi:10.3201/eid2306.161247
154. Gerth H-J, Grimshandl D, Stage B, Döller G, Kunz C. Roe Deer as Sentinels for Endemicity of Tick-Borne Encephalitis Virus [Internet]. Epidemiology and Infection. Cambridge University Press; 1995. pp. 355–365. doi:10.2307/3864481
155. Kříž B, Daniel M, Beneš Č, Maly M. The Role of Game (Wild Boar and Roe Deer) in the Spread of Tick-Borne Encephalitis in the Czech Republic. Vector-Borne Zoonotic Dis. 2014;14: 801–807. doi:10.1089/vbz.2013.1569
156. Cagnacci F, Bolzoni L, Rosà R, Carpi G, Hauffe HC, Valent M, Tagliapietra V, Kazimirova M, Koci J, Stanko M, Lukan M, Henttonen H, Rizzoli A. Effects of deer density on tick infestation of rodents and the hazard of tick-borne encephalitis. I: Empirical assessment. Int J Parasitol. 2012;42: 365–372. doi:10.1016/j.ijpara.2012.02.012
157. Roelandt S, Suin V, Van der Stede Y, Lamoral S, Marche S, Tignon M, Saiz JC, Escribano-Romero E, Casaer J, Brochier B, Van Gucht S, Roels S, Vervaeke M. First TBEV serological screening in Flemish wild boar. Infect Ecol Epidemiol. Taylor & Francis; 2016;6: 31099. doi:10.3402/IEE.V6.31099
158. Böhm B, Schade B, Bauer B, Hoffmann B, Hoffmann D, Ziegler U, Beer M, Klaus C, Weissenböck H, Böttcher J. Tick-borne encephalitis in a naturally infected sheep. BMC Vet Res. BioMed Central; 2017;13: 267. doi:10.1186/s12917-017-1192-3
159. Mansfield KL, Johnson N, Banyard AC, Núñez A, Baylis M, Solomon T, Fooks AR. Innate and adaptive immune responses to tick-borne flavivirus infection in sheep. Vet Microbiol. 2016;185: 20–28. doi:10.1016/j.vetmic.2016.01.015
160. Klaus C, Hoffmann B, Moog U, Schau U, Beer M, Süss J. Can goats BE used as sentinels for tick-borne encephalitis (TBE) in nonendemic areas? Experimental studies and epizootiological observations. Berl Munch Tierarztl Wochenschr. 2010;123: 441–445. doi:10.2376/0005-9366-123-441
161. Süss J, Gelpi E, Klaus C, Bagon A, Liebler-Tenorio EM, Budka H, Stark B, Müller W, Hotzel H. Tickborne encephalitis in naturally exposed monkey (Macaca sylvanus). Emerg Infect Dis. 2007;13: 905–907. doi:10.3201/eid1306.061173
162. Kenyon RH, Rippy MK, McKee KT, Zack PM, Peters CJ. Infection of Macaca radiata with viruses of the tick-borne encephalitis group. Microb Pathog. 1992;13: 399–409. doi:10.1016/0882-4010(92)90083-Z

163. Fokina GI, Malenko G V, Levina LS, Koreshkova G V, Rzhakhova OE, Mamonenko LL, Pogodina V V, Frolova MP. Persistence of tick-borne encephalitis virus in monkeys. V. Virus localization after subcutaneous inoculation. Acta Virol. 1982;26: 369–75. Available: http://www.ncbi.nlm.nih.gov/pubmed/6128905
164. Pogodina V V, Bochkova NG, Levina LS. Persistence of tick-borne encephalitis virus in monkeys. VII. Some features of the immune response. Acta Virol. 1984;28: 407–15. Available: http://www.ncbi.nlm.nih.gov/pubmed/6151355
165. Pogodina V V, Frolova MP, Malenko G V, Fokina GI, Levina LS, Mamonenko LL, Koreshkova G V, Ralf NM. Persistence of tick-borne encephalitis virus in monkeys. I. Features of experimental infection. Acta Virol. 1981;25: 337–43. Available: http://www.ncbi.nlm.nih.gov/pubmed/6120634
166. Daniel M, Kříž B, Danielová V, Beneš Č. Sudden increase in tick-borne encephalitis cases in the Czech Republic, 2006. Int J Med Microbiol. 2008;298: 81–87. doi:10.1016/j.ijmm.2008.02.006
167. Randolph SE. Evidence that climate change has caused 'emergence' of tick-borne diseases in Europe? Int J Med Microbiol Suppl. 2004;293: 5–15. doi:10.1016/S1433-1128(04)80004-4
168. Gray JS. Ixodes ricinus seasonal activity: Implications of global warming indicated by revisiting tick and weather data. Int J Med Microbiol. 2008;298: 19–24. doi:10.1016/j.ijmm.2007.09.005
169. Lu Z, Bröker M, Liang G. Tick-borne encephalitis in mainland China. Vector borne zoonotic Dis. 2008;8: 713–20. doi:10.1089/vbz.2008.0028
170. Sun R-X, Lai S-J, Yang Y, Li X-L, Liu K, Yao H-W, Zhou H, Li Y, Wang L-P, Mu D, Yin W-W, Fang L-Q, Yu H-J, Cao W-C. Mapping the distribution of tick-borne encephalitis in mainland China. Ticks Tick Borne Dis. 2017;8: 631–639. doi:10.1016/j.ttbdis.2017.04.009
171. Wójcik-Fatla A, Cisak E, Zajac V, Zwoliński J, Dutkiewicz J. Prevalence of tick-borne encephalitis virus in Ixodes ricinus and Dermacentor reticulatus ticks collected from the Lublin region (eastern Poland). Ticks Tick Borne Dis. 2011;2: 16–19. doi:10.1016/j.ttbdis.2010.10.001
172. Yun S-M, Song BG, Choi W, Park W Il, Kim SY, Roh JY, Ryou J, Ju YR, Park C, Shin E-H. Prevalence of tick-borne encephalitis virus in ixodid ticks collected from the republic of Korea during 2011-2012. Osong public Heal Res Perspect. 2012;3: 213–21. doi:10.1016/j.phrp.2012.10.004
173. Goodman JL, Dennis DT, Sonenshine DE. Tick-borne diseases of humans. Goodman JL, Dennis DT, Sonenshine DE, editors. Washington, USA: ASM Press; 2005.
174. Randolph SE, Miklisová D, Lysy J, Rogers DJ, Labuda M. Incidence from coincidence: Patterns of tick infestations on rodents facilitate transmission of tick-borne encephalitis virus. Parasitology. 1999;118: 177–186. doi:10.1017/S0031182098003643
175. Randolph SE, Gern L, Nuttall PA. Co-feeding ticks: Epidemiological significance for tick-borne pathogen transmission. Parasitol Today. 1996;12: 472–479. doi:10.1016/S0169-4758(96)10072-7
176. Steere AC, Strle F, Wormser GP, Hu LT, Branda JA, Hovius JWR, Li X, Mead PS. Lyme borreliosis. Nat Rev Dis Prim. Nature Publishing Group; 2016;2: 16090. doi:10.1038/nrdp.2016.90
177. Nuttall PA, Labuda M. Dynamics of infection in tick vectors and at the tick-host interface. Adv Virus Res. 2003;60: 233–272. doi:10.1016/S0065-3527(03)60007-2
178. Gritsun TS, Lashkevich VA, Gould EA. Tick-borne encephalitis. Antiviral Res. 2003;57: 129–146.
179. Labuda M, Jones LD, Williams T, Danielova V, Nuttall PA. Efficient Transmission of Tick-Borne Encephalitis Virus Between Cofeeding Ticks. J Med Entomol. Oxford University Press; 1993;30: 295–299. doi:10.1093/jmedent/30.1.295
180. Labuda M, Nuttall PA, Kožuch O, Elečková E, Williams T, Žuffová E, Sabó A. Non-viraemic transmission of tick-borne encephalitis virus: a mechanism for arbovirus survival in nature [Internet]. Experientia. 1993. doi:10.1007/BF01923553
181. Labuda M, Austyn JM, Zuffova E, Kozuch O, Fuchsberger N, Lysy J, Nuttall PA. Importance of localized

skin infection in tick-borne encephalitis virus transmission. Virology. 1996;219: 357–66. doi:10.1006/viro.1996.0261

182. Karbowiak G, Biernat B, Werszko J, Rychlik L. The transstadial persistence of tick-borne encephalitis virus in Dermacentor reticulatus ticks in natural conditions. Acta Parasitol. 2016;61. doi:10.1515/ap-2016-0028
183. Pfeffer M, Dobler G. Emergence of zoonotic arboviruses by animal trade and migration. Parasit Vectors. 2010;3: 35. doi:10.1186/1756-3305-3-35
184. Danielová V, Holubová J, Pejcoch M, Daniel M. Potential significance of transovarial transmission in the circulation of tick-borne encephalitis virus. Folia Parasitol (Praha). 2002;49: 323–5. Available: https://folia.paru.cas.cz/pdfs/fol/2002/04/15.pdf
185. Pettersson JH-O, Golovljova I, Vene S, Jaenson TGT. Prevalence of tick-borne encephalitis virus in Ixodes ricinus ticks in northern Europe with particular reference to Southern Sweden. Parasit Vectors. Parasites & Vectors; 2014;7: 102. doi:10.1186/1756-3305-7-102
186. Contigiani MS, Diaz LA, Spinsanti L. Flavivirus. Arthropod Borne Diseases. Cham: Springer International Publishing; 2017. pp. 73–88. doi:10.1007/978-3-319-13884-8_6
187. Gould E, Solomon T. Pathogenic flaviviruses. Lancet. 2008;371: 500–509. doi:10.1016/S0140-6736(08)60238-X
188. Gustafson R, Svenungsson B, Forsgren M, Gardulf A, Granstrom M, Granström M, Granstrom M, Granström M, Granstrom M, Granström M, Granstrom M, Granström M. Two-year survey of the incidence of lyme borreliosis and tick-borne encephalitis in a high-risk population in Sweden. Eur J Clin Microbiol Infect Dis. Springer-Verlag; 1992;11: 894–900. doi:10.1007/BF01962369
189. Bogovic P, Lotric-Furlan S, Strle F. What tick-borne encephalitis may look like: Clinical signs and symptoms. Travel Med Infect Dis. Elsevier Ltd; 2010;8: 246–250. doi:10.1016/j.tmaid.2010.05.011
190. Kaiser R. Tick-Borne Encephalitis. Infect Dis Clin North Am. 2008;22: 561–575. doi:10.1016/j.idc.2008.03.013
191. Mickiene A, Laiskonis A, Günther G, Vene S, Lundkvist A, Lindquist L. Tickborne encephalitis in an area of high endemicity in lithuania: disease severity and long-term prognosis. Clin Infect Dis. Oxford University Press; 2002;35: 650–658. doi:10.1086/342059
192. Kaiser R. The clinical and epidemiological profile of tick-borne encephalitis in southern Germany 1994-98. A prospective study of 656 patients. Brain. 1999;122: 2067–2078. doi:10.1093/brain/122.11.2067
193. Růžek D, Dobler G, Mantke OD. Tick-borne encephalitis: Pathogenesis and clinical implications. Travel Med Infect Dis. 2010;8: 223–232. doi:10.1016/j.tmaid.2010.06.004
194. Lotrič-Furlan S, Strle F. Thrombocytopenia - A common finding in the initial phase of tick-borne encephalitis. Infection. Springer-Verlag; 1995;23: 203–206. doi:10.1007/BF01781197
195. Lotrič-Furlan S, Strle F. Thrombocytopenia, Leukopenia and abnormal liver function tests in the initial phase of Tick-borne Encephalitis. Zentralblatt fur Bakteriol. 1995;282: 275–278. doi:10.1016/S0934-8840(11)80127-1
196. Holzmann H. Diagnosis of tick-borne encephalitis. Vaccine. Elsevier; 2003;21: S36–S40. doi:10.1016/S0264-410X(02)00819-8
197. Blom K, Cuapio A, Sandberg JT, Varnaite R, Michaëlsson J, Björkström NK, Sandberg JK, Klingström J, Lindquist L, Gredmark Russ S, Ljunggren H-G. Cell-Mediated Immune Responses and Immunopathogenesis of Human Tick-Borne Encephalitis Virus-Infection. Front Immunol. Frontiers; 2018;9: 2174. doi:10.3389/fimmu.2018.02174
198. Gritsun TS, Frolova T V, Zhankov AI, Armesto M, Turner SL, Frolova MP, Pogodina V V, Lashkevich VA, Gould EA. Characterization of a siberian virus isolated from a patient with progressive chronic tick-borne

encephalitis. J Virol. American Society for Microbiology; 2003;77: 25–36. doi:10.1128/JVI.77.1.25-36.2003

199. Růžek D, Salát J, Palus M, Gritsun TS, Gould EA, Dyková I, Skallová A, Jelínek J, Kopecký J, Grubhoffer L. CD8+ T-cells mediate immunopathology in tick-borne encephalitis. Virology. 2009;384: 1–6. doi:10.1016/j.virol.2008.11.023
200. Mansfield KL, Johnson N, Phipps LP, Stephenson JR, Fooks AR, Solomon T. Tick-borne encephalitis virus - A review of an emerging zoonosis. J Gen Virol. 2009;90: 1781–1794. doi:10.1099/vir.0.011437-0
201. Haglund M, Günther G. Tick-borne encephalitis—pathogenesis, clinical course and long-term follow-up. Vaccine. 2003;21: S11–S18. doi:10.1016/S0264-410X(02)00811-3
202. Poponnikova T V. Specific clinical and epidemiological features of tick-borne encephalitis in Western Siberia. Int J Med Microbiol. 2006;296: 59–62. doi:10.1016/j.ijmm.2006.01.023
203. Monath TP. Pathobiology of the Flaviviruses. The Togaviridae and Flaviviridae. Boston, MA: Springer New York; 1986. pp. 375–440. doi:10.1007/978-1-4757-0785-4_12
204. Zent O, Bröker M. Tick-borne encephalitis vaccines: past and present. Expert Rev Vaccines. Taylor & Francis; 2005;4: 747–755. doi:10.1586/14760584.4.5.747
205. Amicizia D, Domnich A, Panatto D, Lai PL, Cristina ML, Avio U, Gasparini R. Epidemiology of tick-borne encephalitis (TBE) in Europe and its prevention by available vaccines. Hum Vaccin Immunother. Taylor & Francis; 2013;9: 1163–71. doi:10.4161/hv.23802
206. Yoshii K, Song JY, Park S-B, Yang J, Schmitt H-J. Tick-borne encephalitis in Japan, Republic of Korea and China. Emerg Microbes Infect. Nature Publishing Group; 2017;6: e82. doi:10.1038/emi.2017.69
207. Orlinger KK, Hofmeister Y, Fritz R, Holzer GW, Falkner FG, Unger B, Loew-Baselli A, Poellabauer EM, Ehrlich HJ, Barrett PN, Kreil TR. A tick-borne encephalitis virus vaccine based on the European prototype strain induces broadly reactive cross-neutralizing antibodies in humans. J Infect Dis. 2011;203: 1556–1564. doi:10.1093/infdis/jir122
208. Tigabu B, Juelich T, Holbrook MR. Comparative analysis of immune responses to Russian spring–summer encephalitis and Omsk hemorrhagic fever viruses in mouse models. Virology. 2010;408: 57–63. doi:10.1016/j.virol.2010.08.021
209. Heinz FX, Holzmann H, Essl A, Kundi M. Field effectiveness of vaccination against tick-borne encephalitis. Vaccine. 2007;25: 7559–7567. doi:10.1016/j.vaccine.2007.08.024
210. Ransohoff RM, Brown MA. Innate immunity in the central nervous system. J Clin Invest. American Society for Clinical Investigation; 2012;122: 1164–1171. doi:10.1172/JCI58644
211. Frankel SS, Wu S-JL, Grouard-Vogel G, Sun W, Mascola JR, Brachtel E, Putvatana R, Louder MK, Filgueira L, Marovich MA, Wong HK, Blauvelt A, Murphy GS, Robb ML, Innes BL, Birx DL, Hayes CG. Human skin Langerhans cells are targets of dengue virus infection. Nat Med. Nature Publishing Group; 2000;6: 816–820. doi:10.1038/77553
212. Donoso-Mantke O, Karan LS, Růžek D, Mantke OD, Karan LS, Ruzek D. Tick-Borne Encephalitis Virus: A General Overview. Flavivirus Enceph. Robert Koch-Institut, Infektionsepidemiologie; 2011; 133–156. doi:10.5772/847
213. Malkova D, Frankova V. The lymphatic system in the development of experimental tick-borne encephalitis in mice. Acta Virol. 1959;3: 210–214. Available: http://www.ncbi.nlm.nih.gov/pubmed/13853773
214. Maximova OA, Pletnev AG. Flaviviruses and the Central Nervous System: Revisiting Neuropathological Concepts. Annu Rev Virol. Annual Reviews; 2018;5: 255–272. doi:10.1146/annurev-virology-092917-043439
215. Herculano-Houzel S. The glia/neuron ratio: How it varies uniformly across brain structures and species and what that means for brain physiology and evolution. Glia. Wiley-Blackwell; 2014;62: 1377–1391.

doi:10.1002/glia.22683

216. Lui JH, Hansen D V., Kriegstein AR. Development and Evolution of the Human Neocortex. Cell. 2011;146: 18–36. doi:10.1016/j.cell.2011.06.030.Lui

217. Shaw AE, Hughes J, Gu Q, Behdenna A, Singer JB, Dennis T, Orton RJ, Varela M, Gifford RJ, Wilson SJ, Palmarini M. Fundamental properties of the mammalian innate immune system revealed by multispecies comparison of type I interferon responses. Malik H, editor. PLOS Biol. Public Library of Science; 2017;15: e2004086. doi:10.1371/journal.pbio.2004086

218. Jorfi M, D'Avanzo C, Kim DY, Irimia D. Three-Dimensional Models of the Human Brain Development and Diseases. Adv Heal Mater. 2018;7: 1–36. doi:10.1002/adhm.201700723.Three-Dimensional

219. Chiba N, Iwasaki T, Mizutani T, Kariwa H, Kurata T, Takashima I. Pathogenicity of tick-borne encephalitis virus isolated in Hokkaido, Japan in mouse model. Vaccine. 1999;17: 779–787. doi:10.1016/S0264-410X(98)00262-X

220. Hayasaka D, Nagata N, Fujii Y, Hasegawa H, Sata T, Suzuki R, Gould EA, Takashima I, Koike S. Mortality following peripheral infection with Tick-borne encephalitis virus results from a combination of central nervous system pathology, systemic inflammatory and stress responses. Virology. 2009;390: 139–150. doi:10.1016/j.virol.2009.04.026

221. Hirano M, Muto M, Sakai M, Kondo H, Kobayashi S, Kariwa H, Yoshii K. Dendritic transport of tick-borne flavivirus RNA by neuronal granules affects development of neurological disease. Proc Natl Acad Sci. National Academy of Sciences; 2017;114: 201704454. doi:10.1073/pnas.1704454114

222. Edmondson R, Broglie JJ, Adcock AF, Yang L. Three-Dimensional Cell Culture Systems and Their Applications in Drug Discovery and Cell-Based Biosensors. Assay Drug Dev Technol. 2014;12: 207–218. doi:10.1089/adt.2014.573

223. Růžek D, Vancova M, Tesarova M, Ahantarig A, Kopecky J, Grubhoffer L, Růžek D, Vancova M, Tesarova M, Ahantarig A, Kopecky J, Grubhoffer L, Ruzek D, Vancova M, Tesarova M, Ahantarig A, Kopecky J, Grubhoffer L, Růžek D, Vancova M, Tesarova M, Ahantarig A, Kopecky J, Grubhoffer L, Růžek D, Vancova M, Tesarova M, Ahantarig A, Kopecky J, Grubhoffer L, Ruzek D, Vancova M, Tesarova M, Ahantarig A, Kopecky J, Grubhoffer L, Růžek D, Vancova M, Tesarova M, Ahantarig A, Kopecky J, Grubhoffer L, Růžek D, Vancova M, Tesarova M, Ahantarig A, Kopecky J, Grubhoffer L, Ruzek D, Vancova M, Tesarova M, Ahantarig A, Kopecky J, Grubhoffer L. Morphological changes in human neural cells following tick-borne encephalitis virus infection. J Gen Virol. 2009;90: 1649–1658. doi:10.1099/vir.0.010058-0

224. Zhou Y, Ye L, Wan Q, Zhou L, Wang X, Li J, Hu S, Zhou D, Ho W. Activation of Toll-like receptors inhibits herpes simplex virus-1 infection of human neuronal cells. J Neurosci Res. Wiley-Blackwell; 2009;87: 2916–2925. doi:10.1002/jnr.22110

225. Dawes BE, Gao J, Atkins C, Nelson JT, Johnson K, Wu P, Freiberg AN. Human neural stem cell-derived neuron / astrocyte co-cultures respond to La Crosse virus infection with proinflammatory cytokines and chemokines. Journal of Neuroinflammation; 2018;5: 1–15.

226. Couderc T, Guivel-Benhassine F, Calaora V, Gosselin A-S, Blondel B. An ex vivo murine model to study poliovirus-induced apoptosis in nerve cells. J Gen Virol. 2002;83: 1925–1930. Available: http://jgv.microbiologyresearch.org/content/journal/jgv/10.1099/0022-1317-83-8-1925

227. Lafaille FG, Ciancanelli MJ, Studer L, Smith G, Notarangelo L, Casanova JL, Zhang SY. Deciphering human cell-autonomous anti-HSV-1 immunity in the central nervous system. Front Immunol. 2015;6: 1–5. doi:10.3389/fimmu.2015.00208

228. Stefanik M, Formanova P, Bily T, Vancova M, Eyer L, Palus M, Salat J, Braconi CT, Zanotto PM de A, Gould EA, Ruzek D. Characterisation of Zika virus infection in primary human astrocytes. BMC Neurosci. BioMed Central; 2018;19: 5. doi:10.1186/s12868-018-0407-2

229. Hood C, Cunningham AL, Slobedman B, Arvin AM, Sommer MH, Kinchington PR, Abendroth A. Varicella-Zoster Virus ORF63 Inhibits Apoptosis of Primary Human Neurons. J Virol. 2006;80: 1025–1031. doi:10.1128/JVI.80.2.1025

230. Jordan PM, Cain LD, Wu P. Astrocytes Enhance Long-Term Survival of Cholinergic Neurons Differentiated From Human Fetal Neural Stem Cells. J Neurosci Res. 2008;86: 35–47. doi:10.1002/jnr.21460v

231. Lafaille FG, Pessach IM, Zhang S-YY, Ciancanelli MJ, Herman M, Abhyankar A, Ying S-WW, Keros S, Goldstein PA, Mostoslavsky G, Ordovas-Montanes J, Jouanguy E, Plancoulaine S, Tu E, Elkabetz Y, Al-Muhsen S, Tardieu M, Schlaeger TM, Daley GQ, Abel L, Casanova J-LL, Studer L, Notarangelo LD. Impaired intrinsic immunity to HSV-1 in human iPSC-derived TLR3-deficient CNS cells. Nature. Nature Publishing Group; 2012;491: 769–773. doi:10.1038/nature11583

232. Brnic D, Stevanovic V, Cochet M, Agier C, Richardson J, Montero-Menei CN, Milhavet O, Eloit M, Coulpier M. Borna Disease Virus Infects Human Neural Progenitor Cells and Impairs Neurogenesis. J Virol. 2012;86: 2512–2522. doi:10.1128/JVI.05663-11

233. Scordel C, Huttin A, Cochet-Bernoin M, Szelechowski M, Poulet A, Richardson J, Benchoua A, Gonzalez-Dunia D, Eloit M, Coulpier M. Borna Disease Virus Phosphoprotein Impairs the Developmental Program Controlling Neurogenesis and Reduces Human GABAergic Neurogenesis. PLoS Pathog. 2015;11: 1–25. doi:10.1371/journal.ppat.1004859

234. Stoppini L, Buchs P-A, Muller D. A simple method for organotypic cultures of nervous tissue. J Neurosci Methods. Elsevier; 1991;37: 173–182. doi:10.1016/0165-0270(91)90128-M

235. Jandova K, Pasler D, Antonio LL, Raue C, Ji S, Njunting M, Kann O, Kovacs R, Meencke H-J, Cavalheiro EA, Heinemann U, Gabriel S, Lehmann T-N. Carbamazepine-resistance in the epileptic dentate gyrus of human hippocampal slices. Brain. Oxford University Press; 2006;129: 3290–3306. doi:10.1093/brain/awl218

236. Schwarz N, Hedrich UBS, Schwarz H, P A H, Dammeier N, Auffenberg E, Bedogni F, Honegger JB, Lerche H, Wuttke T V, Koch H. Human Cerebrospinal fluid promotes long-term neuronal viability and network function in human neocortical organotypic brain slice cultures. Sci Rep. Nature Publishing Group; 2017;7: 12249. doi:10.1038/s41598-017-12527-9

237. Welsch JC, Talekar A, Mathieu C, Pessi A, Moscona A, Horvat B, Porotto M. Fatal measles virus infection prevented by brain-penetrant fusion inhibitors. J Virol. American Society for Microbiology Journals; 2013;87: 13785–94. doi:10.1128/JVI.02436-13

238. Retallack H, Di Lullo E, Arias C, Knopp KA, Laurie MT, Sandoval-Espinosa C, Mancia Leon WR, Krencik R, Ullian EM, Spatazza J, Pollen AA, Mandel-Brehm C, Nowakowski TJ, Kriegstein AR, DeRisi JL. Zika virus cell tropism in the developing human brain and inhibition by azithromycin. Proc Natl Acad Sci U S A. National Academy of Sciences; 2016;113: 14408–14413. doi:10.1073/pnas.1618029113

239. Braun E, Zimmerman T, Hur T Ben, Reinhartz E, Fellig Y, Panet A, Steiner I. Neurotropism of herpes simplex virus type 1 in brain organ cultures. J Gen Virol. Microbiology Society; 2006;87: 2827–2837. doi:10.1099/vir.0.81850-0

240. Rosenfeld AB, Doobin DJ, Warren AL, Racaniello VR, Vallee RB. Replication of early and recent Zika virus isolates throughout mouse brain development. Proc Natl Acad Sci U S A. National Academy of Sciences; 2017;114: 12273–12278. doi:10.1073/pnas.1714624114

241. Friedl G, Hofer M, Auber B, Sauder C, Hausmann J, Staeheli P, Pagenstecher A. Borna disease virus multiplication in mouse organotypic slice cultures is site-specifically inhibited by gamma interferon but not by interleukin-12. J Virol. American Society for Microbiology Journals; 2004;78: 1212–8. doi:10.1128/JVI.78.3.1212-1218.2004

242. Lancaster MA, Renner M, Martin CA, Wenzel D, Bicknell LS, Hurles ME, Homfray T, Penninger JM, Jackson

AP, Knoblich JA. Cerebral organoids model human brain development and microcephaly. Nature. 2013; doi:10.1038/nature12517

243. Garcez PP, Rodrigo M da C, Loiola EC, Higa LM, Trindade P, Delvecchio R, Tanuri A, Rehen SK. Zika virus impairs growth in human neurospheres and brain organoids. Science (80-). 2016;352: 816–818.

244. Garcez PP, Nascimento JM, de Vasconcelos JM, Madeiro da Costa R, Delvecchio R, Trindade P, Loiola EC, Higa LM, Cassoli JS, Vitória G, Sequeira PC, Sochacki J, Aguiar RS, Fuzii HT, de Filippis AMB, da Silva Gonçalves Vianez Júnior JL, Tanuri A, Martins-de-Souza D, Rehen SK. Zika virus disrupts molecular fingerprinting of human neurospheres. Sci Rep. Nature Publishing Group; 2017;7: 40780. doi:10.1038/srep40780

245. Dang J, Tiwari SK, Lichinchi G, Qin Y, Patil VS, Eroshkin AM, Rana TM. Zika Virus Depletes Neural Progenitors in Human Cerebral Organoids through Activation of the Innate Immune Receptor TLR3. Cell Stem Cell. Cell Press; 2016;19: 258–265. doi:10.1016/j.stem.2016.04.014

246. Birey F, Andersen J, Makinson CD, Islam S, Wei W, Huber N, Fan HC, Metzler KRC, Panagiotakos G, Thom N, Rourke NAO, Steinmetz LM, Bernstein JA, Hallmayer J, Huguenard JR, Pașca SP. Assembly of Functional Forebrain Spheroids from Human Pluripotent Cells. Nature. 2017;545: 54–59. doi:10.1038/nature22330.Assembly

247. Corry J, Arora N, Good CA, Sadovsky Y, Coyne CB. Organotypic models of type III interferon-mediated protection from Zika virus infections at the maternal-fetal interface. Proc Natl Acad Sci U S A. National Academy of Sciences; 2017;114: 9433–9438. doi:10.1073/pnas.1707513114

248. Watanabe M, Buth JE, Vishlaghi N, de la Torre-Ubieta L, Taxidis J, Khakh BS, Coppola G, Pearson CA, Yamauchi K, Gong D, Dai X, Damoiseaux R, Aliyari R, Liebscher S, Schenke-Layland K, Caneda C, Huang EJ, Zhang Y, Cheng G, Geschwind DH, Golshani P, Sun R, Novitch BG. Self-Organized Cerebral Organoids with Human-Specific Features Predict Effective Drugs to Combat Zika Virus Infection. Cell Rep. Cell Press; 2017;21: 517–532. doi:10.1016/J.CELREP.2017.09.047

249. Qian X, Nguyen HN, Song MM, Hadiono C, Ogden SC, Hammack C, Yao B, Hamersky GR, Jacob F, Zhong C, Yoon KJ, Jeang W, Lin L, Li Y, Thakor J, Berg DA, Zhang C, Kang E, Chickering M, Nauen D, Ho CY, Wen Z, Christian KM, Shi PY, Maher BJ, Wu H, Jin P, Tang H, Song H, Ming GL. Brain-Region-Specific Organoids Using Mini-bioreactors for Modeling ZIKV Exposure. Cell. 2016; doi:10.1016/j.cell.2016.04.032

250. Owens T, Khorooshi R, Wlodarczyk A, Asgari N. Interferons in the central nervous system: A few instruments play many tunes. Glia. Wiley-Blackwell; 2014;62: 339–355. doi:10.1002/glia.22608

251. Prat A, Biernacki K, Wosik K, Antel JP. Glial cell influence on the human blood-brain barrier. Glia. Wiley-Blackwell; 2001;36: 145–155. doi:10.1002/glia.1104

252. Růžek D, Salát J, Singh SK, Kopecký J. Breakdown of the Blood-Brain Barrier during Tick-Borne Encephalitis in Mice Is Not Dependent on CD8+ T-Cells. Fooks AR, editor. PLoS One. 2011;6: e20472. doi:10.1371/journal.pone.0020472

253. Li F, Wang Y, Yu L, Cao S, Wang K, Yuan J, Wang C, Wang K, Cui M, Fu ZF. Viral Infection of the Central Nervous System and Neuroinflammation Precede Blood-Brain Barrier Disruption during Japanese Encephalitis Virus Infection. J Virol. American Society for Microbiology Journals; 2015;89: 5602–14. doi:10.1128/JVI.00143-15

254. Palus M, Vancova M, Sirmarova J, Elsterova J, Perner J, Ruzek D. Tick-borne encephalitis virus infects human brain microvascular endothelial cells without compromising blood-brain barrier integrity. Virology. Elsevier Inc.; 2017;507: 110–122. doi:10.1016/j.virol.2017.04.012

255. Dörrbecker B, Dobler G, Spiegel M, Hufert FT. Tick-borne encephalitis virus and the immune response of the mammalian host. Travel Med Infect Dis. 2010;8: 213–222. doi:10.1016/j.tmaid.2010.05.010

256. Nagata N, Iwata-Yoshikawa N, Hayasaka D, Sato Y, Kojima A, Kariwa H, Takashima I, Takasaki T, Kurane

I, Sata T, Hasegawa H. The Pathogenesis of 3 Neurotropic Flaviviruses in a Mouse Model Depends on the Route of Neuroinvasion After Viremia. J Neuropathol Exp Neurol. Oxford University Press; 2015;74: 250–260. doi:10.1097/NEN.0000000000000166

257. Egyed L, Zöldi V, Szeredi L. Subclinical Tick-Borne Encephalitis Virus in Experimentally Infected Apodemus agrarius. Intervirology. Karger Publishers; 2015;58: 369–72. doi:10.1159/000443833
258. Pedrosa PBS, Cardoso TAO. Viral infections in workers in hospital and research laboratory settings: A comparative review of infection modes and respective biosafety aspects. Int J Infect Dis. International Society for Infectious Diseases; 2011;15: e366–e376. doi:10.1016/j.ijid.2011.03.005
259. Környey S. Contribution to the histology of tick-borne encephalitis. Acta Neuropathol. Springer-Verlag; 1978;43: 179–183. doi:10.1007/BF00685013
260. Mazlo M, Szanto J, Mázló M, Szántó J, Mazlo M, Szanto J, Mázló M, Szántó J. Morphological demonstration of the virus of tick-borne encephalitis in the human brain. Acta Neuropathol. Springer-Verlag; 1978;43: 251–253. doi:10.1007/BF00691586
261. Gelpi E, Preusser M, Garzuly F, Holzmann H, Heinz FX, Budka H. Visualization of Central European tick-borne encephalitis infection in fatal human cases. J Neuropathol Exp Neurol. 2005;64: 506–12. doi:10.1093/jnen/64.6.506
262. Gelpi E, Preusser M, Laggner U, Garzuly F, Holzmann H, Heinz FX, Budka H. Inflammatory response in human tick-borne encephalitis: analysis of postmortem brain tissue. J Neurovirol. 2006;12: 322–7. doi:10.1080/13550280600848746
263. Lindqvist R, Kurhade C, Gilthorpe JD, Överby AK. Cell-type- and region-specific restriction of neurotropic flavivirus infection by viperin. J Neuroinflammation. Journal of Neuroinflammation; 2018;15: 1–11. doi:10.1186/s12974-018-1119-3
264. Hirano M, Yoshii K, Sakai M, Hasebe R, Ichii O, Kariwa H. Tick-borne flaviviruses alter membrane structure and replicate in dendrites of primary mouse neuronal cultures. J Gen Virol. 2014;95: 849–861. doi:10.1099/vir.0.061432-0
265. Överby AK, Popov VL, Niedrig M, Weber F, Overby AK, Popov VL, Niedrig M, Weber F, Överby AK, Popov VL, Niedrig M, Weber F, Overby AK, Popov VL, Niedrig M, Weber F, Överby AK, Popov VL, Niedrig M, Weber F, Overby AK, Popov VL, Niedrig M, Weber F. Tick-Borne Encephalitis Virus Delays Interferon Induction and Hides Its Double-Stranded RNA in Intracellular Membrane Vesicles. J Virol. 2010;84: 8470–8483. doi:10.1128/JVI.00176-10
266. Isaeva MP, Leonova GN, Kozhemiako VB, Borisevich VG, Maĭstrovskaia OS, Rasskazov VA. [Apoptosis as a mechanism for the cytopathic action of tick-borne encephalitis virus]. Vopr Virusol. 1998;43: 182–6. Available: http://www.ncbi.nlm.nih.gov/pubmed/9791885
267. Kamalov NI, Novozhilova a P, Kreichman GS, Sokolova ED. Morphological features of cell death in various types of acute tick-borne encephalitis. Neurosci Behav Physiol. 1999;29: 449–53. Available: http://www.ncbi.nlm.nih.gov/pubmed/10582230
268. Prikhod'ko GG, Prikhod'ko EA, Pletnev AG, Cohen JI. Langat Flavivirus Protease NS3 Binds Caspase-8 and Induces Apoptosis. J Virol. 2002;76: 5701–5710. doi:10.1128/JVI.76.11.5701-5710.2002
269. Prikhod'ko GG, Prikhod'ko EA, Cohen JI, Pletnev AG. Infection with Langat Flavivirus or Expression of the Envelope Protein Induces Apoptotic Cell Death. Virology. Academic Press; 2001;286: 328–335. doi:10.1006/VIRO.2001.0980
270. Hamel R, Dejarnac O, Wichit S, Ekchariyawat P, Neyret A, Natthanej L, Perera-Lecoin M, Surasombatpattana P, Talignani L, Thomas F, Cao-Lormeau V-M, Choumet V, Briant L, Desprès P, Amara A, Yssel H, Missé D. Biology of Zika Virus Infection in Human Skin Cells. J Virol. 2015;89: JVI.00354-15-. doi:10.1128/JVI.00354-15

271. Liang Q, Luo Z, Zeng J, Chen W, Foo S-S, Lee S-A, Ge J, Wang S, Goldman SA, Zlokovic BV, Zhao Z, Jung JU. Zika Virus NS4A and NS4B Proteins Deregulate Akt-mTOR Signaling in Human Fetal Neural Stem Cells to Inhibit Neurogenesis and Induce Autophagy. Cell Stem Cell. Cell Press; 2016;19: 663–671. doi:10.1016/J.STEM.2016.07.019
272. Tavian M, Péault B. Embryonic development of the human hematopoietic system. Int J Dev Biol. UPV/EHU Press; 2005;49: 243–50. doi:10.1387/ijdb.041957mt
273. Monier A, Adle-Biassette H, Delezoide A-L, Evrard P, Gressens P, Verney C. Entry and Distribution of Microglial Cells in Human Embryonic and Fetal Cerebral Cortex. J Neuropathol Exp Neurol. Oxford University Press; 2007;66: 372–382. doi:10.1097/nen.0b013e3180517b46
274. Nedergaard M, Ransom B, Goldman SA. New roles for astrocytes: Redefining the functional architecture of the brain. Trends Neurosci. Elsevier Current Trends; 2003;26: 523–530. doi:10.1016/j.tins.2003.08.008
275. Sofroniew M V., Vinters H V. Astrocytes: biology and pathology. Acta Neuropathol. 2010;119: 7–35. doi:10.1007/s00401-009-0619-8
276. Wilhelmsson U, Bushong EA, Price DL, Smarr BL, Phung V, Terada M, Ellisman MH, Pekny M. Redefining the concept of reactive astrocytes as cells that remain within their unique domains upon reaction to injury. Proc Natl Acad Sci U S A. National Academy of Sciences; 2006;103: 17513–8. doi:10.1073/pnas.0602841103
277. Wilkins A, Majed H, Layfield R, Compston A, Chandran S. Oligodendrocytes promote neuronal survival and axonal length by distinct intracellular mechanisms: a novel role for oligodendrocyte-derived glial cell line-derived neurotrophic factor. J Neurosci. Society for Neuroscience; 2003;23: 4967–74. doi:10.1523/JNEUROSCI.23-12-04967.2003
278. Freeman SA, Desmazières A, Fricker D, Lubetzki C, Sol-Foulon N. Mechanisms of sodium channel clustering and its influence on axonal impulse conduction. Cell Mol Life Sci. Springer; 2016;73: 723–35. doi:10.1007/s00018-015-2081-1
279. Tress O, Maglione M, May D, Pivneva T, Richter N, Seyfarth J, Binder S, Zlomuzica A, Seifert G, Theis M, Dere E, Kettenmann H, Willecke K. Panglial gap junctional communication is essential for maintenance of myelin in the CNS. J Neurosci. Society for Neuroscience; 2012;32: 7499–518. doi:10.1523/JNEUROSCI.0392-12.2012
280. Palus M, Bílý T, Elsterova J, Langhansova H, Salat J, Vancova M, Růžek D. Infection and injury of human astrocytes by tick-borne encephalitis virus. J Gen Virol. 2014;95: 2411–2426. doi:10.1099/vir.0.068411-0
281. Lindqvist R, Mundt F, Gilthorpe JD, Wölfel S, Gekara NO, Kröger A, Överby AK. Fast type I interferon response protects astrocytes from flavivirus infection and virus-induced cytopathic effects. J Neuroinflammation. BioMed Central; 2016;13: 277. doi:10.1186/s12974-016-0748-7
282. Kurhade C, Zegenhagen L, Weber E, Nair S, Michaelsen-Preusse K, Spanier J, Gekara NO, Kröger A, Överby AK. Type I Interferon response in olfactory bulb, the site of tick-borne flavivirus accumulation, is primarily regulated by IPS-1. J Neuroinflammation. Journal of Neuroinflammation; 2016;13: 22. doi:10.1186/s12974-016-0487-9
283. Revie D, Salahuddin SZ. Role of macrophages and monocytes in hepatitis C virus infections. World J Gastroenterol. Baishideng Publishing Group Inc; 2014;20: 2777–84. doi:10.3748/wjg.v20.i11.2777
284. Kreil TR, Burger I, Bachmann M, Fraiss S, Eibl MM. Antibodies protect mice against challenge with tick-borne encephalitis virus (TBEC)-infected macrophages. Clin Exp Immunol. Wiley/Blackwell (10.1111); 1997;110: 358–361. doi:10.1046/j.1365-2249.1997.4311446.x
285. Ahantarig A, Růzek D, Vancová M, Janowitz A, St'astná H, Tesarová M, Grubhoffer L. Tick-borne encephalitis virus infection of cultured mouse macrophages. Intervirology. Karger Publishers; 2009;52: 283–90. doi:10.1159/000235741

286. Brandstadter JD, Yang Y. Natural killer cell responses to viral infection. J Innate Immun. Karger Publishers; 2011;3: 274–9. doi:10.1159/000324176

287. Jost S, Altfeld M. Control of Human Viral Infections by Natural Killer Cells. Annu Rev Immunol. Annual Reviews ; 2013;31: 163–194. doi:10.1146/annurev-immunol-032712-100001

288. Azeredo EL, De Oliveira-Pinto LM, Zagne SM, Cerqueira DIS, Nogueira RMR, Kubelka CF. NK cells, displaying early activation, cytotoxicity and adhesion molecules, are associated with mild dengue disease. Clin Exp Immunol. Wiley/Blackwell (10.1111); 2006;143: 345–356. doi:10.1111/j.1365-2249.2006.02996.x

289. Larena M, Regner M, Lobigs M. Cytolytic effector pathways and IFN-γ help protect against Japanese encephalitis. Eur J Immunol. Wiley-Blackwell; 2013;43: 1789–1798. doi:10.1002/eji.201243152

290. Screpanti V, Wallin RPA, Grandien A, Ljunggren H-G. Impact of FASL-induced apoptosis in the elimination of tumor cells by NK cells. Mol Immunol. Pergamon; 2005;42: 495–499. doi:10.1016/J.MOLIMM.2004.07.033

291. Glässner A, Eisenhardt M, Krämer B, Körner C, Coenen M, Sauerbruch T, Spengler U, Nattermann J. NK cells from HCV-infected patients effectively induce apoptosis of activated primary human hepatic stellate cells in a TRAIL-, FasL- and NKG2D-dependent manner. Lab Investig. Nature Publishing Group; 2012;92: 967–977. doi:10.1038/labinvest.2012.54

292. Tomažič J, Poljak M, Popovič P, Matičič M, Beovič B, Avšič-Županc T, Lotrič S, Jereb M, Pikelj F, Gale N. Tick-borne encephalitis: Possibly a fatal disease in its acute stage. PCR amplification of TBE RNA from postmortem brain tissue. Infection. 1997;25: 41–43. doi:10.1007/BF02113507

293. Blom K, Braun M, Pakalniene J, Lunemann S, Enqvist M, Dailidyte L, Schaffer M, Lindquist L, Mickiene A, Michaëlsson J, Ljunggren H-G, Gredmark-Russ S. NK Cell Responses to Human Tick-Borne Encephalitis Virus Infection. J Immunol. American Association of Immunologists; 2016;197: 2762–71. doi:10.4049/jimmunol.1600950

294. Vargin V V, Semenov BF. Changes of natural killer cell activity in different mouse lines by acute and asymptomatic flavivirus infections. Acta Virol. 1986;30: 303–8. Available: http://www.ncbi.nlm.nih.gov/pubmed/2876611

295. Li G, Teleki C, Wang T, Li G, Teleki C, Wang T. Memory T Cells in Flavivirus Vaccination. Vaccines. Multidisciplinary Digital Publishing Institute; 2018;6: 73. doi:10.3390/vaccines6040073

296. Blom K, Braun M, Pakalniene J, Dailidyte L, Béziat V, Lampen MH, Klingström J, Lagerqvist N, Kjerstadius T, Michaëlsson J, Lindquist L, Ljunggren HG, Sandberg JK, Mickiene A, Gredmark-Russ S. Specificity and Dynamics of Effector and Memory CD8 T Cell Responses in Human Tick-Borne Encephalitis Virus Infection. PLoS Pathog. 2015;11: 1–20. doi:10.1371/journal.ppat.1004622

297. Paul S, Ricour C, Sommereyns C, Sorgeloos F, Michiels T. Type I interferon response in the central nervous system. Biochimie. Elsevier; 2007;89: 770–778. doi:10.1016/j.biochi.2007.02.009

298. Carson MJ, Doose JM, Melchior B, Schmid CD, Ploix CC. CNS immune privilege: Hiding in plain sight. Immunol Rev. Wiley/Blackwell (10.1111); 2006;213: 48–65. doi:10.1111/j.1600-065X.2006.00441.x

299. Galea I, Bechmann I, Perry VH. What is immune privilege (not)? Trends Immunol. Elsevier Current Trends; 2007;28: 12–18. doi:10.1016/J.IT.2006.11.004

300. Weller RO, Djuanda E, Yow H-Y, Carare RO. Lymphatic drainage of the brain and the pathophysiology of neurological disease. Acta Neuropathol. Springer-Verlag; 2009;117: 1–14. doi:10.1007/s00401-008-0457-0

301. Pachter JS, de Vries HE, Fabry Z. The Blood-Brain Barrier and Its Role in Immune Privilege in the Central Nervous System. J Neuropathol Exp Neurol. Oxford University Press; 2003;62: 593–604. doi:10.1093/jnen/62.6.593

302. Bauer J, Bradl M, Hickley WF, Forss-Petter S, Breitschopf H, Linington C, Wekerle H, Lassmann H. T-cell apoptosis in inflammatory brain lesions: destruction of T cells does not depend on antigen recognition. Am J Pathol. American Society for Investigative Pathology; 1998;153: 715–24. Available: http://www.ncbi.nlm.nih.gov/pubmed/9736022

303. Bechmann I, Mor G, Nilsen J, Eliza M, Nitsch R, Naftolin F. FasL (CD95L, Apo1L) is expressed in the normal rat and human brain: Evidence for the existence of an immunological brain barrier. Glia. John Wiley & Sons, Ltd; 1999;27: 62–74. doi:10.1002/(SICI)1098-1136(199907)27:1<62::AID-GLIA7>3.0.CO;2-S

304. Trajkovic V, Vuckovic O, Stosic-Grujicic S, Miljkovic D, Popadic D, Markovic M, Bumbasirevic V, Backovic A, Cvetkovic I, Harhaji L, Ramic Z, Mostarica Stojkovic M. Astrocyte-induced regulatory T cells mitigate CNS autoimmunity. Glia. Wiley-Blackwell; 2004;47: 168–179. doi:10.1002/glia.20046

305. Liu Y, Teige I, Birnir B, Issazadeh-Navikas S. Neuron-mediated generation of regulatory T cells from encephalitogenic T cells suppresses EAE. Nat Med. Nature Publishing Group; 2006;12: 518–525. doi:10.1038/nm1402

306. Griffin DE. Immune responses to RNA-virus infections of the CNS. Nat Rev Immunol. Nature Publishing Group; 2003;3: 493–502. doi:10.1038/nri1105

307. Forrester J V., McMenamin PG, Dando SJ. CNS infection and immune privilege. Nat Rev Neurosci. Nature Publishing Group; 2018;19: 655–671. doi:10.1038/s41583-018-0070-8

308. Akira S, Uematsu S, Takeuchi O. Pathogen recognition and innate immunity. Cell. Elsevier; 2006;124: 783–801. doi:10.1016/j.cell.2006.02.015

309. Akira S, Uematsu S, Takeuchi O. Pathogen Recognition and Innate Immunity. Cell. 2006;124: 783–801. doi:10.1016/j.cell.2006.02.015

310. Yoneyama M, Kikuchi M, Matsumoto K, Imaizumi T, Miyagishi M, Taira K, Foy E, Loo Y-M, Gale M, Akira S, Yonehara S, Kato A, Fujita T. Shared and unique functions of the DExD/H-box helicases RIG-I, MDA5, and LGP2 in antiviral innate immunity. J Immunol. American Association of Immunologists; 2005;175: 2851–8. doi:10.4049/JIMMUNOL.175.5.2851

311. Satoh T, Kato H, Kumagai Y, Yoneyama M, Sato S, Matsushita K, Tsujimura T, Fujita T, Akira S, Takeuchi O. LGP2 is a positive regulator of RIG-I- and MDA5-mediated antiviral responses. Proc Natl Acad Sci U S A. National Academy of Sciences; 2010;107: 1512–7. doi:10.1073/pnas.0912986107

312. Sadler AJ, Williams BRG. Structure and Function of the Protein Kinase R. Interferon: The 50th Anniversary. Berlin, Heidelberg: Springer Berlin Heidelberg; 2007. pp. 253–292. doi:10.1007/978-3-540-71329-6_13

313. Xagorari A, Chlichlia K. Toll-like receptors and viruses: induction of innate antiviral immune responses. Open Microbiol J. Bentham Science Publishers; 2008;2: 49–59. doi:10.2174/1874285800802010049

314. Kato H, Takeuchi O, Sato S, Yoneyama M, Yamamoto M, Matsui K, Uematsu S, Jung A, Kawai T, Ishii KJ, Yamaguchi O, Otsu K, Tsujimura T, Koh C-S, Reis e Sousa C, Matsuura Y, Fujita T, Akira S. Differential roles of MDA5 and RIG-I helicases in the recognition of RNA viruses. Nature. Nature Publishing Group; 2006;441: 101–105. doi:10.1038/nature04734

315. Errett JS, Suthar MS, McMillan A, Diamond MS, Gale Jr. M. The essential, nonredundant roles of RIG-I and MDA5 in detecting and controlling West Nile virus infection. J Virol. 2013;87: 11416–11425. doi:10.1128/JVI.01488-13

316. Kawai T, Takahashi K, Sato S, Coban C, Kumar H, Kato H, Ishii KJ, Takeuchi O, Akira S. IPS-1, an adaptor triggering RIG-I- and Mda5-mediated type I interferon induction. Nat Immunol. Nature Publishing Group; 2005;6: 981–988. doi:10.1038/ni1243

317. Liu S, Chen J, Cai X, Wu J, Chen X, Wu Y-T, Sun L, Chen ZJ. MAVS recruits multiple ubiquitin E3 ligases to activate antiviral signaling cascades. Elife. 2013;2. doi:10.7554/eLife.00785

318. Pomerantz JL, Baltimore D, Suzuki S, Graham K, Huang J, Ng M, Itie A, Wakeham A, Shahinian A, Henzel W, Elia A, Shillinglaw W, Mak T, Cao Z, Yeh W. NF-kappa B activation by a signaling complex containing TRAF2, TANK and TBK1, a novel IKK-related kinase. EMBO J. EMBO Press; 1999;18: 6694–6704. doi:10.1093/emboj/18.23.6694

319. Goubau D, Deddouche S, Reis e Sousa C. Cytosolic sensing of viruses. Immunity. Elsevier; 2013;38: 855–69. doi:10.1016/j.immuni.2013.05.007

320. Zhang X, Zheng Z, Liu X, Shu B, Mao P, Bai B, Hu Q, Luo M, Ma X, Cui Z, Wang H. Tick-borne encephalitis virus induces chemokine RANTES expression via activation of IRF-3 pathway. J Neuroinflammation. Journal of Neuroinflammation; 2016;13: 1–18. doi:10.1186/s12974-016-0665-9

321. Zheng Z, Yang J, Jiang X, Liu Y, Zhang X, Li M, Zhang M, Fu M, Hu K, Wang H, Luo M-H, Gong P, Hu Q. Tick-Borne Encephalitis Virus Nonstructural Protein NS5 Induces RANTES Expression Dependent on the RNA-Dependent RNA Polymerase Activity. J Immunol. 2018;201: 53–68. doi:10.4049/jimmunol.1701507

322. Kaisho T, Akira S. Toll-like receptor function and signaling. J Allergy Clin Immunol. Mosby; 2006;117: 979–987. doi:10.1016/j.jaci.2006.02.023

323. Okumura A, Pitha PM, Yoshimura A, Harty RN. Interaction between Ebola virus glycoprotein and host toll-like receptor 4 leads to induction of proinflammatory cytokines and SOCS1. J Virol. American Society for Microbiology Journals; 2010;84: 27–33. doi:10.1128/JVI.01462-09

324. Georgel P, Jiang Z, Kunz S, Janssen E, Mols J, Hoebe K, Bahram S, Oldstone MBA, Beutler B. Vesicular stomatitis virus glycoprotein G activates a specific antiviral Toll-like receptor 4-dependent pathway. Virology. 2007;362: 304–313. doi:10.1016/j.virol.2006.12.032

325. Szomolanyi-Tsuda E, Liang X, Welsh RM, Kurt-Jones EA, Finberg RW. Role for TLR2 in NK cell-mediated control of murine cytomegalovirus in vivo. J Virol. American Society for Microbiology Journals; 2006;80: 4286–91. doi:10.1128/JVI.80.9.4286-4291.2006

326. Lee HK, Lund JM, Ramanathan B, Mizushima N, Iwasaki A. Autophagy-dependent viral recognition by plasmacytoid dendritic cells. Science. American Association for the Advancement of Science; 2007;315: 1398–401. doi:10.1126/science.1136880

327. Dreux M, Garaigorta U, Boyd B, Décembre E, Chung J, Whitten-Bauer C, Wieland S, Chisari FV. Short-Range Exosomal Transfer of Viral RNA from Infected Cells to Plasmacytoid Dendritic Cells Triggers Innate Immunity. Cell Host Microbe. 2012;12: 558–570. doi:10.1016/j.chom.2012.08.010

328. Lund JM, Alexopoulou L, Sato A, Karow M, Adams NC, Gale NW, Iwasaki A, Flavell RA. Recognition of single-stranded RNA viruses by Toll-like receptor 7. Proc Natl Acad Sci U S A. National Academy of Sciences; 2004;101: 5598–603. doi:10.1073/pnas.0400937101

329. Alexopoulou L, Holt AC, Medzhitov R, Flavell RA. Recognition of double-stranded RNA and activation of NF-κB by Toll-like receptor 3. Nature. Nature Publishing Group; 2001;413: 732–738. doi:10.1038/35099560

330. Hemmi H, Takeuchi O, Kawai T, Kaisho T, Sato S, Sanjo H, Matsumoto M, Hoshino K, Wagner H, Takeda K, Akira S. A Toll-like receptor recognizes bacterial DNA. Nature. Nature Publishing Group; 2000;408: 740–745. doi:10.1038/35047123

331. Yamamoto M, Sato S, Hemmi H, Hoshino K, Kaisho T, Sanjo H, Takeuchi O, Sugiyama M, Okabe M, Takeda K, Akira S. Role of adaptor TRIF in the MyD88-independent toll-like receptor signaling pathway. Science. American Association for the Advancement of Science; 2003;301: 640–3. doi:10.1126/science.1087262

332. Sato S, Sugiyama M, Yamamoto M, Watanabe Y, Kawai T, Takeda K, Akira S. Toll/IL-1 receptor domain-containing adaptor inducing IFN-beta (TRIF) associates with TNF receptor-associated factor 6 and TANK-binding kinase 1, and activates two distinct transcription factors, NF-kappa B and IFN-regulatory factor-3, in the Toll-like receptor signaling. J Immunol. American Association of Immunologists; 2003;171: 4304-

10. doi:10.4049/JIMMUNOL.171.8.4304

333. Oganesyan G, Saha SK, Guo B, He JQ, Shahangian A, Zarnegar B, Perry A, Cheng G. Critical role of TRAF3 in the Toll-like receptor-dependent and -independent antiviral response. Nature. Nature Publishing Group; 2006;439: 208–211. doi:10.1038/nature04374

334. Kagan JC, Medzhitov R. Phosphoinositide-Mediated Adaptor Recruitment Controls Toll-like Receptor Signaling. Cell. 2006;125: 943–955. doi:10.1016/j.cell.2006.03.047

335. Fitzgerald KA, Palsson-McDermott EM, Bowie AG, Jefferies CA, Mansell AS, Brady G, Brint E, Dunne A, Gray P, Harte MT, McMurray D, Smith DE, Sims JE, Bird TA, O'Neill LAJ. Mal (MyD88-adapter-like) is required for Toll-like receptor-4 signal transduction. Nature. Nature Publishing Group; 2001;413: 78–83. doi:10.1038/35092578

336. Wesche H, Henzel WJ, Shillinglaw W, Li S, Cao Z. MyD88: an adapter that recruits IRAK to the IL-1 receptor complex. Immunity. 1997;7: 837–47. Available: http://www.ncbi.nlm.nih.gov/pubmed/9430229

337. Wu C-J, Conze DB, Li T, Srinivasula SM, Ashwell JD. Sensing of Lys 63-linked polyubiquitination by NEMO is a key event in NF-κB activation. Nat Cell Biol. Nature Publishing Group; 2006;8: 398–406. doi:10.1038/ncb1384

338. Honda K, Yanai H, Mizutani T, Negishi H, Shimada N, Suzuki N, Ohba Y, Takaoka A, Yeh W-C, Taniguchi T. Role of a transductional-transcriptional processor complex involving MyD88 and IRF-7 in Toll-like receptor signaling. Proc Natl Acad Sci U S A. 2004;101: 15416–21. doi:10.1073/pnas.0406933101

339. Grygorczuk S, Parczewski M, Świerzbińska R, Czupryna P, Moniuszko A, Dunaj J, Kondrusik M, Pancewicz S. The increased concentration of macrophage migration inhibitory factor in serum and cerebrospinal fluid of patients with tick-borne encephalitis. J Neuroinflammation. BioMed Central; 2017;14: 126. doi:10.1186/s12974-017-0898-2

340. Mickienė A, Pakalnienė J, Nordgren J, Carlsson B, Hagbom M, Svensson L, Lindquist L. Polymorphisms in Chemokine Receptor 5 and Toll-Like Receptor 3 Genes Are Risk Factors for Clinical Tick-Borne Encephalitis in the Lithuanian Population. Munderloh UG, editor. PLoS One. Public Library of Science; 2014;9: e106798. doi:10.1371/journal.pone.0106798

341. Kindberg E, Vene S, Mickiene A, Lundkvist Å, Lindquist L, Svensson L. A functional Toll-like receptor 3 gene (TLR3) may be a risk factor for tick-borne encephalitis virus (TBEV) infection. J Infect Dis. 2011;203: 523–528. doi:10.1093/infdis/jiq082

342. Palus M, Sohrabi Y, Broman KW, Strnad H, Šíma M, Růžek D, Volkova V, Slapničková M, Vojtíšková J, Mrázková L, Salát J, Lipoldová M. A novel locus on mouse chromosome 7 that influences survival after infection with tick-borne encephalitis virus. BMC Neurosci. BioMed Central; 2018;19: 39. doi:10.1186/s12868-018-0438-8

343. Baker DG, Woods TA, Butchi NB, Morgan TM, Taylor RT, Sunyakumthorn P, Mukherjee P, Lubick KJ, Best SM, Peterson KE. Toll-like receptor 7 suppresses virus replication in neurons but does not affect viral pathogenesis in a mouse model of Langat virus infection. J Gen Virol. 2013;94: 336–347. doi:10.1099/vir.0.043984-0

344. Carletti T, Zakaria MK, Marcello A. The host cell response to tick-borne encephalitis virus. Biochem Biophys Res Commun. Elsevier Ltd; 2017; 6–13. doi:10.1016/j.bbrc.2017.02.006

345. Hiscott J, Grandvaux N, Sharma S, Tenoever BR, Servant MJ, Lin R. Convergence of the NF-κB and Interferon Signaling Pathways in the Regulation of Antiviral Defense and Apoptosis. Ann N Y Acad Sci. Wiley/Blackwell (10.1111); 2003;1010: 237–248. doi:10.1196/annals.1299.042

346. Szubin R, Chang WLW, Greasby T, Beckett L, Baumgarth N. Rigid Interferon-α Subtype Responses of Human Plasmacytoid Dendritic Cells. J Interf Cytokine Res. 2008;28: 749–763. doi:10.1089/jir.2008.0037

347. Fung KY, Mangan NE, Cumming H, Horvat JC, Mayall JR, Stifter SA, De Weerd N, Roisman LC, Rossjohn J,

Robertson SA, Schjenken JE, Parker B, Gargett CE, Nguyen HPT, Carr DJ, Hansbro PM, Hertzog PJ. Interferon- Protects the Female Reproductive Tract from Viral and Bacterial Infection. Science (80-). 2013;339: 1088–1092. doi:10.1126/science.1233321

348. LaFleur DW, Nardelli B, Tsareva T, Mather D, Feng P, Semenuk M, Taylor K, Buergin M, Chinchilla D, Roshke V, Chen G, Ruben SM, Pitha PM, Coleman TA, Moore PA. Interferon-κ, a Novel Type I Interferon Expressed in Human Keratinocytes. J Biol Chem. 2001;276: 39765–39771. doi:10.1074/jbc.M102502200
349. Adolf GR. Human interferon omega--a review. Mult Scler. 1995;1 Suppl 1: S44-7. Available: http://www.ncbi.nlm.nih.gov/pubmed/9345398
350. de Weerd NA, Nguyen T. The interferons and their receptors-distribution and regulation. Immunol Cell Biol. Nature Publishing Group; 2012;90: 483–491. doi:10.1038/icb.2012.9
351. Levy DE, Darnell JE. STATs: transcriptional control and biological impact. Nat Rev Mol Cell Biol. Nature Publishing Group; 2002;3: 651–662. doi:10.1038/nrm909
352. Ivashkiv LB, Donlin LT. Regulation of type i interferon responses. Nat Rev Immunol. NIH Public Access; 2014;14: 36–49. doi:10.1038/nri3581
353. Farrar MA, Schreiber RD. The Molecular Cell Biology of Interferon-gamma and its Receptor. Annu Rev Immunol. Annual Reviews 4139 El Camino Way, P.O. Box 10139, Palo Alto, CA 94303-0139, USA ; 1993;11: 571–611. doi:10.1146/annurev.iy.11.040193.003035
354. Schoenborn JR, Wilson CB. Regulation of Interferon-γ During Innate and Adaptive Immune Responses. Advances in immunology. 2007. pp. 41–101. doi:10.1016/S0065-2776(07)96002-2
355. Hoffmann H-H, Schneider WM, Rice CM. Interferons and viruses: an evolutionary arms race of molecular interactions. Trends Immunol. NIH Public Access; 2015;36: 124–38. doi:10.1016/j.it.2015.01.004
356. Sommereyns C, Paul S, Staeheli P, Michiels T. IFN-Lambda (IFN-λ) Is Expressed in a Tissue-Dependent Fashion and Primarily Acts on Epithelial Cells In Vivo. Buchmeier MJ, editor. PLoS Pathog. Public Library of Science; 2008;4: e1000017. doi:10.1371/journal.ppat.1000017
357. Egli A, Santer DM, O'Shea D, Tyrrell DL, Houghton M. The impact of the interferon-lambda family on the innate and adaptive immune response to viral infections. Emerg Microbes Infect. 2014;3: e51–e51. doi:10.1038/emi.2014.51
358. Pott J, Mahlakoiv T, Mordstein M, Duerr CU, Michiels T, Stockinger S, Staeheli P, Hornef MW. IFN-λ determines the intestinal epithelial antiviral host defense. Proc Natl Acad Sci. 2011;108: 7944–7949. doi:10.1073/pnas.1100552108
359. Davidson S, Crotta S, McCabe TM, Wack A. Pathogenic potential of interferon αß in acute influenza infection. Nat Commun. 2014;5: 3864. doi:10.1038/ncomms4864
360. Weber E, Finsterbusch K, Lindquist R, Nair S, Lienenklaus S, Gekara NO, Janik D, Weiss S, Kalinke U, Överby AK, Kröger A, Kroger A, Kröger A, Kroger A, Kröger A, Kroger A, Kröger A, Kroger A, Kröger A, Kroger A, Kröger A. Type I Interferon Protects Mice from Fatal Neurotropic Infection with Langat Virus by Systemic and Local Antiviral Responses. J Virol. American Society for Microbiology; 2014;88: 12202–12212. doi:10.1128/JVI.01215-14
361. Best SM, Morris KL, Shannon JG, Robertson SJ, Mitzel DN, Park GS, Boer E, Wolfinbarger JB, Bloom ME. Inhibition of interferon-stimulated JAK-STAT signaling by a tick-borne flavivirus and identification of NS5 as an interferon antagonist. J Virol. 2005;79: 12828–12839. doi:10.1128/JVI.79.20.12828-12839.2005
362. Selinger M, Wilkie GS, Tong L, Gu Q, Schnettler E, Grubhoffer L, Kohl A. Analysis of tick-borne encephalitis virus-induced host responses in human cells of neuronal origin and interferon-mediated protection. J Gen Virol. 2017; doi:10.1099/jgv.0.000853
363. Best SM. The Many Faces of the Flavivirus NS5 Protein in Antagonism of Type I Interferon Signaling. J Virol. American Society for Microbiology (ASM); 2017;91. doi:10.1128/JVI.01970-16

364. Lubick KJ, Robertson SJ, McNally KL, Freedman BA, Rasmussen AL, Taylor RT, Tsuruda S, Sakai M, Ishizuka M, Boer EF, Foster EC, Chiramel AI, Addison CB, Green R, Kastner DL, Katze MG, Holland SM, Forlino A, Freeman AF, Boehm M, Yoshii K, Best SM, Walts AD. Flavivirus antagonism of type i interferon signaling reveals prolidase as a regulator of IFNAR1 surface expression. Cell Host Microbe. Elsevier Inc.; 2015;18: 61–74. doi:10.1016/j.chom.2015.06.007

365. Werme K, Wigerius M, Johansson M. Tick-borne encephalitis virus NS5 associates with membrane protein scribble and impairs interferon-stimulated JAK-STAT signalling. Cell Microbiol. 2008;10: 696–712. doi:10.1111/j.1462-5822.2007.01076.x

366. Wigerius M, Melik W, Elväng A, Johansson M. Rac1 and Scribble are targets for the arrest of neurite outgrowth by TBE virus NS5. Mol Cell Neurosci. 2010;44: 260–271. doi:10.1016/j.mcn.2010.03.012

367. Sadler AJ, Williams BRG. Interferon-inducible antiviral effectors. Nat Rev Immunol. Nature Publishing Group; 2008;8: 559–568. doi:10.1038/nri2314

368. Schoggins JW, Rice CM. Interferon-stimulated genes and their antiviral effector functions. Curr Opin Virol. NIH Public Access; 2011;1: 519–25. doi:10.1016/j.coviro.2011.10.008

369. Schoggins JW. Interferon-stimulated genes: Roles in viral pathogenesis. Curr Opin Virol. 2014;6: 40–46. doi:10.1016/j.coviro.2014.03.006

370. Haller O, Staeheli P, Schwemmle M, Kochs G. Mx GTPases: dynamin-like antiviral machines of innate immunity. Trends Microbiol. 2015;23: 154–163. doi:10.1016/j.tim.2014.12.003

371. Staeheli P, Pitossi F, Pavlovic J. Mx proteins: GTPases with antiviral activity. Trends Cell Biol. 1993;3: 268–72. Available: http://www.ncbi.nlm.nih.gov/pubmed/14731745

372. Yu Z, Wang Z, Chen J, Li H, Lin Z, Zhang F, Zhou Y, Hou J. GTPase activity is not essential for the interferon-inducible MxA protein to inhibit the replication of hepatitis B virus. Arch Virol. Springer Vienna; 2008;153: 1677–1684. doi:10.1007/s00705-008-0168-9

373. Kochs G, Janzen C, Hohenberg H, Haller O. Antivirally active MxA protein sequesters La Crosse virus nucleocapsid protein into perinuclear complexes. Proc Natl Acad Sci U S A. National Academy of Sciences; 2002;99: 3153–8. doi:10.1073/pnas.052430399

374. Verhelst J, Hulpiau P, Saelens X. Mx Proteins: Antiviral Gatekeepers That Restrain the Uninvited. Microbiol Mol Biol Rev. American Society for Microbiology; 2013;77: 551–566. doi:10.1128/MMBR.00024-13

375. Justesen J, Hartmann R, Kjeldgaard NO. Gene structure and function of the 2'-5'-oligoadenylate synthetase family. Cellular and Molecular Life Sciences. 2000. pp. 1593–1612. doi:10.1007/PL00000644

376. Pulit-Penaloza JA, Scherbik S V, Brinton MA. Activation of Oas1a gene expression by type I IFN requires both STAT1 and STAT2 while only STAT2 is required for Oas1b activation. Virology. 2012;425: 71–81. doi:10.1016/j.virol.2011.11.025

377. Scherbik S V, Paranjape JM, Stockman BM, Silverman RH, Brinton MA. RNase L plays a role in the antiviral response to West Nile virus. J Virol. American Society for Microbiology Journals; 2006;80: 2987–99. doi:10.1128/JVI.80.6.2987-2999.2006

378. Yoshii K, Moritoh K, Nagata N, Yokozawa K, Sakai M, Sasaki N, Kariwa H, Agui T, Takashima I. Susceptibility to flavivirus-specific antiviral response of Oas1b affects the neurovirulence of the Far-Eastern subtype of tick-borne encephalitis virus. Arch Virol. 2013;158: 1039–1046. doi:10.1007/s00705-012-1579-1

379. Barkhash A V., Perelygin AA, Babenko VN, Myasnikova NG, Pilipenko PI, Romaschenko AG, Voevoda MI, Brinton MA. Variability in the 2′-5′-Oligoadenylate Synthetase Gene Cluster Is Associated with Human Predisposition to Tick-Borne Encephalitis Virus–Induced Disease. J Infect Dis. 2010;202: 1813–1818. doi:10.1086/657418

380. Silverman RH. Viral encounters with 2',5'-oligoadenylate synthetase and RNase L during the interferon antiviral response. J Virol. American Society for Microbiology Journals; 2007;81: 12720–9. doi:10.1128/JVI.01471-07
381. van Tol S, Hage A, Giraldo MI, Bharaj P, Rajsbaum R. The TRIMendous Role of TRIMs in Virus-Host Interactions. Vaccines. Multidisciplinary Digital Publishing Institute (MDPI); 2017;5. doi:10.3390/vaccines5030023
382. Nisole S, Stoye JP, Saïb A. TRIM family proteins: retroviral restriction and antiviral defence. Nat Rev Microbiol. Nature Publishing Group; 2005;3: 799–808. doi:10.1038/nrmicro1248
383. Zeng W, Sun L, Jiang X, Chen X, Hou F, Adhikari A, Xu M, Chen ZJ. Reconstitution of the RIG-I Pathway Reveals a Signaling Role of Unanchored Polyubiquitin Chains in Innate Immunity. Cell. 2010;141: 315–330. doi:10.1016/j.cell.2010.03.029
384. Yan J, Li Q, Mao A-P, Hu M-M, Shu H-B. TRIM4 modulates type I interferon induction and cellular antiviral response by targeting RIG-I for K63-linked ubiquitination. J Mol Cell Biol. Oxford University Press; 2014;6: 154–163. doi:10.1093/jmcb/mju005
385. Lang X, Tang T, Jin T, Ding C, Zhou R, Jiang W. TRIM65-catalized ubiquitination is essential for MDA5-mediated antiviral innate immunity. J Exp Med. Rockefeller University Press; 2017;214: 459–473. doi:10.1084/JEM.20160592
386. Narayan K, Waggoner L, Pham ST, Hendricks GL, Waggoner SN, Conlon J, Wang JP, Fitzgerald KA, Kang J. TRIM13 Is a Negative Regulator of MDA5-Mediated Type I Interferon Production. J Virol. American Society for Microbiology (ASM); 2014;88: 10748. doi:10.1128/JVI.02593-13
387. Kondo T, Watanabe M, Hatakeyama S. TRIM59 interacts with ECSIT and negatively regulates NF-κB and IRF-3/7-mediated signal pathways. Biochem Biophys Res Commun. 2012;422: 501–507. doi:10.1016/j.bbrc.2012.05.028
388. Shen Y, Li NL, Wang J, Liu B, Lester S, Li K. TRIM56 Is an Essential Component of the TLR3 Antiviral Signaling Pathway. J Biol Chem. 2012;287: 36404–36413. doi:10.1074/jbc.M112.397075
389. Perron MJ, Stremlau M, Song B, Ulm W, Mulligan RC, Sodroski J. TRIM5alpha mediates the postentry block to N-tropic murine leukemia viruses in human cells. Proc Natl Acad Sci U S A. National Academy of Sciences; 2004;101: 11827–32. doi:10.1073/pnas.0403364101
390. Yap MW, Nisole S, Lynch C, Stoye JP. Trim5alpha protein restricts both HIV-1 and murine leukemia virus. Proc Natl Acad Sci U S A. National Academy of Sciences; 2004;101: 10786–91. doi:10.1073/pnas.0402876101
391. Fan W, Wu M, Qian S, Zhou Y, Chen H, Li X, Qian P. TRIM52 inhibits Japanese Encephalitis Virus replication by degrading the viral NS2A. Sci Rep. Nature Publishing Group; 2016;6: 33698. doi:10.1038/srep33698
392. Taylor RT, Lubick KJ, Robertson SJ, Broughton JP, Bloom ME, Bresnahan WA, Best SM. TRIM79α, an interferon-stimulated gene product, restricts tick-borne encephalitis virus replication by degrading the viral RNA polymerase. Cell Host Microbe. Elsevier Inc.; 2011;10: 185–196. doi:10.1016/j.chom.2011.08.004
393. Helbig KJ, Beard MR. The Role of Viperin in the Innate Antiviral Response. J Mol Biol. Academic Press; 2014;426: 1210–1219. doi:10.1016/J.JMB.2013.10.019
394. Fitzgerald KA. The Interferon Inducible Gene: Viperin. J Interf Cytokine Res. Mary Ann Liebert, Inc. 140 Huguenot Street, 3rd Floor New Rochelle, NY 10801 USA ; 2011;31: 131–135. doi:10.1089/jir.2010.0127
395. Upadhyay AS, Vonderstein K, Pichlmair A, Stehling O, Bennett KL, Dobler G, Guo JT, Superti-Furga G, Lill R, Överby AK, Weber F. Viperin is an iron-sulfur protein that inhibits genome synthesis of tick-borne encephalitis virus via radical SAM domain activity. Cell Microbiol. 2014;16: 834–848. doi:10.1111/cmi.12241

396. Vonderstein K, Nilsson E, Hubel P, Nygård Skalman L, Upadhyay A, Pasto J, Pichlmair A, Lundmark R, Överby AK. Viperin targets flavivirus virulence by inducing assembly of non-infectious capsid particles. J Virol. 2017; JVI.01751-17. doi:10.1128/JVI.01751-17

397. Panayiotou C, Lindqvist R, Kurhade C, Vonderstein K, Pasto J, Edlund K, Upadhyay AS, Överby AK. Viperin restricts Zika virus and tick-borne encephalitis virus replication by targeting NS3 for proteasomal degradation. J Virol. American Society for Microbiology; 2018;92: JVI.02054-17. doi:10.1128/JVI.02054-17

398. Lucas S-M, Rothwell NJ, Gibson RM. The role of inflammation in CNS injury and disease. Br J Pharmacol. Wiley-Blackwell; 2006;147 Suppl 1: S232-40. doi:10.1038/sj.bjp.0706400

399. Grossman RM, Krueger J, Yourish D, Granelli-Piperno A, Murphy DP, May LT, Kupper TS, Sehgal PB, Gottlieb AB. Interleukin 6 is expressed in high levels in psoriatic skin and stimulates proliferation of cultured human keratinocytes. Proc Natl Acad Sci U S A. National Academy of Sciences; 1989;86: 6367–71. doi:10.1073/PNAS.86.16.6367

400. Guschin D, Rogers N, Briscoe J, Witthuhn B, Watling D, Horn F, Pellegrini S, Yasukawa K, Heinrich P, Stark GR. A major role for the protein tyrosine kinase JAK1 in the JAK/STAT signal transduction pathway in response to interleukin-6. EMBO J. John Wiley & Sons, Ltd; 1995;14: 1421–1429. doi:10.1002/j.1460-2075.1995.tb07128.x

401. Heinrich PC, Behrmann I, Müller-Newen G, Schaper F, Graeve L. Interleukin-6-type cytokine signalling through the gp130/Jak/STAT pathway. Biochem J. Portland Press Limited; 1998;334 (Pt 2): 297–314. doi:10.1042/BJ3340297

402. Swarup V, Ghosh J, Das S, Basu A. Tumor necrosis factor receptor-associated death domain mediated neuronal death contributes to the glial activation and subsequent neuroinflammation in Japanese encephalitis. Neurochem Int. 2008;52: 1310–1321. doi:10.1016/j.neuint.2008.01.014

403. Smith JA, Das A, Ray SK, Banik NL. Role of pro-inflammatory cytokines released from microglia in neurodegenerative diseases. Brain Res Bull. 2012;87: 10–20. doi:10.1016/j.brainresbull.2011.10.004

404. Hayasaka D, Shirai K, Aoki K, Nagata N, Simantini DS, Kitaura K, Takamatsu Y, Gould E, Suzuki R, Morita K. TNF-α acts as an immunoregulator in the mouse brain by reducing the incidence of severe disease following Japanese encephalitis virus infection. PLoS One. Public Library of Science; 2013;8: e71643. doi:10.1371/journal.pone.0071643

405. Thorburn J, Bender LM, Morgan MJ, Thorburn A. Caspase- and serine protease-dependent apoptosis by the death domain of FADD in normal epithelial cells. Mol Biol Cell. American Society for Cell Biology; 2003;14: 67–77. doi:10.1091/mbc.e02-04-0207

406. Warke R V., Martin KJ, Giaya K, Shaw SK, Rothman AL, Bosch I. TRAIL Is a Novel Antiviral Protein against Dengue Virus. J Virol. American Society for Microbiology Journals; 2008;82: 555–564. doi:10.1128/JVI.01694-06

407. Ishikawa E, Nakazawa M, Yoshinari M, Minami M. Role of Tumor Necrosis Factor-Related Apoptosis-Inducing Ligand in Immune Response to Influenza Virus Infection in Mice. J Virol. American Society for Microbiology Journals; 2005;79: 7658–7663. doi:10.1128/JVI.79.12.7658-7663.2005

408. Vidalain PO, Azocar O, Lamouille B, Astier A, Rabourdin-Combe C, Servet-Delprat C. Measles virus induces functional TRAIL production by human dendritic cells. J Virol. American Society for Microbiology Journals; 2000;74: 556–9. doi:10.1128/JVI.74.1.556-559.2000

409. Moser B, Willimann K. Chemokines: role in inflammation and immune surveillance. Ann Rheum Dis. 2004;63: ii84-ii89. doi:10.1136/ard.2004.028316

410. Williams JL, Holman DW, Klein RS. Chemokines in the balance: maintenance of homeostasis and protection at CNS barriers. Front Cell Neurosci. Frontiers Media SA; 2014;8: 154.

doi:10.3389/fncel.2014.00154

411. Sui Y, Potula R, Dhillon N, Pinson D, Li S, Nath A, Anderson C, Turchan J, Kolson D, Narayan O, Buch S. Neuronal apoptosis is mediated by CXCL10 overexpression in simian human immunodeficiency virus encephalitis. Am J Pathol. American Society for Investigative Pathology; 2004;164: 1557–1566. doi:10.1016/S0002-9440(10)63714-5

412. van Marle G, Antony J, Ostermann H, Dunham C, Hunt T, Halliday W, Maingat F, Urbanowski MD, Hobman T, Peeling J, Power C. West Nile virus-induced neuroinflammation: glial infection and capsid protein-mediated neurovirulence. J Virol. American Society for Microbiology Journals; 2007;81: 10933–49. doi:10.1128/JVI.02422-06

413. Mlera L, Lam J, Offerdahl DK, Martens C, Sturdevant D, Turner C V, Porcella SF, Bloom ME. Transcriptome Analysis Reveals a Signature Profile for Tick-Borne Flavivirus Persistence in HEK 293T Cells. MBio. American Society for Microbiology; 2016;7: e00314-16. doi:10.1128/mBio.00314-16

414. Kindberg E, Mickienė A, Ax C, Åkerlind B, Vene S, Lindquist L, Lundkvist Å, Svensson L. A Deletion in the Chemokine Receptor 5 *(CCR5)* Gene Is Associated with Tickborne Encephalitis. J Infect Dis. 2008;197: 266–269. doi:10.1086/524709

415. Kroemer G, El-Deiry W, Golstein P, Peter M, Vaux D, Vandenabeele P, Zhivotovsky B, Blagosklonny M, Malorni W, Knight R, Piacentini M, Nagata S, Melino G. Molecular mechanisms of cell death: Recommendations of the Nomenclature Committee on Cell Death 2018. Cell Death Differ. 2005;12: 1463–1467. doi:10.1038/sj.cdd.4401724

416. Upton JW, Chan FK-M. Staying alive: cell death in antiviral immunity. Mol Cell. NIH Public Access; 2014;54: 273–80. doi:10.1016/j.molcel.2014.01.027

417. Festjens N, Vanden Berghe T, Cornelis S, Vandenabeele P. RIP1, a kinase on the crossroads of a cell's decision to live or die. Cell Death Differ. 2007;14: 400–410. doi:10.1038/sj.cdd.4402085

418. Micheau O, Tschopp J. Induction of TNF receptor I-mediated apoptosis via two sequential signaling complexes. Cell. 2003;114: 181–90. Available: http://www.ncbi.nlm.nih.gov/pubmed/12887920

419. Cain K, Bratton SB, Langlais C, Walker G, Brown DG, Sun XM, Cohen GM. Apaf-1 oligomerizes into biologically active approximately 700-kDa and inactive approximately 1.4-MDa apoptosome complexes. J Biol Chem. American Society for Biochemistry and Molecular Biology; 2000;275: 6067–70. doi:10.1074/JBC.275.9.6067

420. Vaseva A V., Moll UM. The mitochondrial p53 pathway. Biochim Biophys Acta - Bioenerg. Elsevier B.V.; 2009;1787: 414–420. doi:10.1016/j.bbabio.2008.10.005

421. Ichim G, Tait SWG. A fate worse than death: apoptosis as an oncogenic process. Nat Rev Cancer. 2016;16: 539–548. doi:10.1038/nrc.2016.58

422. Vanlangenakker N, Vanden Berghe T, Vandenabeele P. Many stimuli pull the necrotic trigger, an overview. Cell Death Differ. Nature Publishing Group; 2012;19: 75–86. doi:10.1038/cdd.2011.164

423. Vandenabeele P, Galluzzi L, Vanden Berghe T, Kroemer G. Molecular mechanisms of necroptosis: An ordered cellular explosion. Nat Rev Mol Cell Biol. Nature Publishing Group; 2010;11: 700–714. doi:10.1038/nrm2970

424. Mizushima N. Autophagy in protein and organelle turnover. Cold Spring Harb Symp Quant Biol. 2011;76: 397–402. doi:10.1101/sqb.2011.76.011023

425. Yang Z, Klionsky DJ. Mammalian autophagy: core molecular machinery and signaling regulation. Curr Opin Cell Biol. NIH Public Access; 2010;22: 124–31. doi:10.1016/j.ceb.2009.11.014

426. Chiramel AI, Best SM. Role of autophagy in Zika virus infection and pathogenesis. Virus Res. Elsevier; 2018;254: 34–40. doi:10.1016/j.virusres.2017.09.006

427. Mizushima N, Levine B. Autophagy in mammalian development and differentiation. Nat Cell Biol. 2010;12:

823–830. doi:10.1038/ncb0910-823.Autophagy

428. Mizushima N, Levine B, Cuervo AM, Klionsky DJ. Autophagy fights disease through cellular self-digestion. Nature. Nature Publishing Group; 2008;451: 1069–1075. doi:10.1038/nature06639

429. Kroemer G, Levine B. Autophagic cell death: The story of a misnomer. Nat Rev Mol Cell Biol. 2008;9: 1004–1010. doi:10.1038/nrm2529

430. Hansen M, Rubinsztein DC, Walker DW. Autophagy as a promoter of longevity: insights from model organisms. Nat Rev Mol Cell Biol. Springer US; 2018;19: 611. doi:10.1038/s41580-018-0048-4

431. Tripathi DN, Chowdhury R, Trudel LJ, Tee AR, Slack RS, Walker CL, Wogan GN. Reactive nitrogen species regulate autophagy through ATM-AMPK-TSC2-mediated suppression of mTORC1. Proc Natl Acad Sci U S A. National Academy of Sciences; 2013;110: E2950-7. doi:10.1073/pnas.1307736110

432. Rubinstein AD, Kimchi A. Life in the balance – a mechanistic view of the crosstalk between autophagy and apoptosis. J Cell Sci. 2012;125: 5259–5268. doi:10.1242/jcs.115865

433. Geng J, Klionsky DJ. The Atg8 and Atg12 ubiquitin-like conjugation systems in macroautophagy. 'Protein Modifications: Beyond the Usual Suspects' Review Series. EMBO Rep. 2008;9: 859–864. doi:10.1038/embor.2008.163

434. Hanada T, Noda NN, Satomi Y, Ichimura Y, Fujioka Y, Takao T, Inagaki F, Ohsumi Y. The Atg12-Atg5 conjugate has a novel E3-like activity for protein lipidation in autophagy. J Biol Chem. American Society for Biochemistry and Molecular Biology; 2007;282: 37298–302. doi:10.1074/jbc.C700195200

435. Mizushima N, Kuma A, Kobayashi Y, Yamamoto A, Matsubae M, Takao T, Natsume T, Ohsumi Y, Yoshimori T. Mouse Apg16L, a novel WD-repeat protein, targets to the autophagic isolation membrane with the Apg12-Apg5 conjugate. J Cell Sci. The Company of Biologists Ltd; 2003;116: 1679–1688. doi:10.1242/JCS.00381

436. Kudchodkar SB, Levine B. Viruses and autophagy. Rev Med Virol. NIH Public Access; 2009;19: 359–78. doi:10.1002/rmv.630

437. Levine B, Kroemer G. Autophagy in the pathogenesis of disease. Cell. NIH Public Access; 2008;132: 27–42. doi:10.1016/j.cell.2007.12.018

438. Khakpoor A, Panyasrivanit M, Wikan N, Smith DR. A role for autophagolysosomes in dengue virus 3 production in HepG2 cells. J Gen Virol. Microbiology Society; 2009;90: 1093–1103. doi:10.1099/vir.0.007914-0

439. Panyasrivanit M, Khakpoor A, Wikan N, Smith DR. Linking dengue virus entry and translation/replication through amphisomes. Autophagy. 2009;5: 434–435. doi:10.4161/auto.5.3.7925

440. Kobayashi S, Orba Y, Yamaguchi H, Takahashi K, Sasaki M, Hasebe R, Kimura T, Sawa H. Autophagy inhibits viral genome replication and gene expression stages in West Nile virus infection. Virus Res. Elsevier; 2014;191: 83–91. doi:10.1016/j.virusres.2014.07.016

441. Delgado MA, Elmaoued RA, Davis AS, Kyei G, Deretic V. Toll-like receptors control autophagy. EMBO J. European Molecular Biology Organization; 2008;27: 1110–21. doi:10.1038/emboj.2008.31

442. Shi C-S, Kehrl JH. MyD88 and Trif target Beclin 1 to trigger autophagy in macrophages. J Biol Chem. American Society for Biochemistry and Molecular Biology; 2008;283: 33175–82. doi:10.1074/jbc.M804478200

443. Liang XH, Kleeman LK, Jiang HH, Gordon G, Goldman JE, Berry G, Herman B, Levine B. Protection against fatal Sindbis virus encephalitis by beclin, a novel Bcl-2-interacting protein. J Virol. American Society for Microbiology (ASM); 1998;72: 8586–96. Available: http://www.ncbi.nlm.nih.gov/pubmed/9765397

444. Jounai N, Takeshita F, Kobiyama K, Sawano A, Miyawaki A, Xin K-Q, Ishii KJ, Kawai T, Akira S, Suzuki K, Okuda K. The Atg5 Atg12 conjugate associates with innate antiviral immune responses. Proc Natl Acad Sci U S A. National Academy of Sciences; 2007;104: 14050–5. doi:10.1073/pnas.0704014104

445. Tal MC, Sasai M, Lee HK, Yordy B, Shadel GS, Iwasaki A. Absence of autophagy results in reactive oxygen species-dependent amplification of RLR signaling. Proc Natl Acad Sci U S A. National Academy of Sciences; 2009;106: 2770–5. doi:10.1073/pnas.0807694106

446. Liu BL, Robinson M, Han Z-Q, Branston RH, English C, Reay P, McGrath Y, Thomas SK, Thornton M, Bullock P, Love CA, Coffin RS. ICP34.5 deleted herpes simplex virus with enhanced oncolytic, immune stimulating and anti-tumour properties. Gene Ther. Nature Publishing Group; 2003;10: 292–303. doi:10.1038/sj.gt.3301885

447. Orvedahl A, Alexander D, Tallóczy Z, Sun Q, Wei Y, Zhang W, Burns D, Leib DA, Levine B. HSV-1 ICP34.5 Confers Neurovirulence by Targeting the Beclin 1 Autophagy Protein. Cell Host Microbe. Cell Press; 2007;1: 23–35. doi:10.1016/J.CHOM.2006.12.001

448. Sir D, Chen W-L, Choi J, Wakita T, Yen TSB, Ou J-HJ. Induction of incomplete autophagic response by hepatitis C virus via the unfolded protein response. Hepatology. NIH Public Access; 2008;48: 1054–61. doi:10.1002/hep.22464

449. Kurhade C, Schreier S, Lee Y-P, Zegenhagen L, Hjertqvist M, Dobler G, Kröger A, Överby AK. Correlation of Severity of Human Tick-Borne Encephalitis Virus Disease and Pathogenicity in Mice. Emerg Infect Dis. 2018;24. doi:10.3201/eid2409.171825

450. American Type Culture Collection Standards Development Organization Workgroup ASN-0002. Cell line misidentification: the beginning of the end. Nat Rev Cancer. Nature Publishing Group; 2010;10: 441–448. doi:10.1038/nrc2852

451. Pan C, Kumar C, Bohl S, Klingmueller U, Mann M. Comparative proteomic phenotyping of cell lines and primary cells to assess preservation of cell type-specific functions. Mol Cell Proteomics. American Society for Biochemistry and Molecular Biology; 2009;8: 443–50. doi:10.1074/mcp.M800258-MCP200

452. Sandberg R, Ernberg I. The molecular portrait of in vitro growth by meta-analysis of gene-expression profiles. Genome Biol. BioMed Central; 2005;6: R65. doi:10.1186/gb-2005-6-8-r65

453. Azevedo FAC, Carvalho LRB, Grinberg LT, Farfel JM, Ferretti REL, Leite REP, Filho WJ, Lent R, Herculano-Houzel S. Equal numbers of neuronal and nonneuronal cells make the human brain an isometrically scaled-up primate brain. J Comp Neurol. Wiley-Blackwell; 2009;513: 532–541. doi:10.1002/cne.21974

454. Ginhoux F, Lim S, Hoeffel G, Low D, Huber T. Origin and differentiation of microglia. Front Cell Neurosci. Frontiers Media SA; 2013;7: 45. doi:10.3389/fncel.2013.00045

455. Lum F-M, Low DKS, Fan Y, Tan JJL, Lee B, Chan JKY, Rénia L, Ginhoux F, Ng LFP. Zika Virus Infects Human Fetal Brain Microglia and Induces Inflammation. Clin Infect Dis. Oxford University Press; 2017;64: 914–920. doi:10.1093/cid/ciw878

456. Lannes N, Neuhaus V, Scolari B, Kharoubi-Hess S, Walch M, Summerfield A, Filgueira L. Interactions of human microglia cells with Japanese encephalitis virus. Virol J. Virology Journal; 2017;14: 8. doi:10.1186/s12985-016-0675-3

457. Ormel PR, Vieira de Sá R, van Bodegraven EJ, Karst H, Harschnitz O, Sneeboer MAM, Johansen LE, van Dijk RE, Scheefhals N, Berdenis van Berlekom A, Ribes Martínez E, Kling S, MacGillavry HD, van den Berg LH, Kahn RS, Hol EM, de Witte LD, Pasterkamp RJ. Microglia innately develop within cerebral organoids. Nat Commun. Nature Publishing Group; 2018;9: 4167. doi:10.1038/s41467-018-06684-2

458. Ogata A, Nagashima K, Hall WW, Ichikawa M, Kimura-Kuroda J, Yasui K. Japanese encephalitis virus neurotropism is dependent on the degree of neuronal maturity. J Virol. American Society for Microbiology Journals; 1991;65: 880–6. Available: http://www.ncbi.nlm.nih.gov/pubmed/1987378

459. Kimura-Kuroda J, Ichikawa M, Ogata A, Nagashima K, Yasui K. Specific tropism of Japanese encephalitis virus for developing neurons in primary rat brain culture. Arch Virol. Springer-Verlag; 1993;130: 477–484. doi:10.1007/BF01309676

460. Patabendige A, Michael BD, Craig AG, Solomon T. Brain microvascular endothelial-astrocyte cell responses following Japanese encephalitis virus infection in an in vitro human blood-brain barrier model. Mol Cell Neurosci. Academic Press; 2018;89: 60–70. doi:10.1016/J.MCN.2018.04.002
461. Simonin Y, Loustalot F, Desmetz C, Foulongne V, Constant O, Fournier-Wirth C, Leon F, Molès J-P, Goubaud A, Lemaitre J-M, Maquart M, Leparc-Goffart I, Briant L, Nagot N, Van de Perre P, Salinas S. Zika Virus Strains Potentially Display Different Infectious Profiles in Human Neural Cells. EBioMedicine. Elsevier; 2016;12: 161–169. doi:10.1016/j.ebiom.2016.09.020
462. Hughes BW, Addanki KC, Sriskanda AN, McLean E, Bagasra O. Infectivity of Immature Neurons to Zika Virus: A Link to Congenital Zika Syndrome. EBioMedicine. Elsevier; 2016;10: 65–70. doi:10.1016/J.EBIOM.2016.06.026
463. Cumberworth SL, Barrie JA, Cunningham ME, de Figueiredo DPG, Schultz V, Wilder-Smith AJ, Brennan B, Pena LJ, Freitas de Oliveira França R, Linington C, Barnett SC, Willison HJ, Kohl A, Edgar JM. Zika virus tropism and interactions in myelinating neural cell cultures: CNS cells and myelin are preferentially affected. Acta Neuropathol Commun. Acta Neuropathologica Communications; 2017;5: 50. doi:10.1186/s40478-017-0450-8
464. Rodriguez M, Leibowitz JL, Lampert PW. Persistent infection of oligodendrocytes in Theiler's virus-induced encephalomyelitis. Ann Neurol. John Wiley & Sons, Ltd; 1983;13: 426–433. doi:10.1002/ana.410130409
465. Li Y, Dunphy JM, Pedraza CE, Lynch CR, Cardona SM, Macklin WB, Lynch WP. Ecotropic Murine Leukemia Virus Infection of Glial Progenitors Interferes with Oligodendrocyte Differentiation: Implications for Neurovirulence. J Virol. American Society for Microbiology Journals; 2016;90: 3385–99. doi:10.1128/JVI.03156-15
466. Clase AC, Dimcheff DE, Favara C, Dorward D, McAtee FJ, Parrie LE, Ron D, Portis JL. Oligodendrocytes are a major target of the toxicity of spongiogenic murine retroviruses. Am J Pathol. American Society for Investigative Pathology; 2006;169: 1026–38. doi:10.2353/ajpath.2006.051357
467. Liu H, Xu E, Liu J, Xiong H. Oligodendrocyte Injury and Pathogenesis of HIV-1-Associated Neurocognitive Disorders. Brain Sci. Multidisciplinary Digital Publishing Institute (MDPI); 2016;6. doi:10.3390/brainsci6030023
468. Li X-Q, Sarmento L, Fu ZF. Degeneration of neuronal processes after infection with pathogenic, but not attenuated, rabies viruses. J Virol. American Society for Microbiology Journals; 2005;79: 10063–8. doi:10.1128/JVI.79.15.10063-10068.2005
469. Dimou L, Simon C, Kirchhoff F, Takebayashi H, Götz M. Progeny of Olig2-Expressing Progenitors in the Gray and White Matter of the Adult Mouse Cerebral Cortex. J Neurosci. Society for Neuroscience; 2008;28: 10434–10442. doi:10.1523/JNEUROSCI.2831-08.2008
470. Jakovcevski I, Zecevic N. Olig Transcription Factors Are Expressed in Oligodendrocyte and Neuronal Cells in Human Fetal CNS. J Neurosci. Society for Neuroscience; 2005;25: 10064 –10073. doi:10.1523/JNEUROSCI.22-22-09821.2002
471. Tatsumi K, Isonishi A, Yamasaki M, Kawabe Y, Morita-Takemura S, Nakahara K, Terada Y, Shinjo T, Okuda H, Tanaka T, Wanaka A. Olig2-Lineage Astrocytes: A Distinct Subtype of Astrocytes That Differs from GFAP Astrocytes. Front Neuroanat. Frontiers Media SA; 2018;12: 8. doi:10.3389/fnana.2018.00008
472. Leong SY, Rao VTS, Bin JM, Gris P, Sangaralingam M, Kennedy TE, Antel JP. Heterogeneity of oligodendrocyte progenitor cells in adult human brain. Ann Clin Transl Neurol. Wiley-Blackwell; 2014;1: 272–83. doi:10.1002/acn3.55
473. Nowakowski TJ, Pollen AA, Di Lullo E, Sandoval-Espinosa C, Bershteyn M, Kriegstein AR. Expression Analysis Highlights AXL as a Candidate Zika Virus Entry Receptor in Neural Stem Cells. Cell Stem Cell.

Elsevier Inc.; 2016;18: 1–6. doi:10.1016/j.stem.2016.03.012

474. Pfefferkorn C, Kallfass C, Lienenklaus S, Spanier J, Kalinke U, Rieder M, Conzelmann K-K, Michiels T, Staeheli P. Abortively Infected Astrocytes Appear To Represent the Main Source of Interferon Beta in the Virus-Infected Brain. J Virol. American Society for Microbiology Journals; 2016;90: 2031–8. doi:10.1128/JVI.02979-15

475. Kallfass C, Ackerman A, Lienenklaus S, Weiss S, Heimrich B, Staeheli P. Visualizing production of beta interferon by astrocytes and microglia in brain of La Crosse virus-infected mice. J Virol. American Society for Microbiology Journals; 2012;86: 11223–30. doi:10.1128/JVI.01093-12

476. Diniz JAP, Da Rosa APATATAT, Guzman H, Xu F, Xiao S-Y, Popov VL, Vasconcelos PFC, Tesh RB. West Nile virus infection of primary mouse neuronal and neuroglial cells: the role of astrocytes in chronic infection. Am J Trop Med Hyg. 2006;75: 691–696. Available: http://www.ajtmh.org/content/75/4/691.short

477. Hussmann KL, Samuel MA, Kim KS, Diamond MS, Fredericksen BL. Differential Replication of Pathogenic and Nonpathogenic Strains of West Nile Virus within Astrocytes. J Virol. American Society for Microbiology; 2013;87: 2814–2822. doi:10.1128/JVI.02577-12

478. Delhaye S, Paul S, Blakqori G, Minet M, Weber F, Staeheli P, Michiels T. Neurons produce type I interferon during viral encephalitis. Proc Natl Acad Sci U S A. 2006;103: 7835–40. doi:10.1073/pnas.0602460103

479. Cho H, Proll SC, Szretter KJ, Katze MG, Gale M, Diamond MS. Differential innate immune response programs in neuronal subtypes determine susceptibility to infection in the brain by positive-stranded RNA viruses. Nat Med. Nature Publishing Group; 2013;19: 1–8. doi:10.1038/nm.3108

480. Chhatbar C, Detje CN, Grabski E, Borst K, Spanier J, Ghita L, Elliott DA, Jordão MJC, Mueller N, Sutton J, Prajeeth CK, Gudi V, Klein MA, Prinz M, Bradke F, Stangel M, Kalinke U. Type I Interferon Receptor Signaling of Neurons and Astrocytes Regulates Microglia Activation during Viral Encephalitis. Cell Rep. Elsevier; 2018;25: 118–129.e4. doi:10.1016/j.celrep.2018.09.003

481. Liddelow SA, Guttenplan KA, Clarke LE, Bennett FC, Bohlen CJ, Schirmer L, Bennett ML, Münch AE, Chung W-S, Peterson TC, Wilton DK, Frouin A, Napier BA, Panicker N, Kumar M, Buckwalter MS, Rowitch DH, Dawson VL, Dawson TM, Stevens B, Barres BA, Chung S, Peterson TC, Wilton DK, Frouin A, Napier BA. Neurotoxic reactive astrocytes are induced by activated microglia. Nature. Nature Publishing Group; 2017;541: 481–487. doi:10.1038/nature21029.Neurotoxic

482. Song JH. Human Astrocytes Are Resistant to Fas Ligand and Tumor Necrosis Factor-Related Apoptosis-Inducing Ligand-Induced Apoptosis. J Neurosci. Society for Neuroscience; 2006;26: 3299–3308. doi:10.1002/14651858.CD010875

483. Wallner G, Mandl CW, Ecker M, Holzmann H, Stiasny K, Kunz C, Heinz FX. Characterization and complete genome sequences of high- and low- virulence variants of tick-borne encephalitis virus. J Gen Virol. 1996;77 (Pt 5): 1035–1042.

484. Livak KJ, Schmittgen TD. Analysis of Relative Gene Expression Data Using Real-Time Quantitative PCR and the 2−ΔΔCT Method. Methods. 2001;25: 402–408. doi:10.1006/meth.2001.1262

485. Welsch J, Lionnet C, Terzian C, Horvat B, Gerlier D, Mathieu C. Organotypic Brain Cultures: A Framework for Studying CNS Infection by Neurotropic Viruses and Screening Antiviral Drugs. BIO-PROTOCOL. 2017;7. doi:10.21769/BioProtoc.2605

Supplementary information

Supplementary table 1 - Detailed number of recorded TBEV human infections worldwide between 1985 and 2010.

Data were gathered from (Süss 2011; Donoso Mantke et al. 2011; Poblete-Durán et al. 2016; WHO 2018; Süss 2008).

	1985	1986	1987	1988	1989	1990	1991	1992	1993	1994	1995	1996	1997	1998	1999	2000	2001	2002	2003	2004	2005	2006	2007	2008	2009	2010
Albania	n/a	n/a	n/a	n/a	n/a	1	0	3	0	0	1	2	0	0	1	0	0	0	0	0	n/a	n/a	0	n/a	n/a	23
Andorra	n/a	n/a	n/a	n/a	n/a	n/a	n/a	n/a	n/a	n/a	n/a	n/a	n/a	n/a	0	0	0	n/a	0	n/a	0	0	0	0	n/a	0
Armenia	n/a	n/a	n/a	n/a	n/a	n/a	n/a	n/a	n/a	n/a	n/a	n/a	n/a	n/a	0	n/a	n/a	n/a	n/a	n/a	n/a	n/a	n/a	0	n/a	n/a
Austria	n/a	n/a	n/a	n/a	n/a	n/a	n/a	n/a	n/a	n/a	n/a	n/a	n/a	n/a	6	12	23	36	44	n/a	59	51	n/a	n/a	n/a	58
Azerbaijan	n/a	n/a	n/a	n/a	n/a	n/a	n/a	n/a	n/a	n/a	n/a	n/a	n/a	n/a	0	n/a	0	n/a	n/a	n/a	n/a	n/a	0	n/a	n/a	n/a
Belarus	2	n/a	1	11	4	5	4	2	20	50	66	97	67	78	26	23	61	18	53	44	n/a	108	82	n/a	88	86
Belgium	n/a	n/a	n/a	n/a	n/a	n/a	n/a	n/a	n/a	n/a	n/a	n/a	n/a	n/a	n/a	n/a	n/a	n/a	n/a	n/a	n/a	2	2	9	n/a	n/a
Bosnia and Herzegovina	n/a	n/a	n/a	n/a	n/a	n/a	n/a	n/a	n/a	n/a	n/a	n/a	n/a	n/a	0	n/a	n/a	1	0	0	0	0	n/a	n/a	n/a	2
Bulgaria	33	18	15	10	9	12	14	18	15	45	34	36	14	24	22	0	n/a	0	n/a	0	0	0	n/a	n/a	n/a	n/a
Croatia	n/a	n/a	n/a	n/a	n/a	n/a	n/a	n/a	n/a	n/a	n/a	n/a	25	24	26	18	27	30	36	38	28	20	11	20	44	36
Cyprus	n/a	n/a	n/a	n/a	n/a	n/a	n/a	n/a	n/a	n/a	n/a	n/a	n/a	n/a	n/a	n/a	n/a	n/a	n/a	n/a	n/a	0	n/a	n/a	n/a	n/a
Czech Republic	350	333	178	191	166	182	356	338	629	619	743	571	415	422	490	719	633	647	606	507	643	1029	546	631	n/a	589
Denmark	n/a	n/a	n/a	n/a	n/a	n/a	n/a	n/a	n/a	n/a	n/a	n/a	n/a	n/a	n/a	n/a	n/a	n/a	n/a	n/a	n/a	n/a	n/a	n/a	n/a	0
Estonia	n/a	n/a	n/a	n/a	n/a	n/a	n/a	n/a	n/a	n/a	n/a	n/a	n/a	387	185	272	215	90	237	182	164	171	140	90	179	201
Finland	n/a	n/a	n/a	n/a	n/a	n/a	n/a	n/a	n/a	n/a	5	8	19	16	12	41	33	38	16	29	16	17	20	23	n/a	44
France	n/a	n/a	n/a	n/a	n/a	n/a	n/a	n/a	n/a	n/a	n/a	n/a	n/a	n/a	n/a	n/a	n/a	n/a	n/a	n/a	n/a	n/a	7	n/a	n/a	10
Georgia	n/a	n/a	n/a	n/a	n/a	n/a	n/a	n/a	n/a	n/a	n/a	n/a	n/a	n/a	n/a	n/a	0	n/a	n/a	0	0	0	0	0	n/a	n/a
Germany	n/a	n/a	n/a	n/a	n/a	n/a	n/a	n/a	n/a	n/a	n/a	n/a	n/a	n/a	0	n/a	255	239	278	n/a	431	547	238	n/a	313	n/a
Greece	n/a	n/a	n/a	n/a	n/a	n/a	n/a	n/a	n/a	n/a	n/a	n/a	n/a	n/a	n/a	n/a	n/a	n/a	n/a	n/a	0	n/a	0	0	n/a	n/a
Hungary	226	372	208	218	295	229	288	206	329	278	240	253	107	84	56	46	55	60	73	76	53	57	69	77	70	n/a
Iceland	n/a	n/a	n/a	n/a	n/a	n/a	n/a	n/a	n/a	n/a	n/a	n/a	n/a	n/a	n/a	n/a	n/a	n/a	n/a	n/a	n/a	n/a	n/a	n/a	n/a	n/a
Ireland	n/a	n/a	n/a	n/a	n/a	n/a	n/a	n/a	n/a	n/a	n/a	n/a	n/a	n/a	n/a	n/a	n/a	n/a	n/a	0	0	0	n/a	n/a	n/a	n/a
Israel	n/a	n/a	n/a	n/a	n/a	n/a	n/a	n/a	n/a	n/a	n/a	n/a	n/a	n/a	n/a	n/a	n/a	n/a	n/a	n/a	n/a	n/a	n/a	n/a	n/a	n/a
Italy	0	0	0	0	0	0	0	0	0	0	0	0	0	0	0	0	0	0	0	0	n/a	n/a	n/a	n/a	n/a	n/a
Kazakhstan	n/a	n/a	n/a	n/a	n/a	n/a	n/a	n/a	n/a	n/a	n/a	n/a	n/a	n/a	n/a	n/a	n/a	56	56	n/a	n/a	n/a	32	34	n/a	n/a
Kyrgyzstan	n/a	n/a	n/a	n/a	n/a	n/a	n/a	n/a	n/a	n/a	n/a	n/a	n/a	n/a	n/a	10	36	n/a	5	3	n/a	n/a	15	21	n/a	16
Latvia	150	184	246	119	117	122	226	287	771	1366	1341	736	874	1029	350	544	303	153	365	251	142	170	171	184	n/a	494
Lithuania	10	12	9	17	8	9	14	17	198	284	427	310	645	548	171	419	298	168	763	425	243	462	234	220	n/a	612
Luxembourg	n/a	n/a	n/a	n/a	n/a	n/a	n/a	n/a	n/a	n/a	n/a	n/a	n/a	0	n/a	0	n/a	n/a	0	n/a	0	0	n/a	n/a	n/a	n/a
Malta	n/a	n/a	n/a	n/a	n/a	n/a	n/a	n/a	n/a	n/a	n/a	n/a	n/a	0	0	0	0	0	0	0	0	0	0	0	n/a	n/a
Monaco	n/a	n/a	n/a	n/a	n/a	n/a	n/a	n/a	n/a	n/a	n/a	n/a	n/a	n/a	n/a	n/a	n/a	n/a	n/a	n/a	n/a	n/a	n/a	n/a	n/a	n/a
Montenegro	n/a	n/a	n/a	n/a	n/a	n/a	n/a	n/a	n/a	n/a	n/a	n/a	n/a	n/a	n/a	n/a	n/a	n/a	n/a	n/a	n/a	0	0	0	n/a	n/a
Netherlands	n/a	n/a	n/a	n/a	n/a	n/a	n/a	n/a	n/a	n/a	n/a	n/a	n/a	n/a	n/a	n/a	n/a	n/a	n/a	n/a	n/a	n/a	n/a	n/a	n/a	n/a
Norway	0	0	0	0	0	0	0	0	0	0	0	0	0	0	1	1	1	2	1	5	2	5	13	11	n/a	11
Poland	14	10	24	15	6	8	4	8	249	181	267	257	201	208	101	170	210	126	339	262	262	317	233	n/a	351	294
Portugal	n/a	n/a	n/a	n/a	n/a	n/a	n/a	n/a	n/a	n/a	n/a	n/a	n/a	n/a	n/a	n/a	n/a	n/a	n/a	n/a	n/a	n/a	n/a	n/a	n/a	n/a
Republic of Moldova	n/a	n/a	n/a	n/a	n/a	n/a	n/a	n/a	n/a	n/a	n/a	n/a	n/a	0	n/a	n/a	n/a	n/a	n/a	n/a	0	0	n/a	n/a	n/a	n/a
Romania	n/a	n/a	n/a	n/a	n/a	n/a	n/a	n/a	n/a	n/a	n/a	n/a	n/a	n/a	0	n/a	0	n/a	1	n/a	n/a	n/a	n/a	8	n/a	3
Russian Federation	n/a	n/a	n/a	n/a	n/a	n/a	n/a	n/a	n/a	n/a	n/a	n/a	n/a	n/a	n/a	n/a	6528	n/a	n/a	4156	4566	3494	3138	2796	3720	3094
San Marino	n/a	n/a	n/a	n/a	n/a	n/a	n/a	n/a	n/a	n/a	n/a	n/a	n/a	n/a	0	0	n/a	n/a	0	n/a	0	0	n/a	n/a	n/a	n/a
Serbia	n/a	n/a	n/a	n/a	n/a	n/a	n/a	n/a	n/a	n/a	n/a	n/a	n/a	n/a	n/a	1	n/a	n/a	n/a	1	6	1	0	n/a	n/a	n/a
Slovakia	36	21	24	29	18	14	24	16	51	60	89	106	76	54	63	92	75	62	74	70	50	91	57	85	n/a	90
Slovenia	274	226	106	114	65	104	118	80	197	532	283	406	274	153	151	196	260	262	282	204	297	373	199	251	306	166
Spain	0	0	0	0	0	0	0	0	0	0	0	0	0	0	0	0	0	0	0	0	0	0	0	0	n/a	n/a
Sweden	n/a	n/a	n/a	n/a	n/a	n/a	n/a	n/a	n/a	n/a	n/a	n/a	n/a	n/a	53	198	117	n/a	107	175	131	163	182	224	n/a	174
Switzerland	n/a	n/a	n/a	n/a	n/a	n/a	n/a	n/a	n/a	n/a	n/a	n/a	123	68	112	91	108	53	116	137	202	252	106	121	117	90
Tajikistan	n/a	n/a	n/a	n/a	n/a	n/a	n/a	n/a	n/a	n/a	n/a	n/a	n/a	n/a	n/a	n/a	0	n/a	n/a	n/a	n/a	n/a	0	n/a	n/a	n/a
The former Yugoslav Republic of Macedonia	n/a	n/a	n/a	n/a	n/a	n/a	n/a	n/a	n/a	n/a	n/a	n/a	n/a	0	0	0	n/a	n/a	n/a	n/a	n/a	n/a	n/a	n/a	n/a	n/a
Turkey	n/a	n/a	n/a	n/a	n/a	n/a	n/a	n/a	n/a	n/a	n/a	n/a	n/a	n/a	0	n/a	n/a	n/a	n/a	n/a	n/a	n/a	n/a	n/a	n/a	n/a
Turkmenistan	n/a	n/a	n/a	n/a	n/a	n/a	n/a	n/a	n/a	n/a	n/a	n/a	n/a	n/a	n/a	n/a	0	n/a	n/a	n/a	n/a	n/a	n/a	n/a	n/a	n/a
Ukraine	n/a	n/a	n/a	n/a	n/a	n/a	n/a	n/a	n/a	n/a	n/a	n/a	n/a	25	45	45	n/a	n/a	28	n/a	n/a	n/a	n/a	7	n/a	3
United Kingdom of Great Britain and Northern Ireland	n/a	n/a	n/a	n/a	n/a	n/a	n/a	n/a	n/a	n/a	n/a	n/a	n/a	0	0	0	0	n/a	0	0	0	0	0	0	n/a	n/a
Uzbekistan	n/a	n/a	n/a	n/a	n/a	n/a	n/a	n/a	n/a	n/a	n/a	n/a	n/a	n/a	n/a	n/a	0	n/a	n/a	n/a	n/a	n/a	0	n/a	n/a	n/a

Supplementary table 2 - Cycle threshold (Ct) and fold regulation of genes involved in human apoptosis in hNPCs-derived neural cells using specific PCR arrays (SABiosciences).

Gene symbol	Ct		Fold Regulation
	NI	TBEV	
ABL1	35.00	35.00	1.18
AIFM1	28.62	28.43	1.35
AKT1	25.03	25.57	-1.23
APAF1	26.75	27.73	-1.67
BAD	26.45	27.26	-1.48
BAG1	29.99	30.53	-1.23
BAG3	28.67	28.83	1.06
BAK1	28.57	29.22	-1.33
BAX	25.49	25.47	1.20
BCL10	26.70	26.64	1.23
BCL2	27.93	28.50	-1.26
BCL2A1	35.00	31.65	12.04
BCL2L1	27.07	27.77	-1.38
BCL2L10	35.00	33.16	4.23
BCL2L11	29.39	28.92	1.64
BCL2L2	26.36	27.02	-1.34
BFAR	26.15	26.31	1.06
BID	27.35	27.71	-1.09
BIK	31.33	31.96	-1.31
BIRC2	25.08	25.13	1.14
BIRC3	32.62	28.83	16.34
BIRC5	30.28	31.45	-1.91
BIRC6	25.79	25.95	1.06
BNIP2	25.94	26.47	-1.22
BNIP3	24.93	25.47	-1.23
BNIP3L	24.57	25.51	-1.62
BRAF	28.18	28.98	-1.47
CASP1	30.98	26.03	36.50
CASP10	33.21	32.91	1.45
CASP14	35.00	33.58	3.16
CASP2	26.32	27.37	-1.75
CASP3	25.66	26.48	-1.49
CASP4	33.78	30.89	8.75
CASP5	35.00	32.93	4.96
CASP6	26.59	27.56	-1.66
CASP7	28.63	27.49	2.60
CASP8	31.78	29.47	5.86
CASP9	26.72	27.64	-1.60
CD27	33.21	33.36	1.06
CD40	35.00	32.59	6.28
CD40LG	32.25	33.14	-1.57
CD70	34.53	32.46	4.96
CFLAR	27.01	27.15	1.07
CIDEA	35.00	33.73	2.85
CIDEB	26.93	27.38	-1.16
CRADD	28.99	31.15	-3.78
CYCS	29.07	29.62	-1.24
DAPK1	27.59	28.71	-1.84

Gene symbol	Ct		Fold Regulation
	NI	TBEV	
DFFA	26.90	27.75	-1.53
DIABLO	26.34	26.70	-1.09
FADD	27.24	27.27	1.16
FAS	26.84	26.22	1.82
FASLG	35.00	35.00	1.18
GADD45A	29.29	27.97	2.95
HRK	29.66	27.26	6.23
IGF1R	25.66	26.93	-2.04
IL10	34.75	35.00	-1.01
LTA	32.40	31.26	2.60
LTBR	35.00	35.00	1.18
MCL1	24.06	23.93	1.29
NAIP	24.29	25.39	-1.82
NFKB1	29.12	28.14	2.33
NOD1	28.48	28.00	1.65
NOL3	28.81	29.65	-1.52
PYCARD	30.45	30.25	1.36
RIPK2	28.66	28.65	1.19
TNF	35.00	32.17	8.40
TNFRSF10A	33.80	33.30	1.67
TNFRSF10B	26.71	25.92	2.04
TNFRSF11B	28.86	29.21	-1.08
TNFRSF1A	26.10	26.25	1.06
TNFRSF1B	35.00	32.89	5.10
TNFRSF21	27.95	27.89	1.23
TNFRSF25	28.63	29.61	-1.67
TNFRSF9	35.00	31.90	10.13
TNFSF10	34.31	27.85	103.97
TNFSF8	35.00	35.00	1.18
TP53	25.32	25.17	1.31
TP53BP2	25.29	25.99	-1.38
TP73	35.00	35.00	1.18
TRADD	31.55	32.49	-1.62
TRAF2	28.13	28.20	1.13
TRAF3	27.69	27.92	1.01
XIAP	25.84	26.64	-1.47
ACTB	19.10	19.92	-1.49
B2M	22.38	20.43	4.56
GAPDH	21.63	22.40	-1.44
HPRT1	28.93	29.28	-1.08
RPLP0	20.49	21.70	-1.96
HGDC	34.11	34.87	-1.43
RTC	22.77	22.44	1.48
RTC	22.78	22.42	1.52
RTC	22.81	22.47	1.49
PPC	19.54	19.73	1.04
PPC	19.53	19.68	1.06
PPC	19.49	19.66	1.05

Supplementary table 3 - Cycle threshold (Ct) and fold regulation of genes involved in human autophagy in hNPCs-derived neural cells using specific PCR arrays (SABiosciences).

Gene symbol	Ct		Fold Regulation
	NI	TBEV	
AKT1	35.00	35.00	-1.48
AMBRA1	27.75	26.62	1.48
APP	23.53	23.42	-1.37
Atg10	28.97	28.98	-1.49
Atg12	25.70	25.41	-1.21
Atg16L1	27.63	26.99	1.05
Atg16L2	29.24	29.05	-1.30
Atg3	25.60	25.37	-1.26
Atg4A	28.43	28.53	-1.59
Atg4B	26.51	26.13	-1.14
Atg4C	26.74	27.24	-2.09
Atg4D	27.73	27.27	-1.08
Atg5	26.23	26.02	-1.28
Atg7	27.15	27.02	-1.35
Atg9A	27.94	27.37	1.00
Atg9B	34.59	33.01	2.02
BAD	27.05	26.54	-1.04
BAK1	28.85	28.13	1.11
BAX	25.87	24.97	1.26
BCL2	28.03	27.82	-1.28
BCL2L1	27.78	27.43	-1.16
BECN1	27.21	26.79	-1.11
BID	27.47	26.92	-1.01
BNIP3	25.00	24.99	-1.47
CASP3	25.79	25.97	-1.68
CASP8	31.46	29.08	3.52
CDKN1B	25.11	24.04	1.42
CDKN2A	28.67	27.69	1.33
CLN3	27.60	27.39	-1.28
CTSB	25.67	25.65	-1.46
CTSD	25.46	24.90	-1.00
CTSS	31.86	28.58	6.56
CXCR4	25.17	25.46	-1.81
DAPK1	28.14	28.19	-1.53
DRAM1	29.74	27.74	2.70
DRAM2	26.72	26.70	-1.46
EIF2AK3	27.75	26.11	2.11
EIF4G1	26.11	25.08	1.38
ESR1	34.41	34.76	-1.89
FADD	27.86	26.76	1.45
FAS	26.83	25.47	1.73
GAA	27.41	27.09	-1.19
GABARAP	23.33	23.27	-1.42
GABARAPL1	26.73	26.36	-1.15
GABARAPL2	23.58	23.79	-1.71
HDAC1	26.23	26.14	-1.39
HDAC6	26.37	26.03	-1.17
HGS	28.95	28.14	1.18

Gene symbol	Ct		Fold Regulation
	NI	TBEV	
HSP90AA1	23.35	22.57	1.16
HSPA8	22.27	21.82	-1.08
HTT	27.47	26.85	1.04
IFNG	35.00	35.00	-1.48
IGF1	33.50	30.86	4.21
INS	35.00	35.00	-1.48
IRGM	35.00	35.00	-1.48
LAMP1	24.81	24.45	-1.15
MAP1LC3A	26.55	26.50	-1.43
MAP1LC3B	24.48	24.46	-1.46
MAPK14	26.70	26.39	-1.19
MAPK8	24.95	25.54	-2.23
MTOR	26.60	26.21	-1.13
NFKB1	29.38	27.05	3.40
NPC1	27.70	27.11	1.02
PIK3C3	25.97	25.82	-1.33
PIK3CG	35.00	35.00	-1.48
PIK3R4	27.56	27.21	-1.16
PRKAA1	25.96	25.80	-1.33
PTEN	25.26	24.79	-1.07
RAB24	30.11	29.05	1.41
RB1	25.66	25.41	-1.24
RGS19	29.85	29.02	1.20
RPS6KB1	26.14	25.82	-1.19
SNCA	26.65	27.10	-2.02
SQSTM1	24.30	23.02	1.64
TGFB1	27.78	27.41	-1.15
TGM2	33.49	30.85	4.21
TMEM74	32.20	30.06	2.98
TNF	34.53	31.45	5.71
TNFSF10	35.00	27.31	139.49
TP53	25.48	24.49	1.34
ULK1	27.85	27.87	-1.50
ULK2	26.26	26.27	-1.49
UVRAG	29.14	27.63	1.92
WIPI1	27.87	27.81	-1.42
ACTB	19.32	19.27	-1.43
B2M	22.39	19.56	4.80
GAPDH	21.92	21.70	-1.27
HPRT1	28.65	28.31	-1.17
RPLP0	20.36	20.97	-2.26
HGDC	33.26	32.94	-1.19
RTC	22.82	22.95	-1.62
RTC	22.77	23.00	-1.74
RTC	22.81	22.96	-1.64
PPC	19.67	19.59	-1.40
PPC	19.67	19.57	-1.38
PPC	19.66	19.56	-1.38

Supplementary table 4 - Cycle threshold (Ct) and fold regulation of genes involved in human antiviral response in hNPCs-derived neural cells using a specific PCR array (SABiosciences).

Gene symbol	Ct		Fold Regulation
	NI	TBEV	
AIM2	32.97	33.03	1.68
APOBEC3G	39.34	34.20	6.41
Atg5	26.79	27.04	1.09
AZI2	26.39	26.37	1.69
CARD9	n.d.	33.86	-1.30
CASP1	31.21	27.70	37.01
CASP10	33.23	34.57	-3.16
CASP8	31.37	31.28	-1.21
CCL3	41.57	36.03	1.04
CCL5	43.49	25.47	207.94
CD40	43.95	n.d.	-3.89
CD80	35.43	41.75	1.13
CD86	n.d.	n.d.	2.97
CHUK	28.51	28.60	1.31
CTSB	26.48	26.85	1.24
CTSL	26.49	27.13	1.09
CTSS	33.84	31.63	3.27
CXCL10	43.64	24.88	719.08
CXCL11	n.d.	26.80	188.71
CXCL9	30.76	29.77	5.70
CYLD	28.93	28.14	1.72
TKFC	30.55	30.51	-1.16
DDX3X	25.08	25.36	1.13
DDX58	27.86	24.35	17.63
DHX58	35.28	31.16	99.04
FADD	28.93	29.37	1.46
FOS	27.24	26.86	1.67
HSP90AA1	23.08	23.12	1.25
IFIH1	29.90	24.75	42.81
IFNA1	n.d.	35.11	-1.68
IFNA2	n.d.	n.d.	1.30
IFNAR1	25.69	26.18	-1.09
IFNB1	33.74	26.40	44.32
IKBKB	27.96	28.02	1.20
IL12A	30.19	30.55	1.78
IL12B	35.59	35.01	2.19
IL15	34.82	32.78	6.45
IL18	33.00	34.45	1.17
IL1B	39.11	34.31	-2.07
IL6	34.41	31.40	-1.10
CXCL8	37.46	30.05	12.55
IRAK1	29.70	29.54	1.29
IRF3	27.94	27.66	1.15
IRF5	32.90	32.90	-1.09
IRF7	31.06	28.63	5.03
ISG15	30.05	23.98	203.66
JUN	28.24	27.72	1.62
MAP2K1	27.85	27.84	1.10

Gene symbol	Ct		Fold Regulation
	NI	TBEV	
MAP2K3	29.16	28.59	1.46
MAP3K1	27.95	28.19	1.32
MAP3K7	26.58	26.90	1.30
MAPK1	24.96	25.16	1.23
MAPK14	27.69	28.00	1.04
MAPK3	28.12	28.31	-1.04
MAPK8	26.01	26.65	1.19
MAVS	28.34	28.59	-1.03
MEFV	33.87	35.09	3.18
MX1	32.55	23.91	522.76
MYD88	29.03	27.64	3.14
NFKB1	30.59	29.38	2.28
NFKBIA	28.71	27.45	3.03
NLRP3	n.d.	n.d.	-4.06
NOD2	41.52	35.41	2.41
OAS2	42.50	27.13	541.19
PIN1	27.56	27.80	1.04
PSTPIP1	32.96	32.43	-1.48
PYCARD	33.06	33.49	-1.05
PYDC1	34.99	36.14	2.19
RELA	27.67	27.46	1.31
RIPK1	29.37	28.72	2.20
SPP1	30.22	29.52	1.15
STAT1	26.78	24.13	11.63
SUGT1	25.57	25.93	1.36
TBK1	28.40	28.26	1.35
TICAM1	30.78	29.84	1.46
TLR3	30.61	27.85	8.40
TLR7	37.65	37.79	1.04
TLR8	n.d.	n.d.	1.04
TLR9	34.15	42.40	-1.04
TNF	40.18	32.70	-1.16
TRADD	33.63	33.08	1.59
TRAF3	29.00	28.98	1.04
TRAF6	27.70	27.47	1.14
TRIM25	27.49	25.52	6.41
ACTB	19.49	19.60	-1.42
B2M	23.00	20.63	3.93
GAPDH	21.91	21.86	-1.27
HPRT1	28.64	28.70	-1.37
RPLP0	20.67	20.95	-1.60
HGDC	33.93	35.00	-2.76
RTC	22.76	22.40	-1.02
RTC	22.76	22.43	-1.05
RTC	22.77	22.43	-1.04
PPC	19.80	19.77	-1.29
PPC	19.76	19.71	-1.27
PPC	19.76	19.70	-1.26

Supplementary table 5 - Cycle threshold (Ct) and fold regulation of genes involved in human antiviral response in unsorted cultures, En-Neurons and En-Astrocytes using specific PCR arrays (SABiosciences).

Unsorted cultures

Gene symbol	Ct		Fold Regulation
	NI	TBEV	
AIM2	32.97	33.03	-1.13
APOBEC3G	35.00	34.20	1.60
Atg5	26.79	27.04	-1.29
AZI2	26.39	26.37	-1.07
CARD9	35.00	33.86	2.03
CASP1	31.21	27.70	10.48
CASP10	33.23	34.57	-2.75
CASP8	31.37	31.28	-1.02
CCL3	35.00	35.00	-1.09
CCL5	35.00	25.47	680.29
CD40	35.00	35.00	-1.09
CD80	35.00	35.00	-1.09
CD86	35.00	35.00	-1.09
CHUK	28.51	28.60	-1.16
CTSB	26.48	26.85	-1.40
CTSL	26.49	27.13	-1.69
CTSS	33.84	31.63	4.26
CXCL10	35.00	24.88	1024.00
CXCL11	35.00	26.80	270.60
CXCL9	30.76	29.77	1.83
CYLD	28.93	28.14	1.59
TKFC	30.55	30.51	-1.06
DDX3X	25.08	25.36	-1.32
DDX58	27.86	24.35	10.48
DHX58	35.00	31.16	13.18
FADD	28.93	29.37	-1.47
FOS	27.24	26.86	1.20
HSP90AA1	23.08	23.12	-1.12
IFIH1	29.90	24.75	32.67
IFNA1	35.00	35.00	-1.09
IFNA2	35.00	35.00	-1.09
IFNAR1	25.69	26.18	-1.53
IFNB1	33.74	26.40	149.09
IKBKB	27.96	28.02	-1.13
IL12A	30.19	30.55	-1.39
IL12B	35.00	35.00	-1.09
IL15	34.82	32.78	3.78
IL18	33.00	34.45	-2.97
IL1B	35.00	34.31	1.48
IL6	34.41	31.40	7.41
CXCL8	35.00	30.05	28.44
IRAK1	29.70	29.54	1.03
IRF3	27.94	27.66	1.12
IRF5	32.90	32.90	-1.09
IRF7	31.06	28.63	4.96
ISG15	30.05	23.98	61.82
JUN	28.24	27.72	1.32
MAP2K1	27.85	27.84	-1.08

Gene symbol	Ct		Fold Regulation
	NI	TBEV	
MAP2K3	29.16	28.59	1.37
MAP3K1	27.95	28.19	-1.28
MAP3K7	26.58	26.90	-1.36
MAPK1	24.96	25.16	-1.25
MAPK14	27.69	28.00	-1.35
MAPK3	28.12	28.31	-1.24
MAPK8	26.01	26.65	-1.69
MAVS	28.34	28.59	-1.29
MEFV	33.87	35.00	-2.38
MX1	32.55	23.91	367.09
MYD88	29.03	27.64	2.41
NFKB1	30.59	29.38	2.13
NFKBIA	28.71	27.45	2.20
NLRP3	35.00	35.00	-1.09
NOD2	35.00	35.00	-1.09
OAS2	35.00	27.13	215.27
PIN1	27.56	27.80	-1.28
PSTPIP1	32.96	32.43	1.33
PYCARD	33.06	33.49	-1.46
PYDC1	34.99	35.00	-1.09
RELA	27.67	27.46	1.06
RIPK1	29.37	28.72	1.44
SPP1	30.22	29.52	1.49
STAT1	26.78	24.13	5.78
SUGT1	25.57	25.93	-1.39
TBK1	28.40	28.26	1.01
TICAM1	30.78	29.84	1.77
TLR3	30.61	27.85	6.23
TLR7	35.00	35.00	-1.09
TLR8	35.00	35.00	-1.09
TLR9	34.15	35.00	-1.96
TNF	35.00	32.70	4.53
TRADD	33.63	33.08	1.35
TRAF3	29.00	28.98	-1.07
TRAF6	27.70	27.47	1.08
TRIM25	27.49	25.52	3.61
ACTB	20.81	21.21	-1.43
B2M	23.06	21.86	2.11
GAPDH	23.12	23.33	-1.26
HPRT1	29.24	29.12	1.00
RPLP0	21.33	22.08	-1.83
HGDC	34.13	35.00	-1.99
RTC	21.23	21.43	-1.25
RTC	21.26	21.36	-1.16
RTC	21.28	21.46	-1.23
PPC	19.46	19.46	-1.09
PPC	19.44	19.40	-1.06
PPC	19.47	19.44	-1.06

En-Neurons

Gene symbol	Ct		Fold Regulation
	NI	TBEV	
AIM2	32.73	33.05	1.01
APOBEC3G	35.00	35.00	1.27
Atg5	26.97	27.56	-1.19
AZI2	26.50	26.61	1.17
CARD9	32.71	33.51	-1.38
CASP1	33.39	31.08	6.28
CASP10	32.98	33.60	-1.21
CASP8	31.62	32.51	-1.46
CCL3	35.00	34.45	1.85
CCL5	33.93	26.22	265.03
CD40	35.00	35.00	1.27
CD80	33.96	35.00	-1.62
CD86	35.00	35.00	1.27
CHUK	28.34	28.72	-1.03
CTSB	26.95	27.60	-1.24
CTSL	27.77	28.08	1.02
CTSS	32.86	32.85	1.27
CXCL10	35.00	26.64	415.87
CXCL11	35.00	28.36	126.24
CXCL9	30.55	30.17	1.65
CYLD	27.96	28.23	1.05
TKFC	30.68	31.61	-1.51
DDX3X	25.63	26.04	-1.05
DDX58	28.61	26.43	5.74
DHX58	35.00	31.94	10.56
FADD	29.19	30.17	-1.56
FOS	28.88	29.03	1.14
HSP90AA1	23.72	24.35	-1.22
IFIH1	31.25	27.29	19.70
IFNA1	35.00	33.48	3.63
IFNA2	35.00	35.00	1.27
IFNAR1	26.36	27.10	-1.32
IFNB1	32.91	27.09	71.51
IKBKB	28.51	29.15	-1.23
IL12A	32.92	32.43	1.78
IL12B	35.00	32.77	5.94
IL15	34.97	33.60	3.27
IL18	31.39	32.42	-1.61
IL1B	35.00	34.98	1.28
IL6	34.43	31.36	10.63
CXCL8	35.00	31.83	11.39
IRAK1	29.76	30.84	-1.67
IRF3	28.93	29.16	1.08
IRF5	32.93	33.52	-1.19
IRF7	30.81	31.27	-1.09
ISG15	30.99	26.34	31.78
JUN	28.87	29.17	1.03
MAP2K1	28.39	28.95	-1.16

Gene symbol	Ct		Fold Regulation
	NI	TBEV	
MAP2K3	30.14	30.01	1.39
MAP3K1	28.17	28.74	-1.17
MAP3K7	26.72	26.83	1.17
MAPK1	25.73	26.22	-1.11
MAPK14	27.52	28.17	-1.24
MAPK3	28.50	29.10	-1.20
MAPK8	25.39	26.01	-1.21
MAVS	28.72	29.50	-1.36
MEFV	35.00	35.00	1.27
MX1	32.36	27.41	39.12
MYD88	29.36	29.61	1.06
NFKB1	30.97	30.54	1.71
NFKBIA	28.41	28.05	1.62
NLRP3	35.00	35.00	1.27
NOD2	35.00	35.00	1.27
OAS2	34.03	29.79	23.92
PIN1	27.86	28.63	-1.35
PSTPIP1	32.73	33.50	-1.35
PYCARD	31.60	32.44	-1.41
PYDC1	35.00	35.00	1.27
RELA	28.09	28.47	-1.03
RIPK1	30.08	29.92	1.41
SPP1	30.60	31.39	-1.37
STAT1	28.01	27.02	2.51
SUGT1	25.52	25.94	-1.06
TBK1	28.77	28.85	1.20
TICAM1	31.80	31.58	1.47
TLR3	31.35	30.92	1.71
TLR7	35.00	35.00	1.27
TLR8	34.89	35.00	1.17
TLR9	32.28	33.48	-1.82
TNF	35.00	33.96	2.60
TRADD	34.98	35.00	1.25
TRAF3	29.90	29.94	1.23
TRAF6	28.06	28.64	-1.18
TRIM25	29.26	28.46	2.20
ACTB	20.90	21.88	-1.56
B2M	24.77	24.20	1.88
GAPDH	23.73	24.63	-1.47
HPRT1	29.01	29.35	1.00
RPLP0	22.21	22.73	-1.13
HGDC	35.00	34.19	2.22
RTC	20.99	20.89	1.36
RTC	20.90	20.88	1.28
RTC	20.96	20.92	1.30
PPC	19.56	19.42	1.39
PPC	19.46	19.40	1.32
PPC	19.47	19.45	1.28

En-Astrocytes

Gene symbol	Ct		Fold Regulation
	NI	TBEV	
AIM2	32.78	31.09	4.00
APOBEC3G	35.00	33.73	2.99
Atg5	26.55	27.05	-1.14
AZI2	26.23	26.22	1.25
CARD9	35.00	35.00	1.24
CASP1	30.97	26.66	24.59
CASP10	33.70	33.23	1.72
CASP8	31.26	30.84	1.66
CCL3	35.00	34.73	1.49
CCL5	35.00	25.64	814.63
CD40	35.00	35.00	1.24
CD80	35.00	35.00	1.24
CD86	35.00	35.00	1.24
CHUK	28.14	28.82	-1.29
CTSB	26.03	27.01	-1.59
CTSL	26.01	26.93	-1.53
CTSS	34.59	32.53	5.17
CXCL10	34.53	24.60	1209.34
CXCL11	35.00	26.71	388.02
CXCL9	30.31	29.66	1.95
CYLD	28.55	28.10	1.69
TKFC	29.83	31.33	-2.28
DDX3X	24.60	25.46	-1.46
DDX58	27.42	23.73	16.00
DHX58	35.00	30.49	28.25
FADD	28.60	29.34	-1.35
FOS	26.57	27.07	-1.14
HSP90AA1	22.74	22.84	1.16
IFIH1	28.84	24.01	35.26
IFNA1	35.00	35.00	1.24
IFNA2	35.00	35.00	1.24
IFNAR1	25.21	26.35	-1.78
IFNB1	35.00	26.24	537.45
IKBKB	27.48	28.17	-1.30
IL12A	29.11	29.47	-1.04
IL12B	35.00	35.00	1.24
IL15	34.26	33.37	2.30
IL18	32.51	33.22	-1.32
IL1B	34.50	35.00	-1.14
IL6	34.78	32.06	8.17
CXCL8	35.00	30.78	23.10
IRAK1	29.35	30.30	-1.56
IRF3	27.36	27.38	1.22
IRF5	33.44	35.00	-2.38
IRF7	30.67	28.58	5.28
ISG15	29.28	22.87	105.42
JUN	27.96	27.51	1.69
MAP2K1	27.29	27.87	-1.21

Gene symbol	Ct		Fold Regulation
	NI	TBEV	
MAP2K3	28.45	28.39	1.29
MAP3K1	27.58	28.16	-1.21
MAP3K7	25.95	26.48	-1.16
MAPK1	24.56	25.31	-1.36
MAPK14	27.32	27.93	-1.23
MAPK3	27.69	28.72	-1.65
MAPK8	26.28	27.31	-1.65
MAVS	27.88	29.11	-1.89
MEFV	35.00	33.89	2.68
MX1	32.82	23.20	975.50
MYD88	28.40	26.81	3.73
NFKB1	30.02	29.55	1.72
NFKBIA	28.45	27.77	1.99
NLRP3	35.00	35.00	1.24
NOD2	35.00	35.00	1.24
OAS2	35.00	26.35	498.00
PIN1	27.35	28.45	-1.73
PSTPIP1	31.57	33.28	-2.64
PYCARD	33.15	33.43	1.02
PYDC1	35.00	35.00	1.24
RELA	27.43	27.80	-1.04
RIPK1	29.06	29.04	1.26
SPP1	29.29	28.68	1.89
STAT1	26.05	23.45	7.52
SUGT1	25.27	25.75	-1.13
TBK1	27.69	27.87	1.09
TICAM1	30.38	29.75	1.92
TLR3	29.49	27.13	6.36
TLR7	35.00	35.00	1.24
TLR8	35.00	35.00	1.24
TLR9	34.11	35.00	-1.49
TNF	35.00	33.41	3.73
TRADD	32.70	33.04	-1.02
TRAF3	28.27	29.00	-1.34
TRAF6	27.44	27.42	1.26
TRIM25	26.87	25.02	4.47
ACTB	20.32	21.26	-1.55
B2M	22.35	21.24	2.68
GAPDH	22.51	23.16	-1.27
HPRT1	29.23	29.54	1.00
RPLP0	20.73	21.70	-1.58
HGDC	34.75	34.67	1.31
RTC	20.97	20.92	1.28
RTC	21.01	20.92	1.32
RTC	21.01	20.96	1.28
PPC	19.47	19.45	1.26
PPC	19.45	19.45	1.24
PPC	19.44	19.52	1.17

Title: Pathological modeling of tick-borne encephalitis Virus infection and induced antiviral response in neurons and astrocytes using human neural progenitor-derived cells.

Keywords: Tick-borne encephalitis virus, Antiviral immunity, Human neural progenitor cells, Neurons, Astrocytes, Flavivirus

Tick-borne encephalitis virus (TBEV), a member of the *Flaviviridae* family, genus *Flavivirus*, is, from a medical point of view, the most important arbovirus in Europe and North-East Asia. It is responsible for febrile illness and, in some cases, for neurological manifestations ranging from mild meningitis to severe encephalomyelitis that can be fatal. Despite its medical importance, the neuropathogenesis induced by this zoonotic agent remains poorly understood. Here, we used human neural cells differentiated from fetal neural progenitor cells (hNPCs) to model the infection *in vitro* and to decipher the mechanisms by which the virus damages the human brain. Our results showed that neurons and glial cells, namely astrocytes and oligodendrocytes, were permissive to TBEV. Neurons were massively infected and subjected to a dramatic cytopathic effect (60% loss 7 days post-infection). Astrocytes were also infected, although at lower levels, and the infection had a moderate effect on their survival (30% loss 7 days post-infection), inducing a hypertrophied morphology characteristic of astrogliosis. Thus, two major cellular events described in TBEV-infected human brain (i.e. neuronal loss and astrogliosis) were reproduced in this *in vitro* cellular model, showing its relevance to study TBEV-induced neuropathogenesis. We therefore used it to tackle TBEV-induced antiviral response. Using PCR arrays, we first showed that TBEV induced a strong antiviral response characterized by the overexpression of viral sensors, cytokines and interferon-stimulated genes (ISGs). Then, setting up enriched cultures of human neurons and human astrocytes, we further showed that the two cellular types were participating in the global antiviral response. However, astrocytes developed a stronger antiviral response than neurons. These results, by demonstrating that human neurons and human astrocytes have unique antiviral potential, suggest that their particular susceptibility to TBEV infection is due to their different capacity to mount a protective antiviral response.

Titre : Modélisation pathologique de l'infection par le virus de l'encéphalite à tiques et réponse antivirale induite dans les neurones et astrocytes dérivés de progéniteurs neuraux fœtaux humains

Mots-clés : Virus de l'encéphalite à tiques, Immunité antivirale, Cellules progénitrices neurales humaines, Neurones, Astrocytes, Flavivirus

Le virus de l'encéphalite à tiques (TBEV), membre de la famille des *Flaviviridae* et du genre *Flavivirus*, est d'un point de vue médical, l'arbovirus le plus important en Europe et en Asie du Nord-Est. Il est responsable de symptômes fébriles et de manifestations neurologiques allant de la méningite légère à l'encéphalomyélite sévère pouvant être fatale. En dépit de son importance médicale, la neuropathogenèse induite par cet agent zoonotique reste peu caractérisée. Ici, nous avons utilisé des cellules neurales humaines différenciées à partir de progéniteurs neuraux fœtaux pour modéliser l'infection *in vitro* et élucider les mécanismes par lesquels le virus endommage le cerveau humain. Nos résultats ont montré que les neurones et les cellules gliales (astrocytes et oligodendrocytes) étaient permissifs au TBEV. Les neurones étaient massivement infectés et la cible d'un effet cytopathique important (perte de 60 % des neurones 7 jours après l'infection). Les astrocytes étaient également infectés, bien qu'à des niveaux inférieurs, et l'infection avait un effet modéré sur leur survie (perte de 30 % des astrocytes 7 jours après l'infection), induisant une hypertrophie caractéristique d'une astrogliose. Ainsi, deux événements majeurs décrits dans les cerveaux de patients infectés par TBEV (perte neuronale et astrogliose) étaient reproduits dans ce modèle cellulaire *in vitro*, démontrant ainsi sa pertinence pour des études de neuropathogenèse. Nous l'avons donc utilisé pour étudier la réponse antivirale induite par TBEV. En utilisant des PCR arrays, nous avons d'abord montré que le virus induisait une forte réponse antivirale caractérisée par une surexpression de senseurs viraux, de cytokines et de gènes stimulés par l'interféron. Puis, en établissant des cultures enrichies en neurones humains et astrocytes humains, nous avons montré que ces deux types cellulaires participaient à la réponse antivirale globale. Cependant, les astrocytes élaboraient une réponse antivirale plus forte que les neurones. Ces résultats, en démontrant que les neurones humains et les astrocytes humains élaboraient chacun une réponse antivirale unique suite à l'infection, suggèrent que leur sensibilité particulière à TBEV serait due à leur capacité différente à établir une réponse antivirale protectrice.